

**NDOT Research Report**

**Report No. 554-14-803**

---

**Toward Successful Implementation of  
Prefabricated Deck Panels to Accelerate the  
Bridge Construction Process**

---

**August 2016**

**Nevada Department of Transportation  
1263 South Stewart Street  
Carson City, NV 89712**



## Disclaimer

This work was sponsored by the Nevada Department of Transportation. The contents of this report reflect the views of the authors, who are responsible for the facts and the accuracy of the data presented herein. The contents do not necessarily reflect the official views or policies of the State of Nevada at the time of publication. This report does not constitute a standard, specification, or regulation.

Report No. CCEER 16-05

**TOWARD SUCCESSFUL IMPLEMENTATION OF  
PREFABRICATED DECK PANELS TO ACCELERATE THE  
BRIDGE CONSTRUCTION PROCESS**

Jared Jones  
Keri Ryan  
Mehdi “Saiid” Saiidi

A report sponsored by the Nevada Department of Transportation

---

**Center for Civil Engineering Earthquake Research**

University of Nevada, Reno  
Department of Civil and Environmental Engineering, MS 258  
1664 N. Virginia St.  
Reno, NV 89557

August 2016

## **Abstract**

The development of accelerated bridge construction (ABC) techniques and connection details has become a national research focus. With the aging of the interstate system and many bridges on key routes requiring extensive rehabilitation or replacement, the economic impact of construction time has become a key factor in the design of bridges. Several states have successfully standardized the ABC approach with high rates of public satisfaction. Compared to other ABC techniques, the technologies for pre-fabricated bridge decks are relatively mature. However, this technology has not been incorporated in Nevada. The goal of this research project is to develop design guidelines and specifications on the use of pre-fabricated bridge decks for Nevada based on existing techniques.

A state-of-the-art literature review summarizing existing practices for the implementation of prefabricated deck panels was prepared. This information was used to assemble a survey that was sent to representatives of all state DOTs. The survey requested information from each DOT on their experience with prefabricated deck panels, connection details that were used, and the field performance of the panels and connections. Information from the literature review and survey was used to develop design specifications and recommendations for the Nevada Department of Transportation (NDOT). These specifications were supplemented with a design aid spreadsheet and finite element models to validate the provisions in the specifications and aid in the implementation of this technology. As part of this implementation, two design methods were developed: a simplified (design aid spreadsheet) method and a model based method.

Survey results showed that full-depth prefabricated deck panels performed better and saved time compared to partial depth panels. Because of this, full-depth deck panels were the primary focus in this project. Results from the survey showed that guidelines and connection details developed by the Precast/Prestressed Concrete Institute (PCI) Northeast committee (PCI, 2011a) were widely used and led to satisfactory performance. These guidelines were used as the foundation for the proposed design specifications for NDOT. Information from the survey and literature review were used to supplement the PCI guidelines and add information specific to Nevada's needs.

The guidelines were used to design full-depth deck panel systems for two existing bridges. The simplified and model based methods were applied to both design examples to determine whether the design specifications could be used to appropriately design full-depth deck systems for different cases. The results from the two design examples showed that the full-depth deck panel systems performed as expected and could be designed using the existing AASHTO and PCI provisions. Additional modeling beyond simple hand calculations was required for skewed and curved bridges. Based on these findings, prefabricated full-depth deck panels are recommended for use in ABC projects in Nevada using the assembled design specifications and design procedures created for this project.

## **Acknowledgements**

This project was sponsored by the Nevada Department of Transportation. We would like to thank Mr. Martin, Mr. Elicegui, Mr. Harrison, and Mr. Hornback from NDOT who helped guide the project and assisted in reviewing the developed survey and design aid spreadsheet.

Also, thank you to the many state DOTs that filled out our survey. The survey became a critical part of the project after receiving so many detailed responses. The findings and conclusions we made from the survey would not have been possible without the large amount of feedback we received.

This document is based on an MS thesis prepared by the first author and supervised by the other authors.

# Table of Contents

Abstract.....	i
Acknowledgements.....	ii
Table of Contents.....	iii
List of Figures.....	vi
List of Tables.....	viii
Chapter 1. Introduction.....	1
1.1 Motivation and Background.....	1
1.2 Objectives and Scope.....	1
1.3 Organization of Thesis.....	2
Chapter 2. Literature Review.....	4
2.1 Introduction.....	4
2.2 Overview of Prefabricated Deck Systems.....	4
2.2.1 Full Depth Deck Panel Systems.....	4
2.2.2 Partial Depth Deck Panel Systems.....	5
2.2.3 Corrugated Steel Decks.....	5
2.2.4 Steel Grids.....	5
2.3 Terminology.....	7
2.4 NCHRP 12-65 Project.....	8
2.4.1 Project Overview.....	8
2.4.2 Survey Results.....	9
2.4.3 Findings from NCHRP 12-65 Project.....	10
2.5 Current Practice, Standards and Specifications for Full Depth Deck Panels.....	10
2.5.1 General Guidelines.....	10
2.5.2 Oregon DOT Specifications and Construction Guidelines.....	19
2.5.3 Utah DOT Specifications and Lessons Learned.....	23
2.5.4 NCHRP 584 Connection Designs.....	27
2.6 Current Practice, Standards and Specifications for Partial Depth Deck Panels.....	33
2.6.1 General Fabrication and Construction Procedures.....	33
2.6.2 Texas Specifications and Experience.....	36
2.6.3 Colorado Experience.....	39
2.7 Noteworthy Projects.....	41
2.7.1 Utah Interstate Exchange Ramp Deck Replacement Project (Skewed Bridge).....	41
2.7.2 Missouri Bill Emerson Memorial Bridge.....	42
2.7.3 Iowa US 6 Over Keg Creek.....	44
2.8 Literature Review Conclusions.....	45
3. State DOT Prefabricated Deck Panel Survey Results.....	46

3.1 Introduction and Prior Research .....	46
3.2 Total Responses and Number of Decks Constructed .....	46
3.3 Trends in Application of Prefabricated Deck Panels .....	48
3.3.1 Full-Depth Longitudinal and Transverse Reinforcement .....	48
3.3.2 Connection Details .....	50
3.3.4 Usage of Overlays .....	58
3.4 Deck Panel Evaluations .....	59
3.4.1 Deck Panel Performance Problems .....	59
3.4.2 Ratings of Deck Panel Performance .....	63
3.4.3 Preference Trends for Full-Depth vs Partial-Depth Panels .....	64
3.5 Deck Panel Limitations .....	65
3.6 Implementation of Site Casting .....	67
3.7 Recommendations for Nevada Implementation .....	68
Chapter 4: Specification Development and Overview .....	74
4.1 Introduction .....	74
4.2 Design Specifications Overview .....	74
Chapter 5: Full-Depth Panel Design Process .....	76
5.1 Introduction .....	76
5.2 Simplified Design Method .....	76
5.2.1 General Properties .....	76
5.2.2 Loads and Load Combinations .....	77
5.2.3 Design of Transverse Prestressing Steel .....	77
5.2.4 Panel to Girder Connection Design .....	81
5.2.5 Longitudinal Post-Tensioning Design .....	82
5.2.6 UHPC Design .....	82
5.2.7 Overhang Design .....	83
5.3 Model Based Design Method .....	85
Chapter 6: Design Example 1: West Mesquite Interchange .....	86
6.1 Introduction .....	86
6.2 Bridge Description .....	86
6.3 Simplified Design Method .....	89
6.3.1 Design Moments and Loads .....	89
6.3.2 Prestress Steel Design .....	91
6.3.3 Panel-to-Girder Connection Design .....	101
6.3.4 Post-Tensioning Design .....	103
6.3.5 Overhang Design .....	104
6.4 Model Based Design Method .....	110

6.4.1 Overview.....	110
6.4.2 Material Definitions.....	110
6.4.3 Geometric and Element Definitions.....	111
6.4.4 Loads and Analysis Assumptions.....	114
6.4.5 Dead and Live Load Analysis and Post-Tensioning.....	114
6.4.6 Analysis with Post-Tensioning.....	116
6.5 Validation and Comparison of Results.....	118
Chapter 7: Design Example 2: SR 170 Bunkerville Road.....	120
7.1 Introduction.....	120
7.2 Bridge Description.....	120
7.3 Simplified Design Method.....	122
7.3.1 Design Moments and Loads.....	122
7.3.2 Prestress Steel Design.....	125
7.3.3 Panel-to-Girder Connection Design.....	134
7.3.4 Post-Tensioning Design.....	136
7.3.5 Overhang Design.....	138
7.4 Model Based Design Method.....	143
7.4.1 Overview.....	143
7.4.2 Material Definitions.....	143
7.4.3 Geometric and Element Definitions.....	144
7.4.4 Loads and Analysis Assumptions.....	145
7.4.5 Dead and Live Load Analysis and Post-Tensioning.....	146
7.4.6 Analysis with Post-Tensioning.....	148
7.5 Validation and Comparison of Results.....	148
Chapter 8: Summary and Conclusions.....	150
8.1 Project Summary.....	150
8.2 Conclusions.....	151
References.....	153
Appendix A: NCHRP Report 584 DOT Survey.....	156
Appendix B: NDOT Prefabricated Deck Panel Survey.....	159
Appendix C: NDOT Design Specifications.....	177
LIST OF CCEER PUBLICATIONS.....	251

## List of Tables

Table 3.1 Transportation limits placed on full-depth deck panels by states.....	67
Table 6.1 Summary of transverse and longitudinal moments .....	90
Table 6.2 Prestressing steel properties .....	92
Table 6.3 Initial prestressing steel design .....	93
Table 6.4 Elastic shortening losses .....	94
Table 6.5 Prestress losses prior to deck installation.....	96
Table 6.6 Prestress losses at final age of the deck .....	97
Table 6.7 Panel stress checks.....	99
Table 6.8 Panel moment capacity iterations .....	100
Table 6.9 Panel moment capacity and minimum reinforcement limit .....	101
Table 6.10 Panel-to-girder connection design.....	102
Table 6.11 Post-tensioning steel properties .....	103
Table 6.12 Post-tensioning steel calculations .....	104
Table 6.13 Temperature and shrinkage reinforcement.....	104
Table 6.14 Overhang design for section 1-1 .....	110
Table 6.15 Overhang design for section 2-2 .....	110
Table 6.16 Post-tensioning calculations.....	116
Table 7.1 Summary of transverse and longitudinal moments .....	124
Table 7.2 Prestressing steel properties .....	125
Table 7.3 Initial prestressing steel design .....	126
Table 7.4 Elastic shortening losses .....	127
Table 7.5 Prestress losses prior to deck installation.....	129
Table 7.6 Prestress losses at final age of the deck .....	130
Table 7.7 Panel stress checks.....	132
Table 7.8 Panel moment capacity iterations .....	133
Table 7.9 Panel moment capacity and minimum reinforcement limit .....	134
Table 7.10 Panel-to-girder connection design.....	135
Table 7.11 Post-tensioning steel properties .....	137
Table 7.12 Post-tensioning steel calculations .....	137
Table 7.13 Temperature and shrinkage reinforcement.....	138
Table 7.14 Overhang design for section 1-1 .....	141
Table 7.15 Overhang design for section 2-2 .....	142
Table 7.16 Post-tensioning calculations.....	148

## List of Figures

Figure 2.1: Full depth precast concrete deck .....	4
Figure 2.2: Partial depth concrete deck.....	5
Figure 2.3: Cross section of corrugated steel deck.....	5
Figure 2.4: Open grid deck .....	6
Figure 2.5: Half-filled grid deck .....	6
Figure 2.6: Fully filled grid deck .....	7
Figure 2.7: Exodermic bridge deck.....	7
Figure 2.8: Definition of terms for prefabricated deck panels .....	8
Figure 2.9: Skewed profile of bridge with skew $<15^\circ$ .....	11
Figure 2.10: Skewed profile of bridge with skew $>15^\circ$ .....	12
Figure 2.11: Deck-to-steel girder connection.....	13
Figure 2.12: Deck to concrete girder connection .....	14
Figure 2.13: Transverse panel-to-panel connection .....	15
Figure 2.14: Joint spacing for backer rod installation .....	15
Figure 2.15: Longitudinal cast-in-place joint.....	17
Figure 2.16: Typical section of leveling device .....	19
Figure 2.17: Plan view of panel layout .....	20
Figure 2.18: Plan view of skewed panel layout .....	21
Figure 2.19: Prestressed concrete girder-to-deck panel connection.....	21
Figure 2.20: Steel girder-to-deck panel connection .....	22
Figure 2.21: Longitudinal deck panel joint .....	22
Figure 2.22: As-designed and as-built welded tie connection for 800 N overpass on I-15 rapid deck replacement project .....	24
Figure 2.23: UDOT current standard transverse panel connection detail with longitudinal post-tensioning.....	25
Figure 2.24: Plan view for transversely pretensioned system .....	28
Figure 2.25: First transverse connection for transversely pretensioned panel.....	28
Figure 2.26: Second transverse connection for transversely pretensioned panel .....	29
Figure 2.27: Plan view for transverse conventionally reinforced deck .....	30
Figure 2.28: Transverse connection for conventionally reinforced panel .....	30
Figure 2.29: Steel girder-to-deck panel connection .....	31
Figure 2.30: Prestressed concrete girder-to-deck panel connection for transversely pretensioned panels.....	32
Figure 2.31: Prestressed concrete girder-to-deck panel connection for transversely conventionally reinforced panels.....	33
Figure 2.32: Partial depth deck detail .....	34
Figure 2.33: Partial depth deck with prestressed concrete girder.....	35
Figure 2.34: Partial depth deck with steel girder .....	35

Figure 2.35: Girder detail showing grout dam width.....	36
Figure 2.36: Typical panel placement for Texas partial-depth decks.....	37
Figure 2.37: Typical panel placement with overhang and projected girder reinforcement.....	37
Figure 2.38: Typical transverse panel connection for Texas partial-depth decks.....	38
Figure 2.39: Skewed panel layout.....	39
Figure 2.40: Colorado prestressed girder-to-deck section.....	40
Figure 2.41: Colorado steel girder-to-deck section.....	40
Figure 2.42: Colorado transverse panel joint.....	40
Figure 2.43: Utah panel layout.....	41
Figure 2.44: Deck placement of Utah ramp.....	42
Figure 2.45: Deck panel placement of Bill Emerson Memorial Bridge.....	43
Figure 2.46: Panel with reinforcement and shear key.....	44
Figure 3.1: Number of new bridges built with prefabricated deck panels in past 10 years.....	47
Figure 3.2: Number of bridge deck replacement projects using prefabricated deck in past 10 years.....	47
Figure 3.3: Percentage of DOT's with various experience levels using prefabricated deck panels by number of bridges.....	48
Figure 3.4: Implementation of longitudinal reinforcement details.....	49
Figure 3.5: Implementation of transverse reinforcement details.....	49
Figure 3.6: Various panel-to-panel connection details.....	50
Figure 3.7: Number of DOT's implementing various panel-to-panel connection details.....	51
Figure 3.8: Type of use for each panel-to-panel connection detail, counted as number of states selecting each usage rating.....	52
Figure 3.9: Various panel-to-girder connection details.....	53
Figure 3.10: Number of DOT's implementing various deck-to-girder connection details.....	54
Figure 3.11: Type of use for each deck-to-panel connection, counted as number of states selecting each usage rating.....	55
Figure 3.12: Various partial-depth connection details: a-d. panel-to-girder connection detail, and e. panel-to-panel connection detail.....	56
Figure 3.13: Number of DOT's that use each partial depth connection.....	57
Figure 3.14: Type of use for each connection detail, counted as number of states selecting each usage rating.....	58
Figure 3.15: Number of DOT's that use each panel overlay type for full-depth decks.....	59
Figure 3.16: Number of DOT's that use each panel overlay type for partial depth decks.....	59
Figure 3.17: Number of DOT's indicating a frequently observed problem for full-depth deck panels.....	60
Figure 3.18: Evaluation of performance problems for full-depth panels, shown as percentage of states selecting each rating of the problem.....	61
Figure 3.19: Number of DOT's indicating a frequently observed problem for partial depth deck panels.....	62
Figure 3.20: Evaluation of performance problems for partial depth panels, shown as percentage of states selecting each rating of the problem.....	63

Figure 3.21: Full-depth deck panel performance rating .....	64
Figure 3.22: Partial depth deck panel performance rating .....	64
Figure 3.23: Preferred deck panel system .....	65
Figure 3.24: Percentage of states limiting the use of prefabricated deck panels .....	66
Figure 3.25: Percentage of states using site casting of various bridge components .....	68
Figure 3.26: Connection ratings for full-depth panel-to-panel connections .....	71
Figure 3.27: Connection ratings for full-depth panel-to-girder connections .....	72
Figure 3.28: Connection ratings for partial-depth panel-to-girder connections and panel-to-panel connections ...	73
Figure 5.1: Load cases for overhang design.....	83
Figure 6.1: Mesquite Bridge cross-section.....	87
Figure 6.2: Mesquite plan view .....	87
Figure 6.3: Mesquite girder cross-section .....	87
Figure 6.4: Girder prestress steel schedule .....	88
Figure 6.5: Mesquite panel layout.....	88
Figure 6.6: Pocket Layout.....	102
Figure 6.7: Mesquite duct layout .....	104
Figure 6.8: 3-D view of CSiBridge model .....	110
Figure 6.9: Girder properties .....	112
Figure 6.10: Model bridge deck cross-section .....	112
Figure 6.11: Discretization of the deck .....	113
Figure 6.12: Girder prestress steel along girder .....	113
Figure 6.13: Deck stress for refined model subjected to dead load .....	115
Figure 6.14: Deck stress for simplified model subjected to dead load .....	115
Figure 6.15: Moment diagram due to dead load .....	115
Figure 6.16: Stress due to live load .....	116
Figure 6.17: Post-tensioning layout for model based design .....	117
Figure 6.18: Stress in the deck after post-tensioning .....	117
Figure 6.19: Moment due to dead load including post-tensioning.....	118
Figure 7.1: Bunkerville Road Bridge cross-section .....	121
Figure 7.2: Bunkerville Road elevation view .....	121
Figure 7.3: Bunkerville Road girder cross-section.....	122
Figure 7.4: Pocket layout .....	136
Figure 7.5: Bunkerville Road Bridge duct layout .....	137
Figure 7.6: 3-D view of CSiBridge model .....	143
Figure 7.7: Girder properties .....	144
Figure 7.8: Model bridge deck cross-sectio .....	145
Figure 7.9: Discretization of the deck .....	145

Figure 7.10: Deck stress for model subjected to dead load .....	146
Figure 7.11: Moment diagram due to dead load .....	147
Figure 7.12: Stress due to live load .....	147
Figure 7.13: Stress in the deck after post-tensioning .....	148

# **Chapter 1. Introduction**

## **1.1 Motivation and Background**

The development of accelerated bridge construction (ABC) techniques and connection details has become a national research focus. Several states have successfully standardized the ABC approach with high rates of public satisfaction. Precast concrete deck panels are used in ABC to decrease the construction time of installing the deck. Two different types of panels are primarily used. Full-depth panels are designed to span the full-depth of the deck, and therefore comprise the entire deck upon installation. Partial-depth panels are designed to span only part of the deck depth, and upon installation can act as formwork for a cast-in-place (CIP) pour that completes the deck. Both types of panels decrease construction time as formwork for a CIP pour does not need to be installed along the entire length of the bridge.

Compared to other ABC techniques, the technologies for pre-fabricated bridge decks are relatively mature. For instance, full-depth panels have been in use for over 20 years (Culmo, 2011). Partial-depth panels are extensively used in some states; for example, Texas first developed methods for using precast deck panels as formwork in the 1960's and now applies such methods to 85 percent of bridges (Merrill, 2002). Due to aging of the national bridge inventory, many of the bridges in the United States have significant deterioration, often centered on the bridge superstructure. Therefore, concrete deck replacement projects are becoming increasingly common, and can be expedited efficiently with minimal disruption to traffic using ABC.

## **1.2 Objectives and Scope**

The main objective of this project was to develop specifications and design guidelines for the implementation of prefabricated deck panels in Nevada. This goal was accomplished by completing the following objectives:

1. Determining the types and applications of prefabricated deck panels that lead to the best performance
2. Determining which connections should be used for different panel configurations
3. Developing construction procedures for proper deck installation
4. Developing methods to calculate panel capacity that is sufficient to handle all sustained loads
5. Creating modeling procedures and methods for determining correct application of deck panel design

This project used existing standards for prefabricated deck panels as a basis but expanded on the results to customize specifications for Nevada. The current information and practices were used to develop guidelines that meet Nevada's needs. A survey was used to collect the most up-to-date information on performance and details for nationwide use of prefabricated deck panels. Specifications were developed based on the most commonly used details, which were then expanded upon with the experiences of other states as

needed. This information was used to shape the provisions that were recommended for Nevada.

Existing provisions from AASHTO and PCI were used to develop design specifications for the various deck panel components. These provisions were used to develop two design methods that were implemented on example bridges. The first one was a simplified method that incorporated AASHTO and PCI provisions into a design aid spreadsheet to assist in calculations. The second was a model based method that used computer modeling to determine design sufficiency. The design procedures were applied to the Mesquite Interchange and the SR 170 Bunkerville Road Bridge, both existing bridges in Nevada. These bridges were used because they were both designed by NDOT and resemble design cases that are anticipated for Nevada's implementation of prefabricated deck panels. The bridges were modeled using CSiBridge and dead and live load analyses were completed. The results from the design aid spreadsheet were used to determine the connection and reinforcement requirements for full-depth deck panels under standard loads. The computer models were used to determine load and resultant force information, which were used as inputs for the design aid spreadsheet to calculate the capacity of each component. These calculations were used to check the design for all appropriate load cases at each design section.

### **1.3 Organization of Thesis**

This thesis is organized as follows:

Chapter 1 contains a summary of the background information for the project and reviews the objectives and scope of this thesis. Chapter 2 expands on the background information and contains a literature review that summarizes the current design and construction practices for prefabricated deck panels.

Chapter 3 discusses the findings of the prefabricated deck panel survey. The results received from each state DOT are summarized and the findings are discussed and used to establish the project focus. Chapter 4 discusses how the design guidelines were developed using the conclusions formed from the prefabricated deck panel survey. Additional information gathered from the literature review that was added as supplementary commentary is discussed.

Chapter 5 summarizes the design procedure used for the design of the deck panels. Both the simplified (spreadsheet based) method and model based methods are developed. The spreadsheet calculations for the applied loads, amount of prestressing steel, panel-to-girder connection properties, amount of post-tensioning steel, and overhang reinforcement designs procedures are explained. The methodology behind the model based method is also discussed.

Chapter 6 describes the application of both design methods to the Mesquite Interchange Bridge, which is a skewed bridge. The findings from the design procedure are used to determine the applicability of each design method for skewed bridges. The process is repeated in Chapter 7 for the Bunkerville Road Bridge, a three span bridge. The results from this bridge are used to determine the applicability of each design method for multispan bridges.

Chapter 8 summarizes the project findings and the conclusions. The recommended design procedure based on each design example is discussed as well as the limitations for each design method. The final design recommendations are based on combinations of the design guidelines and the findings from the design examples.

## Chapter 2. Literature Review

### 2.1 Introduction

This chapter contains a literature review detailing the uses and applications of prefabricated deck panels. This literature review will discuss various precast panel systems, development of standard connection details and construction methods, state specific guidelines and practices, and representative and innovative bridge projects.

### 2.2 Overview of Prefabricated Deck Systems

#### 2.2.1 Full Depth Deck Panel Systems

Full depth precast concrete decks are prefabricated deck panels that are installed without needing forms. The main advantage to using full depth decks is the decrease in construction or closure time for the deck installation (Sullivan, 2007). Full-depth precast panels are normally produced in a controlled plant environment, which leads to higher quality of the concrete and therefore better performance of the panels (PCI, 2011b). Generally, full depth decks are designed as one-way slabs between the supporting beams and girders and use either mild reinforcement or post-tensioning (Culmo, 2011). Typically, panels span the width of the bridge and extend 8 to 12 ft in the direction of traffic. Bridges that are wider than 50 ft are normally designed so the panels span half the width of the bridge. Full-depth precast panels have pockets or block-outs that are used to connect the deck panels to the girders. The deck is connected to the girder by placing shear connectors in the pockets and filling the pockets with grout. This connection forces the deck to act compositely with the girders. An example of a full-depth precast deck with pockets is shown in Figure 2.1. Full-depth precast decks are typically more expensive in material and construction costs than a conventional cast-in-place deck but the extra cost is often offset by decreased construction time and less required maintenance. (PCI, 2011b).



Figure 2.1: Full depth precast concrete deck (Culmo, 2011)

### 2.2.2 Partial Depth Deck Panel Systems

Partial depth precast concrete decks are a cross between full depth decks and stay in place forms in that a panel is used as a form for concrete but a cast-in-place pour is still required. Partial depth decks are normally 3.5 to 4" thick, 8 ft long and are designed to span between the girders in interior bays. The panels are placed directly on top of the girders or on top of a sealant or backer rod barrier (Figure 2.2). The panels are used to support the cast concrete in the same way as a stay-in-place form, and the remaining deck is cast in place over and around the precast panels (Culmo, 2011).



Figure 2.2: Partial depth concrete deck (Culmo, 2011)

### 2.2.3 Corrugated Steel Decks

Corrugated steel deck forms are an alternative to partial depth concrete decks. The steel decks run in the same direction as the girders and are placed to span between girders. CONTECH makes three different sizes of corrugated steel decks: 6"x2", 9"x3", and 12"x4-1/4". These range in thickness from 12 gauge steel to 3/8" steel. Figure 2.3 shows a cross section of a CONTECH corrugated steel deck (CONTECH, 2012). They are similar to partial depth concrete decks in that the deck panels are installed, the reinforcement is placed, and the concrete is poured to complete the deck. These steel decks remain on the bridge for the life of the project (Culmo, 2011).

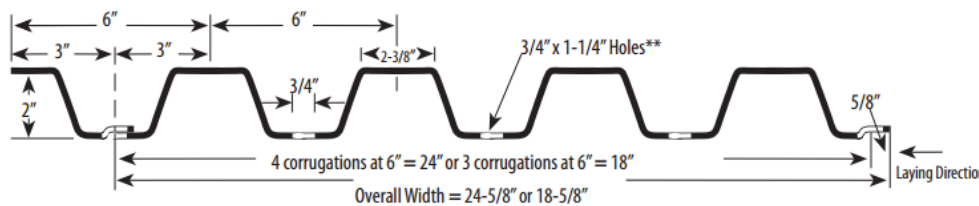


Figure 2.3: Cross section of corrugated steel deck (CONTECH, 2012)

### 2.2.4 Steel Grids

In steel grid deck systems, a steel grid and filler concrete are prefabricated together. Steel grid options include open grid, partially or fully filled grid, and exodermic decks. The partially or fully filled grid and exodermic decks use concrete, while the open grid contains no concrete and uses steel as the riding surface. The open grid has main bars that span both directions and either diagonal or intermediate cross bars in between the main bars. The spacing between the main bars ranges from 2" to 8". This system is the lightest

of the steel grid options. Figure 2.4 shows a steel open grid with diagonal intermediate bars. Partially and fully filled grid decks are steel grids with concrete poured within part or all of the steel portion of the assembly, respectively. These decks are installed in one piece and completed with a CIP pour on the grid to produce the final surface. Figure 2.5 shows a half-filled grid deck and Figure 2.6 shows a fully-filled grid deck. An exodermic deck uses the same concept as a partially filled grid except the top concrete layer is a reinforced deck that is cast on top of the steel section prior to placement of the panel (Culmo, 2011). Figure 2.7 shows sections of an exodermic deck.

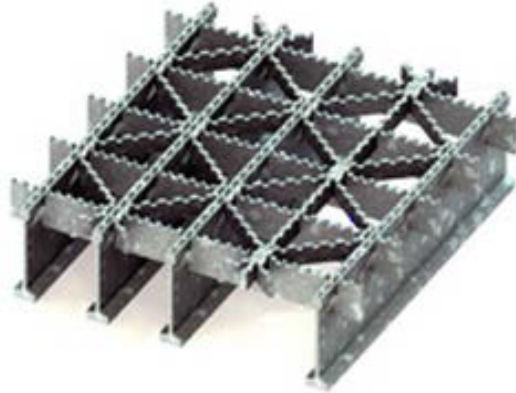


Figure 2.4: Open grid deck (BGFMA, 2015)

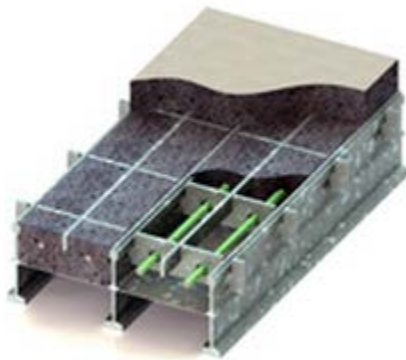


Figure 2.5: Half-filled grid deck (BGFMA, 2015)

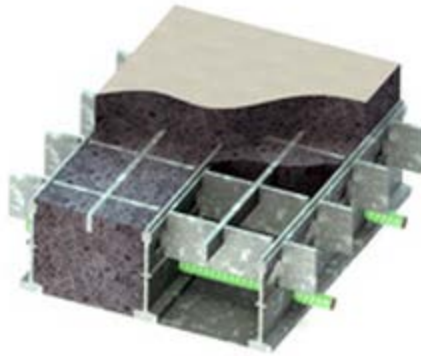


Figure 2.6: Fully filled grid deck (BGFMA, 2015)

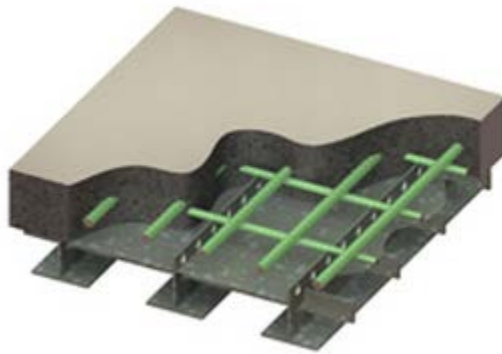


Figure 2.7: Exodermic bridge deck (BGFMA, 2015)

### 2.3 Terminology

Figure 2.8 shows a bridge with panels and joints labeled, and is used to define terminology used to describe prefabricated deck panels. The longitudinal direction refers to the direction of traffic flow, which is from top to bottom in Figure 2.8, while the transverse direction is normal to traffic flow. Label “a” denotes a precast panel. Line “b” designates the longitudinal joint of the deck and line “c” designates the transverse joint. Labels “e” and “f” designate the floor beams and the longitudinal girders, respectively.

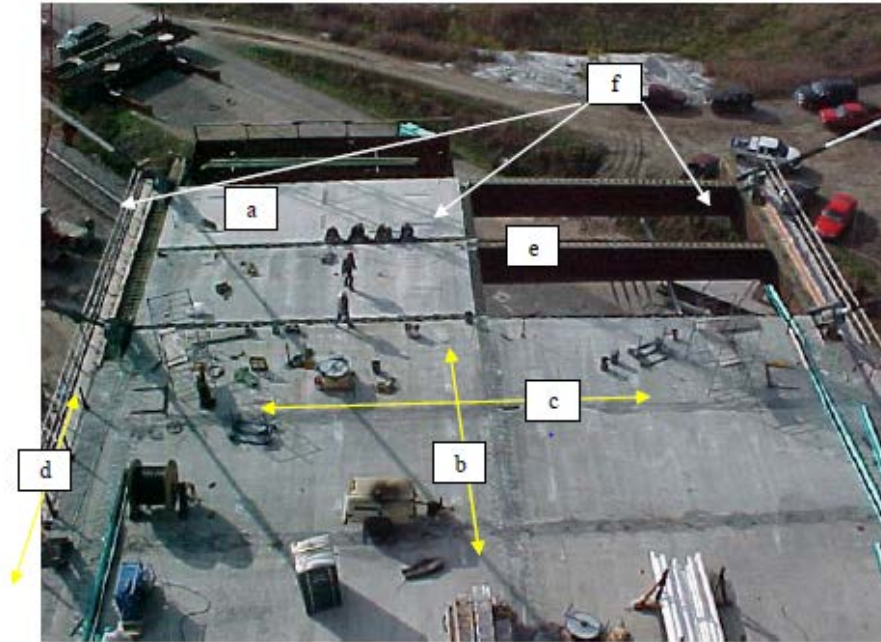


Figure A.2.4.6-2 Top view of the new Bill Emerson Memorial Bridge

(a) Typical Precast Panel, (b) CIP Longitudinal Joint, (c) Transverse CIP Joint, (d) Short CIP Cantilever, (e) Typical Floor Beam, and (f) Longitudinal Girders

Figure 2.8: Definition of terms for prefabricated deck panels (Badie and Tadros, 2008)

## 2.4 NCHRP 12-65 Project

### 2.4.1 Project Overview

The NCHRP 12-65 project was conducted to develop, test, and make design recommendations for full-depth precast panel systems with no overlays and no longitudinal post-tensioning (Badie and Tadros, 2008). Both measures were intended to speed the construction or deck replacement process and cost by eliminating field work. During this project, the researchers conducted a comprehensive literature review on bridges incorporating full-depth, precast panel systems and a national survey to document available specifications and policies developed by highway authorities experienced with precast panel systems. The main goal of the project was to develop guidelines and LRFD specifications for design fabrication and construction of full-depth, precast-concrete bridge deck panel systems without the use of post-tensioning or overlays and to develop connection details for new deck panel systems. Information was collected on all full depth deck projects, but emphasis was placed on projects that did not use longitudinal post-tensioning.

A 14 question survey was distributed to all state and Canadian provincial DOT's, members of the PCI Bridge Committee, and members of the TRB A2C03 Concrete Bridges Committee; totaling 110 requests. Respondents were asked whether full depth precast deck panels had been used within the past 10 years, and if so to evaluate their experience with the panels. Survey respondents that indicated no recent use of full-depth deck panels were asked if there were any reasons why they had not been used. Information was requested on project size, reinforcement and connection type, overlay

type, and the grouting method used for connections. An evaluation of the panel systems was requested based on the experience of each respondent. The respondent was also asked if guidelines on full-depth precast concrete panels systems had been developed by their organization, and if so a copy was requested. The original survey questions are included in Appendix A. 32 responses were received, of which 10 reported application of a full depth precast deck panel system in the prior 10 years.

#### **2.4.2 Survey Results**

In the survey, 22 of 32 total respondents reported not using full-depth precast deck panels. The 22 states/provinces were the following: Alberta, Arizona, California, Florida, Hawaii, Kansas, Massachusetts, Maryland, Minnesota, Mississippi, North Carolina, North Dakota, New Jersey, New Mexico, Nevada, Ohio, Ontario, Oregon Tennessee, Washington, Wisconsin, and Wyoming all indicated they had not used full-depth prefabricated deck panels but would be interested in the findings of the survey. Reasons for not using full-depth precast deck panels included: cost, questions about construction issues, lack of specifications or guidelines, long-term durability questions, riding surface concerns, and concerns about joint issues. Each DOT indicated they were interested in the results of the survey and requested to be informed of the findings.

9 states and 1 province responded that full depth precast deck panel systems had been used in the past 10 years. The respondents were: Alaska, California, Colorado, Illinois, Kentucky, New Brunswick, New York, Texas, Utah, and Virginia. All of the state DOTs reported using full depth deck panels that were constructed to act compositely with the girder for every bridge project except one. All but one respondent rated the overall performance of the deck panels to be good, and the remaining rated the performance as excellent. Of the states that responded, Alaska, Illinois, New York, Texas, Utah, and Virginia reported that guidelines and specifications for design, fabrication or construction of full depth precast concrete panel systems had been developed.

Alaska used full depth panels on two bridges within the prior 10 years of the study, but had constructed about 20 total bridges using the panels in the prior 20 years. Neither of the two most recent bridges used post-tensioning in the longitudinal direction or had an overlay. Both bridges used a female-to-female shear key for the panel connections and shear pockets with connectors to make the deck composite with the steel girders. Inspections to date indicated that the joints and deck were performing satisfactorily and were in very good condition.

Colorado used full depth panels for a deck replacement and widening project on an arch bridge. The deck was supported by cross piers, which were supported by vertical posts that extended to the arch. The panel design included eight total panels with a thick asphalt overlay applied on the panels. This bridge was post-tensioned in the longitudinal direction. A CIP concrete side barrier was connected to the deck using a shear connector. The transverse joint was created by extending conventional reinforcement and placing a CIP closure pour between the panels.

Illinois completed a full depth project, where the deck panels were made composite with the 6 steel girders by using shear pockets and shear connectors. Conventional

reinforcement was used in both directions and post-tensioning was applied in the longitudinal direction. Barriers were connected to each side panel by threading bolts through the panel into nuts seated within the barriers.

Kentucky completed one project that used full depth deck panels. The bridge was conventionally reinforced with no post-tensioning. A unique feature about this bridge was that shear connectors between the deck and girders were only applied at exterior girder locations. This eliminated the need for shear pockets. The sides of the exterior panels had a female shear key that allowed a CIP parapet to be installed.

New York used full depth panels on a deck replacement project for a large interstate bridge with a 32 degree skew. The bridge had 9 spans and six steel open box girders and was constructed in three sections. Each section was constructed and post-tensioned separately so that the bridge could be kept in service. Because of the high skew a CIP pour was made at each abutment.

The report included project details from Missouri, Nebraska, New Hampshire, Texas, Utah, Virginia, Wisconsin, and Ontario. These bridges mentioned above are representative of the projects described in the report.

### **2.4.3 Findings from NCHRP 12-65 Project**

Many of the example bridges discussed within the report had similar specifications. Almost all bridges developed composite action between the deck and the girders through shear connectors. Some of the bridges took advantage of the deck configuration and connected the deck to the girders along the outside perimeter of the deck panels so that shear pockets were not needed in the deck. This allowed the deck panels and the girder to be connected with one CIP pour. Every bridge used a female-to-female connection for the panel-to-panel connection. Many of the bridges used leveling screws during construction to allow the decks to be centered upon placement.

The results of the survey were compiled to list common practices for prefabricated full-depth deck panels and incorporated into a design guide (Badie and Tadros, 2008). Suggestions for modifications to the AASHTO LRFD code were also developed (Badie and Tadros, 2008). The connection details developed as part of the research from this project are discussed in Section 2.5.4.

## **2.5 Current Practice, Standards and Specifications for Full Depth Deck Panels**

### **2.5.1 General Guidelines**

The PCI NE chapter is one organization that has taken the lead on developing specifications and recommendation for use of full-depth deck panels. Two documents have been developed: (1) “Full Depth Deck Panels Guidelines for Accelerated Bridge Deck Replacement or Construction” (PCI, 2011a) provides general guidelines and specifications, and (2) “State-of-the-Art Report on Full-Depth Precast Concrete Bridge Deck Panels” (PCI, 2011b) is a more extensive reference with background information and commentary. These two documents serve as general guidelines for the use of full-

depth deck panels, and are the primary sources for the general information presented in this section.

Full depth precast concrete deck panels are normally made of high strength ( $f'_c > 6$  ksi), high quality concrete as they originate from a precast concrete plant. Typically, the panels are prestressed in the transverse direction during the fabrication process. PCI recommends that the deck panel width in the longitudinal direction be specified in increments of 2 ft, with a maximum of 12 ft to facilitate shipping (PCI, 2011b). A common method for assembling full depth panels is to post-tension the entire deck once all of the panels are in place during construction. To accommodate the post-tensioning, 2" diameter post-tensioning ducts are commonly included in deck panels. The post-tensioning ducts are normally placed in the center of the cross-section of the panel with no eccentricity to prevent deflection in the panels prior to placement (PCI, 2011a). Bridges with curved geometry or skew can still accommodate prefabricated full depth deck panels. If the bridge has a curved profile, the decks can be fabricated with curved ducts to incorporate post-tensioning. PCI has developed separate recommendations for bridges with both large and small skew. If the bridge is skewed less than 15 degrees, the panels are recommended to be designed as trapezoids to match the bridge profile. A typical layout for a skewed full depth deck is shown in Figure 2.9. If the skew is greater than 15 degrees, the panels are recommended to be set straight but the panels on both sides have to be trimmed down to meet the abutment. A typical layout for a full depth deck with skew greater than 15 degrees is shown in Figure 2.10.

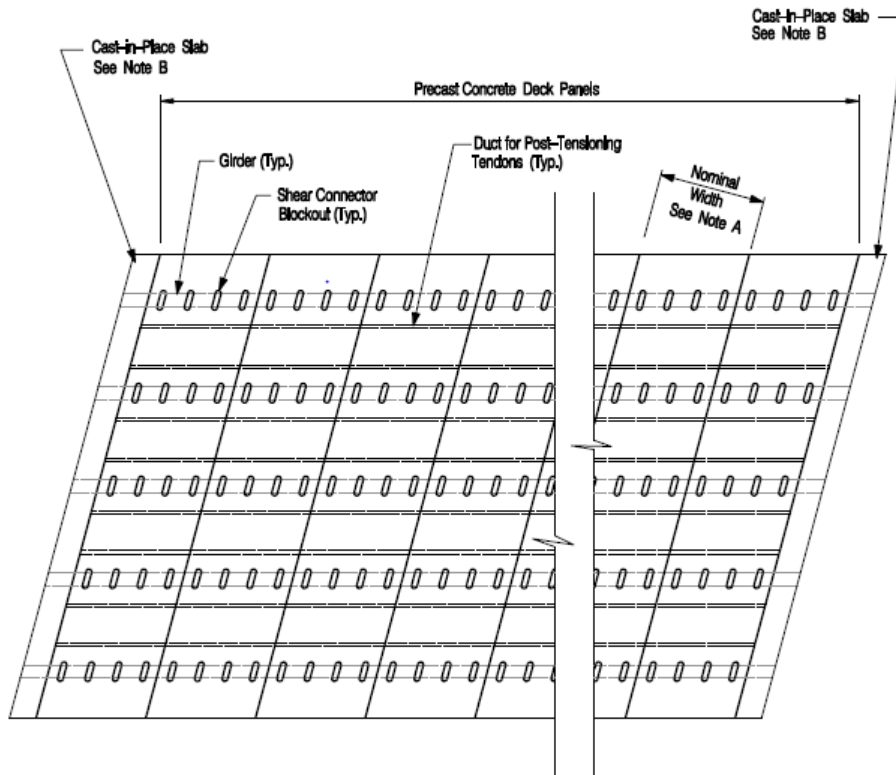


Figure 2.9: Skewed profile of bridge with skew <math>< 15^\circ</math> (PCI, 2011a)

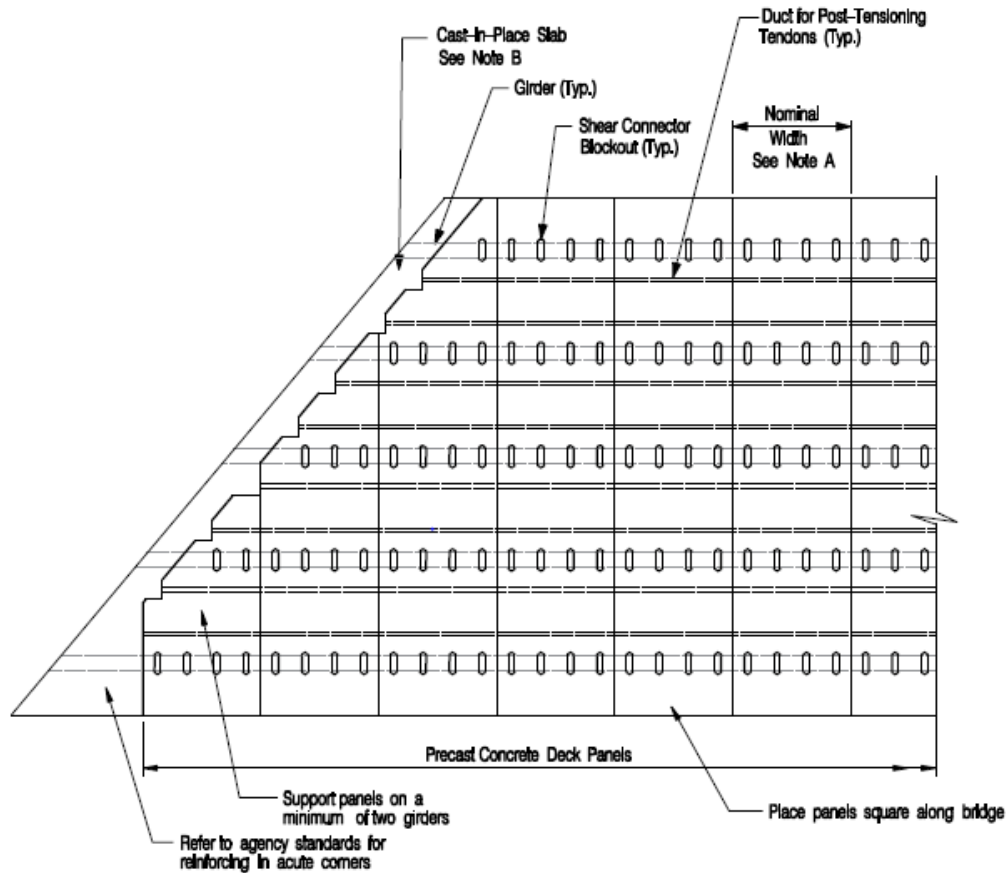


Figure 2.10: Skewed profile of bridge with skew  $>15^\circ$  (PCI, 2011a)

### 2.5.1.1 Deck-to-Girder Connection Details

A deck that is composite with the girder is considered an essential component for a precast deck system to work. Without the composite action, joint leakage occurs commonly (Badie and Tadros, 2008). Section 3.11 of PCI (2011a) titled Composite Deck Design recommends that deck panels should be made composite with the supporting members. Composite action can be achieved by placing steel shear studs or channels into prefabricated pockets, welding the studs/channels to the girder, and filling the pocket with grout as shown in Figure 2.11 (Badie and Tadros, 2008). Non-shrink, flowable, moderate strength (5 ksi), and low permeability grout should be used for the shear connector pockets (PCI, 2011a). Shear pockets should be spaced 2 ft on center when possible to attain full composite action. However research has shown that spacing of up to 4 ft may be used to attain full composite action (Badie and Tadros, 2008). Studs should be spaced a minimum of 2.5" from the edge of the shear pocket, and welded at least 1.5" away from the edge of the girder (PCI, 2011b).

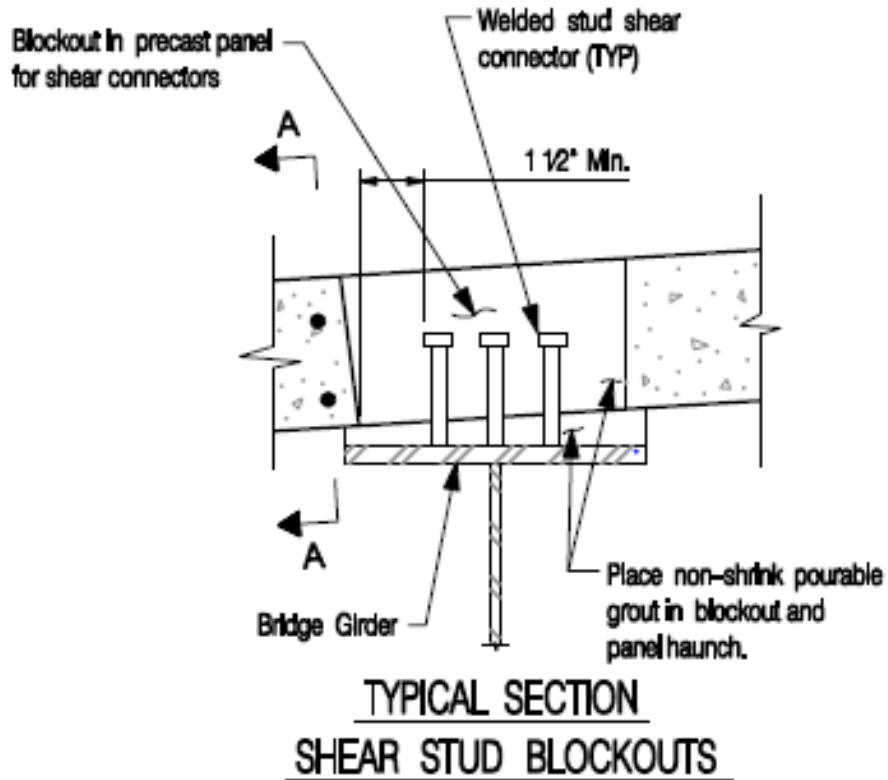
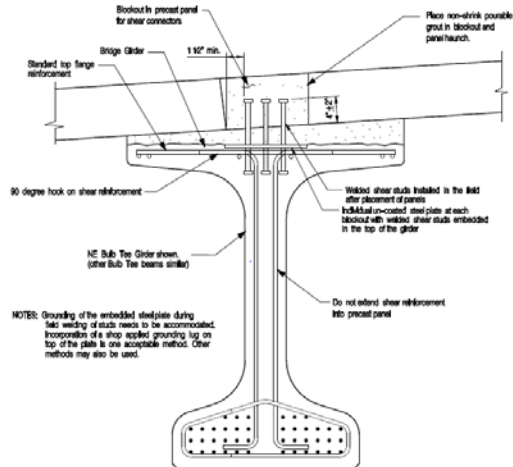


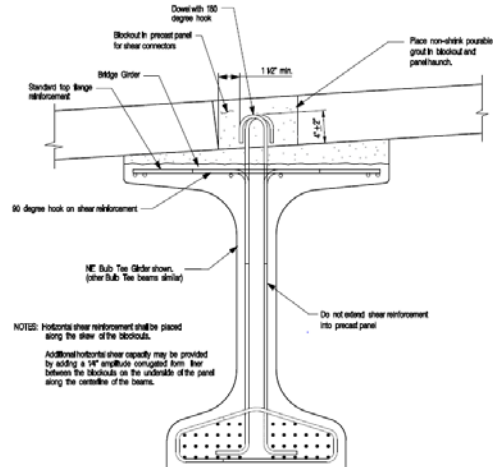
Figure 2.11: Deck-to-steel girder connection (PCI, 2011a)

For a steel girder, the studs or channels are welded to the top flange of the girder as shown in Figure 2.11. For a concrete girder, studs welded to a steel plate or hooked reinforcing steel from the top of concrete girders form the shear connectors (Figure 2.12). The deck panel-to-girder connection can also be designed similarly to the steel girder connection by casting a plate in the top of the girder and welding the studs in place (PCI, 2011a). In the case of hooked reinforcing steel, the reinforcement is extended out of the top of the girder and hooked a full 180 degrees in the pocket (Figure 2.12). Since the steel is embedded in the girder and grout is used in the same way as the system with shear studs, composite action is achieved.



TYPICAL SECTION - BULB TEE BEAMS

NEW CONSTRUCTION WITH WELDED STUD CONNECTION



TYPICAL SECTION - BULB TEE BEAMS

NEW CONSTRUCTION WITH PROJECTING REINFORCING CONNECTION

Figure 2.12: Deck to concrete girder connection (PCI, 2011a)

### 2.5.1.2 Transverse Panel-to-Panel Connection Details

Two main types of connections are used for the transverse panel to panel connection: shear keys and shear keys with post-tensioning. The transverse connection must transfer two primary forces: the vertical shear force and the bending moment resulting from the loads applied to the bridge (PCI, 2011b). The shear key connection used most often is a grouted female to female joint. The shear is transferred by the interaction between the grout and panel. The surface of the shear key should be roughened by using sand or water blasting to achieve the maximum interaction between the panel and the grout. A wood form must be installed under the panel to contain the grout during installation but may be removed after curing is complete (Badie and Tadros, 2008). A closed cell polyethylene foam backer rod can also be used to contain the grout as shown in Figure 2.13. The backer rod should be secured firmly at the bottom of the joint. Figure 2.14 shows the appropriate spacing for the joint and backer rod as well as the results of installation errors.

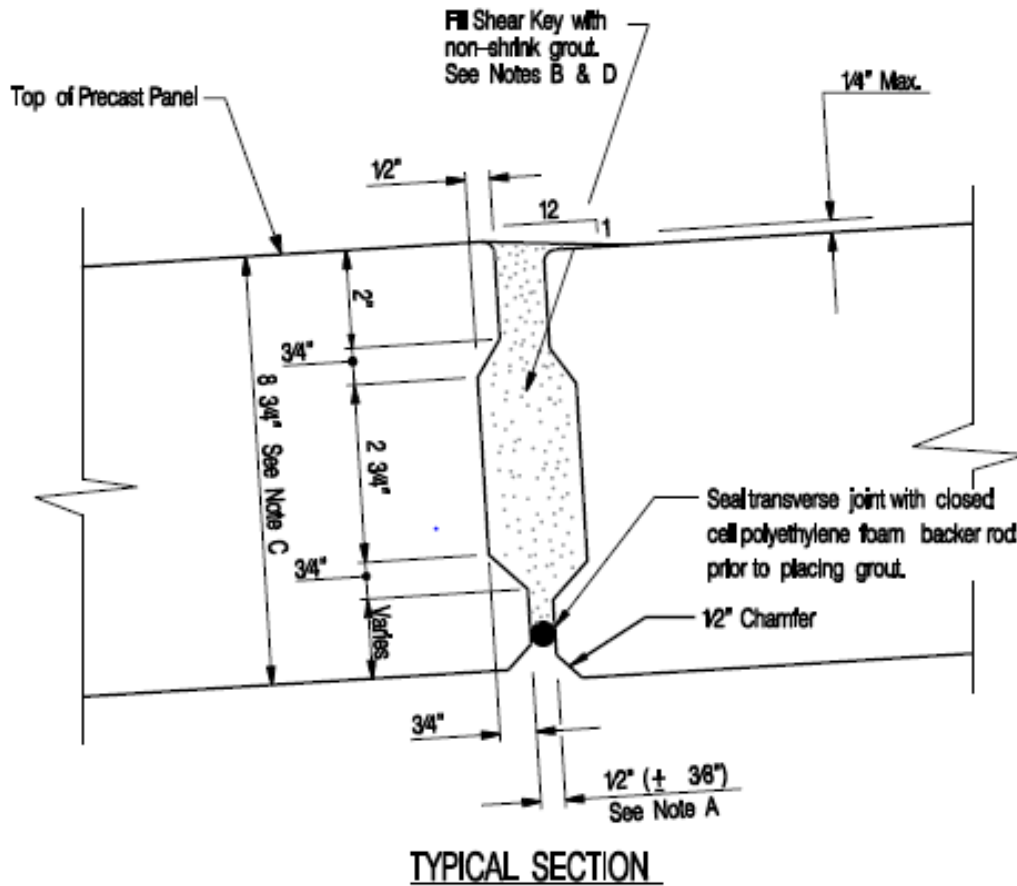


Figure 2.13: Transverse panel-to-panel connection (PCI, 2011a)

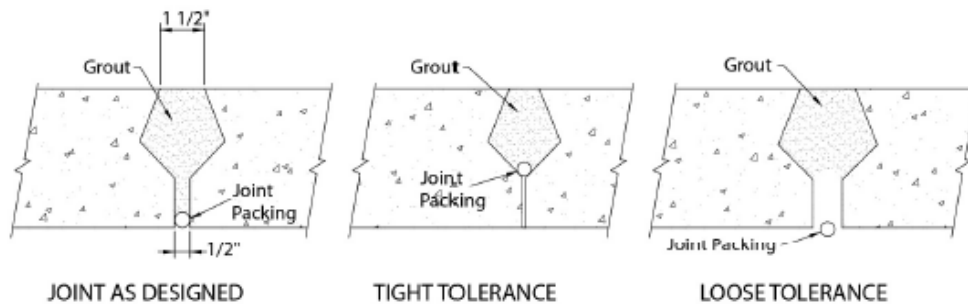


Figure 2.14: Joint spacing for backer rod installation (PCI, 2011b)

If post-tensioning is used, the shear key detailing is similar but ducts are incorporated into the deck panels to allow post-tensioning strands to be installed after the deck is placed (Sullivan, 2007). Applying post-tensioning is widely recognized as the most reliable way to prevent leakage (Badie and Tadros, 2008). Utah experimented with conventional reinforcement and post-tensioning, and concluded that longitudinal post-tensioning is necessary in all situations. Utah observed no leakage in post-tensioned joints even in negative moment regions of the bridge, while bridges constructed with welded tie connections (no post-tensioning) had some connection leakage but still performed adequately structurally (Culmo, 2013). Further details about Utah's experience

are provided in Section 2.5.3. Alaska does not use post-tensioning, but relies on the interaction between the shear key and grout for each panel (Badie and Tadros, 2008).

Some states have experimented with ultra-high performance concrete (UHPC) in panel-to-panel connection joints because of the greater resistance UHPC offers against cracking and leakage. By using UHPC in combination with conventional reinforcement, joint lengths can be made smaller than connections that use normal grout and post-tensioning can be eliminated. Elimination of post-tensioning makes fabrication simpler. An FHWA researcher found that UHPC could be used as a direct substitute for traditional joint concrete and grout and the deck would perform as well as or better than a CIP deck (Graybeal, 2010). The most widely available UHPC mix in the United States is a proprietary product sold by a multinational construction materials supplier (Graybeal, 2011).

Male to female joints have been attempted before, but they are difficult to implement because of the tolerances required for installation. Because the tolerances are often not met, leakage has been a problem for many bridges that have used this method (Badie and Tadros, 2008).

### **2.5.1.3 Longitudinal Panel-to-Panel Connection Details**

Many smaller bridges use only one panel in the transverse direction, which eliminates the need for a longitudinal joint. On larger bridges that have a longitudinal joint, the longitudinal connection detailing between panels is similar to the transverse connection details. A female-to-female joint is the most commonly used longitudinal panel-to-panel connection type. Prestressing can be used in the transverse direction to help prevent leakage but is less common. For instance, Utah does not use prestressing in the transverse direction.

An alternate to female-to-female grouted connection is available for bridges with two panels spanned transversely over the width of the bridge where both panels overlap with a center girder. In this case, a CIP concrete pour is used instead of grout and shear pockets. The shear studs used for composite action are connected to the girder, the panels are placed, and a high early concrete pour is applied. The CIP pour creates the longitudinal joint and interaction is still maintained because of the female joints on each panel. Several states have used this technique and Figure 2.15 shows an example of this type of longitudinal joint applied to a bridge in Missouri. This method is advantageous because it consolidates the panel-to-panel and panel-to-girder connections into one, eliminating the time and expense associated with manufacturing the panels with pockets. However, to use this approach the panels must be sized to span between the girders (Badie and Tadros, 2008).



Figure 2.15: Longitudinal cast-in-place joint (Badie and Tadros, 2008)

#### 2.5.1.4 Production and Construction Guidelines

PCI recommends that the panels are designed so that the long side is oriented in the transverse direction of the bridge (PCI, 2011b). The panel framing should be designed with a slope to allow the bridge to drain, and a crown can be incorporated by casting a closure pour. Design parameters such as allowable concrete stresses, transverse flexure, post-tensioning, and the panel overhang dimensions should meet the specifications in the AASHTO LRFD Bridge Design Specifications (AASHTO, 2014). Expected losses in the post-tensioning should be accounted for in the design process. Losses that should be factored into the prestress force are elastic shortening, anchorage set, and friction. Creep and shrinkage do not need to be included; small losses in the post-tensioning are considered acceptable since the applied post-tensioning is usually higher than what is required (PCI, 2011b). The panel transportation plan should be specified in the shop drawings.

Several quality control items should be checked during the production of full-depth panels. The following is a list of items from PCI (2011b):

- Location and alignment of post-tensioning ducts
- Deck thickness to satisfy cover requirements
- Positioning and rigidity of the transverse shear key
- Uniformity of the surface finish
- Influence of shrinkage, creep, and camber on the final alignment
- Location of attachments for traffic barrier service
- Location and coordination of the shear pocket positioning with respect to the existing or proposed girder alignment
- Accurate location of lifting hardware for handling of the deck panels
- Conflicts between reinforcement, ducts, anchorages, and local reinforcement around pockets as well as the main transverse and longitudinal reinforcement.

Clearances, dimensions, and tolerances must be addressed in the development of shop drawings and the setup of formwork, and then routinely verified in the pre-pour and post-pour inspection phase of production. Concrete should not be deposited in the forms until the engineer and/or the QA/QC inspector has inspected and approved the placements of ducts, anchorages and all other materials in the panels and marked as approved on each item.

Shear studs can be included on the girders prior to installation. For steel girders, it may be easier to weld the studs onto the girders after the panels are in place. Structural angles may be used to hold panels in place during installation. The angles act as a type of form for the panels and allow the proper elevations to be achieved. However, either structural angles or leveling bolts can be used during installation to keep the panels level. For full-depth decks that incorporate a crown, the crown can be created by screeding the panels down to the desired thickness or creating an internal hinge in the center of the panel that allows the panel to rotate under its own weight. The transverse joints are prepared by installing the backer rod and grinding the panel edges down to create a smooth transition from panel-to-panel. Once the panels are in place, grout should be applied to the panel connections (PCI, 2011b). The construction guidelines state that post-tensioning should be applied after the transverse joints have been grouted, but before forming the composite connection with the girder to prevent inducing any undesirable stresses in the girders.

In summary, a general sequence of construction for full depth panels is outlined below (PCI, 2011a). The construction sequence should be included on the plans.

1. Clean surfaces of shear keys.
2. Preset leveling bolts to anticipated height.
3. Place all precast deck panels on girders in a span.
4. Adjust leveling devices on deck panels to bring panels to grade. (Figure 2.16)
5. All leveling bolts shall be torqued to approximately the same value (20 percent maximum deviation).
6. Install longitudinal post-tensioning strand (un-tensioned) in ducts and seal joints in ducts between deck panels.
7. Place a flowable non-shrink grout in all transverse joints. The grout shall be rodded or vibrated to ensure all voids are filled.
8. After the grout in the transverse joints has attained a strength of 1000 psi (based on grout manufacturers' recommendations), the longitudinal post-tensioning strands may be stressed. The contractor shall determine the jacking force required to achieve the minimum final post-tensioning force shown on the plans accounting for all losses.
9. Grout post-tensioning ducts.
10. Install shear connectors in all blockouts.
11. Form haunches between the top of the girders and the bottom of the deck panels.
12. Grout all haunches and shear connector blockouts with a flowable non-shrink grout.
13. Cast end closure pours.
14. Cast parapets and/or sidewalks.
15. Place overlay (if required) and open bridge.

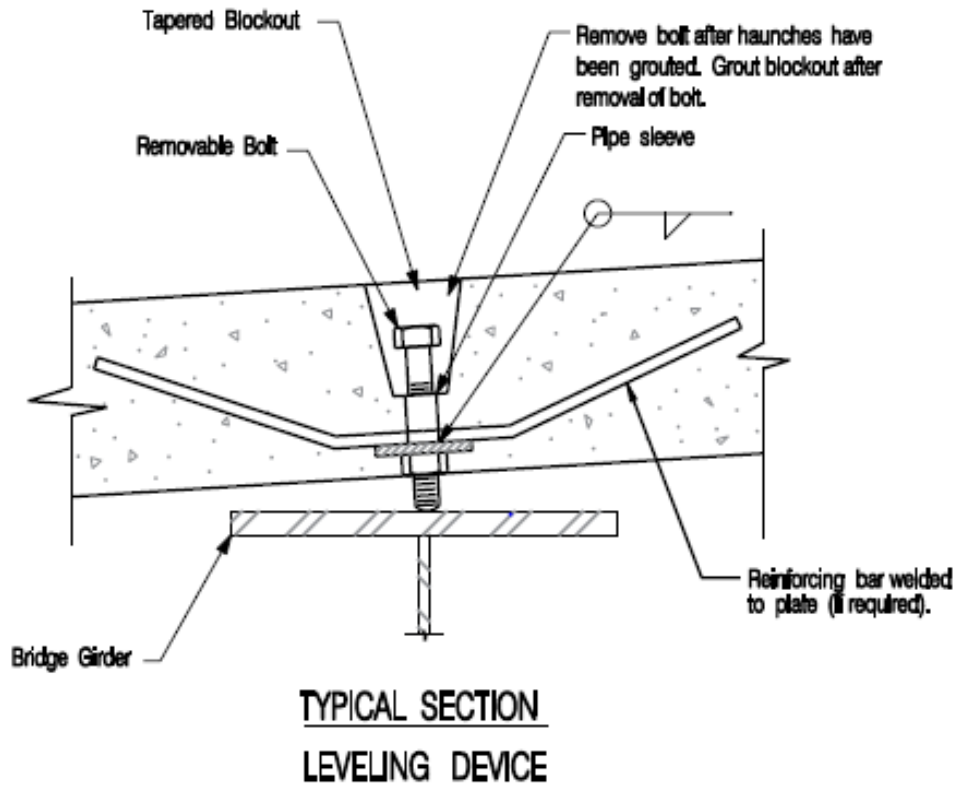


Figure 2.16: Typical section of leveling device (PCI, 2011b)

### 2.5.2 Oregon DOT Specifications and Construction Guidelines

Oregon DOT (ODOT) responded to the NCHRP 12-65 survey that full-depth prefabricated decks had not been used, but they would be interested in the findings of the survey (Badie and Tadros, 2008). In 2011, ODOT developed standards and specifications for full-depth prefabricated deck panels. The information presented next is based on a webinar presented by Bruce Johnson, a State Bridge Engineer with ODOT, for the Florida International University ABC series that outlined ODOT's process in creating guidelines for full-depth prefabricated deck panels (Johnson, 2011).

ODOT aimed to design a concrete mix for prefabricated deck panels that would be abrasion and chemical resistant. Silica fume and slag were used for chloride and wear resistance. The developed concrete mix included 8 ksi concrete, 7% silica fume, 15% slag and a 0.3 water/cement ratio. The standards specified that the panels should be steam cured, use a curing compound, and preferably be fabricated in a PCI certified plant. Because the panels were created with a concrete mix that emphasized chemical and wear resistance, ODOT opted not to use an overlay and rather let the panels take the wear and weathering directly. If the concrete in the panels was shown to inadequately resist corrosion, an overlay could be used.

ODOT evaluated the potential options for each connection type before specifying a selection. For the transverse reinforcement, ODOT considered pre-tensioning the panels or alternatively using mild steel reinforcement. Pre-tensioning was observed to remove

tensile cracks and take advantage of the increased durability of the concrete; as well as making the panels more resistant to damage from lifting and transporting the panels. The longitudinal reinforcement was reviewed similarly by comparing a post-tensioning approach with traditional mild steel reinforcement. ODOT has been a proponent of UHPC, and decided that mild steel longitudinal reinforcement lap spliced within narrow joints and filled with UHPC were the best option for the transverse connection. By using UHPC, post-tensioning work was not needed, which would speed up construction time.

ODOT specified a panel thickness of 8.5” to account for 0.5” of sacrificial topping and an 8” structural component for the deck. The width and length of the deck is controlled by the transportation limits of the fabricator. However, ODOT limited the panel width to 10 ft and the length to 50 ft. ODOT used a lifecycle cost analysis to determine the feasibility of using full-depth deck panels in Oregon. The initial cost of using full-depth deck panels was determined to be higher than a CIP deck, but because of the decreased maintenance costs the panels would be cheaper over the life of the bridge.

ODOT’s completed specifications included a plan set for panel layouts and connections. The panel layout is shown in Figure 2.17, with a maximum panel width of 50 ft and pocket spacing of 2 ft in the longitudinal direction. The longitudinal steel is extended in both directions and connected with a lap splice along the transverse joint. Figure 2.18 shows a plan view of a skewed panel. Figures 2.19 and 2.20 show the girder to deck panel connection for a prestressed concrete girder and steel girder, respectively. The prestressed concrete girder uses steel stirrups for composite action while the steel girder uses welded steel studs. Figure 2.21 shows the longitudinal joint with UHPC and spanning reinforcement.

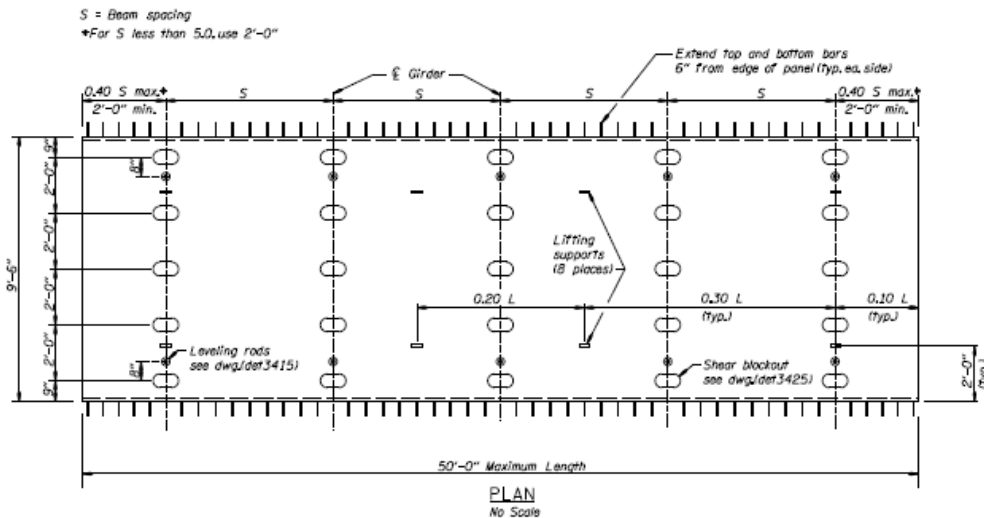


Figure 2.17: Plan view of panel layout (ODOT, 2015)

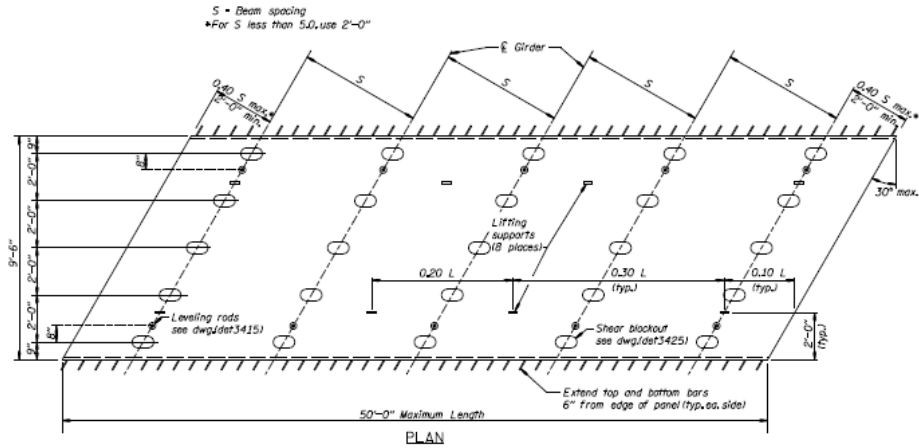


Figure 2.18: Plan view of skewed panel layout (ODOT, 2015)

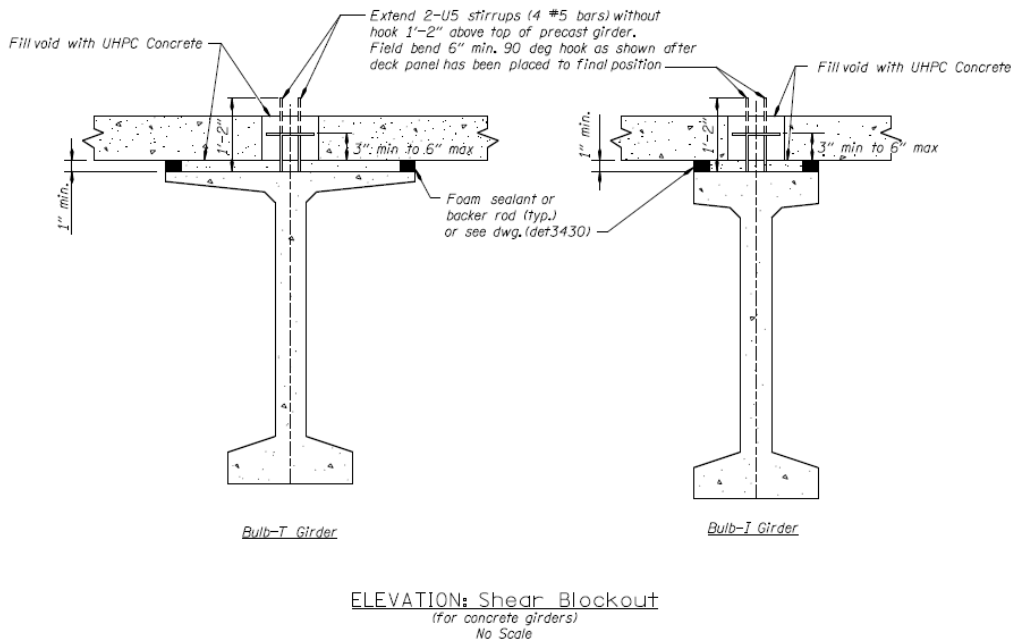
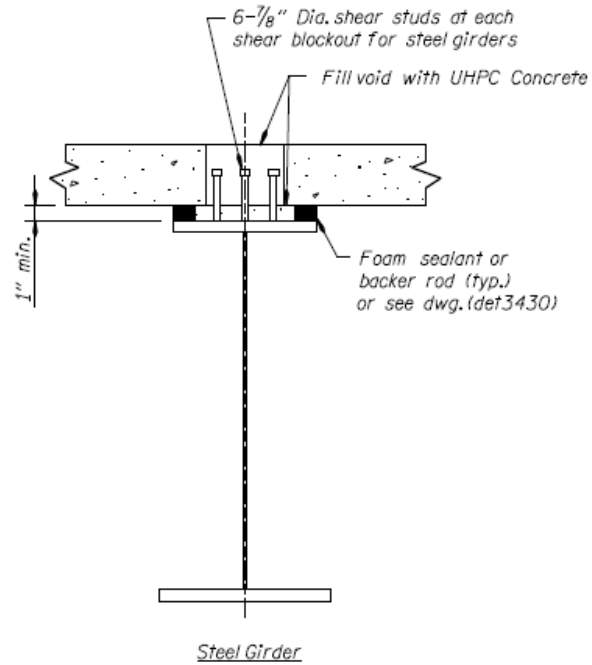
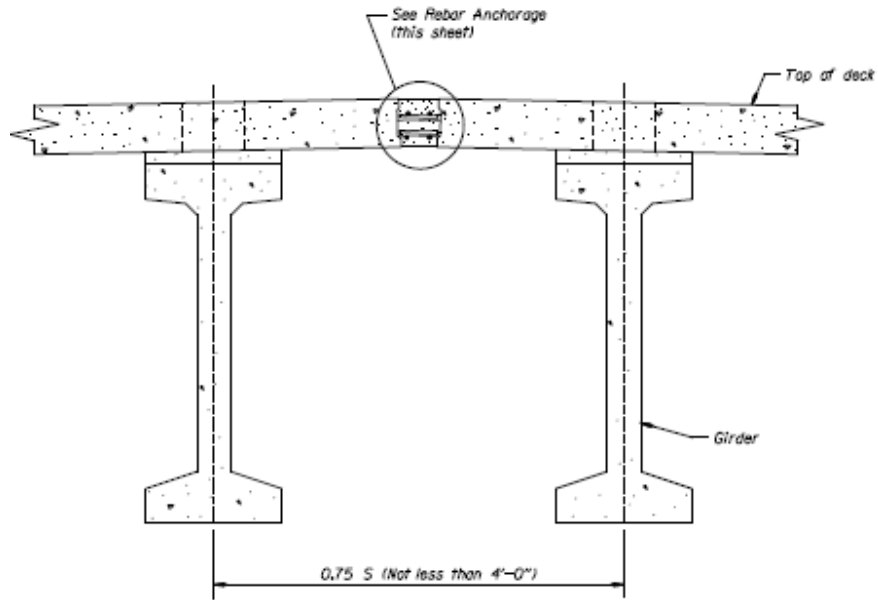


Figure 2.19: Prestressed concrete girder-to-deck panel connection (ODOT, 2015)



ELEVATION: Shear Blockout  
 (for steel girders)  
 No Scale

Figure 2.20: Steel girder-to-deck panel connection (ODOT, 2015)



LONGITUDINAL JOINT WITHOUT STAGE CONSTRUCTION  
 No Scale

Figure 2.21: Longitudinal deck panel joint (ODOT, 2015)

### **2.5.3 Utah DOT Specifications and Lessons Learned**

Utah has been a leader in the development of ABC methods. UDOT contracted with CME Associates to develop standards for ABC that were first completed in 2009 (Culmo, 2013). The current standards are integrated into UDOT's Structures Design and Detailing Manual (UDOT, 2015a) and various specification sheets and design drawings (UDOT, 2015b) that are publicly available on UDOT's website. Currently, Utah's policy is to evaluate ABC for all projects, and select ABC when an overall cost benefit is expected, where both direct construction costs and indirect costs such as user delays are considered. UDOT uses a standard rating procedure and decision flowchart to determine if an ABC approach is required. Standard procedures include both offline approaches, where the complete bridge is constructed offsite and moved into place, and online approaches, where prefabricated bridge elements are rapidly assembled onsite (UDOT, 2015b). Guidelines on the construction and placement of prefabricated full-depth deck panels apply generally to the online construction approach, and have been developed in this context.

UDOT's very early experiences with ABC consisted of several rapid deck replacement projects. As a result, critical assessments of process and structural details were performed for several of these projects and assembled in "Lessons Learned" reports (e.g. URS, 2004; Deloy Dye, 2005; Ackerman, 2007). The first project was to replace the decks on a skewed steel plate girder bridge originally constructed in 1967, located remotely on I-80 in Summit County (URS, 2004). The report described the construction process in detail. The contractor Ralph L. Wadsworth was required to obtain a Prefabricator License, which took six months and cost several thousand dollars. During the project, the contractor encountered numerous problems with the concrete mix used to construct the panels and the non-shrink grout used to construct the shear stud pockets and to fill the pocket joints onsite. In addition, significant differences between the design and as-built (based on survey) bridge measurements were detected, and lateral distortion of the top girder flanges occurring after deck removal made placement of the prefabricated panels very difficult. Despite the many difficulties, the project was completed in 6.5 days of full closure of the local bridge and partial closures of I-80.

A 4-span steel curved girder bridge over I-15 at 800 N in Salt Lake City, originally built in 1965, necessitated a rapid deck displacement due to a sudden blowout in span 1 (Ackerman, 2007). UDOT had planned to use traditional CIP decks, but opted for experimental use of prefabricated panels because the incremental cost increase (less than 30% threshold) was considered reasonable, traffic impacts could be significantly reduced, and transportation costs would be minimal as the bridge was located very close to Granite Construction's fabrication yard. Granite Construction, who was the pre-selected contractor due to funding considerations, was also required by UDOT to obtain pre-cast certification at a cost of \$20,000. Post-project evaluation suggested this expense could be avoided by adding a site-casting specification that addresses such details as shop drawing submittals, leveling pad, and match casting requirement. Nonetheless, to date UDOT has not indicated any current use or experimentation with site-casting.

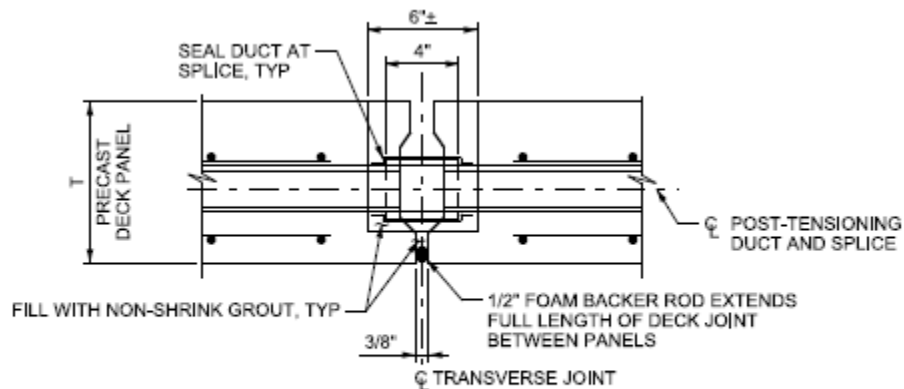
The original structure was designed with chorded girders, while the deck and parapets followed the bridge alignment (Ackerman, 2007). To simplify design and construction,



performance based on Culmo (2013) is restricted to bridges constructed using online approaches.

Eight of the bridges inspected incorporated a welded tie plate/gouted shear key detail without post-tensioning, similar to that shown in Figure 2.22, for the transverse panel-to-panel connection. The performance of this connection detail has been poor. Specific issues include widespread leakage through the joints, especially in the negative moment region; and the inability of the joint to transfer moment across the panels. Leakage is more problematic on bridges with polymer overlays compared to those with asphalt. As an extreme case, significant joint deterioration has occurred on Bridge C-325, such that the pavement on the top of the deck has popped out and exposed several of the connections. CME estimates the remaining life of this type of connection to be 15 years from when the leakage evidence is first observed. Joint performance may be influenced by quality of the grout, which also applies to panel-to-girder connections (see below). Repair of the joints through epoxy injection of grout may be possible, but is expected to be difficult, time consuming and costly. As a result of the poor performance, this connection detail has been retired, and does not reflect UDOT's current standards.

Ten of the bridges inspected incorporated a grouted shear key detail with post-tensioning for the transverse panel-to-panel connection. This detail has performed well to date, and reflects UDOT's current standard (Fig. 2.23). A few bridges have isolated areas of leakage, effluorescence, and rust staining near the deck ends; however, such problems are not accelerating quickly and CME estimates that the joints should last through the life of the deck (up to 75 years). Most of these bridges included a CIP concrete closure pour. Shrinkage of the closure pour concrete has led to some cracking and joint leakage; CME estimates that this problem can be reduced by relaxing the existing concrete specification as the high early strength requirements tends to lead to more shrinkage issues with the concrete.



### **SECTION B-B**

Figure 2.23: UDOT current standard transverse panel connection detail with longitudinal post-tensioning (UDOT, 2015b)

One of the bridges inspected incorporated the standard transverse connection detail without longitudinal post-tensioning that was developed as a result of the NCHRP 12-65 project (Badie and Tadros, 2008). The detail, which incorporates a reinforcing bar grouted into steel pockets that are cast into the deck, is discussed further in Section 2.5.4. The bridge was first inspected in 2011 almost immediately after construction, and no problems were detected. However, in the 2013 inspection unexpected deterioration of the transverse connection joint was detected. CME estimates that the joint will last 20-30 years, which is less optimistic than NCHRP findings. However, the NCHRP conclusions appeared to be based on simple span bridges with only positive moments, and therefore CME recommends that the connection detail be avoided in negative moment regions. Furthermore, the detail was found to be costly relative to the standard with longitudinal post-tensioning, and thus likely will not be further pursued.

Nineteen of the bridges inspected incorporated full-depth pockets through the panels to form the girder-to-panel shear connections. The pockets are filled with grout. This detail is used with both steel girder and concrete girders. The performance of these connections has been mixed; some of the bridges show signs of minor leakage through the pockets. CME estimates that the primary cause of the leakage is due to shrinkage of grout in the pockets, and recommends that the grout specifications should be modified to include a prequalification procedure and different grouts should be evaluated against a performance standard. The issues are relatively minor and the shear connectors are expected to last 40-75 years.

Most of the inspected bridges incorporated a 3/8" polymer overlay without a waterproofing membrane. Many of the overlays were observed to have cracks at the deck expansion joints or at the transverse deck panel joints. CME estimates that lack of a waterproofing system allows salts and chlorides to seep through the cracks and exacerbate the leakage problems that are observed in the deck joints. In addition, delamination of the overlays was observed in some bridges. CME estimates that this overlay system will need major maintenance or replacement every 10-15 years, and has recommended that UDOT replace the existing polymer overlay with a waterproofing membrane on the bare concrete deck, covered by a 3" thick bituminous wearing surface (asphalt layer). Instead, UDOT updated the standard in early 2014 to require the polymer overlay provider to provide 5 year warranty against material and installation defects (UDOT, 2014).

In addition to details already mentioned, the following guidelines related to precast decks are provided in UDOT's Structures Design and Detailing Manual (UDOT, 2015a). Precast deck elements are designed using the strip method based on Articles 9.7.3 and 4.6.2.1, and Table A4-1 in the Appendix to Section 4 of the AASHTO *LRFD Specifications* (AASHTO, 2014). The design table also specifies the concrete deck reinforcing. Skew is considered in the detailing of deck reinforcing for skew angles greater than 20 degrees, which is slightly more conservative than the LRFD recommendations of 25 degrees. General size guidelines restrict the panel maximum width (including projecting reinforcement) to 14 ft. The minimum panel thickness is 8 3/4".

The connection between panels is generally provided by post-tensioning. The post-tensioning system should be designed to provide at least 0.25 ksi across the joint after all losses. The losses associated with panel creep can be ignored because the deck-girder interaction tends to restrain the creep. Use of lap splices with a closure pour or other alternative details providing reinforcing across the joint are also permitted.

Deck haunches are used to account for construction variations, tolerance, and beam camber. The haunch can vary along the length of the girder due to flange thickness variation, camber variation, and roadway profile. The minimum haunch thickness is 1 3/4" for full-depth precast deck panels.

The designer is to provide a placing sequence for full-depth panels, and a construction sequence for all activities including connecting the panels to each other and the girder. Transverse construction joints are to be placed parallel to any skew, and avoid the girder field splice locations. Longitudinal construction joints are to be avoided unless dictated by exceptional circumstances, e.g. deck width exceeding 120 ft. Longitudinal construction joints should not be located under a wheel line. Closure pours are not required but can be useful in phased construction projects. Closure pours should be a minimum width of 3 ft, and lap splices of the transverse reinforcing should be located within the closure pour.

#### **2.5.4 NCHRP 584 Connection Designs**

The results and findings of NCHRP 12-65 were used to assemble optimal designs for full-depth prefabricated deck panels. The main goal of the research was to develop and validate a system that did not require longitudinal post-tensioning or an overlay. Two different panel systems were developed through the research; a transversely pretensioned system and a transversely conventionally reinforced system.

The transversely pretensioned system used an 8 ft long panel that spanned the entire width of the bridge with a structural thickness of 8". The transverse prestressing was applied through eight 1/2" diameter strands that are distributed in two layers. No. 6 bars at 13.3" spacing were used in the longitudinal direction. Figure 2.24 shows the plan view of the panel design.

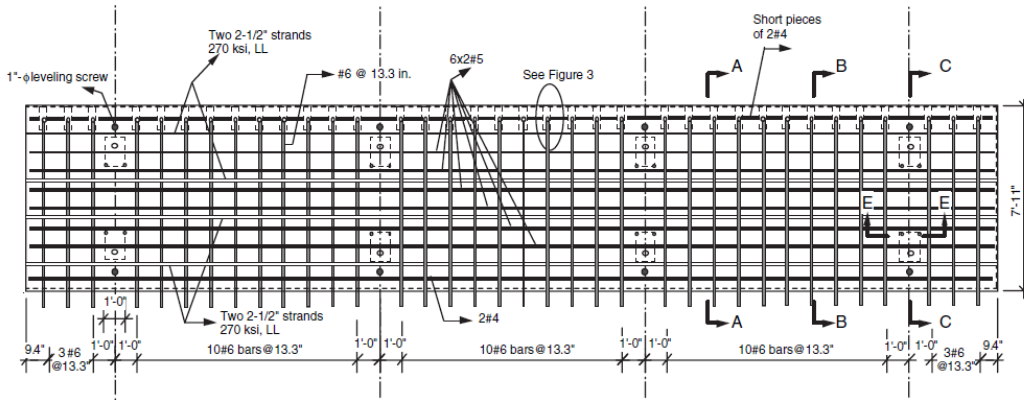


Figure 2.24: Plan view for transversely pretensioned system (Badie and Tadros, 2008)

Two alternative details were proposed as viable options to splice the longitudinal reinforcement across the transverse connection for use with the transversely pretensioned panel system. The first transverse connection consisted of placing an HSS section in one side of the panel and embedding the reinforcement within the section. Reinforcement from the adjacent panel is extended into the HSS section when the panels are placed during construction and the HSS is filled with grout. Figure 2.25 shows different views of the first transverse connection. The second transverse connection used an extra reinforcing bar that was dropped into the connection through a slot in the top of the panel and then covered in grout. Figure 2.26 shows this connection.

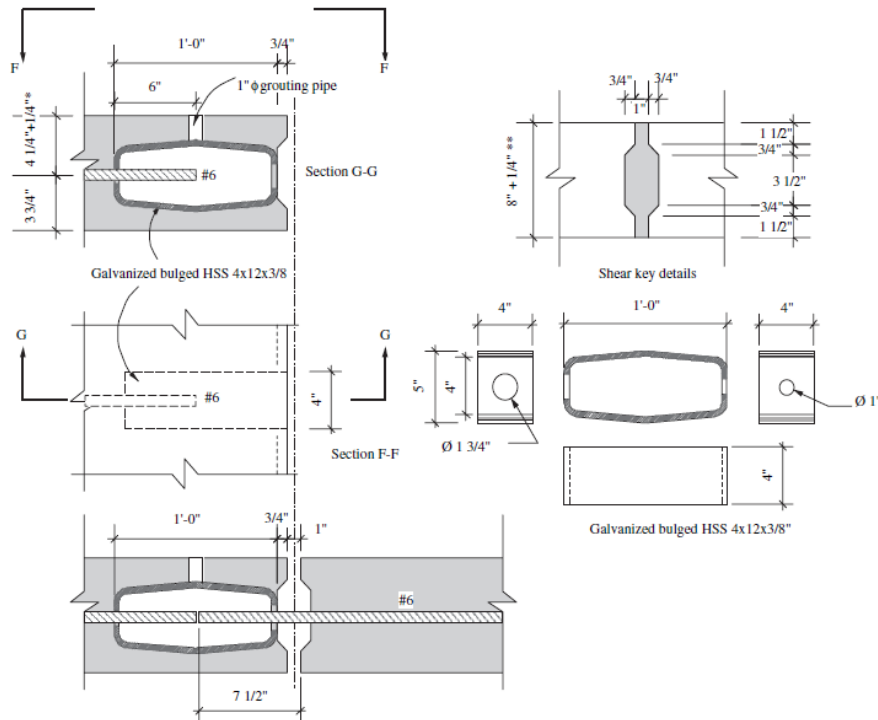


Figure 2.25: First transverse connection for transversely pretensioned panel (Badie and Tadros, 2008)

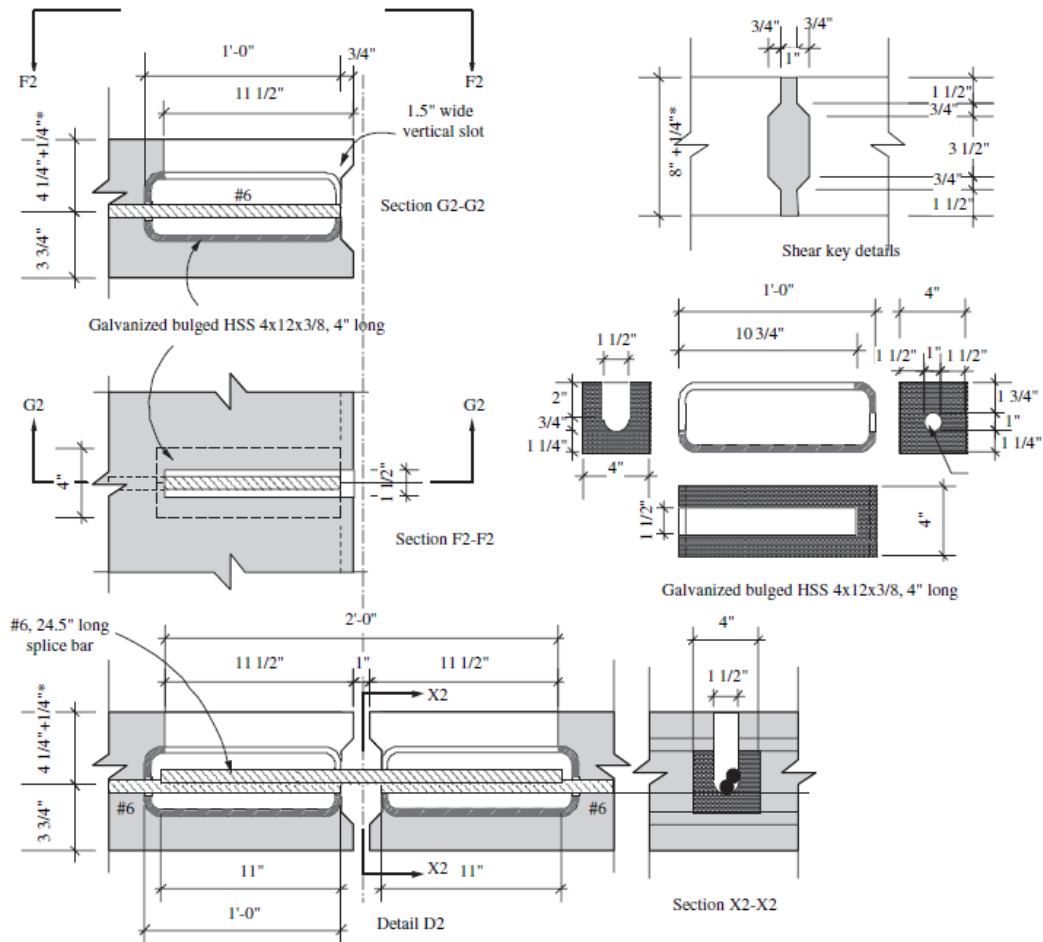


Figure 2.26: Second transverse connection for transversely pretensioned panel (Badie and Tadros, 2008)

The transversely conventionally reinforced panel is also 8" thick. The panel uses three layers of reinforcement; a top and bottom layer in the transverse direction and a longitudinal layer. No. 6 bars spaced at 18 inches are used for both the top and bottom transverse layer. The longitudinal reinforcement is 1 No. 8 bar with threaded ends. The longitudinal reinforcement is spliced using HSS tubes. The plan view of the panel is shown in Figure 2.27 and the transverse connection is shown in Figure 2.28.

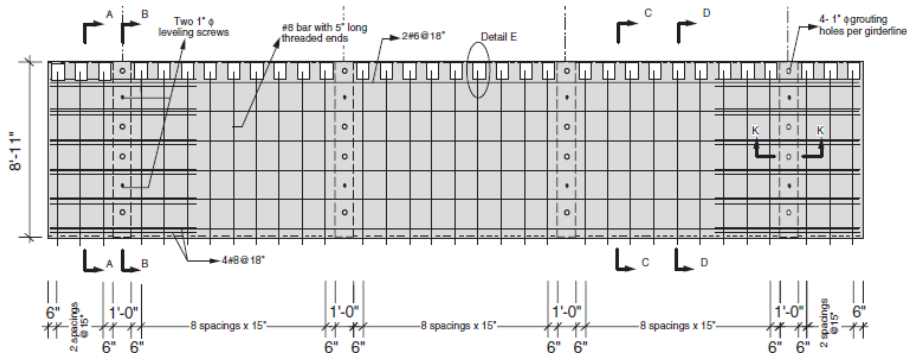


Figure 2.27: Plan view for transverse conventionally reinforced deck (Badie and Tadros, 2008)

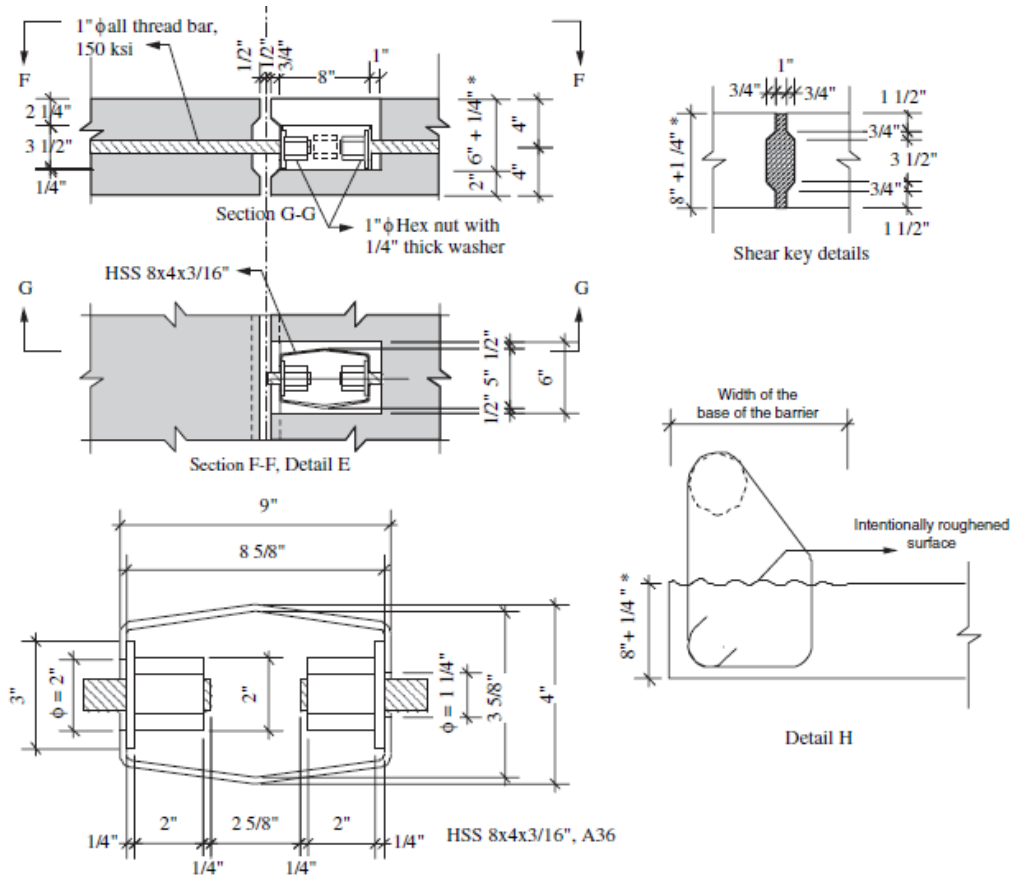


Figure 33. CD-2, Details E and H (\*1/4 in. is used as a sacrificial layer for texturing).

Figure 2.28: Transverse connection for conventionally reinforced panel (Badie and Tadros, 2008)

For steel girders, both the pretensioned and conventionally reinforced panel configurations used the same girder-to-deck panel connection (Figure 2.29). The connections were spaced 48" apart and used eight 1 1/4" studs for each pocket. For concrete girders, the girder-to-deck panel connection differed for the two panel

configurations. The transversely prestressed panel used a stud configuration with clusters of three 1 1/4" studs spaced 48" apart (Figure 2.30). Studs were used for this connection to minimize the pocket size required to accommodate the connection. The conventionally reinforced panel configuration used projected shear reinforcement from the girder for the connection (Figure 2.31).

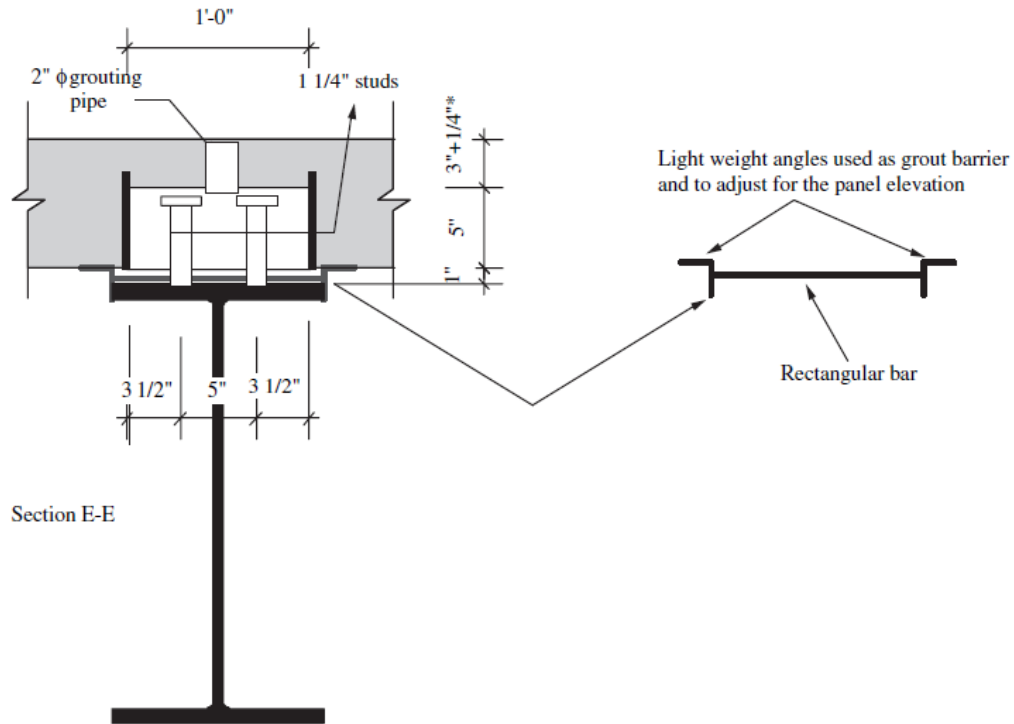


Figure 2.29: Steel girder-to-deck panel connection (Badie and Tadros, 2008)

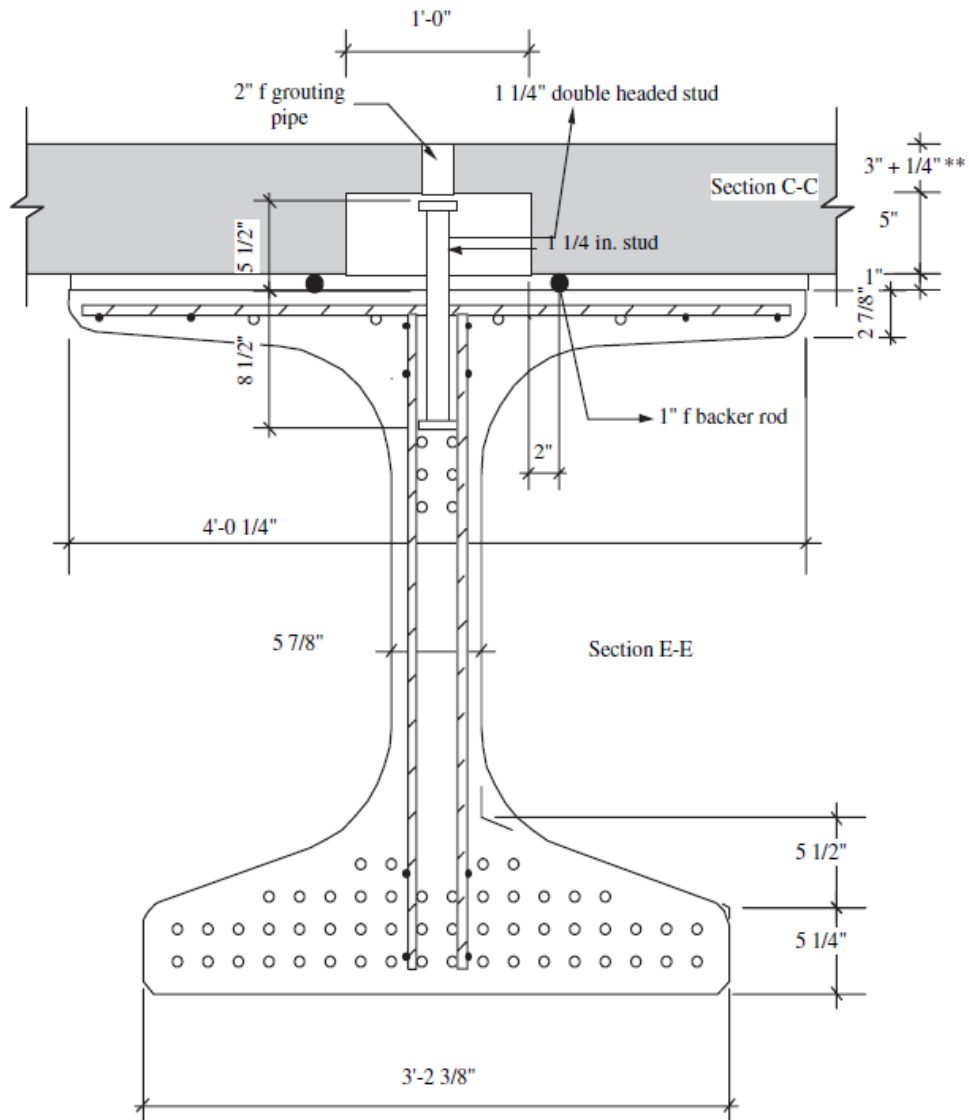


Figure 2.30: Prestressed concrete girder-to-deck panel connection for transversely pretensioned panels (Badie and Tadros, 2008)

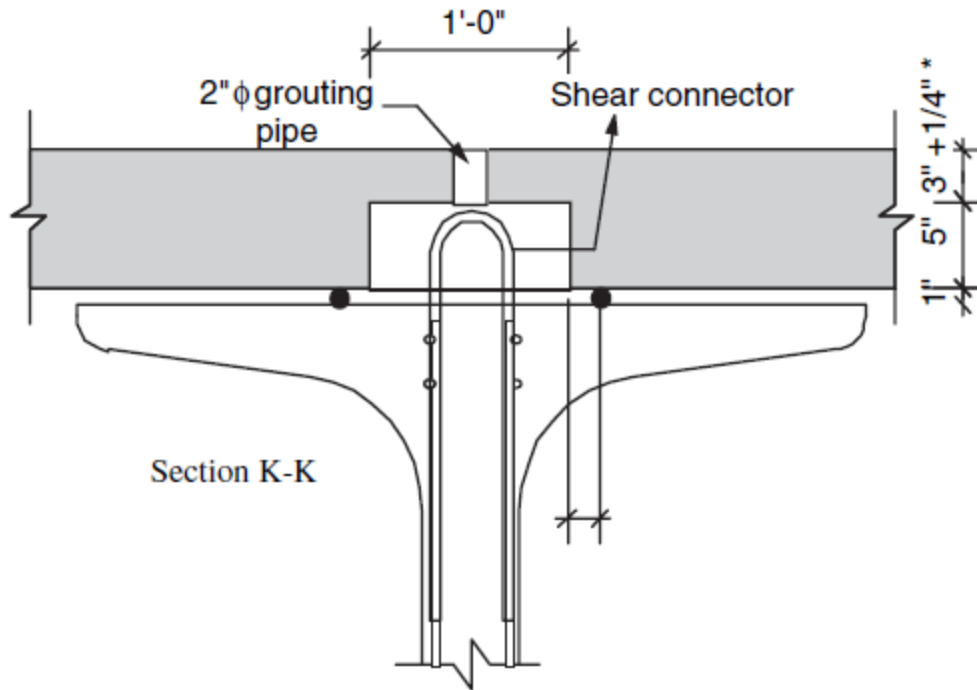


Figure 2.31: Prestressed concrete girder-to-deck panel connection for transversely conventionally reinforced panels (Badie and Tadros, 2008)

## 2.6 Current Practice, Standards and Specifications for Partial Depth Deck Panels

### 2.6.1 General Fabrication and Construction Procedures

Two different fabrication processes are used for partial depth precast panels, and both are considered viable (Hieber and Wacker, 2005). The first method is to place spacers between the panels in the casting bed, and cut the prestressing strands after the concrete has cured. This allows the panels to be separated at the completion of the cure time. The second method is to cast one large panel and to cut out individual panels once the concrete is cured. According to the PCI Precast Deck Panel Guidelines (PCI, 2001), partial depth panels should be at least 3.5" thick and use 6000 psi 28 day strength concrete. Once the panels are in place the CIP portion of the deck should be at least 4.5" thick. Prestressing strands, if incorporated, should be 3/8" diameter and located at least 4" away from the outside of the panels (PCI, 2001).

During construction, partial depth panels should be handled as little as possible to prevent cracking or warping. Panels developing cracks that span across more than one prestressing strand or expanding beyond 1/3 of the total length of the panel should not be used on the bridge. To install the panels, temporary supports are placed on the girders and leveling screws are used to adjust the panels to the correct elevation. Once the temporary supports are constructed, the panels can be placed and grouted to the girders to prevent movement. After the panels are grouted to the girder, the leveling screws used for the panels should be removed. The deck reinforcement can then be placed and the final CIP deck poured and allowed to set.

PCI (2001) specifies standard drawings for panel placement and installation. Figure 2.32 shows a plan view of the deck and specifies general dimensions. Figure 2.33 illustrates the prestressed concrete girder to deck connection. This connection is similar to the full-depth connection shown in Figure 2.12 except the partial depth connection is made composite with a CIP pour while the full-depth connection uses grout. Figure 2.34 illustrates the steel girder to deck connection. This connection is similar to the full-depth connection shown in Figure 2.11. Figure 2.35 shows how the grout dam should be designed.

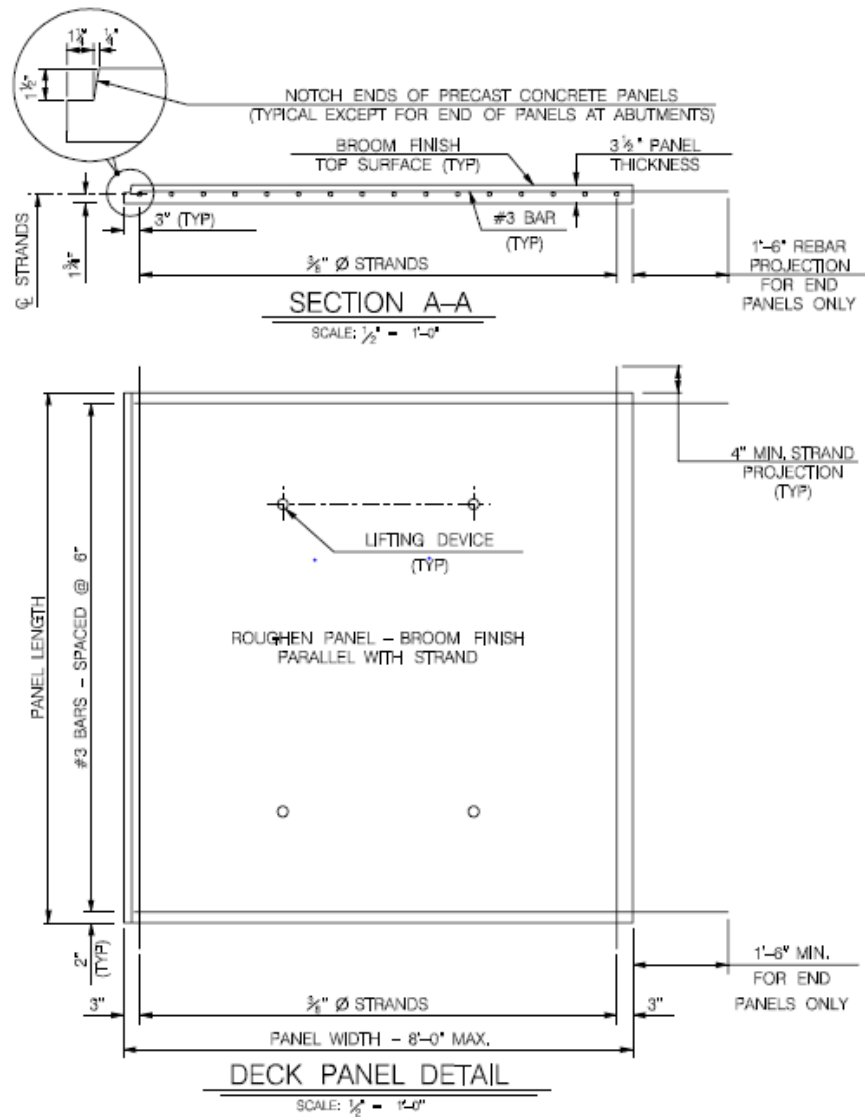


Figure 2.32: Partial depth deck detail (PCI, 2001)

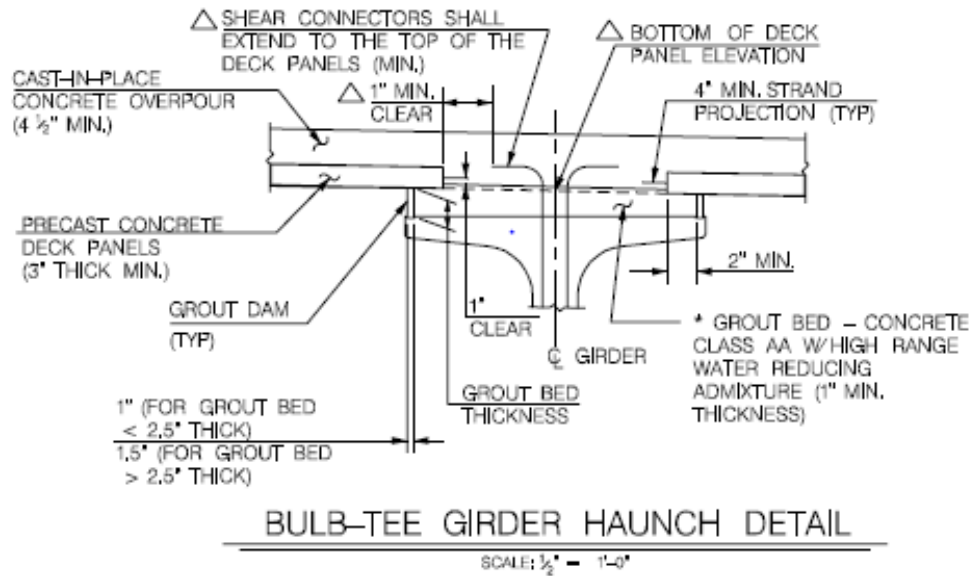
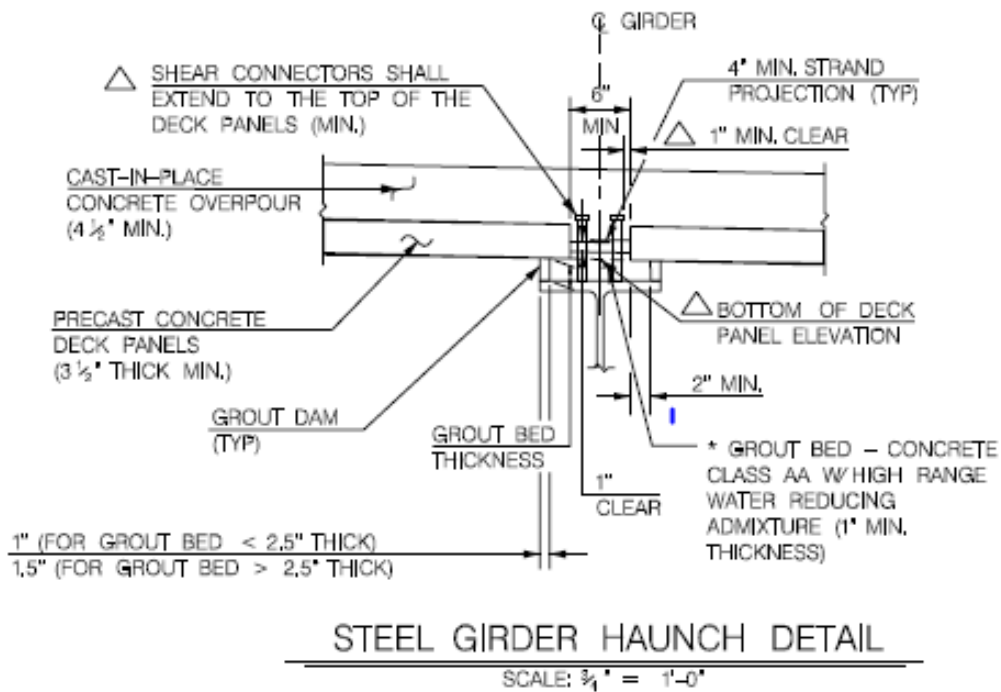


Figure 2.33: Partial depth deck with prestressed concrete girder (PCI, 2001)



\* ENSURE GROUT FLOWS UNDER PANEL FOR COMPLETE BEARING

Figure 2.34: Partial depth deck with steel girder (PCI, 2001)

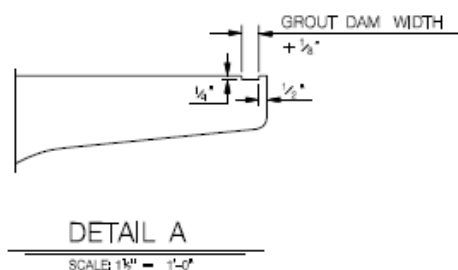
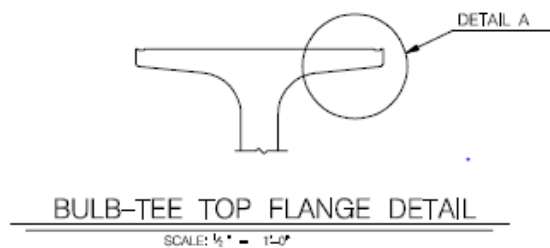


Figure 2.35: Girder detail showing grout dam width (PCI, 2001)

## 2.6.2 Texas Specifications and Experience

Texas has been a leader in the development of partial-depth precast panels (Merrill, 2002). Texas first designed a bridge with precast partial depth panels to act as stay in place formwork for the CIP portion of the deck in 1963. The method did not immediately gain popularity because of the difficulty in cantilevering the panels on the exterior edges. However, Texas began using partial-depth panels spanning over the interior girders, and currently uses partial-depth panels on most girder bridges in every part of the state. Standard details and specifications have been iterated based on lessons learned from construction challenges, in-house research projects, and evolution in materials over time. Texas explains the benefit of using a partial-depth panel system as follows. Construction is accelerated because the panels can be placed for the formwork within hours, and the CIP finishing pour takes less time due to the decreased amount of concrete compared to a full CIP deck. The decrease in construction time translates to cost savings, both in decreased work for the contractor and less traffic delay. Texas has also found that partial-depth panels are safer to install than a conventional deck. Since the panels are significantly heavier than wood or steel formwork, the formwork cannot blow away. Form removal is unnecessary as the panels stay in place for the life of the bridge. Texas has also seen positive impacts from the prestressing steel applied to the precast panels in the positive moment region of the deck. High quality concrete is achieved through this method of construction because the panels are fabricated in precast plants (Merrill, 2002). When asked whether Texas has considered implementing fully prefabricated decks for further benefit, current designers responded that full-depth decks are not used extensively as a widespread need has not been developed. However, full-depth decks have been

found useful for certain projects, and the state is working with the precast industry to develop best practices (Holt, 2015).

Texas uses panels that are 4" thick with a 4" thick CIP layer for a total deck thickness of 8". The precast panels are typically cast at a fabrication plant in casting beds that are 350 to 500 ft long, and prestressed to the appropriate level based on AASHTO Bridge Design Specifications (AASHTO, 2014). The largest producers of partial-depth panels can manufacture about 300 panels per day. The panels are typically cast with approximately 6" gap between panels to allow for panel movement at the release of the prestressing strands. The required concrete strength is 5 ksi. After the panels are placed, #5 bars spaced at 6" are normally placed in the panels that experience negative moment. Figure 2.36 shows the typical panel-to-girder section with bedding strips and spacing and does not show reinforcement. Figure 2.37 shows the panel placement over both an interior and exterior girder as well as the projected girder reinforcement. Composite action between the girder and the deck is achieved by projecting #4 bars from the girder with a full closed loop as shown in Figure 2.37. Figure 2.38 shows a transverse section between panel ends; the panels are placed with a maximum 1" gap and sealed to prevent joint leakage (Merrill, 2002).

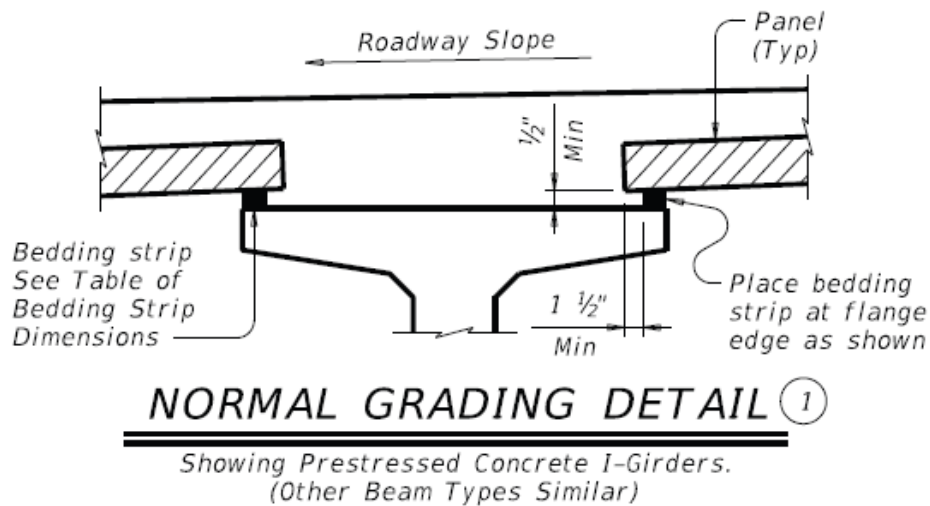


Figure 2.36: Typical panel placement for Texas partial-depth decks (TXDOT, 2006)

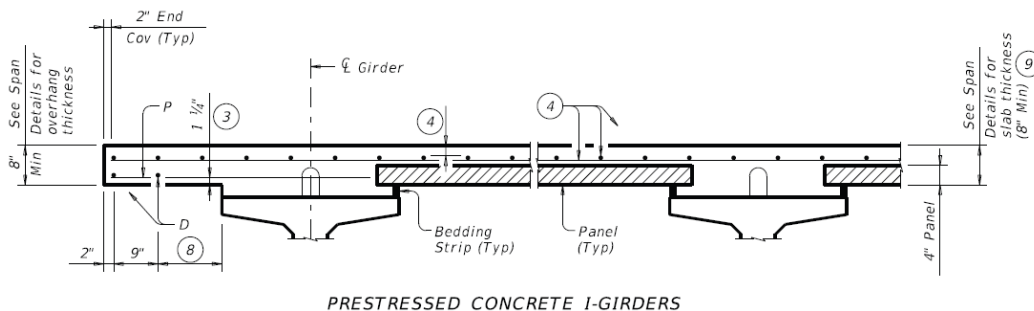
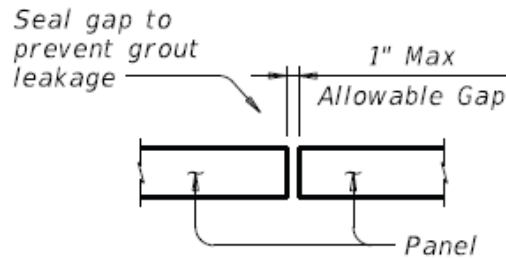


Figure 2.37: Typical panel placement with overhang and projected girder reinforcement (TXDOT, 2006)



## **TYPICAL SECTION AT PANEL JOINT**

(Panel reinforcing not shown for clarity.)  
The gap cannot be considered as a  
panel fabrication tolerance.

Figure 2.38: Typical transverse panel connection for Texas partial-depth decks (TXDOT, 2006)

Texas has placed limitations on the use of partial-depth precast deck panels. Precast deck panels are not permitted on curved steel girder bridges due to the complicated interaction between the deck, girder, and the diaphragm. Texas prefers to use a monolithic deck for this scenario. Partial-depth panels are not permitted on deck widening and phased construction projects, because the panels cannot usually be placed properly with the existing or currently built part of the structure. Partial-depth panels are impractical to install on steel girders with flange widths less than 12” because it is difficult to weld the shear studs within such a small opening (Merrill, 2002).

Texas has recently started using precast deck panels for the entire superstructure. Previously partial-depth panels were not applied over the expansion joints because of the geometric requirement for skewed panels. However, Texas experimented with different panel configurations and determined that trapezoidal panels could be used over expansion joints and remain structurally sound. Tests showed that either a parallel or fanned strand pattern would provide the required strength for the deck to meet required design loads (Wood et. al, 2008). Figure 2.39 illustrates Texas’ specifications for a skewed panel layout.

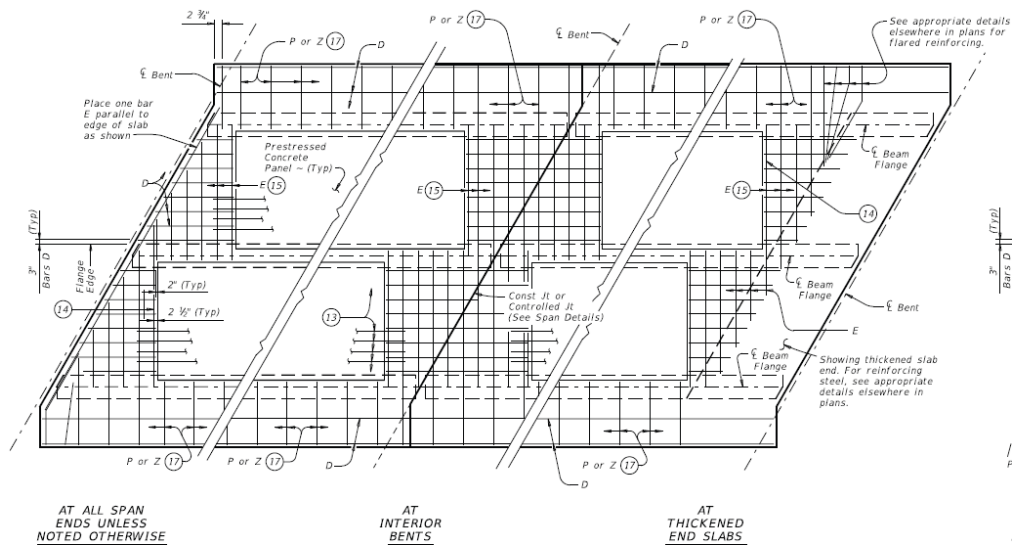


Figure 2.39: Skewed panel layout (TXDOT, 2006)

Texas has historically encountered longitudinal cracking on decks that use partial-depth precast panels. The longitudinal cracking was found to be caused by placement of the bedding strip too far from the edge of the girders, which led to insufficient bearing for the panels, or by placement of the bedding strips too far in advance of the panel placement. The latter approach caused the bedding strips, which prevent the CIP concrete from flowing under the panel edges, to crush. Texas mitigated the longitudinal cracking by ensuring the bedding strips were placed as specified, so that the design panel bearing stresses were achieved. Besides the longitudinal cracking, Texas has had positive experiences with partial depth deck panels and has been happy with the performance they have produced (Merrill, 2002).

### 2.6.3 Colorado Experience

Colorado DOT has also used precast partial-depth panels for many years. Policies dating from 1991 are listed on the CODOT website (CDOT, 1991). Panels are between 2 and 10 ft in length and no less than 3” in depth. Concrete used for the panels must have a minimum 28 day strength of 6 ksi.

CODOT uses similar specifications to the ones mentioned in Section 2.5.2. Figure 2.40 shows a section view of prestressed concrete deck panels spanning between interior girders. CODOT uses projected reinforcement bent 90° at the top, rather than Texas’ closed hoop configuration (Figure 2.37). Steel studs are used to achieve composite action between the deck and girder for partial-depth decks with steel girders (Figure 2.41). In general, the transverse joint is formed by fitting the panel ends tight against each other (Figure 2.42). After the panels are placed during construction, the deck panel surfaces are roughened to create more interaction between the panels and the CIP concrete.

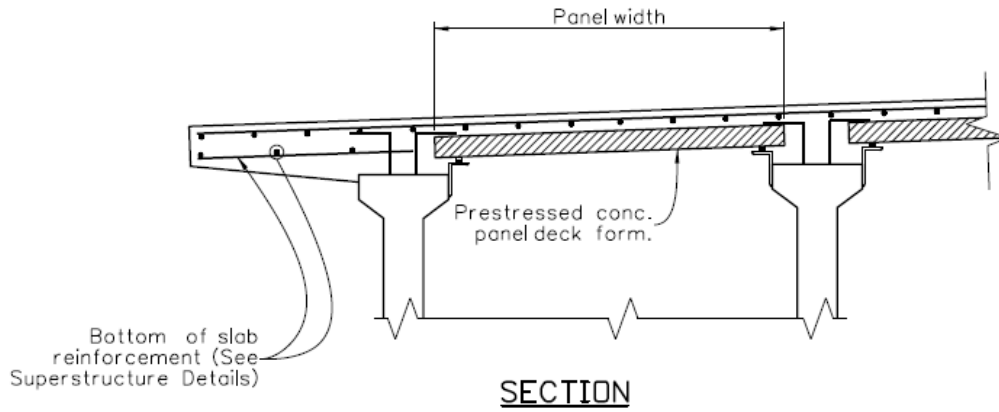


Figure 2.40: Colorado prestressed girder-to-deck section (CODOT, 2015)

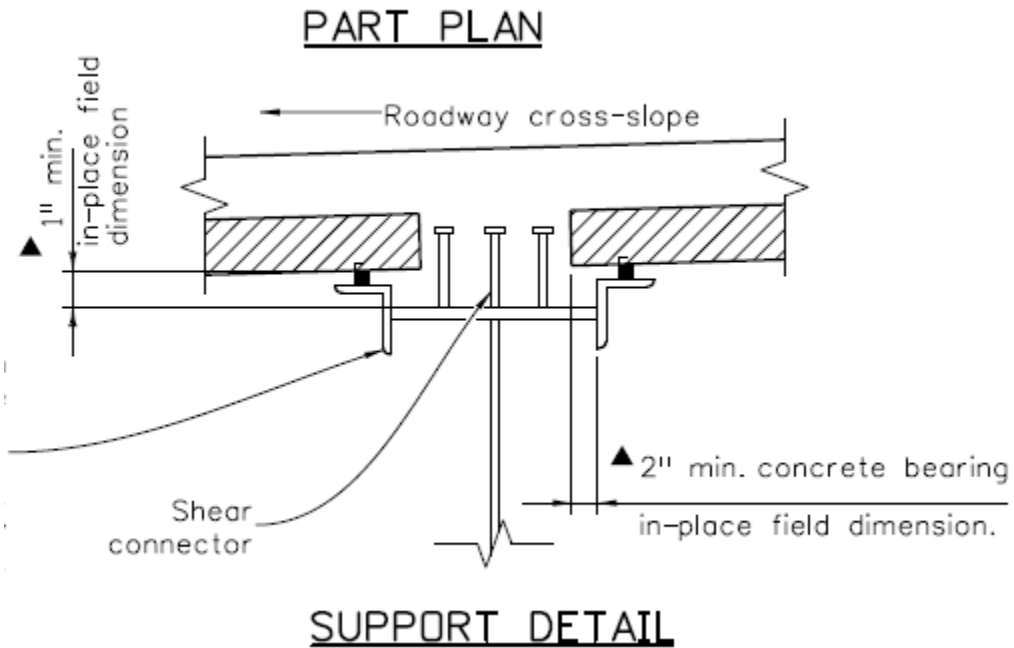


Figure 2.41: Colorado steel girder-to-deck section (CODOT, 2015)

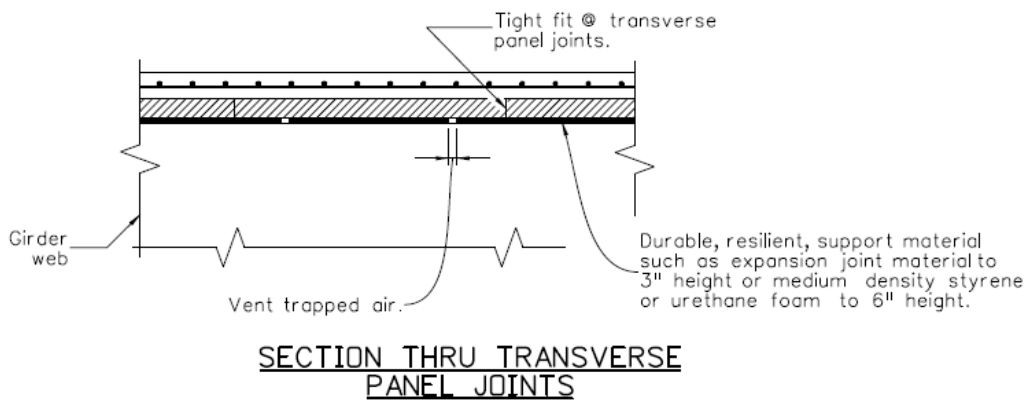


Figure 2.42: Colorado transverse panel joint (CODOT, 2015)

## 2.7 Noteworthy Projects

### 2.7.1 Utah Interstate Exchange Ramp Deck Replacement Project (Skewed Bridge)

In 2014, UDOT replaced the deck of a 4-span 48.5° skewed interstate-to-interstate exchange ramp with full-depth precast concrete deck panels (Scoles et al., 2014). The bridge was built in 1967 and the deck had been repaired several times to extend the life of the bridge. The inspections prior to the most recent deck replacement revealed crumbling of the deck, expansion joint failure, heavily rusted bearings at the abutments, and cracking and concrete spalling around the bearing pedestals at the abutments. UDOT decided to perform a full deck replacement to extend the life of the ramp.

Minimizing the traffic impact was a goal of this project, so the construction closure was desired to take 14 days or less. As a result, three different approaches using full-depth deck panels were considered to optimize construction speed. The selected design used an approach that oriented the deck panels perpendicular to the centerline of the structure. This approach eliminated the need for a skewed joint, and allowed for quicker panel construction and placement than if panel joints had followed the skew of the bridge. The main disadvantage was the lack of a performance history for this type of panel configuration. Figure 2.43 shows the final panel layout that was chosen for the project.

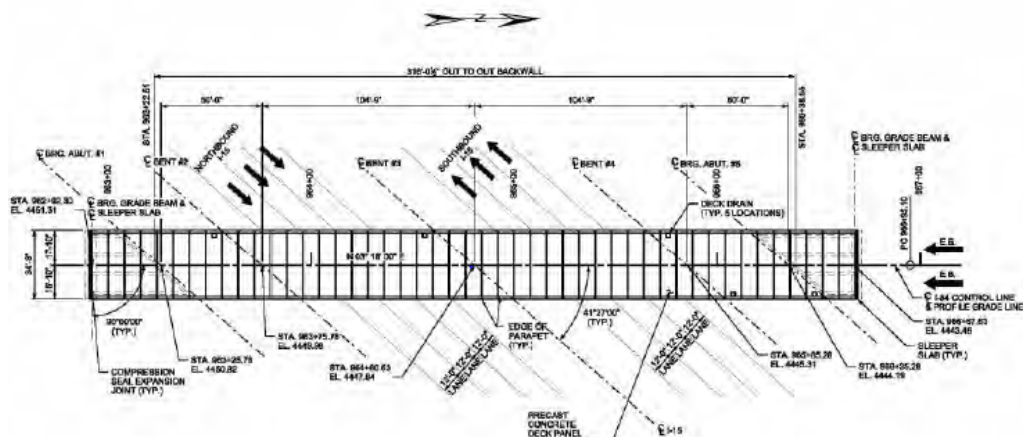


Figure 2.43: Utah panel layout (Scoles et al, 2014)

The bridge had a superelevation transition along each span. In the existing deck, the change in superelevation had been built into the panels. For the deck replacement, the panels were made flat to simplify construction and fabrication. Varying haunch heights and large post-tensioning ducts allowed the panels to be assembled in this manner. Composite action was achieved by using shear studs and blockouts in the panels. All of the transverse reinforcement was designed using UDOT's method for a CIP deck.

Because many of the components of the bridge were unique, several parts of the design were checked to ensure the system would perform as expected. The post-tensioning was analyzed thoroughly, and the transfer of the post-tensioning force from the deck to the girder was examined. Long term creep losses were calculated using a finite element model to validate the results of hand calculations from AASHTO LRFD.

The removal of the existing deck was more difficult than was expected as the girder flanges were 5/8" thick and were prone to damage using traditional removing techniques. The girders also rebounded more than expected after the dead load of the previous deck had been removed. This caused damage to the abutment bearings. However, the replacement was completed in 6 days, much shorter than the 14 day target. No post-construction reports were included with the summary. Figure 2.44 shows the placement of the deck panels during construction.



Figure 2.44: Deck placement of Utah ramp (Scoles et al, 2014)

### **2.7.2 Missouri Bill Emerson Memorial Bridge**

In 2003, the Missouri DOT (MODOT) used full depth precast deck panels in the construction of the Bill Emerson Memorial Bridge (Badie and Tadros, 2008). The bridge was a complete replacement of the original bridge that was built in 1927. The main span of the cable-stay bridge is 4000 ft long and 100 ft wide. The superstructure is supported by three longitudinal girders spaced at about 50 ft and transverse floor beams spaced at 18 ft.

The deck consists of two adjacent 10" deep precast panels spanning the width of the bridge, replicated in the longitudinal direction. The panel face on the interior side of the bridge rests on the center girder and floor beams. Because the bridge was not skewed, straight panels were used and the longitudinal joint was created over the center girder of the bridge. Figure 2.45 is a duplicate of Figure 2.15, repeated here for convenience, and shows the panel layout for the bridge.



Figure 2.45: Deck panel placement of Bill Emerson Memorial Bridge (Badie and Tadros, 2008)

The precast deck panels were conventionally reinforced with top and bottom meshes of epoxy coated bars. CIP concrete was used for the side and median barriers, transverse connections, and longitudinal connections. The transverse connection was a shear key with reinforcement projected out of the panel and a CIP pour used to complete the joint. Because the longitudinal connection was formed over a girder, shear keys were not needed for that connection. The panels were made composite with the girder by welding shear studs on the steel girder and completing the longitudinal connection with CIP concrete. The longitudinal direction also used post-tensioning spaced at 12". The deck was completed with a 3" silica fume overlay. Figure 2.49 shows an individual panel with post-tension ducts and shear keys for the longitudinal joint.

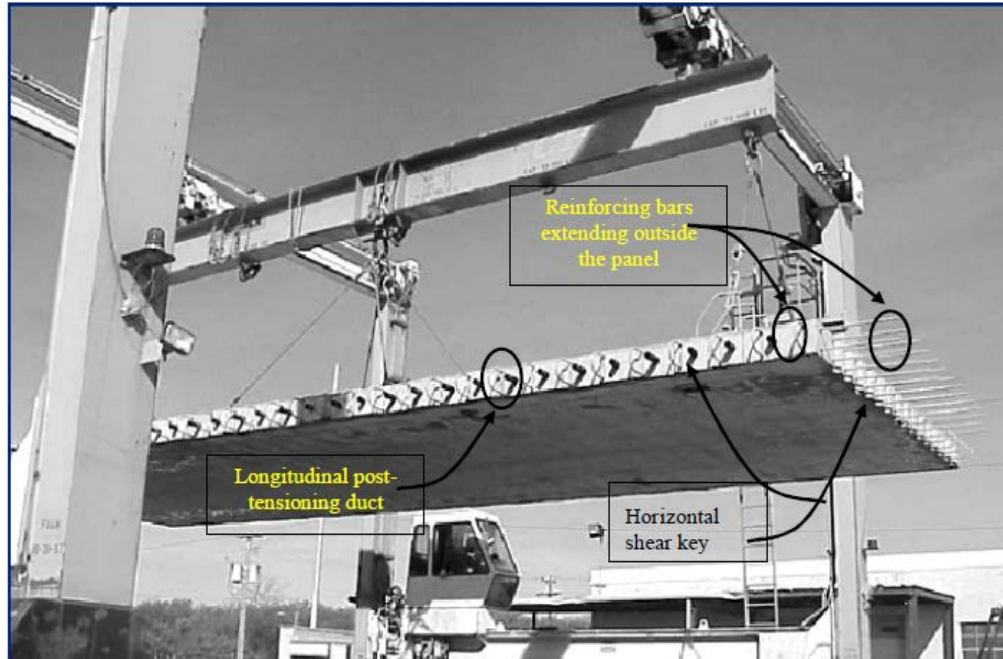


Figure 2.46 Panel with reinforcement and shear key (Badie and Tadros, 2008)

### 2.7.3 Iowa US 6 Over Keg Creek

The Strategic Highway Research Program (SHRP2) and the HNTB engineering firm wanted to demonstrate an ABC modular design concept for common multi-span stream crossings. Designing and demonstrating a successful design for this type of crossing would allow ABC to be used on typical small scale bridge replacements. The US 6 over Keg Creek Bridge was chosen as an example because of the moderate size and simplicity of the project (Iowa DOT, 2014).

The project used a precast modular deck system with steel girders, precast pier columns and bent caps, precast abutment footings and wings, precast approach pavement slabs, semi-integral abutments, and UHPC joints between the deck modules. The contractor decided to use site casting for the bridge components rather than using a precast plant because of the cost-savings for this project.

Bridge construction was begun by closing the highway and demolishing the old bridge. The abutments and columns were installed and the abutments were placed within the first five days of construction. When the abutments and columns were in place the cap beams were installed. The cap beam installation included the largest precast lift Iowa had performed. Girders were placed and the deck modules were then installed. The approach slabs were set and the joint and closure pours were installed using UHPC. The girders were post-tensioned using rods. Final surface work was completed and the bridge was opened to traffic. There were no major problems during the construction of the bridge and the entire construction took 16 days to complete. Minor issues, such as the field casting of UHPC and field welds, will need to be addressed on future ABC projects, but the incorporation of ABC into this bridge was deemed a success (Iowa DOT, 2014).

## **2.8 Literature Review Conclusions**

Prefabricated deck panels are an innovative way to decrease construction time and reduce maintenance requirements. The panels can be incorporated in several ways, including installation of the whole deck in one piece using full-depth prefabricated panels, or incorporating panels as a stay-in-place form for a concrete pour using partial-depth prefabricated panels. Experience with prefabricated deck panels varies widely state-to-state. Some states, such as Texas, have used prefabricated panels for 30+ years while others are just recently experimenting with different panel types. Because of the diversity of experiences, it is instructive to evaluate the methodologies and detailing that other states have incorporated for their use of deck panels along with corresponding successes and failures. The next part of the project attempts to determine the best practices for the use of deck panels by surveying every DOT and assembling the positive and negative experiences for each panel and connection type.

## **3. State DOT Prefabricated Deck Panel Survey Results**

### **3.1 Introduction and Prior Research**

The literature review on prefabricated panels indicated that a variety of deck panel details have been developed and implemented throughout the United States. As a follow-up to this literature review, additional information was gathered to identify the best options for prefabricated deck panels. Specifically, other state experiences with deck panels were investigated to identify best options for Nevada.

A survey was designed for this project to gather information on prefabricated deck panel systems, specifically full-depth and partial-depth panels. This survey was modeled after the NCHRP 12-65 project survey (Section 2.4), with the goal to update the NCHRP survey results (Badie and Tadros, 2008) and investigate additional issues that were of interest to Nevada DOT. The final 32-question survey included a variety of questions about the use of prefabricated deck panels. The complete blank survey form sent to the DOTs is included in Appendix B. All 50 state DOTs were invited to complete the survey online. The representatives from each DOT were requested to complete the survey within three weeks. At the end of the survey deadline, 31 states had responded to the survey.

### **3.2 Total Responses and Number of Decks Constructed**

Several questions were asked to identify the volume of bridges that had been constructed using prefabricated deck panels and to differentiate between various DOTs by their levels of experience. Of the 32 DOTs, 20 reported they had constructed new bridges or performed deck replacement projects with prefabricated deck panels in the past 10 years. Figure 3.1 shows the total number of new bridges constructed in the last 10 years, differentiated by deck and girder type. Figure 3.2 shows the total number of deck replacements performed in the last 10 years, also differentiated by deck and girder type. Because of the difference in experience levels with prefabricated deck panels across different states, it is important to look at the number of bridges each DOT has designed using deck panels. Figure 3.3 shows the percentage of DOTs with varying levels of experience using prefabricated deck panels, tabulated from among the 32 states that responded. For example, 37% of DOTs had no experience, 34% had limited experience (designed between 1 and 5 bridges), 16% had some experience (6 to 15 bridges), and 13% had extensive experience (>20 bridges).

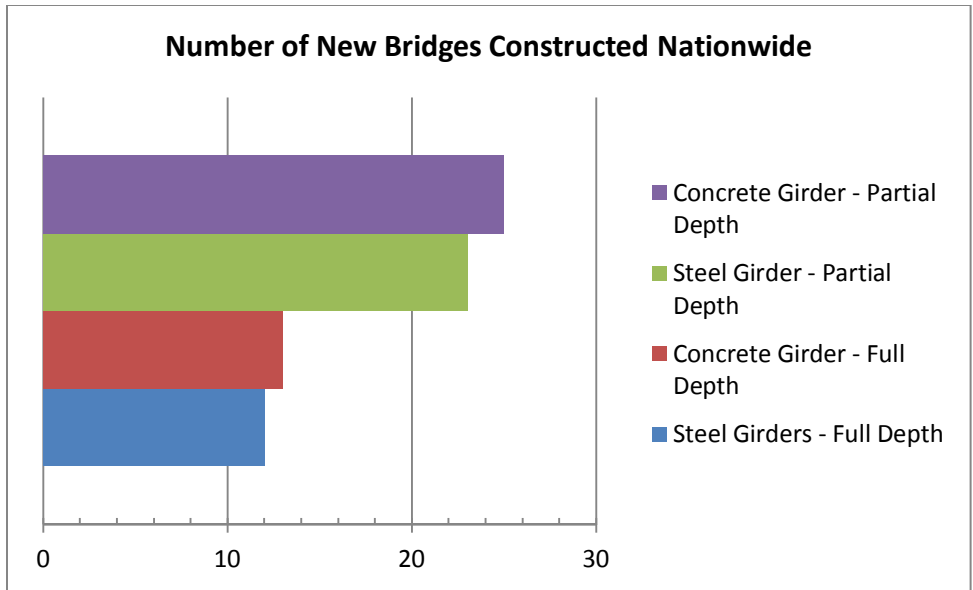


Figure 3.1: Number of new bridges built with prefabricated deck panels in past 10 years

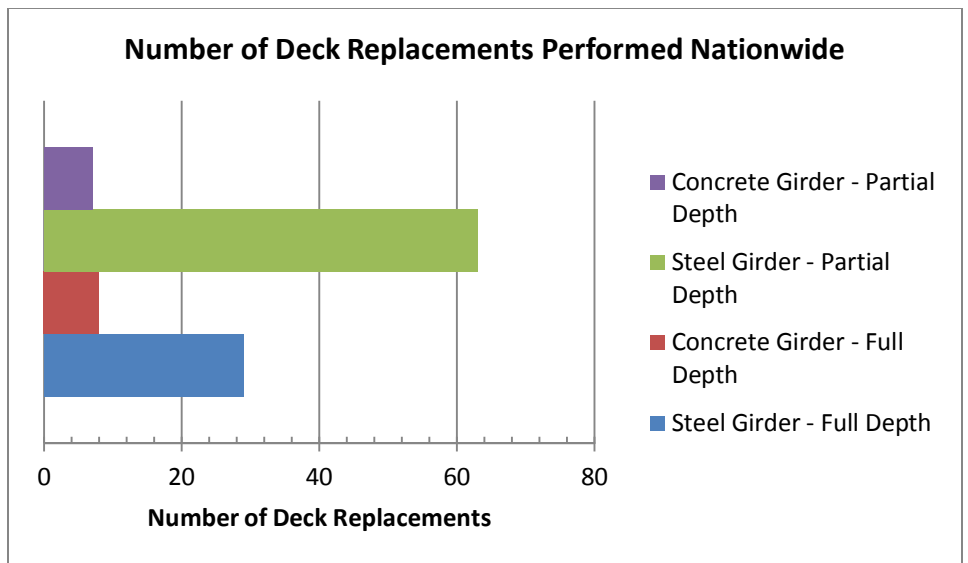


Figure 3.2: Number of bridge deck replacement projects using prefabricated deck panels in past 10 years

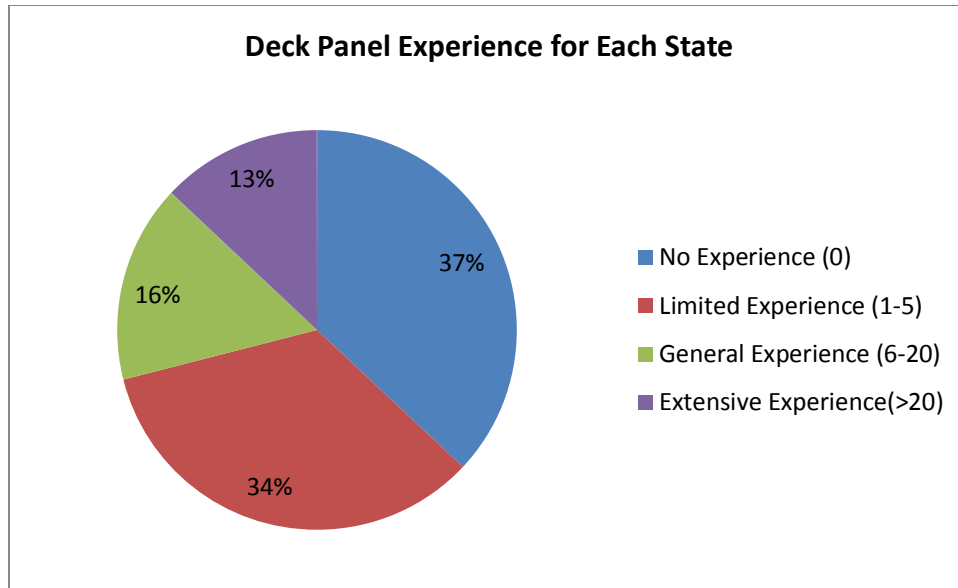


Figure 3.3: Percentage of DOT's with various experience levels using prefabricated deck panels by number of bridges

Figure 3.1 shows that for new bridge construction, both partial depth and full depth panels have been used with both steel and concrete girders. Not included in Figure 3.1 due to scaling issues, Texas reported constructing 2000 new bridges with partial depth panels and prestressed concrete girders in the past 10 years. This number was much larger than other states because Texas uses partial depth panels almost exclusively for new bridge construction. Based on Figure 3.2, both partial depth and full depth deck panels are commonly used for deck replacements on steel girder bridges. However, prestressed concrete girder bridges incorporating prefabricated deck panels are much less common. Figures 3.1 and 3.2 imply that partial depth panels are more commonly used than full-depth panels, however this is misleading. Multiple DOTs use partial depth panel construction as the default for all bridge construction. Because of this, these DOTs have constructed large numbers of bridges that use partial depth deck panels; at a higher proportion than DOTs that use full-depth panels. In summary, full-depth panels are used by more DOTs, but more bridges are constructed using partial depth panels.

### 3.3 Trends in Application of Prefabricated Deck Panels

#### 3.3.1 Full-Depth Longitudinal and Transverse Reinforcement

DOTs were surveyed to identify the most common methods for connecting full-depth panels in the longitudinal and transverse direction. Figures 3.4 and 3.5 show how many times each reinforcement type was used. The two most common longitudinal reinforcement types were spliced reinforcement with UHPC and longitudinal post-tensioning with standard grout. Tennessee has applied HSS with epoxy grout and New Jersey has tried a rapid set latex modified concrete on two bridges. For the transverse reinforcement, spliced reinforcement with UHPC or standard grout was the most commonly used connection type. Bridges that did not have a longitudinal joint were identified as “Not Applicable” in Figure 3.5.

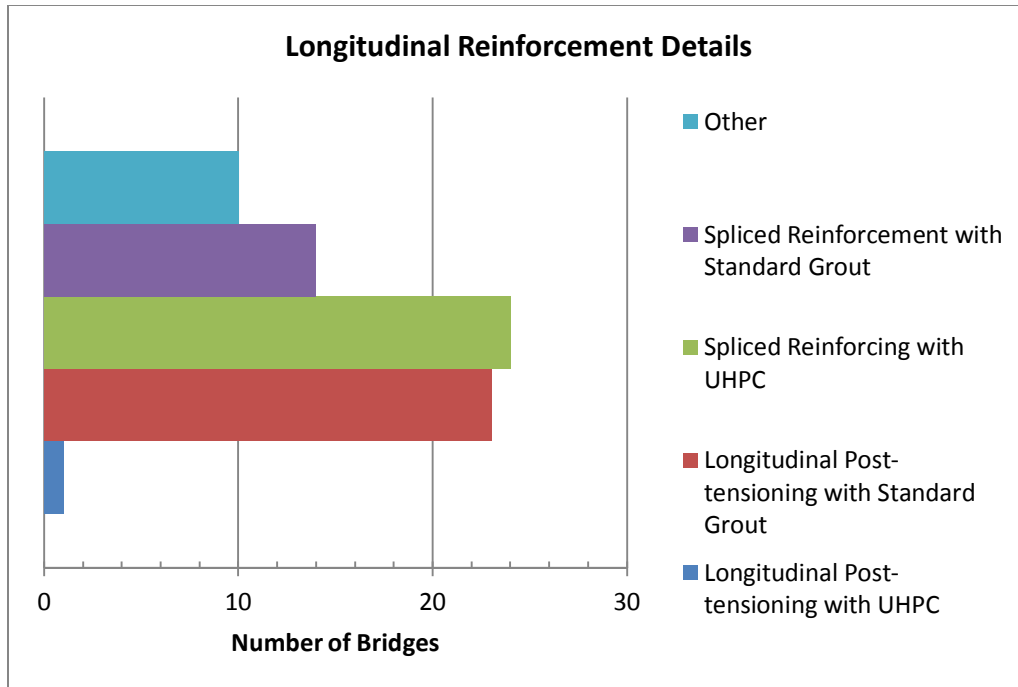


Figure 3.4: Implementation of longitudinal reinforcement details

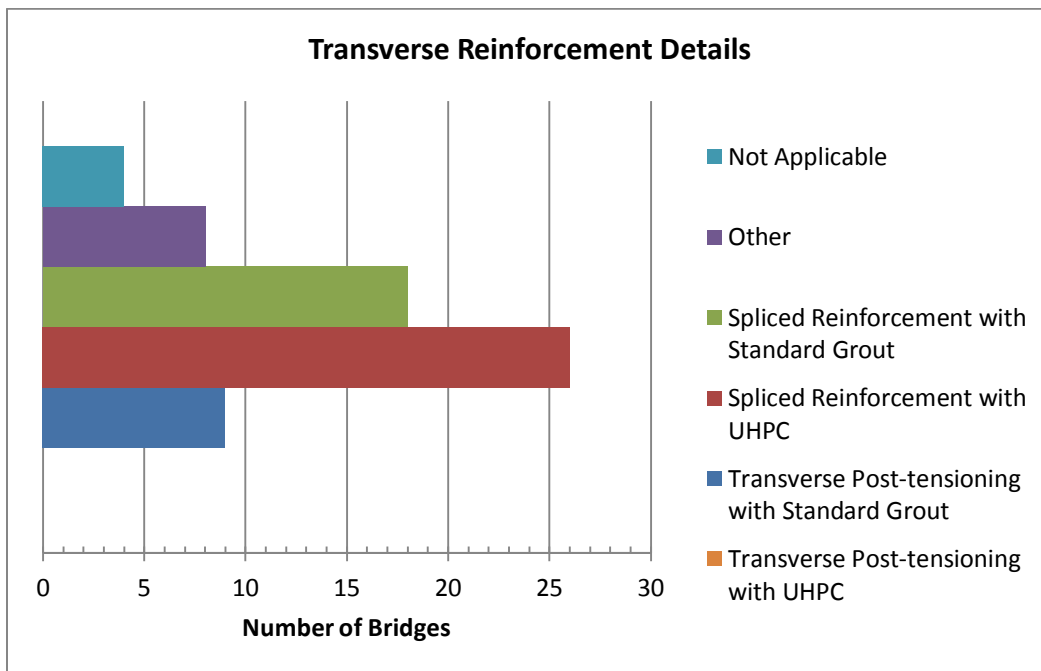


Figure 3.5: Implementation of transverse reinforcement details

### 3.3.2 Connection Details

#### 3.3.2.1 Full Depth Panel-to-Panel Connections

To assess use of full-depth panel-to-panel connections, the survey presented a variety of details, and respondents were asked to rate implementation of each detail (usage rating) as: “regularly used”, “used but not standard practice”, “used but would not use again”, and “never used”. Figure 3.6 shows the panel-to-panel connections that were included in the survey and Figure 3.7 shows the number of DOTs reporting successful application of each connection detail. DOTs reporting either regular use or used but not as standard practice were included in the count in Figure 3.7. Figure 3.8 shows the number of DOTs that selected each usage rating in pie chart format.

The general female-to-female shear key detail developed by PCI (2011a) shown in Figure 3.6a was the most commonly used transverse connection type and the longitudinal joint resembling that developed by Oregon DOT (Figure 3.6g) was the most commonly used longitudinal connection. The female-to-female shear key with welded shear plate (Figure 3.6b), transverse shear key with steel plate (Figure 3.6c), female-to-female shear key with HSS (Figure 3.6d) and longitudinal joint with spliced reinforcement (Figure 3.6i) were all never used or seldom used.

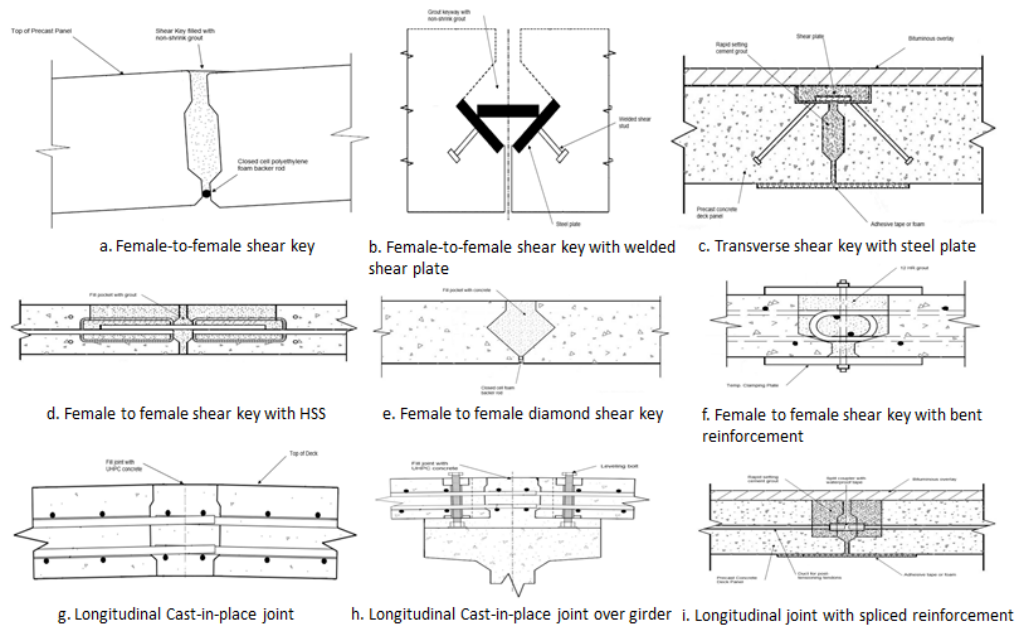


Figure 3.6: Various panel-to-panel connection details

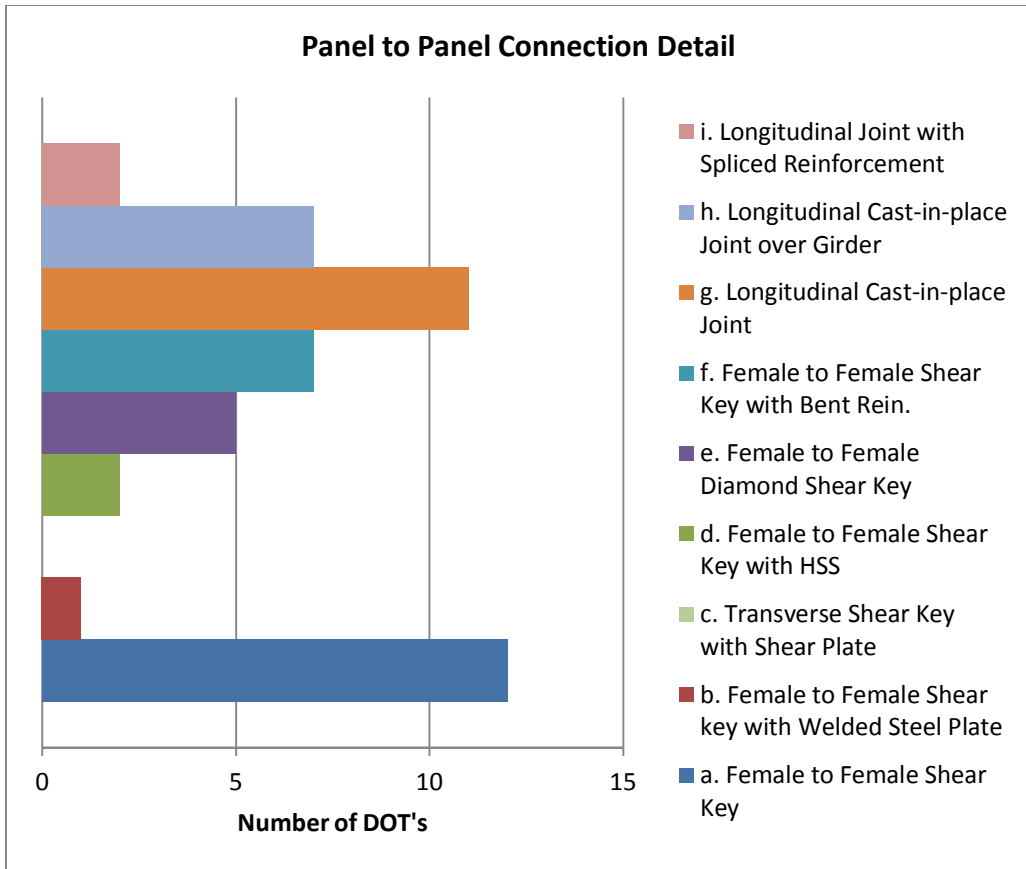
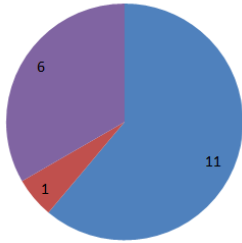
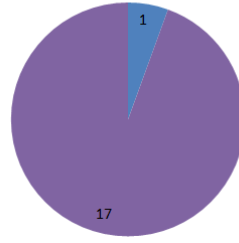


Figure 3.7: Number of DOTs implementing various panel-to-panel connection details

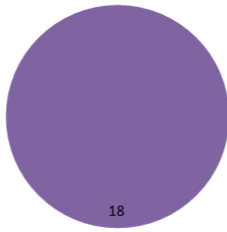
a. Female to Female Shear Key



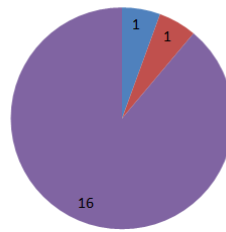
b. Female to Female Shear Key with Welded Shear Plate



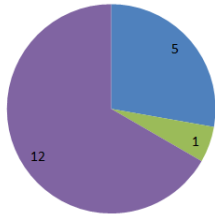
c. Transverse Shear Key with Shear Plate



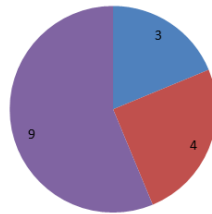
d. Female to Female Shear Key with HSS



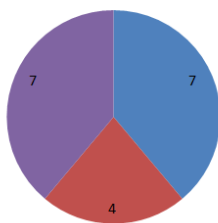
e. Female to Female Diamond Shear Key



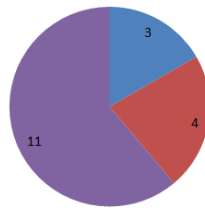
f. Female to Female Shear Key with Bent Reinforcement



g. Longitudinal Cast-In-Place Joint



h. Longitudinal Cast-In-Place Joint Over Girder



i. Longitudinal Joint with Spliced Reinforcement

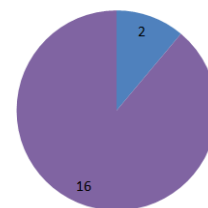


Figure 3.8: Type of use for each panel-to-panel connection detail, counted as number of states selecting each usage rating.

### 3.3.2.2 Full Depth Panel-to-Girder Connections

Implementation of various full-depth panel-to-girder connections was surveyed in the same way as the full-depth panel-to-panel connections. Figure 3.9 shows the panel-to-girder connections and Figure 3.10 shows the number of DOTs indicating successful application of each connection detail. Figure 3.11 shows the number of states that indicated each usage rating in pie chart format.

The steel girder with welded steel studs detail developed by PCI (Figure 3.9a, PCI, 2011a) was the most commonly used steel girder connection. The prestressed concrete girder with studs detail (Figure 3.9d, PCI, 2011a) was commonly implemented with prestressed concrete girders. Thus details utilizing shear studs were most commonly implemented for both steel and concrete girders. A projected reinforcement detail (Figure 3.9e, PCI, 2011a) and stirrups (Figure 3.9f, DET 3425 of ODOT, 2015) were used for the concrete girder but not as commonly as the shear stud detail. The other connection types that were included in the survey were seldom or never used.

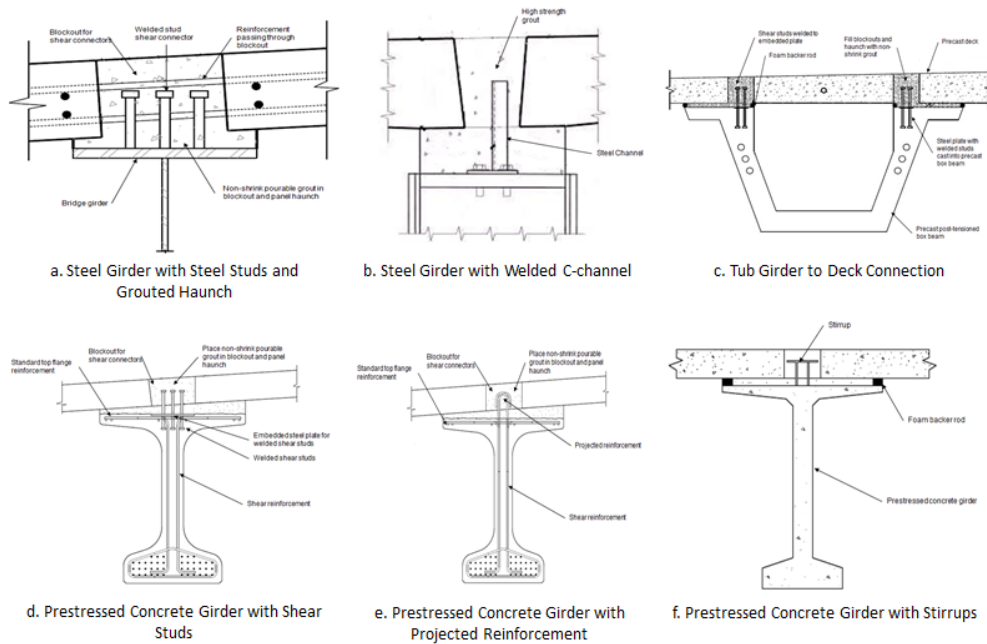


Figure 3.9: Various panel-to-girder connection details

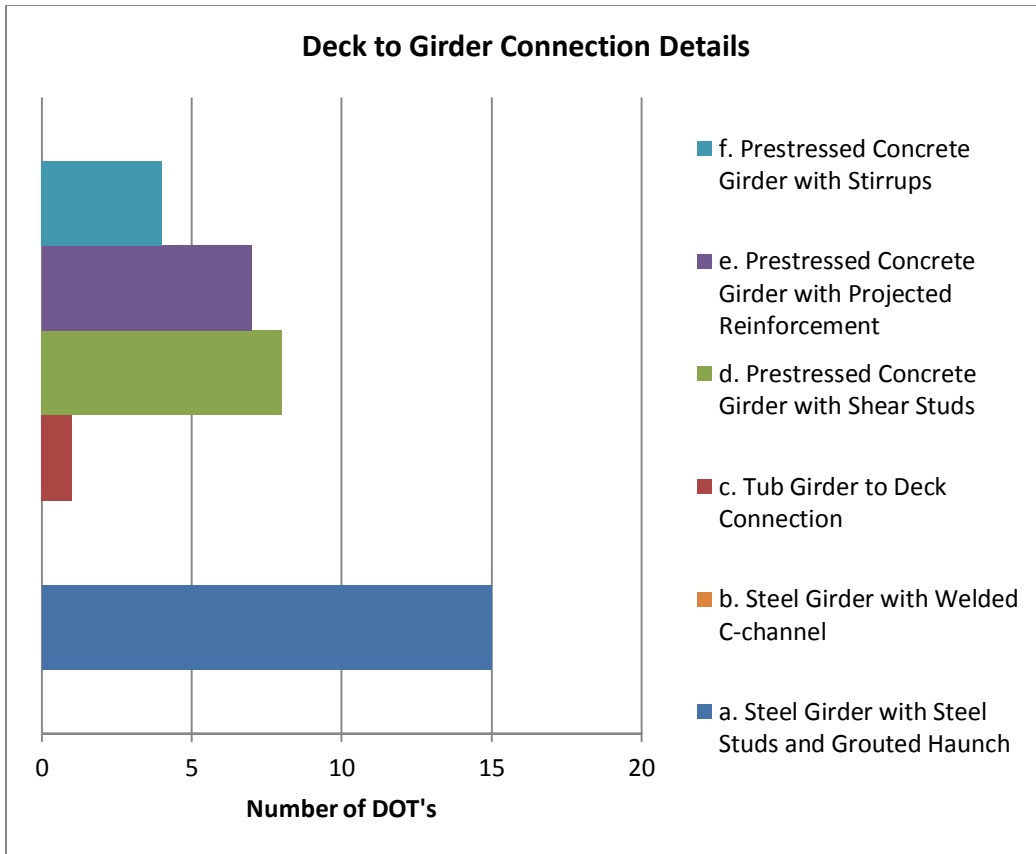


Figure 3.10: Number of DOT's implementing various deck-to-girder connection details

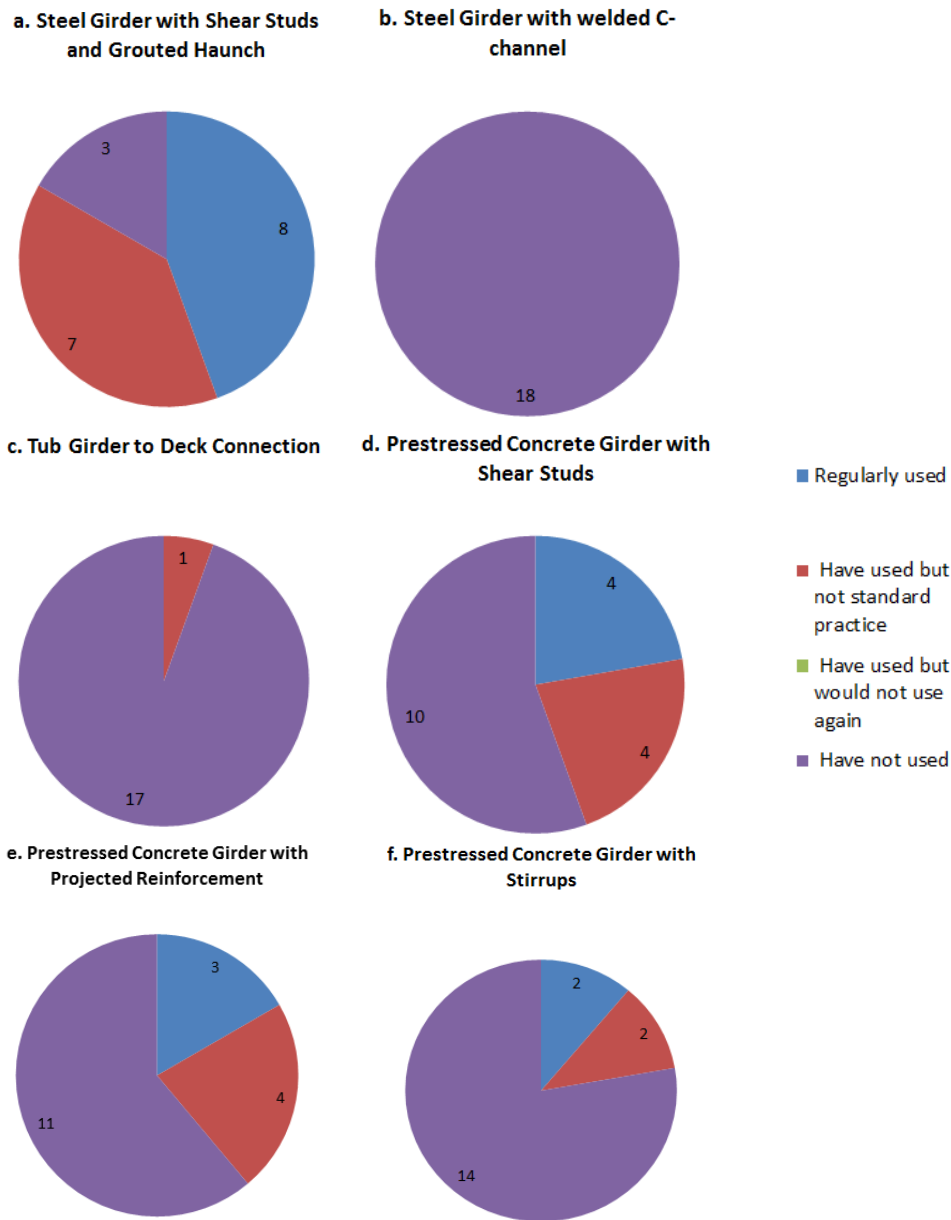


Figure 3.11: Type of use for each deck-to-panel connection, counted as number of states selecting each usage rating

### 3.3.2.3 Partial Depth Connections

Usage ratings were surveyed for partial depth panel-to-girder and panel-to-panel connections in the same way as for the full-depth panels. Figure 3.12 shows the partial depth panel-to-panel and panel-to-girder connections. Figure 3.13 shows how many DOTs used each connection type, and Figure 3.14 shows the number of states selecting each usage rating in pie chart format.

The most commonly used partial depth panel-to-girder connection was a detail with welded steel studs extending from steel girders (Figure 3.12a, PCI, 2001) and a

prestressed concrete girder with haunch reinforcement (Figure 3.12b, TXDOT, 2006). U-girders with partial depth panels (Figure 3.12c, TXDOT, 2006) were also a common configuration among different DOTs.

Only one type of partial depth panel-to-panel connection was identified by the authors to include in the survey. As a result, DOTs were asked an open ended question to indicate differences in their own implementation relative to the model connection (Figure 3.12e, TXDOT, 2006). Most DOTs indicated that instead of leaving a 1 inch gap, the panels are pushed directly against each other and a concrete deck pour is used to seal the joint.

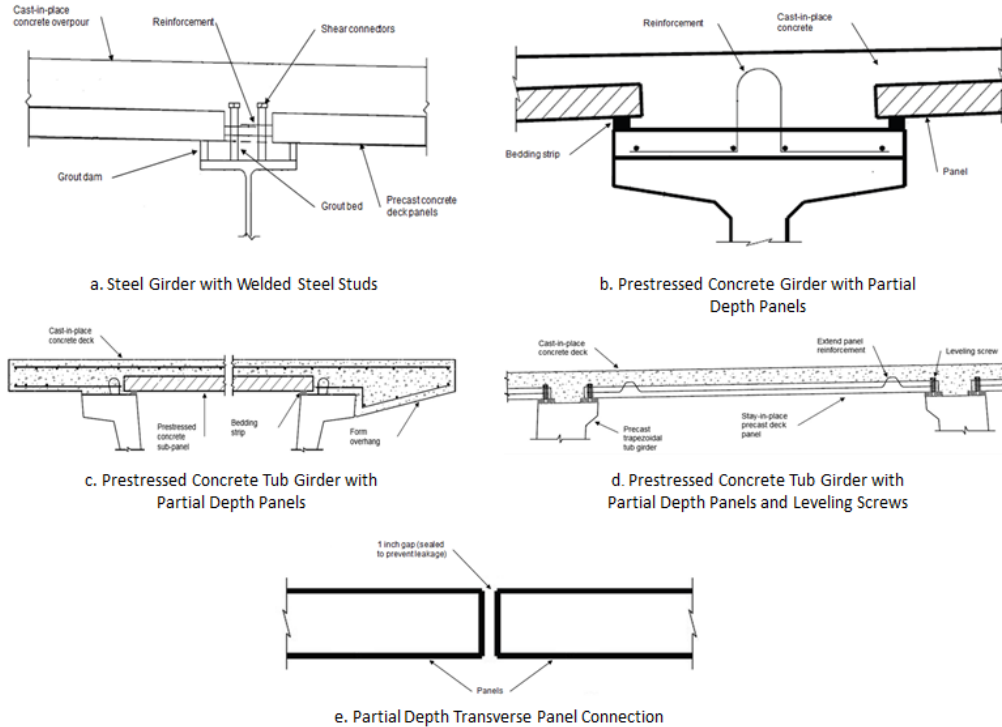


Figure 3.12: Various partial-depth connection details: a-d. panel-to-girder connection detail, and e. panel-to-panel connection detail

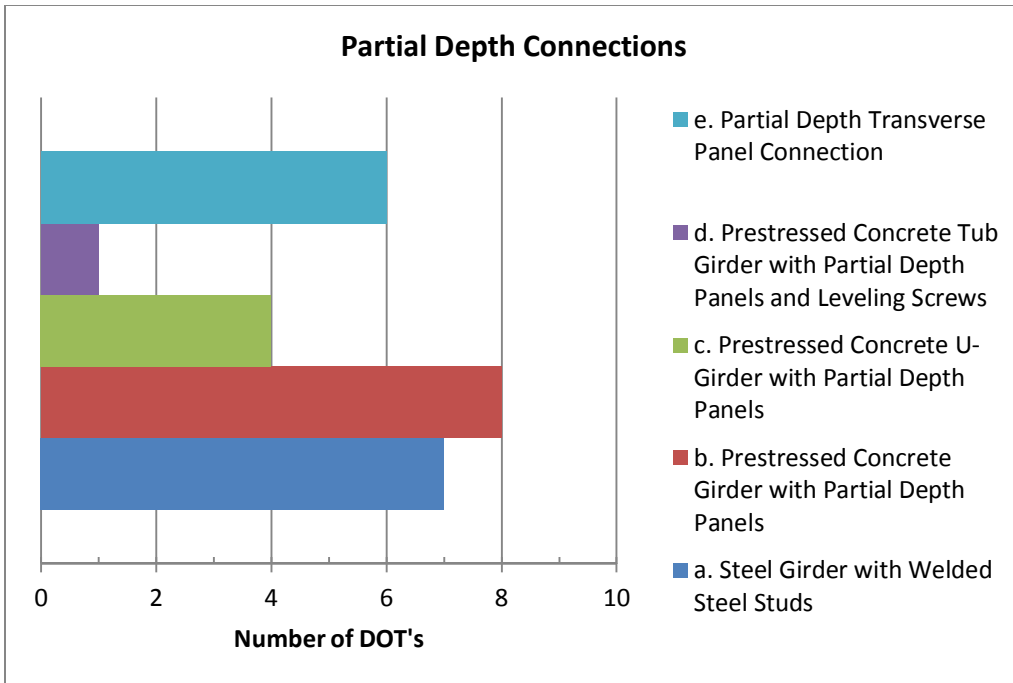


Figure 3.13: Number of DOT's that use each partial depth connection

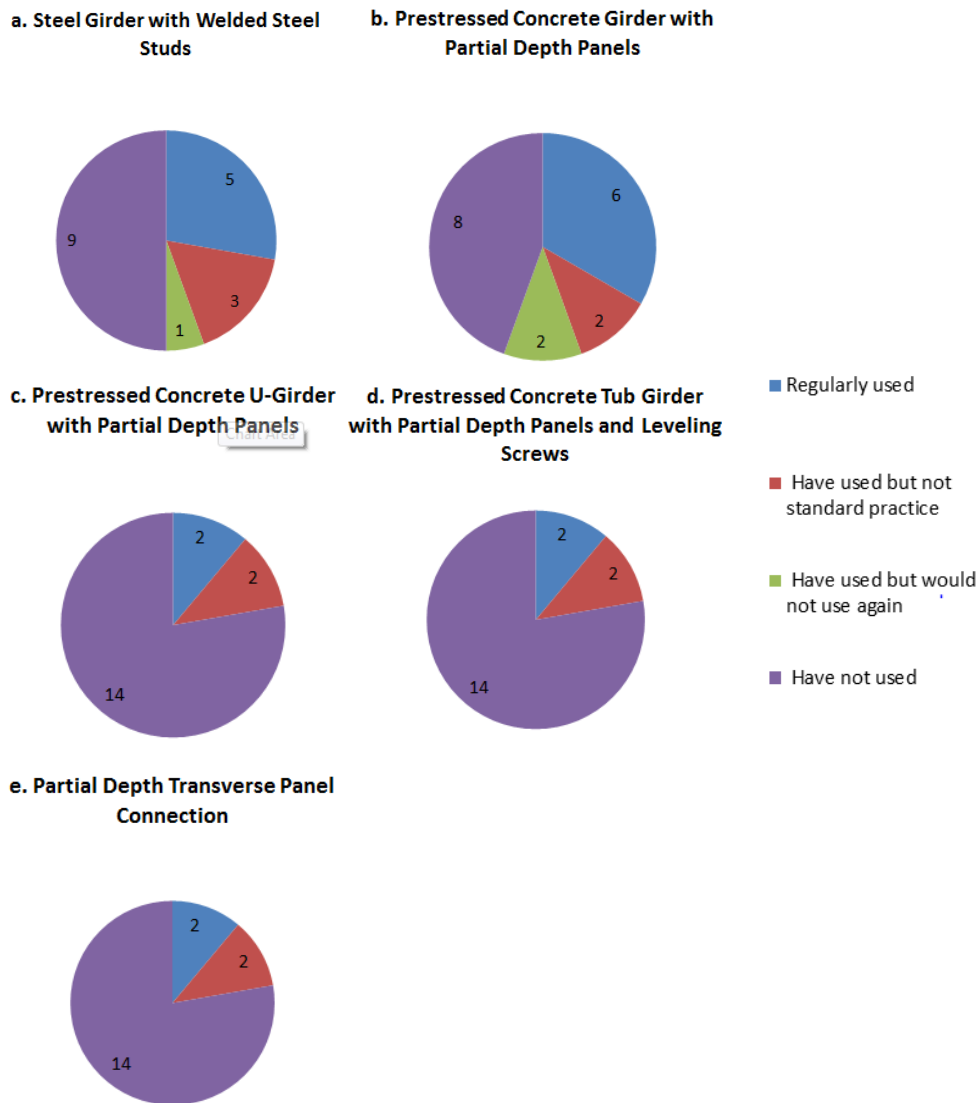


Figure 3.14: Type of use for each connection detail, counted as number of states selecting each usage rating

### 3.3.4 Usage of Overlays

DOTs were asked to indicate the standard practice for application of overlays to bridges with both partial-depth and full-depth deck panels. DOTs preferred a variety of options for full depth deck panels including asphalt, concrete, a 3/8" polymer multilayer, and no overlay. Asphalt overlays and no overlay were selected most frequently among the options. No overlay was the most commonly chosen option for partial depth deck panels. Figures 3.15 and 3.16 show the number of DOTs that used each overlay option for full-depth and partial depth deck panels.

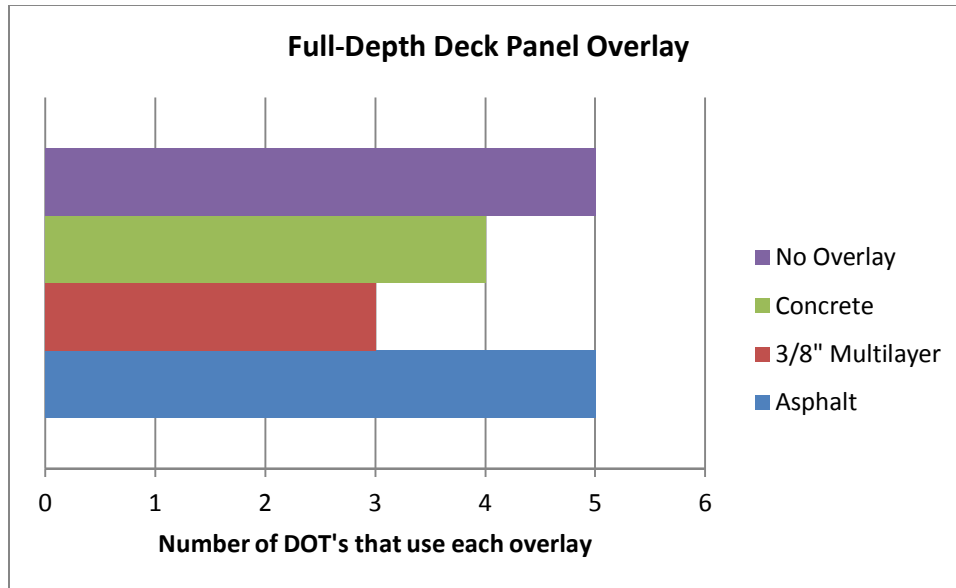


Figure 3.15: Number of DOT's that use each panel overlay type for full-depth decks

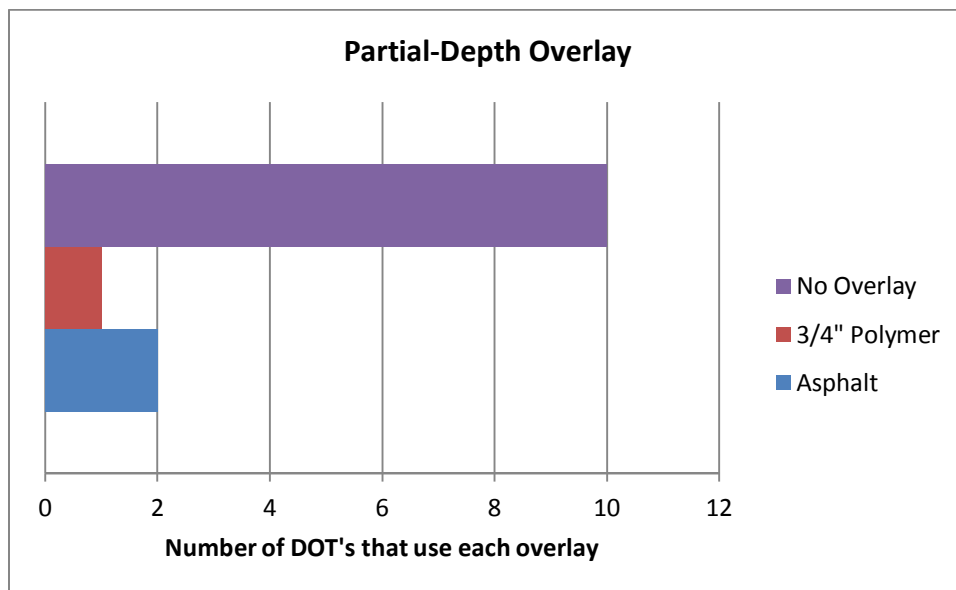


Figure 3.16: Number of DOTs that use each panel overlay type for partial depth decks

### 3.4 Deck Panel Evaluations

#### 3.4.1 Deck Panel Performance Problems

Common performance problems with the prefabricated deck panels were also included in the survey. To evaluate the performance of the deck panels in the field, DOTs were presented with a list of potential performance problems and asked to evaluate the frequency of the problem as: being “observed frequently”, “observed in the past but it was not common”, or had “never been observed”. Figure 3.17 shows the number of responses indicating a frequently observed problem for full-depth panels and Figure 3.19

shows the number of responses indicating a frequently observed problem for partial-depth panels. Figures 3.18 and 3.20 show the percentage of states selecting each rating for each performance issue for full-depth and partial depth deck panels, respectively. The performance problems observed most frequently for full-depth deck panels were closure pour cracking and joint leakage. The respondents that reported these as common problems indicated that both of these problems could be corrected by applying UHPC for the joints and closure pour. DOTs indicated that reflective cracking, excessive surface wear, concrete spalling, and differential panel movement were not commonly observed. Reflective cracking was the most commonly observed performance problem for partial depth deck panels while differential panel movement, closure pour cracking, concrete spalling, excessive surface wear, and joint leakage were not indicated as frequently occurring problems for DOTs. Reflective cracking was reported as a major issue for several states and resulted in multiple DOTs prohibiting the use of partial depth panels. Other partial depth deck panel performance problems such as joint leakage and closure pour cracking could be corrected with UHPC.

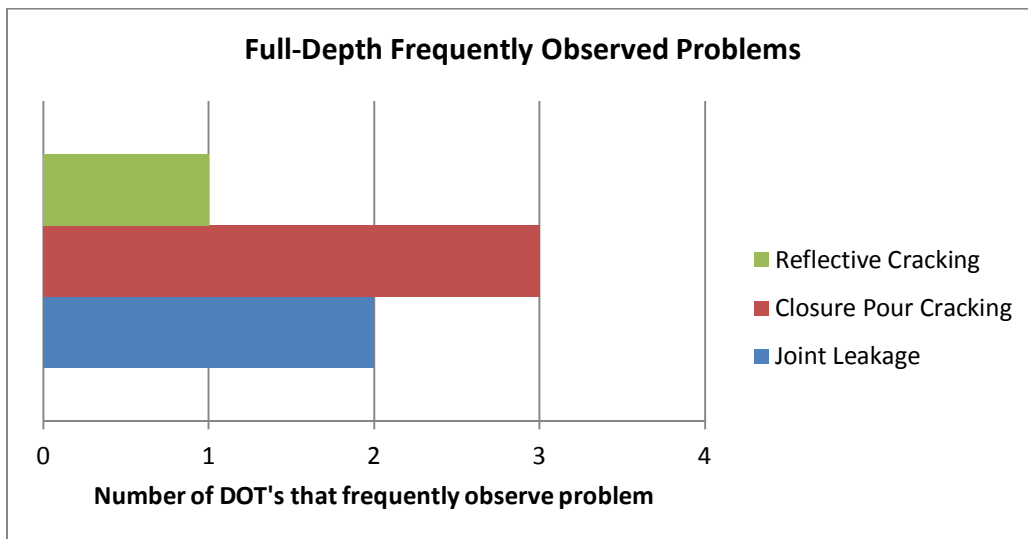


Figure 3.17: Number of DOTs indicating a frequently observed problem for full-depth deck panels

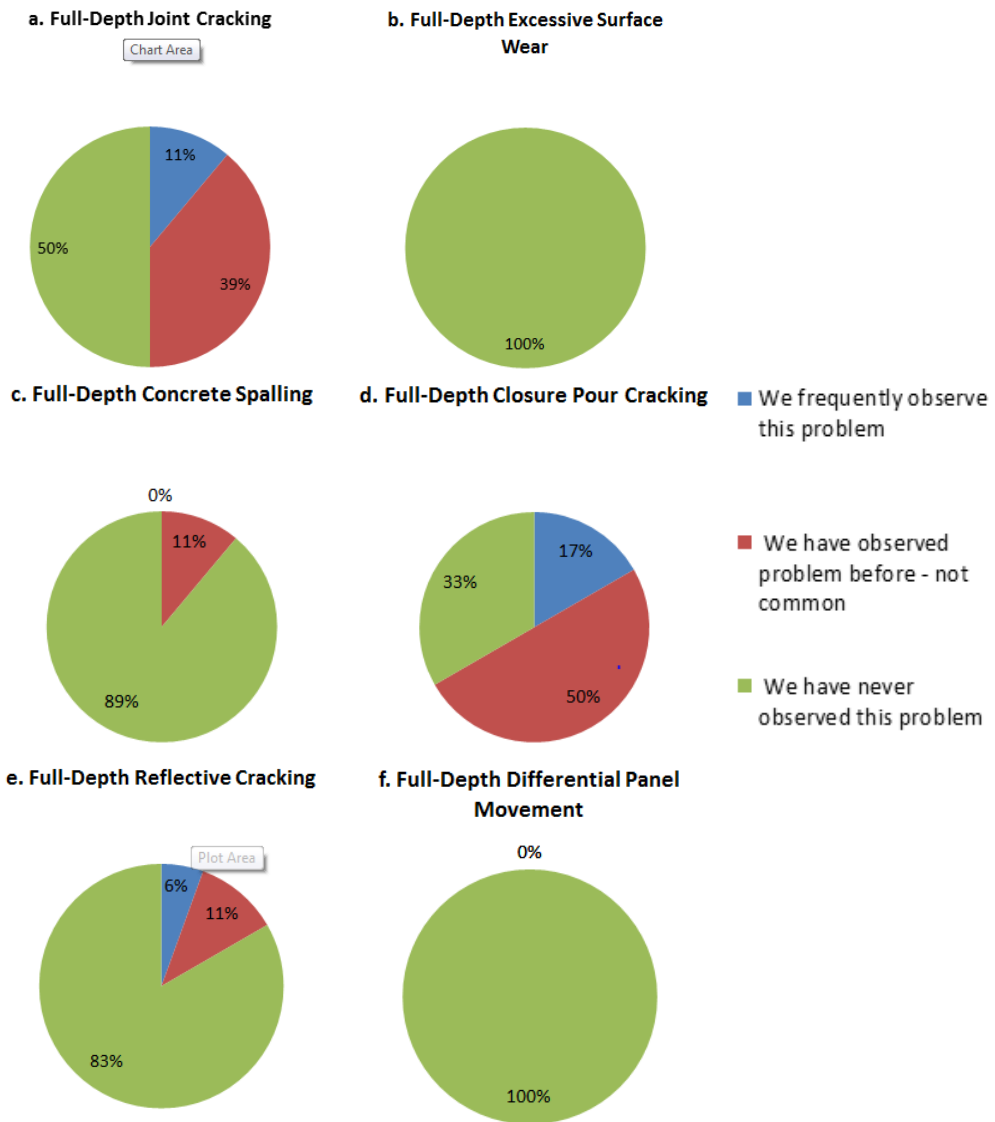


Figure 3.18: Evaluation of performance problems for full depth panels, shown as percentage of states selecting each rating of the problem

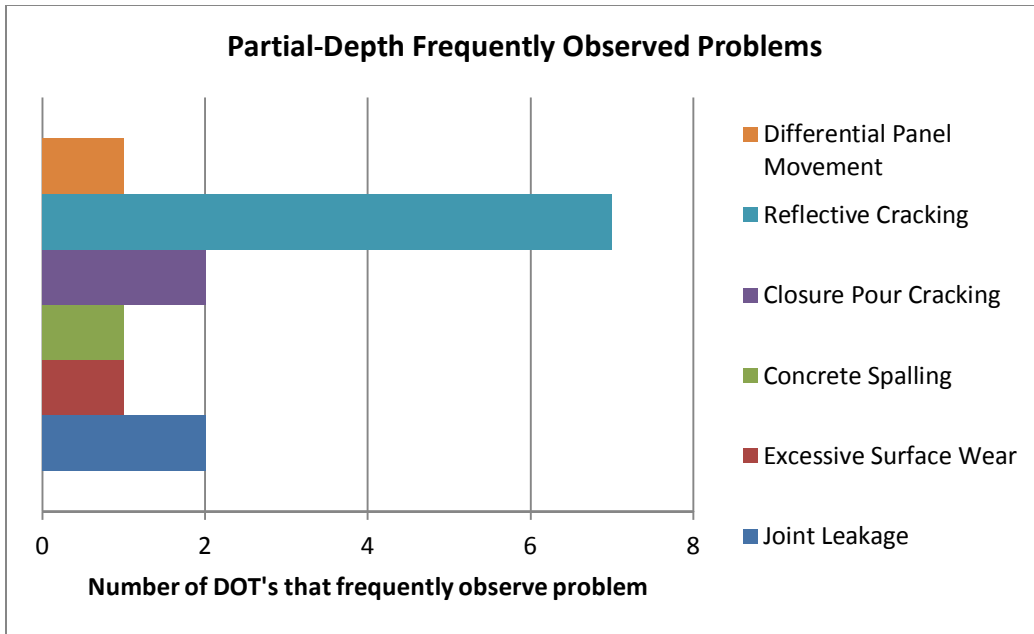


Figure 3.19: Number of DOTs indicating a frequently observed problem for partial depth deck panels

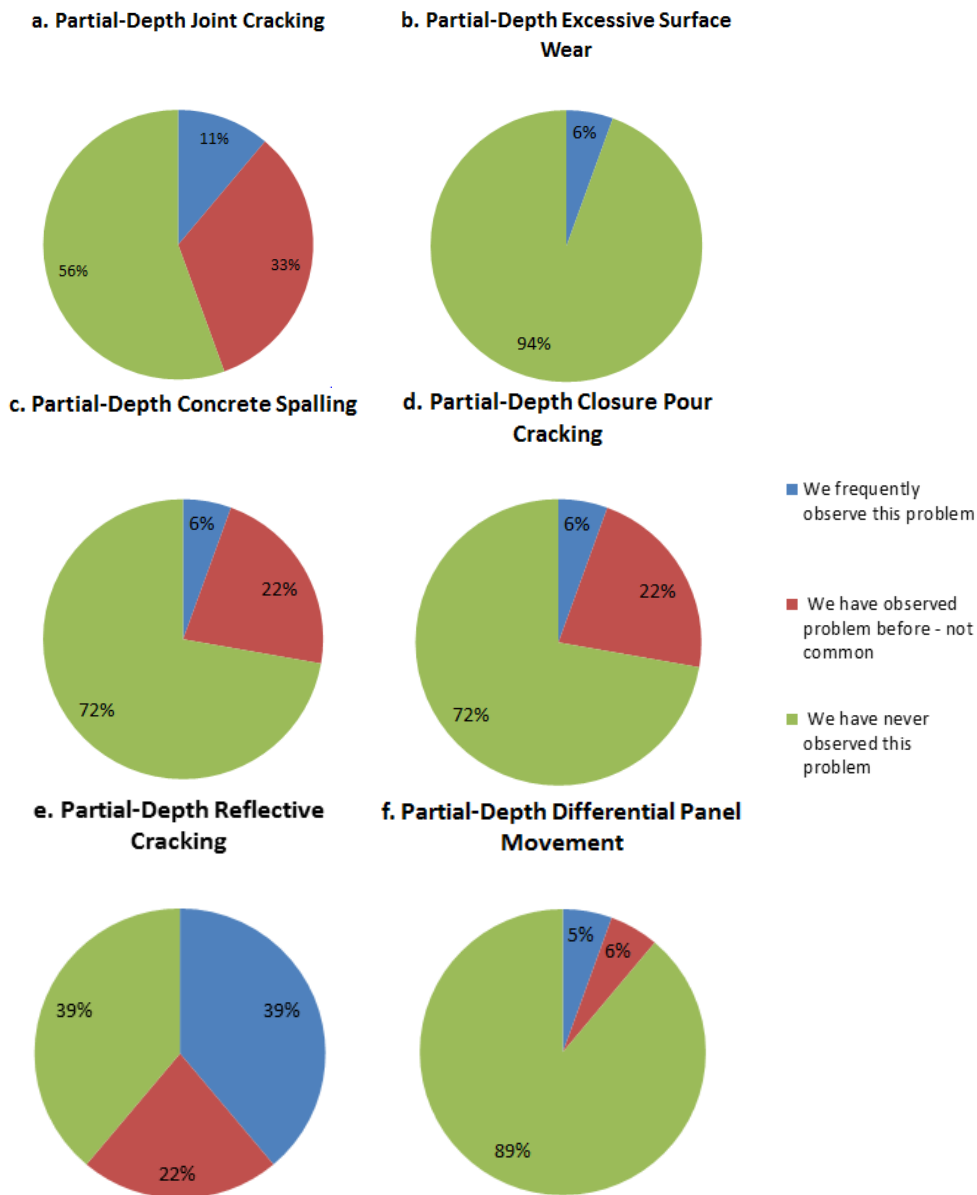


Figure 3.20: Evaluation of performance problems for partial depth panels, shown as percentage of states selecting each rating of the problem

### 3.4.2 Ratings of Deck Panel Performance

At the conclusion of the survey, DOTs were asked to evaluate the overall performance of full-depth and partial depth deck panel systems. Respondents were asked to rate the panels on a scale with four options: “poor”, “fair”, “good” and “excellent”. A rating of “poor” indicated that the prefabricated deck panel system had numerous problems and did not perform as expected, while a rating of “excellent” meant that the system had no issues and only required standard maintenance. The performance of full depth deck panels was rated highly by the DOTs with 17 out of 20 selecting a rating of good or excellent. The partial depth panels received mixed reviews with 11 out of 20 DOTs

selecting a rating of fair or poor. The poor rating of partial depth deck panels was largely due to performance issues and is related to the reflective cracking discussed above. Even though many DOTs indicated an unsatisfactory rating for partial depth deck panels, Texas, which uses the most partial depth panels, indicated an excellent rating for partial depth deck panel systems. Figures 3.21 and 3.22 show the number of DOTs that indicated each performance rating for full and partial depth deck panels.

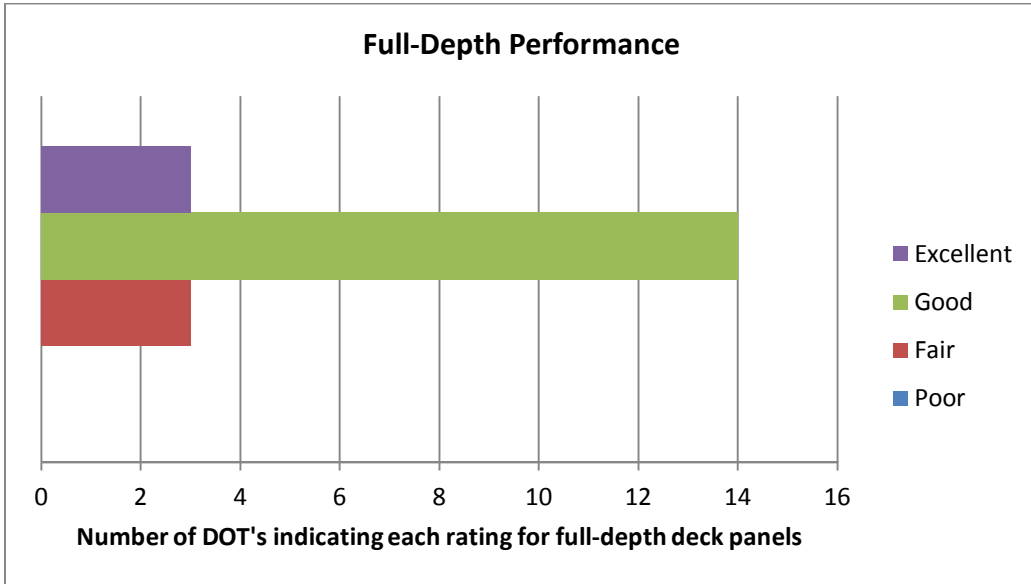


Figure 3.21: Full-depth deck panel performance rating

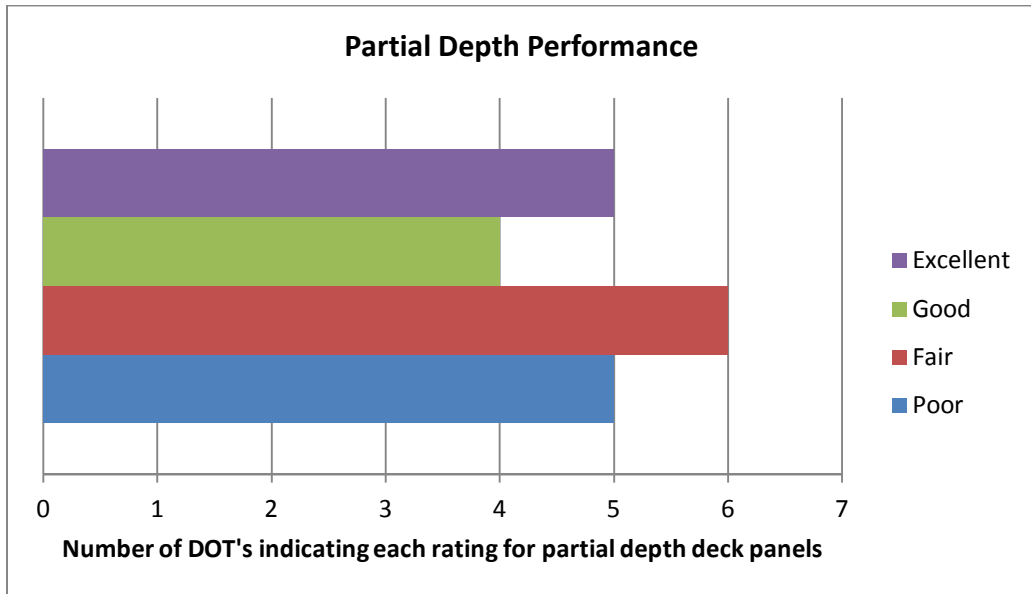


Figure 3.22: Partial-depth deck panel performance rating

### 3.4.3 Preference Trends for Full-Depth vs Partial-Depth Panels

An open ended question was asked to determine whether state DOTs preferred full-depth or partial-depth panel systems. Figure 3.23 shows the percentage of states preferring

partial depth or full-depth deck panels and percentage indicating no preference. The majority of respondents either prefer full-depth panels or currently do not have a preference. Multiple DOTs reported being in the experimental phase for full-depth panels and therefore, currently do not have an opinion. Colorado reported preferring partial-depth to full-depth deck panels because using partial-depth panels is standard practice in the state. Iowa, Minnesota, and Louisiana reported preferring full-depth deck panels because severe performance issues had been observed with partial depth panels.

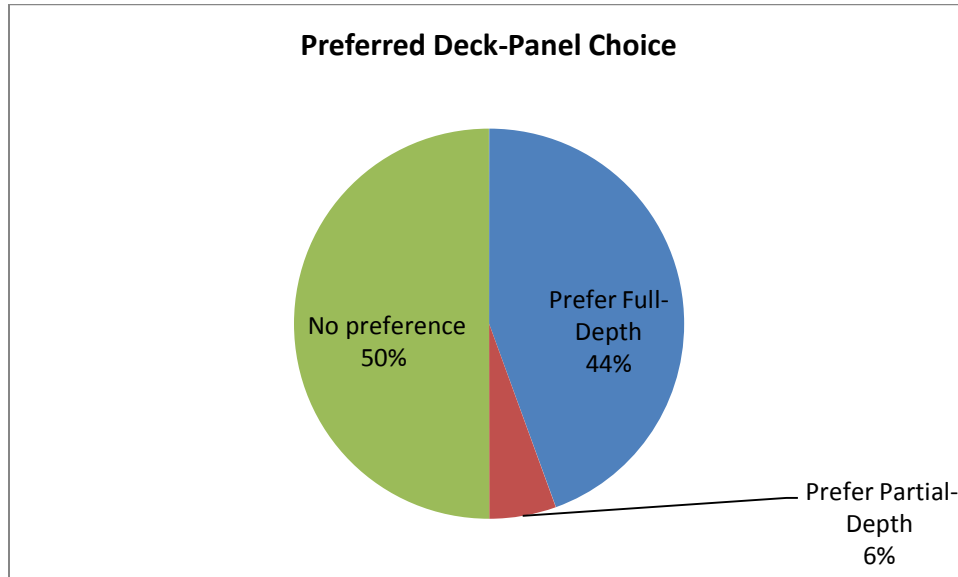


Figure 3.23: Preferred deck panel system

### 3.5 Deck Panel Limitations

Consensus regarding limitations on the use of prefabricated deck panel systems appears to be lacking in the literature. Questions regarding skew, curvature and superelevation were included in the survey to determine if DOTs had made decisions to limit deck panel implementation under certain circumstances. Figure 3.24 shows the percentage of states fully restricting, partially restricting, or not restricting the use of full-depth or partial-depth panels for bridges with skew, curvature and superelevation. Figure 3.24 shows that use of full-depth deck panels was less restricted than partial-depth panels. Most DOTs did not place a restriction on the use of full-depth deck panels regardless of skew, curvature or superelevation. Among all parameters, curvature prompted restrictions for the greatest number of states; for instance 28% of states disallowed the use of full-depth deck panels for bridges with curvature. In general, DOTs did not indicate specific limits, but four states indicated maximum skew angle of 30 degrees, and two states indicated a maximum superelevation (2% and 4%). Some DOTs indicated that limitations had not been placed on the implementation of deck panels was because the panels had not been used enough to develop guidelines for the use of deck panels.

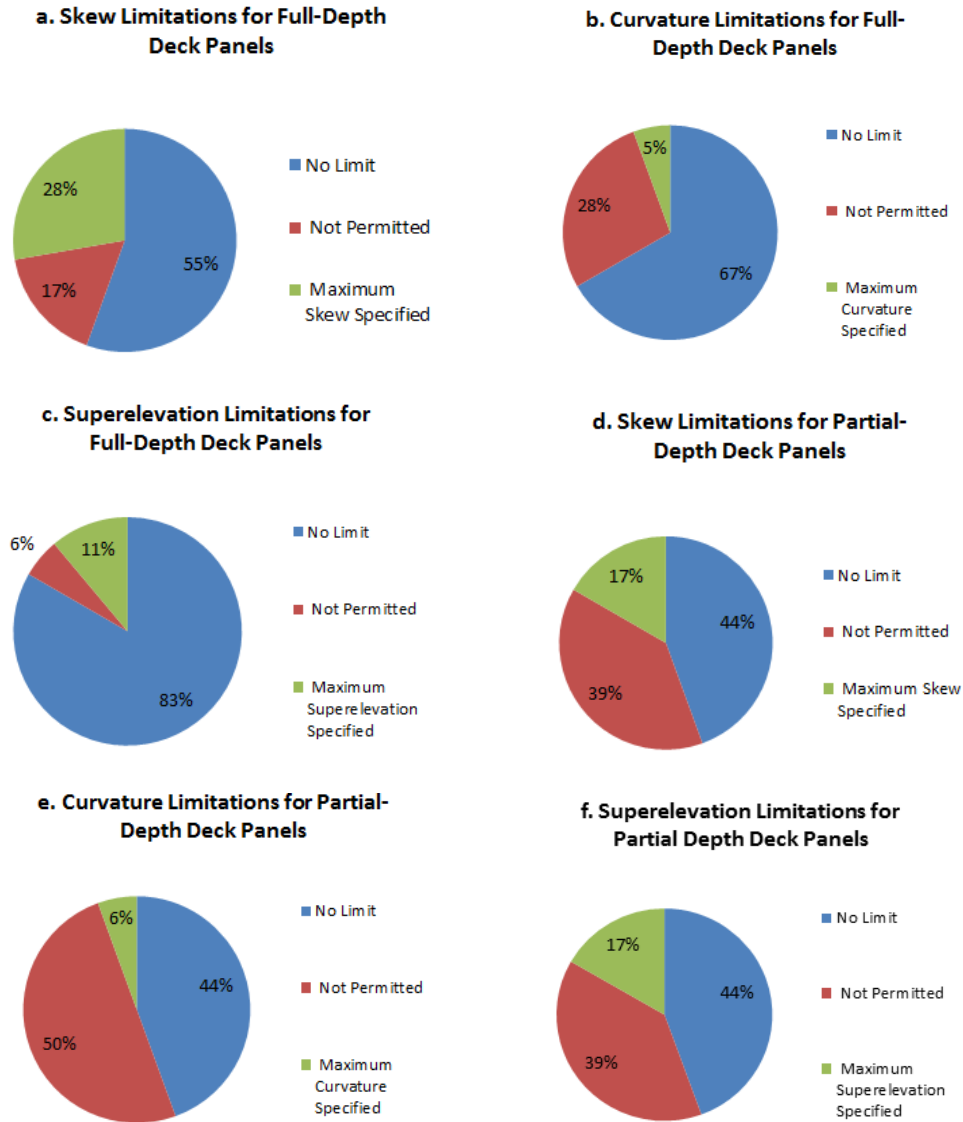


Figure 3.24: Percentage of states limiting the use of prefabricated deck panels

More restrictions were placed on the implementation of partial-depth deck panels than full-depth deck panels. Partial depth deck panels were not permitted in almost half of the DOTs when the bridge had skew, curvature or superelevation. However, 44% of DOTs indicated no limit had been placed on the implementation of partial depth deck panels when the project included skew, curvature or superelevation. Specific limits that were indicated were a maximum skew angle of 40 degrees, and maximum superelevation in the range of 3-5%.

Another limitation on prefabricated deck panels is the maximum panel size as governed by transportation considerations. Several states specified a minimum or maximum length, width, or depth applied to deck panels based on transportation limits. Table 3.1 shows the ranges for the maximum length and width that states had imposed for the transportation of panels, as well as a minimum depth.

Table 3.1: Transportation limits placed on full-depth deck panels by states

Transportation Limits Range Among States	
Length (maximum allowed)	10 to 41 ft.
Width (maximum allowed)	6 to 12 ft.
Depth (minimum allowed)	3.5 in. to 8.25 in.

### 3.6 Implementation of Site Casting

Nevada has an added challenge in implementing ABC due to the current lack of a certified precast concrete plant in the state. Because of this, it was important to determine the feasibility of site casting different components of a bridge. The survey asked whether site casting had been used for girders, columns, pier caps, footings, abutments, full-depth deck panels and partial-depth deck panels. For each component, respondents were asked whether site casting: has been “used regularly”, “used sometimes depending on the project details”, “attempted once or twice”, or “never been attempted”. Figure 3.25 shows the percentage of DOTs that indicated the frequency of site-casting for each type of component. The responses from the DOTs indicated that site casting has not been attempted for any bridge components in a majority of states. Pier caps and abutments were reported as being site-cast the most often compared to other components. Full-depth and partial-depth deck panels have been site cast in a few states, but site casting of these components is very infrequent. If NDOT desires to use site casting for deck panels, the authors recommend contacting Texas and Utah for specifics on usage of site casting. The numbers reported in Figure 3.25 should be interpreted with caution. Based on the authors’ knowledge of site casting in various states, it appears that a small number of respondents may have misinterpreted site casting as CIP construction.

As discussed in Section 2.5.3, when Utah began implementing ABC construction, contractors were selected that were not certified for precast construction. Rather than opt for site casting, Utah responded to this situation by requiring the contractor to obtain certification prior to building the project, but provided financial compensation for requiring the certification.

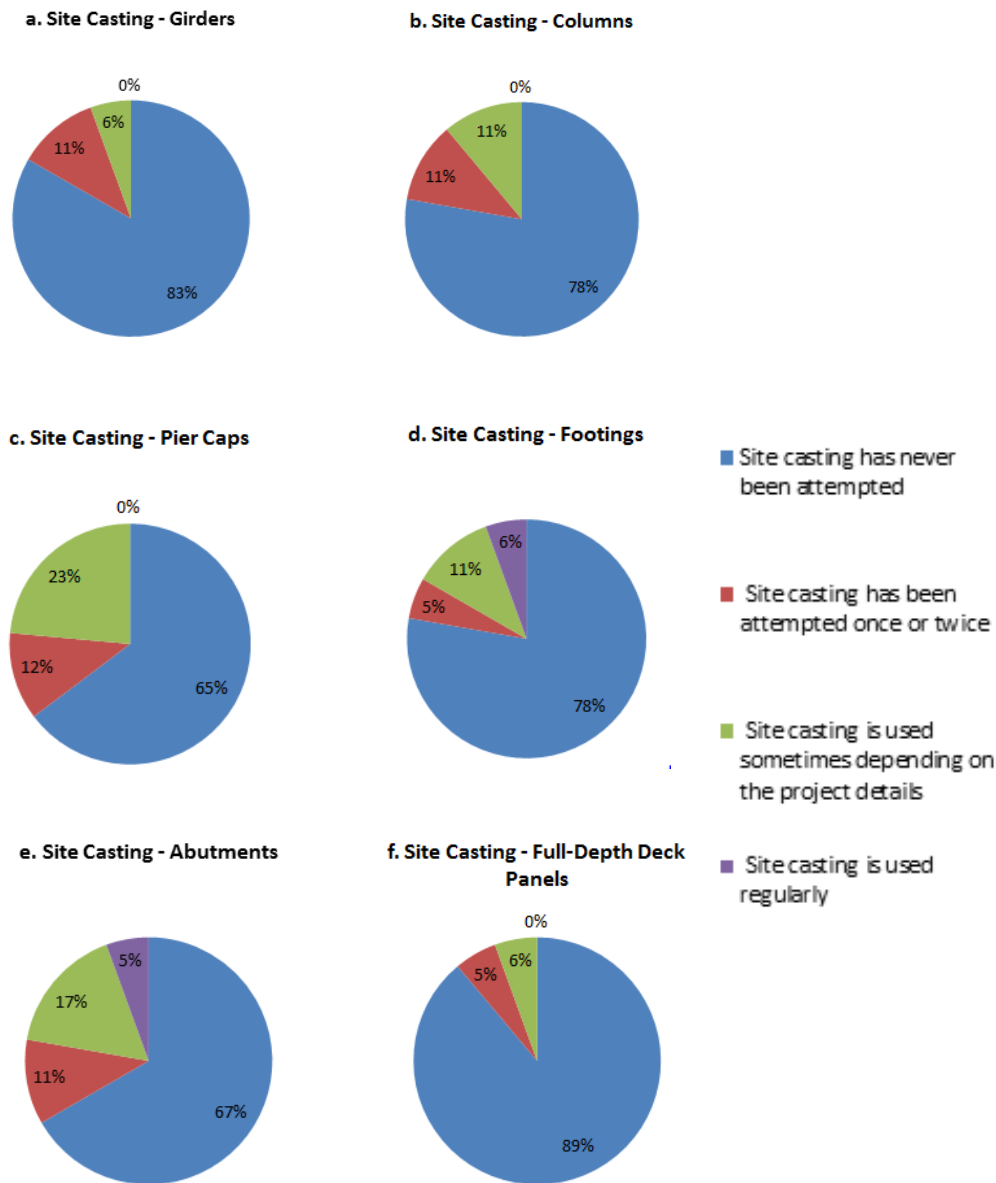


Figure 3.25: Percentage of states using site casting of various bridge components

### 3.7 Recommendations for Nevada Implementation

The main goal of the survey was to develop recommendations on panel and connection type for the Nevada DOT by determining what has been successfully applied in other states. To develop an overall perception of performance for each connection detail, survey responses on implementation of specific connection details (Figures 3.6, 3.9, 3.12) were superimposed with performance evaluation responses for corresponding full-depth and partial depth panels (Figures 3.21, 3.22). Figures 3.26, 3.27, and 3.28 present the implicit performance ratings for each connection detail according to this method. Specifically, if a DOT indicated frequent use of a specific connection, the DOT's

associated general rating for the panels was applied toward that connection. For example, one DOT indicated frequent use of the female-to-female shear key connection and rated their experience with full-depth deck panels as “good”; thus the female-to-female shear key was assigned one “good” rating. Increasing number of “good” and “excellent” ratings in Figures 3.26 – 3.28 indicates more widespread favorable impression of the connection.

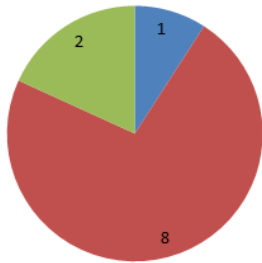
Recall that the full-depth panel-to-panel connections reported as frequently used by the most states were the PCI female-to-female connection (Figure 3.6a) for the transverse connection and the Oregon DOT cast-in-place joint (Figure 3.6g) for the longitudinal connection. Each of these connections were used by DOTs that rated full-depth panel performance as good, and the connections did not have any poor ratings associated with their use. The other full-depth panel-to-panel connections such as the diamond shear key were not commonly used or were associated with DOTs that did not rate performance of full-depth deck panels as favorable as the DOTs that used the PCI or ODOT connections. Two alternative approaches for panel-to-panel connections have been found to help prevent leakage: post-tensioning and UHPC. The use of UHPC will lead to less space between the panel-to-panel connections because of the decreased anchorage length requirements and also will simplify the fabrication and installation of the panels. However, little long-term performance data is available for full-depth decks with UHPC joints. Post-tensioning has been used by many DOTs to prevent leakage. Because of the tradeoffs between the two methods, it is believed that either approach could be effective.

DOTs indicated four options for full-depth panel-to girder connections that were commonly used. The steel girder with shear studs and grouted haunch connection (Figure 3.9a), which is the only steel girder connection in current use by DOT’s, was associated with DOT’s that rated full-depth deck panel performance as generally favorable. Specifically, the connection received seven good ratings and one fair rating, and thus appears to be an acceptable connection for steel girder panel-to-girder connections. All three commonly used options for concrete girders: steel studs, hooked reinforcement, and steel stirrups (Figure 3.9d, e, and f) received good reviews and were all used with the same frequency among states. Because the shear stud configuration (Figure 3.9a) and the prestressed concrete girder shear stud connection (Figure 3.9d) were used the most frequently among states with favorable performance reviews, both of these full-depth deck panel-to-girder connections are recommended.

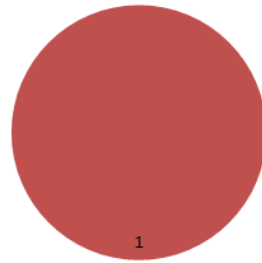
The performance of partial depth panels was rated by DOTs to be significantly less satisfactory than the performance of full-depth panels. Because the majority of DOTs indicated having no preference between full-depth or partial-depth deck panels or preferring full-depth panels, the application of full-depth panels by Nevada is recommended prior to attempting to include partial-depth panels in standard construction practices. If partial-depth panel systems are selected by NDOT, the survey results suggest that any of the options for partial depth panel-to-girder connections are acceptable and no strong preference is indicated (Figure 3.28). Both steel and concrete girder panel-to-girder connection details were highly rated as well as the tub girder connection detail. The transverse panel connection detail developed by Texas DOT was the only panel-to-panel connection included in the survey, and was used frequently by states that rated the performance of partial-depth panels systems to be good.

In summary, full-depth deck panels are recommended for Nevada because of the higher ratings for full-depth deck panels compared to partial-depth deck panels. The recommended panel-to-panel connection details are the PCI female-to-female shear key (Figure 3.6a) for the transverse connection and the ODOT cast-in-place connection (Figure 3.6g) for the longitudinal connection. Either longitudinal post-tensioning or UHPC should be used to help prevent joint leakage. The recommended full-depth panel-to-girder connection is the PCI detail for both steel (Figure 3.9a) and prestressed concrete (Figure 3.9d) girders. If partial depth deck panels are implemented in Nevada, the Texas specifications on partial-deck panel connections (Figure 3.12b, c, e) are recommended for NDOT because of their positive ratings of partial-depth deck panels and extensive experience.

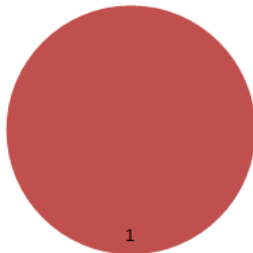
a. Female to Female Shear Key



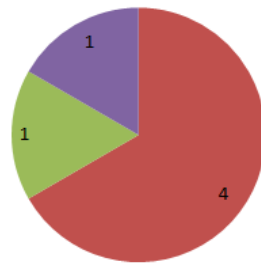
b. Female to Female Shear Key with Welded Steel Plate



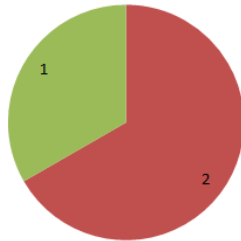
c. Female to Female Shear Key With HSS



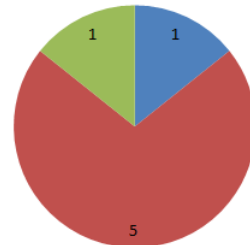
d. Female to Female Diamond Shear Key



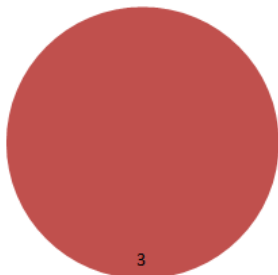
e. Female to Female Shear Key with Bent Reinforcement



f. Longitudinal Cast-In-Place Joint



g. Longitudinal Cast-In-Place Joint Over Girder



h. Longitudinal Joint With Spliced Reinforcement

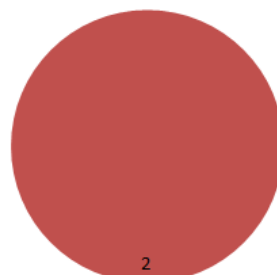
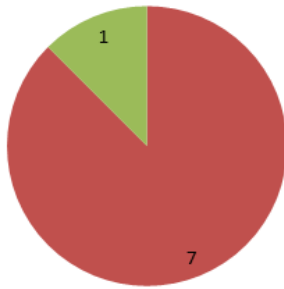
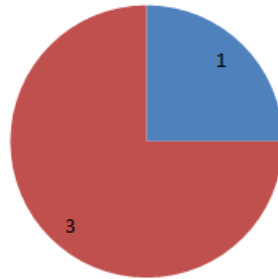


Figure 3.26: Connection ratings for full-depth panel-to-panel connections

**a. Steel Girder with Shear Studs and Grouted Haunch**



**b. Prestressed Concrete Girder with Shear Studs**



**c. Prestressed Concrete Girder with Projected Reinforcement**

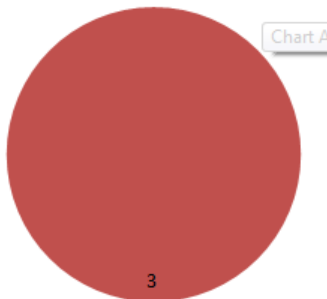


Chart A

**d. Prestressed Concrete Girder with Stirrups**

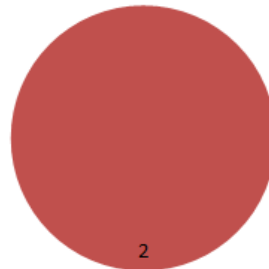


Figure 3.27: Connection ratings for full-depth panel-to-girder connections

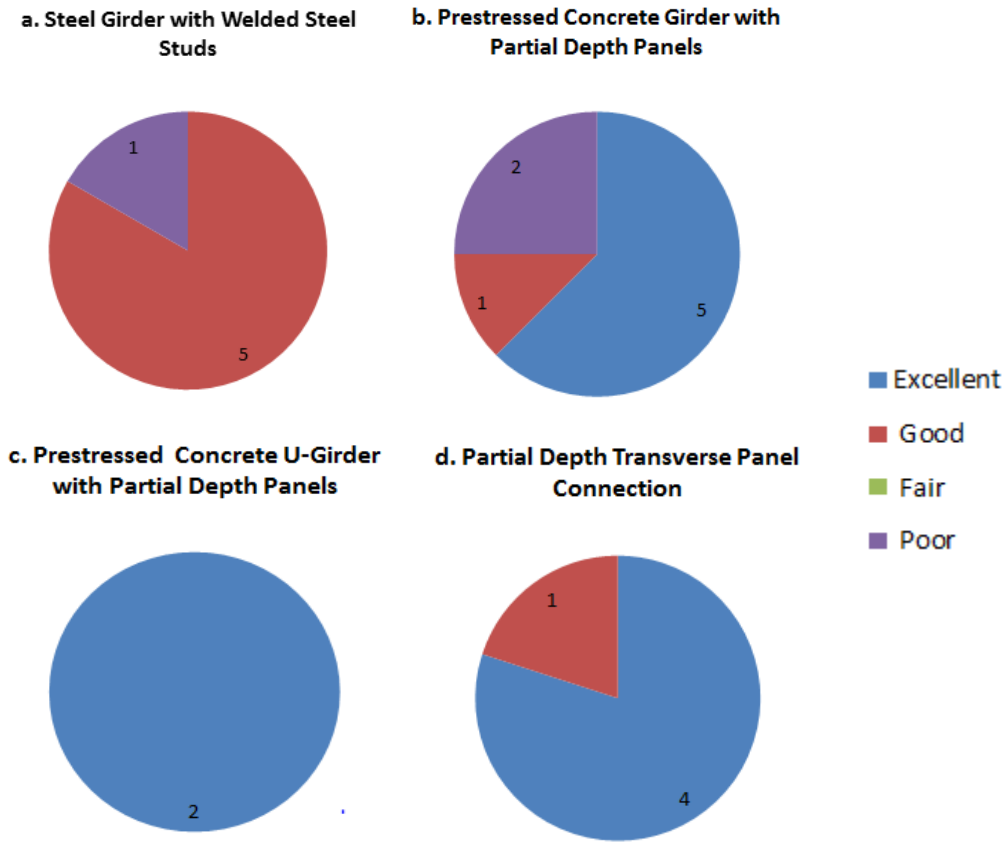


Figure 3.28: Connection ratings for partial-depth panel-to-girder connections and panel-to-panel connections

## **Chapter 4: Specification Development and Overview**

### **4.1 Introduction**

Project Task 2 consisted of assembling specifications for NDOT's implementation of prefabricated deck panels. The guidelines were developed from a review of existing national and state-adopted guidelines as described in Chapter 2, and a survey of current practices by state DOTs as described in Chapter 3. The survey results indicated that specifications and drawings from the PCI Northeast Full Depth Deck Panel Guidelines (PCI, 2011a) were the most widely used, and have been evaluated favorably by most agencies that have adopted them. As a result, the PCI Northeast Guidelines with modifications are recommended for adoption by NDOT. The guidelines presented here represent the PCI Northeast Guidelines with supplemental information as needed from other sources. Sources of supplemental information include: 1) the State of the Art Report on Full-Depth Deck Panels (PCI, 2011b), 2) Oregon Department of Transportation (ODOT) prefabricated deck panel guidelines (ODOT, 2015), 3) Utah Department of Transportation (UDOT) deck guidelines (UDOT, 2015), and 4) results from the survey of DOT current practices.

The specifications can be found in Appendix C, formatted as follows: the main numbered sections (e.g. 1.1) and corresponding commentary sections preceded by C (e.g. C1.1) are exact replications of the PCI Northeast Full Depth Deck Panel Guidelines (PCI, 2011a). Supplemental commentary sections that correspond to the numbered sections are preceded by SC (e.g. SC1.1). Appendix A of the specifications contains the drawings from Appendix A of PCI (2011a). An example illustrating the design of full-depth deck panels taken from PCI (2011b) can be found in Appendix B of the specifications.

### **4.2 Design Specifications Overview**

Section 1 of the design specifications contains general information about the use of full-depth prefabricated deck panels. The PCI specifications outline the types of bridge structures and characteristics of bridges (e.g. skew, curvature) that can accommodate full-depth panels.

Section 2 describes the material properties of typical prefabricated deck panels. The original PCI document erroneously specifies concrete properties with a description of rebar. Because of this, supplementary commentary from the PCI State of the Art Report (PCI, 2011b) is used to specify the concrete properties. Other material properties outlined in the specifications include the mild steel reinforcement, the prestressing steel, the post-tensioning ducts, the anchorage devices, and the grout used for the joints. Additional information from a UDOT report containing a grout mix design is included as supplementary commentary in Section 2.6.

Section 3 summarizes the design requirements. Sections 3.2, 3.6, 3.8, 3.10, 3.12 and 3.13 required additional commentary beyond what was provided by PCI. These extra provisions are described below. In the survey, multiple states limited prefabricated full-depth deck panels to bridges with skews no greater than 30° as shown in Figure 2.24a. To account for this input, supplementary commentary is included in Section 3.2 regarding

skew limitations as limitations are not discussed in the PCI document (PCI, 2011a). Also, extra information from the PCI State of the Art Report (PCI, 2011b) is included regarding longitudinal joints, cross slopes, superelevation, panel overhang, and longitudinal reinforcement. Additional information from PCI (2011b) is also included in the supplementary commentary of Section 3.6 that describes how to design the panel in the transverse direction, and is detailed later in Chapter 5. Transportation limits are an additional design requirement that have been a controlling factor for several states. Information about the limits from the survey are included Section 3.8. Section 3.10 summarizes the longitudinal post-tensioning used for deck panels. Because UHPC joints are not discussed in the PCI documentation but are used as a substitution for longitudinal post-tensioning, a UHPC joint design method based on information from ODOT (2015) is included in the supplementary commentary. In the supplementary commentary of Section 3.12, design specifications from UDOT describe the use of closure pours with full-depth deck panels (UDOT, 2015). Section 3.13 describes issues related to curved bridges. In this section, PCI allows for the use of full-depth panels on bridges with curvature. However, because of the problems with curved bridge applications reported in the survey, the supplementary commentary recommends that initial implementation of full-depth deck panels by NDOT are limited to bridges without curvature. Postponing implementation of prefabricated panel on curved bridges will allow NDOT to gain experience before attempting complicated bridge configurations.

Section 4 reviews construction procedures and other considerations for the implementation of full-depth deck panels. In Section 4.3, casting tolerances are discussed. PCI and most DOTs reported that certified precast plants are located in the vicinity of construction and generally contracted to cast the panels. Because Nevada does not have a certified precast plant, provisions for site casting are included as this technique will most likely be employed by NDOT. All other construction information directly replicates PCI (2011a).

## **Chapter 5: Full-Depth Panel Design Process**

### **5.1 Introduction**

While the existing specifications, as described in the previous chapter, can be used to set the general design properties of full-depth panels; every panel system must be designed to handle all appropriate loads. The individual deck panels, panel-to-panel connections, panel-to-girder connections, and the composite deck system should all be designed to accommodate any applied loads. The primary loads are dead loads (self-weight) and live loads (traffic), which induce shear and flexure in the panels. Because the deck is composed by connecting several individual panels, the following components must be checked to ensure proper deck behavior: the transverse panel-to-panel joints, panel-to-girder connections, transverse prestressing steel, longitudinal post-tensioning or UHPC, and the longitudinal joint if applicable. Deck joints are typically weaker than the panels, and have experienced a number of problems as reported by state DOTs. Special attention should be given to the joints to ensure that joint integrity is maintained throughout the life of the bridge. The overall design approach and many of the design considerations discussed in this chapter are taken from Appendix D – Design Example of PCI (2011b).

To expedite the design procedure, a design aid spreadsheet has been created using Microsoft Excel for this project. The spreadsheet can be used to design the full-depth deck panel system from start to finish without requiring extensive modeling or other outside resources. However, because spreadsheet calculations alone may not account for all complexities encountered in design, two design methods have been considered. With the simplified design method, each component is designed solely based on equations embedded into the design aid spreadsheet. If the deck panel system is sufficiently simple, it can be designed using the spreadsheet alone and no additional analysis is needed. The model based design method also uses the design aid spreadsheet for many of the design calculations, but allows the user to input information determined from other sources such as a computational or finite element model to improve the accuracy of the results. Also, the model based design method incorporates iteration for some components; for instance, longitudinal post-tensioning is designed initially using the spreadsheet equations, followed by validation and or possible adjustment of the details using a structural model. The simplified design method applies to bridges with basic geometry while the model based design method applies to complex bridges that have unique properties such as large skew or curvature.

### **5.2 Simplified Design Method**

#### **5.2.1 General Properties**

The design aid spreadsheet is organized into several sections, each of which calculates the properties for different components of the panel design. The Bridge Properties section in the spreadsheet requires user input for all of the geometric information for the bridge. Span length, number of spans, bridge width, overhang width, panel depth, panel width, and parapet height are all specified. These properties are used to determine the design dead load and its effects on the bridge. Information about the girders, including the girder type, spacing, geometry, and number of girders is also input; these details are used to

calculate the girder contribution to the dead load and the moment due to live load in the transverse direction of the bridge. Material properties for the deck panel concrete, girder steel or concrete, conventional steel reinforcement, and the prestressing steel are also input into the spreadsheet. All of these properties are entered into cells A1:C59.

### 5.2.2 Loads and Load Combinations

The design aid spreadsheet calculates both the dead load and live load applied to the panels in the Load Assignments section using the properties mentioned in Section 5.2.1. The self-weights of the deck panels and wearing surface are found by multiplying the unit weight of the concrete or asphalt by the corresponding depths. These properties are used to calculate unfactored area loads for the whole deck for both structural component (DC) and wearing surface (DW) loads in cells F2 and F3. These unfactored area loads are then multiplied by the corresponding load factor from AASHTO LRFD Table 3.4.1-1 and 3.4.1-2 (AASHTO, 2012). In the deck panel design, load combinations Strength I, Service I and Service III are all used for various components.

### 5.2.3 Design of Transverse Prestressing Steel

The deck is designed with the strip method as described in AASHTO LRFD 4.6.2.1 (AASHTO, 2012). For this method, the deck is assumed to be a continuous beam in the transverse direction and the transverse cross-section (concrete and steel reinforcement) are designed accordingly. The maximum positive and negative moment are calculated, followed by the required amount of steel, and the depth of the concrete section is checked for sufficiency. In this design aid spreadsheet, the user can conservatively estimate the maximum moment across the width of the deck from Eq. 5.1:

$$M = \frac{wl^2}{y} \quad (5.1)$$

where  $w$  is the distributed load calculated from panel properties,  $l$  is the specified girder spacing, and  $y$  is a coefficient with recommended value of 10 or 12 as determined by the user. Alternatively, the user can compute and input an exact moment using a structural analysis package or formula. The estimated moment for DC and DW by Eq. (5.1) is computed in cells F7 and F8, while the user may enter the exact moment for both dead load components, and live loads in cells F10-F15.

Transverse reinforcement of full-depth deck panels is generally prestressed. The spreadsheet assumes two layers of prestressing strands, one layer each in the top and bottom of the panel. The required amount of prestressing steel is calculated iteratively because of the losses associated with prestressing. Initial values for prestress loss, tendon size, and bar quantity are assumed to start the process. The input for the number of prestressing strands and the preliminary prestressing steel calculations are performed in the Prestress Steel Estimate section. The allowable tensile stress or modulus of rupture  $f_r$  in prestressed members is  $0.19\sqrt{f'_c}$  where  $f'_c$  is the compressive strength of the deck concrete. This allowable tensile stress is equated to the demand stress due to bending and axial force, and used to solve for the prestress force,  $P_{pe}$  with the following equation:

$$\sigma_{allowable} = \frac{P_{pe}}{A} - \frac{M}{S} \quad (5.2)$$

where  $M$  is the transverse moment,  $A$  is the calculated cross sectional area and  $S$  is the calculated gross section modulus of the deck panel. Equation (5.2) is rearranged to calculate the force  $P_{pe}$  required by the prestressing steel. The number of strands,  $n$ , is then found using:

$$n = \frac{P_{pe}}{A_{ps}f_{pe}}, \quad (5.3)$$

where  $A_{ps}$  is the user defined area of one prestress strand, and  $f_{pe}$  is the calculated effective stress in the strands after losses. These assumed initial values are found within cells E36-G45.

The exact losses must be calculated in subsequent iterations until the results converge. All prestress loss calculations are completed in the Prestress Losses section of the design aid spreadsheet. Elastic shortening is calculated according to AASHTO LRFD 5.9.4.2.3a-1 (AASHTO, 2012). Elastic shortening losses are assumed to be 1% of the initial prestress. The loss is then calculated using:

$$\Delta f_{pES} = \frac{E_p}{E_{ct}} f_{cgp}, \quad (5.4)$$

where  $E_p$  is the user defined modulus of elasticity of the prestress strand,  $E_{ct}$  is the user defined modulus of elasticity of the concrete at the time of transfer, and  $f_{cgp}$  is the concrete stress at the center of gravity of the prestressing tendons due to the prestressing force immediately after transfer and the self-weight of the member at the section of maximum moment, calculated as  $\frac{P_{pe}}{A}$  where  $P_{pe}$  is the total calculated prestressing force applied to the panel. If the loss is not close to the assumed value, the user is directed to recalculate using the updated values. The design aid spreadsheet calculates elastic shortening losses in cells K1-M10.

Long-term losses are also factored into the design including creep, shrinkage and relaxation. These losses are calculated considering the time between transfer and deck installation, and at the end of the service life of the panel. These losses are calculated according to AASHTO LRFD 5.9.5.4 and 5.4.2.3 (AASHTO, 2012). Shrinkage loss is calculated as:

$$\Delta f_{pSR} = \varepsilon_{sh} E_p K_{id} \quad (5.5)$$

for loss between transfer of prestress force and deck placement and

$$\Delta f_{pSD} = \varepsilon_{bdf} E_p K_{id}, \quad (5.6)$$

for loss between deck placement and end of service life, where  $\varepsilon_{sh}$  is the calculated concrete shrinkage strain of the girder between the time of transfer and deck placement,  $\varepsilon_{bdf}$  is the calculated shrinkage strain of the girder between time of deck placement and end of service life, and  $K_{id}$  is the calculated transformed section coefficient that accounts for time-dependent interaction between concrete and bonded steel in the section being

considered for time period between transfer and deck placement. Creep loss is calculated as:

$$\Delta f_{pCR} = \frac{E_p}{E_{ci}} f_{cgp} \psi_b(t_d, t_i) K_{id}, \quad (5.7)$$

for loss between transfer of prestress force and deck placement and

$$\Delta f_{pCD} = \frac{E_p}{E_{ci}} f_{cgp} \psi_b[(t_f, t_i) - \psi_b(t_d, t_i)] K_{df} + \frac{E_p}{E_{ci}} \Delta f_{cd} \psi_b(t_f, t_d) K_{df}, \quad (5.8)$$

for loss between deck placement and end of service life, where  $\psi_b(t_d, t_i)$  is the calculated creep coefficient at time of deck placement due to loading introduced at transfer,  $\psi_b(t_f, t_d)$  is the calculated creep coefficient at end of service life due to loading at deck placement,  $E_{ci}$  is the user defined elastic modulus of the concrete at transfer, and  $K_{df}$  is the calculated transformed section coefficient that accounts for time-dependent interaction between concrete and bonded steel in the section considered for the time period between deck placement and end of service life. The time-dependent creep coefficients used to calculate long term losses are controlled by the following user-defined factors: relative humidity of the area, the time between casting and loading, and the anticipated lifespan of the deck. Relaxation loss is calculated as:

$$\Delta f_{pR} = \frac{f_{pt}}{K_L} \left( \frac{f_{pt}}{f_{py}} - 0.55 \right), \quad (5.9)$$

where  $f_{pt}$  is the calculated stress (updated value) in the prestressing strands immediately after transfer,  $f_{py}$  is the calculated yield stress of the prestressing tendon and  $K_L$  is a user defined coefficient equal to 30 for low relaxation strands and 7 for prestressing steel. Equation (5.9) applies to relaxation losses both at time of transfer and at end of service life as half of the relaxation is assumed to occur between transfer and deck placement and the other half is assumed to occur between deck placement and the end of the service life. Creep and shrinkage losses between transfer and deck installation are computed in cells K11-M27, while the losses between deck installation and end of service life are computed in K34-M46. Losses due to relaxation are computed in cells K28-M32 and L48.

Once losses have been calculated and factored into the prestress force, the maximum concrete stress and moment are checked using the Strength 1 load combination. The stresses due to positive and negative moment and the capacity calculations are found in the Panel Capacity section. Compressive stress limits are found in AASHTO Table 5.9.4.2.1-1 (AASHTO, 2012), where two limits are defined. The first case limits stresses due to the sum of effective prestress and permanent loads to be less than  $0.45f'_c$  in ksi (computed in cell Q4). The second case limits the total stress due to all effective prestress, permanent loads and transient loads to be less than  $0.6f'_c$  (computed in cell Q6). The allowable tensile stress is set at  $0.19\sqrt{f'_c}$ . The stresses in the section are then recalculated using Equation (5.2) with exact prestress losses using Service 1 moment. The updated stresses with exact losses are compared to the stress limits. If any of the stress limits (compression or tension) are exceeded, a design iteration is required.

The flexural strength check is performed using a strain compatibility approach from Section 8.2.2.5 of the PCI Bridge Design Manual and explained in detail in Appendix D of PCI (2011b). The tension force  $T$  in the prestressing tendons is computed iteratively starting with an initial estimate. The initial estimate for tension is:

$$T = A_{ps} f_{py} n, \quad (5.10)$$

where  $n$  is the user defined number of prestressing strands per panel (cell Q21). Equation (5.10) assumes that the combination of prestress and flexure will cause the tension force in the prestressing strands to approach the yield stress. Setting the tension force  $T$  equal to the compression force, the corresponding idealized depth of compression,  $a$ , is calculated using:

$$a = \frac{T}{0.85 f'_c b} \quad (5.11)$$

The neutral axis depth of the panel,  $c$ , is equal to:

$$c = \frac{a}{\beta_1}, \quad (5.12)$$

where  $\beta_1 = 0.85$  for 4 ksi and weaker concrete, 0.65 for 8 ksi and stronger concrete with linear interpolation for concrete strengths between the two values. The strain in the prestressing strand is calculated using the assumed values with the formula:

$$\varepsilon_p = \frac{0.003(d-c)}{c} + \frac{f_{pe}}{E_p}, \quad (5.13)$$

where  $d$  is the user defined distance from the top of the panel to the center of the prestress force for each layer. The strain compatibility approach uses a power stress-strain formula to compute the stress  $f_{ps}$  in the prestressing strands as a function of strain:

$$f_{ps} = \varepsilon_p E_p \left\{ Q + \frac{(1-Q)}{\left[ 1 + \left( \frac{E_p \varepsilon_p}{K f_{py}} \right)^R \right]^{\frac{1}{R}}} \right\} < 270 \text{ ksi}, \quad (5.14)$$

where  $Q$ ,  $R$  and  $K$  are calibration factors of 0.031, 7.36, and 1.04 respectively. The stress computed from Eq. (5.14) is compared to the assumed stress for both layers. If the computed stress  $f_{ps}$  is not close to the assumed stress  $f_{pe}$ , this computed stress replaces the assumed value in Eq. (5.10), and the calculations are repeated until the solution converges. These iterative calculations take place in cells P24-R58 of the design aid spreadsheet.

The converged solution, which represents the actual stress in the prestressing strands, is used to calculate the flexural strength of the panel. The ultimate capacity of the panel is computed using the conventional concrete flexural strength formula (cell Q60):

$$\phi M_N = \phi \left[ \frac{n}{2} A_{ps \text{ Top}} f_{ps \text{ Top}} \left( d_{\text{Top}} - \frac{a}{2} \right) + \frac{n}{2} A_{ps \text{ Bottom}} f_{ps \text{ Bottom}} \left( d_{\text{Bottom}} - \frac{a}{2} \right) \right], \quad (5.15)$$

and compared against the ultimate Strength 1 moment demand.

The final prestressing check is a minimum reinforcement limit. AASHTO LRFD 5.7.3.3.2 (AASHTO, 2012) specifies the minimum reinforcement as the amount sufficient to develop a nominal moment greater than 1.2 times the cracking moment. The cracking moment is calculated with the formula (cell Q70):

$$M_{cr} = S \left( f_r + \frac{P_{pe}}{A_{ps}} \right), \quad (5.16)$$

If the nominal moment is greater than the factored cracking moment, the design is sufficient. Otherwise, reinforcement must be added to the panel section.

#### 5.2.4 Panel to Girder Connection Design

The deck panels are made to form a composite section with the girders through welded studs or projected reinforcement from the girders that extend into pockets in the panel. To achieve full composite action between the deck and the girder, the connections must be checked to ensure adequate shear transfer. The connections are designed by making assumptions for pocket dimensions, spacing, and stud or rebar detailing per pocket, and then checking the capacity. These calculations are found in the Panel to Girder Connection Design section.

The demand for each girder line is calculated using the ultimate shear in the bridge. The ultimate shear is found using either basic mechanics formulas or a structural model. The shear demand per unit length,  $V_{h1}$  is calculated using C5.8.4.2-7 (AASHTO, 2012):

$$V_{h1} = \frac{V_1}{d_v} \quad (5.17)$$

where  $V_1$  is the maximum factored vertical shear in the bridge and  $d_v$  is the distance between the centroid of the tension steel and the mid-thickness of the slab.  $V_{h1}$  is divided by the number of girders to get a shear flow per girder line. This demand is divided by a resistance factor of 0.9 and multiplied by the width of the panel to get the factored shear for each girder line.

The capacity of the connection is calculated according to AASHTO LRFD 5.8.4.1-3 (AASHTO, 2012) (cell V12):

$$V_n = cA_{cv} + \mu(A_{vf}f_y + P_c) \quad (5.18)$$

where  $c$  is the cohesion factor (assumed to be 0.24 ksi for this application),  $A_{cv}$  is the area of concrete engaged in shear transfer,  $\mu$  is the friction factor (=1 assuming concrete placed against clean, hardened concrete with surface intentionally roughened to an amplitude of 0.25 in),  $A_{vf}$  is the area of the shear reinforcement crossing the shear plane,  $f_y$  is the specified shear reinforcement strength, and  $P_c$  is the specified permanent net compressive force normal to the shear plane. The shear capacity must be greater than the shear demand.  $A_{cv}$  and  $A_{vf}$ , and thus the capacity of the section, are controlled by the pocket dimensions, number of pockets per panel, and the number of welded studs or

projected U-bars. These parameters can be adjusted by the user to increase the capacity or optimize the design.

### 5.2.5 Longitudinal Post-Tensioning Design

AASHTO LRFD 9.7.5.3 (AASHTO, 2012) prescribes that the transverse joint have an average effective prestress of 0.25 ksi compression. Longitudinal post-tensioning is one approach that can be used to attain this level of compression. To keep all joints at 0.25 ksi compression, the applied post-tensioning should balance tension resulting from the bridge loads in addition to supplying the required prestress. The calculations for the longitudinal post-tensioning are located in the Longitudinal Post-tensioning section. First, the maximum negative moment  $M_{Long}^-$  across a joint due to bridge loading is computed from a deck analysis. From this moment, the maximum tensile stress is calculated from (cell V16):

$$\sigma_{Tension} = \frac{My}{I} \quad (5.19)$$

In a single span bridge, tension resulting from the bridge loading is 0 because the typical loading produces a positive moment at all superstructure locations that puts the deck in compression. In general, the required post-tensioning force  $P_{long}$  can be found with the following equation (cell V18):

$$P_{long} = (\sigma_{Tension} + 0.25 \text{ ksi})A_{long} \quad (5.20)$$

where  $A_{long}$  is the deck cross-sectional area in the longitudinal direction in square inches. The required number of post-tensioning bars is computed by dividing the required post-tensioning force by the effective prestress force,  $f_{pe}$  for one bar.

Temperature and shrinkage reinforcement is added to the section in addition to post-tensioning bars per AASHTO LRFD 5.10.8 (AASHTO, 2012). The design calculations are found in the Temperature and Shrinkage Reinforcement section. The required reinforcement area  $A_s$  per foot of panel is found using the formula:

$$A_s \geq \frac{1.3bh}{2(b+h)f_y}, 0.11 \text{ in}^2 \leq A_s \leq 0.60 \text{ in}^2, \quad (5.21)$$

where  $b$  is the width of the panel in inches,  $h$  is the depth of the panel in inches and  $f_y$  is the yield strength of the reinforcing bars in ksi. For this application, the user can specify either reinforcing mesh or rebar, and the calculations are performed in cells U21-W26.

### 5.2.6 UHPC Design

In contrast to longitudinal post-tensioning, designing full-depth deck panels with UHPC allows the deck joints to experience tension due to the ability of UHPC to carry a tensile load. This method eliminates the need for post-tensioning which decreases construction time and simplifies the design. Oregon Department of Transportation's (ODOT) design method was requested for this project as ODOT uses UHPC routinely for full-depth decks. ODOT uses a connection developed by FHWA (2010a). As this connection has already been tested, ODOT does not capacity check the connection for individual design cases; rather, the same connection is used for all applications. If the design case is simple,

the connection can be used without checking the capacity. If the connection integrity is a concern, each transverse connection is checked to determine the applied axial load at the location of the joint. The post-cracking tensile strength of UHPC is reported to be between 1 and 1.5 ksi by FHWA (2010b). The applied tensile force is compared to the UHPC tensile capacity to determine if the UHPC connection is sufficient for the application. If not, post-tensioning may be required.

### 5.2.7 Overhang Design

Additional considerations must be given to the overhang section of prefabricated deck panels to account for additional loads due to the barrier rail and vehicle impact. The overhang design method is based on a design example from PCI (PCI, 2011b), and uses the provisions from AASHTO LRFD 13.4.1 (AASHTO, 2012). The design approach is in the Overhang Design section in cells V32-V78. The calculations assume a standard cast-in-place rail. Currently, research to design precast barrier rails is underway, and though the technology has not been sufficiently developed to include in this report it may be an option in the future (ABC-UTC, 2016).

Two separate load cases are considered for the overhang design, as illustrated in Figure 5.1. For both cases, the overhang capacity is checked using the pretensioning reinforcement calculated in Section 5.2.3, and reinforcement is added as needed. The first case includes a horizontal vehicular collision load that is applied to the rail. The forces due to the collision load are evaluated in the deck cross-section at the inside edge of the rail, and 3 inches from the outside edge of the exterior girder. The design aid spreadsheet requires the user to specify the rail moment capacity  $M_{base}$  (cell V32) (used in the service moment summation), horizontal collision force  $R_w$  (cell V33) due to vehicle impact, and the critical length  $L_c$  (cell V34) of the wall failure mechanism. The properties for different rail configurations may be calculated per the user's choice, using the provisions from AASHTO LRFD (2012). The tension force in the deck per unit length is related to the horizontal collision force  $R_w$  using the following formula (AASHTO, 2012):

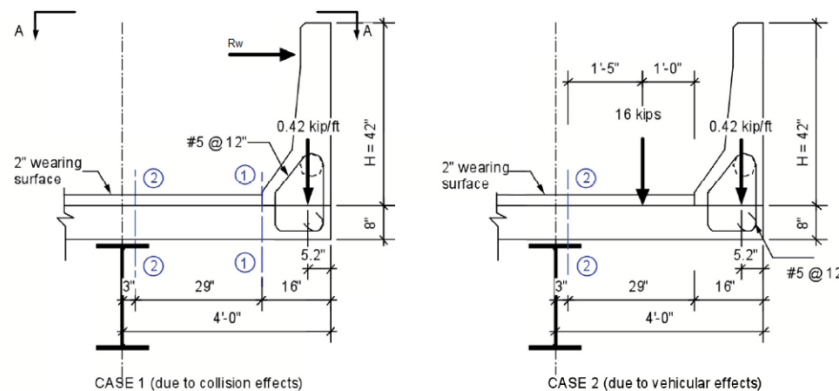


Figure 5.1: Load cases for overhang design (PCI, 2011b)

$$T_{base} = \frac{R_w}{L_c + 2H}, \quad (5.22)$$

where  $H$  is the user defined height of the rail. Essentially, the concentrated collision force is distributed over an effective deck length  $L_c+2H$ . The tensile force due to vehicle impact [Eq. (5.21)] is added to the tensile force due to bending from the rail and slab weight; the corresponding moment demand is evaluated and multiplied by the corresponding load factor for Extreme Event II for both sections 1-1 and 2-2.

Next, the panel capacities at Sections 1-1 and 2-2 are evaluated assuming the required amount of prestressing steel calculated from Section 5.2.3. If the initial amount of steel is inadequate, the steel area is increased until the required capacity is satisfied. The prestressing strands resisting the moment in the panels usually do not have sufficient development length at the ends to contribute to the overhang capacity, thus non-prestressed steel hooks are added at the end of the panels to attain sufficient bond between the concrete and the rebar. The development length of the steel hook is found using AASHTO LRFD Eq. 5.11.2.4.1-1 (AASHTO, 2012).

$$l_d = \frac{38d_b}{\sqrt{f'_c}} \quad (5.23)$$

where  $f'_c$  is in ksi,  $l_d$  is the development length and  $d_b$  is the diameter of the bar, both defined in inches. The calculated value of  $l_d$  is multiplied by 1.2 for epoxy coated rebar. The developed strength of the bars at distance  $l$  in inches from the end of the overhang is found using:

$$f_s = f_y \frac{(l-2 \text{ in})}{l_d}, \quad (5.24)$$

where  $f_y$  is the specified yield stress of the rebar, and the bar is assumed to be recessed 2 inches into the panel. Using the stress in the steel evaluated from Eq. (5.23), the capacity of the overhang section is calculated using the standard formulas for reinforced concrete. Lengths  $a$  and  $c$  are evaluated using Eqs. (5.11) and (5.12), which are then used to evaluate the strain in the rebar [Eq (5.24)] and the moment capacity of the section [Eq (5.25)]:

$$\varepsilon_s = \frac{0.003(d-c)}{c}, \quad (5.25)$$

$$\phi M_N = A_s f_s \left(d - \frac{a}{2}\right), \quad (5.26)$$

The moment capacity from Eq. (5.25) should exceed the applied moment due to the collision load. If the capacity is insufficient, additional steel must be added to the section. The above calculations are applied independently both at Sections 1-1 and 2-2.

The second load case uses a 16 kip axle load placed 1 foot from the edge of the rail per Section 3.6 of AASHTO (2012) (Figure 5.1). For this load case, section 2-2 clearly controls and it alone is evaluated. The width of the strip considered for live load effects is calculated using AASHTO LRFD Table 4.6.2.1.3-1 (AASHTO, 2012):

$$L = 45.0 + 10.0X, \quad (5.27)$$

where  $X$  is the distance from the wheel load to the section being considered. The 16 kip live load is factored by a multiple presence factor  $m$  and an impact factor  $IM$ . The live load moment per unit length of panel is found using:

$$M_{LL+IM} = \frac{16 IM \cdot m \cdot X}{L}, \quad (5.28)$$

The moments from the dead and live load are combined using the Strength I load case. This moment is then compared to the moment capacity of Section 2-2 that was found for the first load case. Again, if the capacity is insufficient, the amount of hooked steel should be increased.

### 5.3 Model Based Design Method

The model based design method is similar to that of the simplified design method. All properties are entered into the design aid spreadsheet described in Section 5.2, and the spreadsheet calculates the required amounts of prestressing steel and post-tensioning steel, and checks the sufficiency of the panel-to-girder connections. However, the model-based design method expands on the results of the spreadsheet by accepting precise input values for the panel stresses and moments computed using finite element modeling. In the cases described in this study, CSiBridge models were used, however any finite element modeling program may be used. If the bridge contains complicated geometry or materials, simplified spreadsheet calculations may lead to an unconservative or overly conservative design. Alternative design details can be incorporated into the model and quickly evaluated, allowing the user to update the spreadsheet calculations and iterate to an improved solution.

As an example, errors may occur in either the loads or resulting forces evaluated from simplified calculations. Refined values of forces and moments can be collected from a finite element model to replace the approximate spreadsheet calculations. The model also allows detailed evaluation of force concentrations or other abnormalities that may arise from geometric irregularities and cannot be evaluated by hand. For example, if a bridge contains a high degree of skew, stresses may accumulate at certain areas such as the bridge corners. The user can then design according to these stresses and ensure that the unique geometry does not lead to stress concentrations or other unique behavior in the deck system that might lead to insufficient reinforcement.

The quantity and placement of the post-tensioning and prestressing steel can also be refined in the model based approach. As stated in Section 5.2.4, multi-span bridges force tension into the deck panels and joints because of the negative moments over the intermediate supports. If the deck geometry is complex, the resulting tensile stresses in the top of the deck may not be adequately represented with simple formulas. In this case, a computational model that includes the entire deck surface is developed, and longitudinal post-tensioning and transverse prestressing stresses are applied. The cumulative deck stresses are then analyzed and compared against the compression and tension limits from AASHTO LRFD (2012). In summary, the user designs the prestressing system with the design aid spreadsheet, and validates it with advanced computational modeling. If the model shows that the prestressing is insufficient or overly conservative, the design is iterated using the model until an optimal solution is achieved.

## **Chapter 6: Design Example 1: West Mesquite Interchange**

### **6.1 Introduction**

Chapter 5 presented two design procedures for full-depth prefabricated deck panels: the simplified method and the model based method. Both approaches are recommended for the design of full-depth deck panels, and may be implemented selectively depending on the bridge characteristics. The design methods have been applied to example bridges to: (1) demonstrate the design calculations, (2) validate the simplified method, including the design aid spreadsheet, against a more accurate modeling approach, and (3) develop insight as to the applicability of each method. The bridge examples were chosen from among plan sets provided by NDOT for several existing bridges in Nevada. The first bridge example is the West Mesquite Interchange Bridge, which is part of the I-975 highway and consists of separate bridges for northbound and southbound traffic. Partial depth prefabricated deck panels were incorporated into the design of this bridge. However, the deck did not perform adequately and required repairs and additional upkeep. Because this bridge had been built with partial depth prefabricated deck panels, it was considered an optimal design example for full depth prefabricated deck panels. Also, this bridge contained a significant amount of skew, which several states had considered to be a limiting factor for application. Because other states had limited the incorporation of full-depth deck panels on skewed bridges, attention was given to discrepancies that may arise in the design methods resulting from the skew. This chapter describes the application of both design methods to the southbound Mesquite Bridge. Section 6.2 briefly describes the bridge geometry, and Sections 6.3 and 6.4 describe the implementation of the simplified design method and the model-based method, respectively, for the bridge. Finally, Section 6.5 discusses the findings from the Mesquite Bridge design example and implications for the design philosophy.

### **6.2 Bridge Description**

The southbound bridge is a single span bridge with a span length of 111'-6" oriented at a skew angle of 31°7'7". The overall width is 45'-11" with 3'-6" overhangs and a superelevation of 4.7%. Five prestressed concrete girders are spaced at 9'-9". The abutments are seat type, resting on a spread footing with bearing pads. Figure 6.1 displays the cross section of the bridge and Figure 6.2 shows the plan view. Figure 6.3 shows the girder dimensions and Figure 6.4 shows the girder prestressing steel.

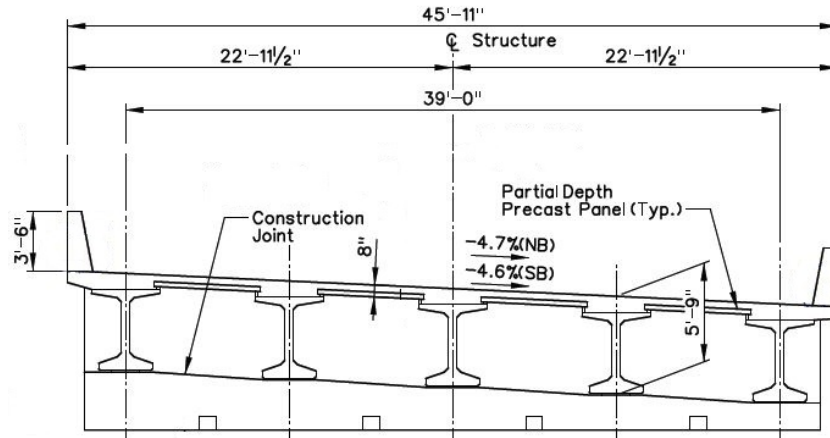


Figure 6.1: Mesquite Bridge cross-section

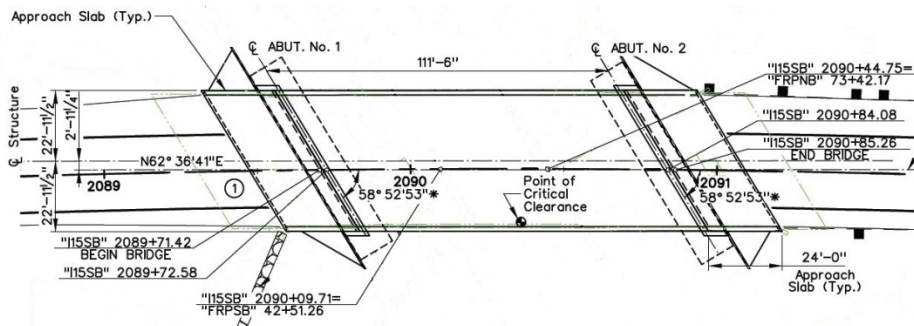


Figure 6.2: Mesquite plan view

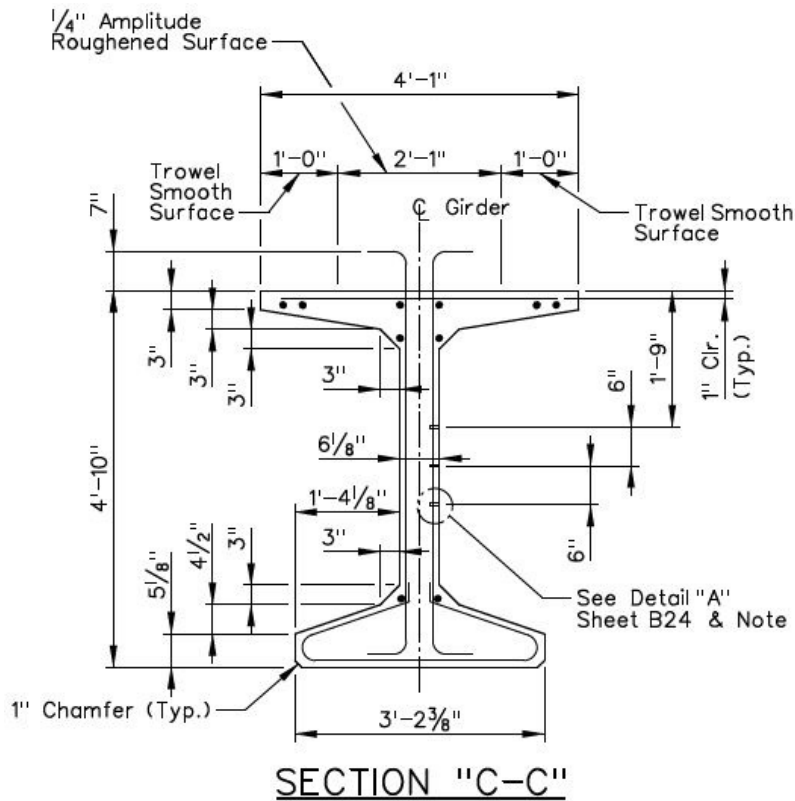
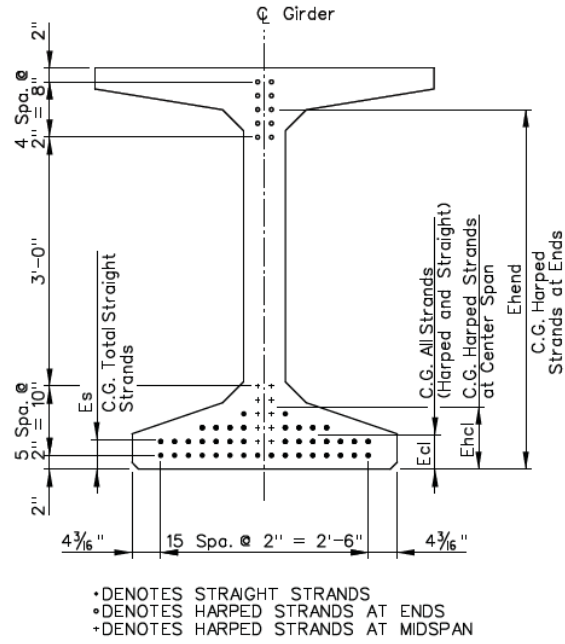


Figure 6.3: Mesquite girder cross-section



- DENOTES STRAIGHT STRANDS
- DENOTES HARPED STRANDS AT ENDS
- DENOTES HARPED STRANDS AT MIDSPAN

**STRAND PATTERN**  
 (See Girder Schedule Table  
 For C.G. Dimensions)

Figure 6.4: Girder prestress steel schedule

For the design example, all geometric properties of the bridge have been assumed to remain consistent with the original design. The main difference is that in the design example, the deck is modified from a partial depth to a full-depth panel configuration. Because the deck is 45'-9" wide, less than the 50'-0" transportation limit, the panels are designed to span the entire width of the bridge with no longitudinal joint. Also, since the deck is highly skewed, the panels are designed to be triangular or trapezoidal near the abutments and rectangular over the rest of the span. The rectangular panels are 45'-11" long (equivalent to the bridge width) by 10 feet wide and 8 inches in depth. A 2 inch concrete overlay is assumed. A drawing showing the panel layout is shown in Figure 6.5. The concrete strength is specified as 6 ksi.

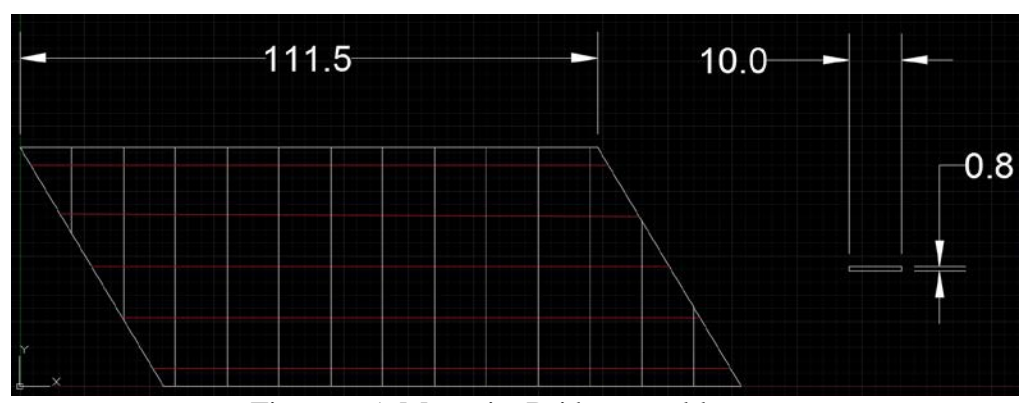


Figure 6.5: Mesquite Bridge panel layout

## 6.3 Simplified Design Method

The following sections describe the implementation of the simplified design method on the southbound Mesquite Bridge, supported by output from the design aid spreadsheet. For interpretation of the spreadsheet data, orange highlighted cells are user input values, while grey highlighted cells with orange text represent values calculated within the spreadsheet.

### 6.3.1 Design Moments and Loads

Area loads and moments due to dead and live load were calculated first, and the output from the design aid spreadsheet is shown in Table 6.1. Assuming an 8 inch deck with a 2 inch wearing surface (from the overlay), the DC and DW area loads due to self-weight were calculated as:

$$DC = 0.15 \text{ kcf} * \frac{8 \text{ in}}{12 \frac{\text{in}}{\text{ft}}} = 0.1 \text{ ksf},$$

$$DW = 0.15 \text{ kcf} * \frac{2 \text{ in}}{12 \frac{\text{in}}{\text{ft}}} = 0.025 \text{ ksf}$$

These DC and DW loads were then used to calculate the moment demands in a deck panel for the transverse and longitudinal directions. In this example, the transverse direction moments were calculated using two different methods to demonstrate alternative approaches. Per Method 1, the moment was estimated using a simplified equation [Eq. (5.1)]. First, the distributed dead load (per unit length in the transverse direction) was calculated as:

$$w_{DC} = 0.1 \text{ ksf} * 1 \text{ ft} = 0.1 \text{ klf}$$

$$w_{DW} = 0.025 \text{ ksf} * 1 \text{ ft} = 0.025 \text{ klf}$$

Then,  $w_{DC}$  and  $w_{DW}$  were substituted for  $w$  in Eq. (5.1), with  $y = 10$ , and girder spacing  $l = 9.75$  ft, to compute the DC and DW moments ( $M_{DC}$  and  $M_{DW}$ ):

$$M_{DC} = \frac{0.1 \text{ klf} * (9.75 \text{ ft})^2}{10} = 0.95 \frac{\text{k-ft}}{\text{ft}}$$

$$M_{DW} = \frac{0.025 \text{ klf} * (9.75 \text{ ft})^2}{10} = 0.24 \frac{\text{k-ft}}{\text{ft}}.$$

This result, which applies to both positive and negative moment regions, is shown as Estimated  $M_{DC}$  and Estimated  $M_{DW}$  in Table 6.1. Method 2 computed the moments using a simple structural analysis model built from basic line elements with applied distributed loads  $w_{DC}$  and  $w_{DW}$  as defined above. The results from this analysis are shown as transverse direction moments  $M_{DC}^+$ ,  $M_{DC}^-$ ,  $M_{DW}^+$ , and  $M_{DW}^-$  in Table 6.1. Subsequent design is based on the moments computed from Method 2, which is a more accurate procedure; however, the moments from Method 1 could be used if more conservatism was desired.

The maximum positive and negative transverse moments due to live load were found using Table A4-1 in the AASHTO LRFD specifications (AASHTO, 2012), and are shown as  $M_{LL}^+$  and  $M_{LL}^-$  in Table 6.1. The live load calculation assumed a girder spacing of 9'-9" and distance from the girder centerline to the design section of 0 inches for the negative moment.

Moments in the longitudinal direction were calculated using simplified beam formulas, and the resulting values were entered into Table 6.1. The maximum negative and positive longitudinal moments for DC and DW loads were calculated as:

$$M_{DC}^+ = \frac{w_{DC-Long} l^2}{8} = \frac{0.1 \text{ ksf} * 45.9 \text{ ft} * (111.5 \text{ ft})^2}{8} = 4567 \text{ k-ft}$$

$$M_{DC}^- = 0$$

$$M_{DW}^+ = \frac{w_{DW-Long} l^2}{8} = \frac{0.025 \text{ ksf} * 45.9 \text{ ft} * (111.5 \text{ ft})^2}{8} = 1783 \text{ k-ft}$$

$$M_{DW}^- = 0$$

Table 6.1: Summary of transverse and longitudinal moments

Load Assignments 3.4.1			
DC:	0.1	ksf	
DW:	0.025	ksf	
LL:	HL-93 with lane load and multi presence factor		
Moments in transverse direction			
c =	10		
Estimated $M_{DC}^+$	0.951	k-ft/ft	Calculated using estimate of $wl^2/c$
Estimated $M_{DW}^+$	0.238	k-ft/ft	
$M_{DC}^+$	0.4	k-ft/ft	Calculated using standard formulas or structural analysis program
$M_{DC}^-$	-0.8	k-ft/ft	
$M_{DW}^+$	0.1	k-ft/ft	
$M_{DW}^-$	-0.21	k-ft/ft	
$M_{LL}^+$	6.74	k-ft/ft	
$M_{LL}^-$	-7.51	k-ft/ft	
Moments in longitudinal direction			
$M_{DC}^+$	7135.593	k-ft	
$M_{DC}^-$	0	k-ft	
$M_{DW}^+$	1783.898	k-ft	
$M_{DW}^-$	0	k-ft	

These transverse direction moments were combined according to the load combinations, Strength I, Service I and Service III. Each load combination is used for a different part of the design calculations. The moment demands for each load combination were calculated as:

$$M_{Strength I}^+ = \left(0.4 \frac{k-ft}{ft} * 1.25 + 0.1 \frac{k-ft}{ft} * 1.5 + 6.74 \frac{k-ft}{ft} * 1.75\right) * 10 ft = 124 \frac{k-ft}{panel}$$

$$\begin{aligned} M_{Strength I}^- &= \left(-0.84 \frac{k-ft}{ft} * 1.25 - 0.21 \frac{k-ft}{ft} * 1.5 - 7.51 \frac{k-ft}{ft} * 1.75\right) * 10 ft \\ &= -145 \frac{k-ft}{panel} \end{aligned}$$

$$M_{Service I without LL}^+ = \left(0.4 \frac{k-ft}{ft} * 1 + 0.1 \frac{k-ft}{ft} * 1\right) * 10 ft = 5 \frac{k-ft}{panel}$$

$$M_{Service I without LL}^- = \left(-0.84 \frac{k-ft}{ft} * 1 - 0.21 \frac{k-ft}{ft} * 1\right) * 10 ft = -14 \frac{k-ft}{panel}$$

$$M_{Service I with LL}^+ = \left(0.4 \frac{k-ft}{ft} * 1 + 0.1 \frac{k-ft}{ft} * 1 + 6.74 \frac{k-ft}{ft} * 1\right) * 10 ft = 72 \frac{k-ft}{panel}$$

$$M_{Service I with LL}^- = \left(-0.84 \frac{k-ft}{ft} * 1 - 0.21 \frac{k-ft}{ft} * 1 - 7.51 \frac{k-ft}{ft} * 1\right) * 10 ft = -85 \frac{k-ft}{panel}$$

$$M_{Service III}^+ = \left(0.4 \frac{k-ft}{ft} * 1 + 0.1 \frac{k-ft}{ft} * 1 + 6.74 \frac{k-ft}{ft} * 0.8\right) * 10 ft = 58.5 \frac{k-ft}{panel}$$

$$M_{Service III}^- = \left(-0.84 \frac{k-ft}{ft} * 1 - 0.21 \frac{k-ft}{ft} * 1 - 7.51 \frac{k-ft}{ft} * 0.8\right) * 10 ft = -70.6 \frac{k-ft}{panel}$$

### 6.3.2 Prestress Steel Design

An overview of the prestressing steel design process is as follows. The Service III moment is used to estimate an initial amount of prestressing steel (based on assumed losses) to satisfy tensile stress limits in the concrete. The initial amount of prestressing is used in the calculation of losses and capacity. The updated prestress force including losses is incorporated into the calculations, and used to iterate the amount of prestressing steel as needed. The updated prestress force is used to check the compressive and tensile stresses in the section against Service I and Service III loads, respectively. The moment capacity of the design is checked against the moment factored for Strength I load combinations. If the capacity is insufficient, the number of prestressing strands are adjusted until adequate capacity is attained and all stress limits are also met.

First, the initial amount of prestressing steel was estimated. Table 6.2 shows the prestress steel properties assumed for transverse panel reinforcement, which included ½” diameter 7-wire (Grade 270) prestressing strands. The ultimate stress,  $f_{pu}$ , of the strand was defined as 270 ksi, and other values assumed by the design aid spreadsheet were: strand yield stress  $f_{py} = 90\%$  of  $f_{pu}$ , initial prestress  $f_{pi} = 75\%$  of  $f_{pu}$ , and effective prestress  $f_{pe} = 90\%$  of  $f_{pi}$ .

Table 6.2: Prestressing steel properties

Steel Properties - Prestressing Steel		
$f_{pu} =$	270	ksi
$f_{py} =$	243	ksi
$E_p =$	28500	ksi
$f_{pi} =$	203	ksi
1/2" diameter - 7 wire strands	0.153	in <sup>2</sup>
$f_{pe} =$	182	ksi

The larger of the two Service III moments,  $M_{Service III Max}$ , was used to calculate an initial value for the number of prestressing strands per panel. The allowable tensile stress in the concrete,  $\sigma_{allowable}$ , was computed as:

$$\sigma_{allowable} = 0.19\sqrt{f'_c} = 0.19\sqrt{6 \text{ ksi}} = 0.465 \text{ ksi}.$$

The initial prestress force was calculated by rearranging Eq. (5.2) and solving for  $P_{pe}$ :

$$P_{pe} = \left( \sigma_{allowable} + \frac{M_{Service III}}{S} \right) * A = \left( -0.465 \text{ ksi} + \frac{70.6 \text{ k-ft} * 12 \frac{\text{in}}{\text{ft}}}{1280 \text{ in}^3} \right) * 960 \text{ in}^2 = 188.9 \text{ kips}.$$

Note that compression is positive in the above calculation. The initial number of prestressing strands,  $n$ , rounded up to the nearest even number, was calculated per Eq. (5.3) as:

$$n = \frac{188.9 \text{ k}}{0.153 \frac{\text{in}^2}{\text{strand}} * 182 \text{ ksi}} = 8 \text{ strands}.$$

Thus, the required number of prestressing strands was initially estimated as 8. Table 6.3 shows the initial prestress steel calculations.

Next, the subsequent calculations and prestress design checks are described, which are based on the specified number of strands. As part of the design process, the number of strands was iteratively adjusted until all checks are satisfied. Application of this iterative process led to a final calculation of 12 strands required to satisfy all design checks. All subsequent calculations are based on this final value (12 strands), shown as the highlighted orange input cell in Table 6.3. The strands were placed in two layers; each located 2.25 inches from the outside edge of the panel.

Table 6.3: Initial prestressing steel design

Prestress Steel Estimate		
$M_{service III} Max =$	70.63	k-ft
$\sigma_{allowed} =$	-0.465	ksi
$P_{pe} =$	188.9	k
$n =$	6.8	strands
Use	12	- 1/2" strands
Try 2 layers	6	strands/layer
$A_{ps} =$	1.836	in <sup>2</sup>
$\beta_1 =$	0.75	

This uses the service moment to calculate a required number of strands based off of estimated properties. These calculations are checked in the following sections

Losses were calculated for the prestress steel according to the equations found in Section 5.2.3. Elastic shortening loss was initially assumed to be 1%, and the actual loss was subsequently calculated. The initial prestress value,  $f_{pi}$ , was multiplied by 99% to reflect the prestress in the strand after elastic shortening loss,  $f_{pes}$ .

$$f_{pes} = 0.99 * 203 \text{ ksi} = 200.5 \text{ ksi}.$$

The updated total prestress force (with 12 bars) was computed as:

$$P_{pe} = nA_{ps}f_{pes} = 12 * 0.153 \text{ in}^2 * 200.5 \text{ ksi} = 368 \text{ kips}.$$

This prestress force was used to find the stress  $f_{cgp}$  in the concrete due to prestressing:

$$f_{cgp} = \frac{P_{pe}}{A} = \frac{368 \text{ k}}{960 \text{ in}^2} = 0.382 \text{ ksi}.$$

Using Eq. (5.4) with  $E_p = 28500$  ksi and  $E_{ct} = 4031$  ksi, the losses due to elastic shortening were found to be 2.71 ksi, which is equivalent to a prestress loss of 1.34%. Because the calculated elastic shortening loss was not close to the assumed loss, the procedure was repeated using an assumed initial loss of 1.33%. This resulted in an elastic shortening loss of 2.70 ksi and a loss percentage of 1.33%, which was close enough to the assumed value to be considered converged. The elastic shortening loss calculations are shown in Table 6.4.

Table 6.4: Elastic shortening losses

Prestress Losses		
Elastic Shortening		
Try 1% initial loss	1.33%	
Assumed strand stress =	199.8	ksi
$P_i =$	366.8	k
$f_{cp} =$	0.382	ksi
$\Delta f_{pss} =$	2.702	ksi
% Loss =	1.33%	Should be close to assumed value, if not recalculate

After the calculation of short term losses (elastic shortening), long term losses due to shrinkage, creep, and relaxation were determined. Panel properties prior to deck installation differed from the properties after deck installation, so shrinkage and creep losses were calculated both before and after deck installation. The following input values were defined: volume-to-surface area ratio of one deck panel  $V/SA = 3.75$ , relative humidity  $H = 40\%$  for this bridge location (Figure 5.4.2.3.3-1 in AASHTO, 2012), time between curing and loading  $t = 89$  days, and the overall lifespan of the deck  $t_f = 75$  years or 27375 days. Based on these inputs, the following factors were calculated: volume-to-surface ratio factor  $k_s$ , humidity factor for shrinkage  $k_{hs}$ , humidity factor for creep  $k_{hc}$ , factor for the effect of concrete strength  $k_f$ , time development factor at time of transfer  $k_{td}$ , and time development factor at the end of the service life of the deck  $k_{tdf}$ , according to AASHTO 5.4.2.3.2-(2-5) and 5.4.2.3.3-2:

$$k_s = 1.45 - 0.13 \left( \frac{V}{SA} \right) \geq 1.0, 1.45 - 0.13(3.75): k_s = 1$$

$$k_{hs} = 2 - 0.014H = 2 - 0.014(40): k_{hs} = 1.44$$

$$k_{hc} = 1.56 - 0.008H = 1.56 - 0.008(40): k_{hc} = 1.24$$

$$k_f = \frac{5}{1 + f'_{ci}} = \frac{5}{1 + 5 \text{ ksi}}: k_f = 0.83$$

$$k_{td} = \frac{t}{61 - 4f'_{ci} + t} = \frac{89 \text{ days}}{61 - 4 * 5 \text{ ksi} + 89 \text{ days}}: k_{td} = 0.68$$

$$k_{tdf} = \frac{t_f}{61 - 4f'_{ci} + t_f} = \frac{27375 \text{ days}}{61 - 4 * 5 \text{ ksi} + 27375 \text{ days}}: k_{tdf} = 0.99$$

These factors were used to calculate the strain due to shrinkage,  $\epsilon_{sh}$  per AASHTO 5.4.2.3.3-1 (2012), and the creep coefficient at time of installation,  $\psi_b(t, t_i)$  and final service life of the deck,  $\psi_b(t_f, t_i)$  per AASHTO 5.4.2.3.2-1 (2012).

$$\varepsilon_{sh} = k_s k_{hs} k_f k_{td} 0.48 * 10^{-3} = 1(1.44)(0.83)(0.68)(0.48 * 10^{-3}) \\ = 0.000394$$

$$\psi_b(t, t_i) = 1.9 k_s k_{hc} k_f k_{td} t_i^{-0.118} = 1.9(1)(1.24)(0.83)(0.68)(89^{-0.118}) = 1.34$$

$$\psi_b(t_f, t_i) = 1.9 k_s k_{hc} k_f k_{td} t_f^{-0.118} = 1.9(1)(1.24)(0.83)(0.68)(27375^{-0.118}) = 1.96$$

The transformed section coefficient,  $K_{id}$  was found using AASHTO 5.9.5.4.2a-2 (2012):

$$K_{id} = \frac{1}{1 + \frac{E_p A_{ps}}{E_{ci} A_g} \left(1 + \frac{A_g e_{pg}^2}{I_g}\right) [1 + 0.7 \psi_b(t_f, t_i)]} = \frac{1}{1 + \frac{28500 \text{ ksi}}{4287 \text{ ksi}} \left(\frac{1.836 \text{ in}^2}{960 \text{ in}^2}\right) (1 + 0) [1 + 0.7(1.96)]} \\ = 0.97$$

Each of the above factors were used to find the losses due to shrinkage and creep prior to deck installation using Eqs. (5.5) and (5.7):

$$\Delta f_{pSR} = \varepsilon_{sh} E_p K_{id} = 0.000394 * 28500 \text{ ksi} * 0.97 = 10.9 \text{ ksi}$$

$$\Delta f_{pCR} = \frac{E_p}{E_{ci}} f_{cgp} \psi_b(t, t_i) K_{id} = \frac{28500 \text{ ksi}}{4287 \text{ ksi}} 0.382 \text{ ksi} (1.34)(0.97) = 3.52 \text{ ksi}$$

Relaxation before deck installation was calculated according to Eq. (5.9):

$$\Delta f_{pR1} = \Delta f_{pR2} = \frac{f_{pt}}{K_L} \left( \frac{f_{pt}}{f_{py}} - 0.55 \right) = \frac{198.9 \text{ ksi}}{30} \left( \frac{198.9 \text{ ksi}}{243 \text{ ksi}} - 0.55 \right) = 1.8 \text{ ksi}$$

The shrinkage strain of concrete over the whole life of the deck,  $\varepsilon_{bif}$ , and the shrinkage strain of concrete between time of deck placement and final age,  $\varepsilon_{bdf}$ , were calculated as:

$$\varepsilon_{bif} = k_s k_{hs} k_f k_{tdf} 0.48 * 10^{-3} = 1(1.44)(0.83)(0.999)(0.48 * 10^{-3}) \\ = 0.000575$$

$$\varepsilon_{bdf} = \varepsilon_{bif} - \varepsilon_{sh} = 0.000575 - 0.000394 = 0.000181$$

Shrinkage and creep losses at the end of the deck life were then calculated per Eqs. (5.6) and (5.8) as:

$$\Delta f_{pSD} = \varepsilon_{bdf} E_p K_{id} = 0.000181 * 28500 \text{ ksi} * 0.97 = 5.0 \text{ ksi}$$

$$\Delta f_{pCD} = \frac{E_p}{E_c} f_{cgp} \psi_b[(t_f, t_i) - \psi_b(t_a, t_i)] K_{df} + \frac{E_p}{E_{ci}} \Delta f_{cd} \psi_b(t_f, t_a) K_{df} \\ = \frac{28500 \text{ ksi}}{4415 \text{ ksi}} 0.382 \text{ ksi} (1.96 - 1.34)(0.97) + 0 = 1.47 \text{ ksi}$$

The relaxation loss after deck placement was assumed to be identical to that before deck placement. Prestress loss calculations prior to deck installation and at the end of service life are shown in Tables 6.5 and 6.6, respectively. The total long term prestress loss (24.5 ksi) was calculated by summing all individual losses before and after deck placement. This led to a final prestress value of 175.3 ksi with a net loss of 13.4% over the life of the deck.

Table 6.5: Prestress losses prior to deck installation

Creep & Shrinkage (Between Transfer and Deck Installation)		5.9.5.4
V/SA	3.75	
H	40	Relative Humidity
t =	89 days	Time between curing and loading
t <sub>r</sub> =	27375 days	Overall life of panels
k <sub>s</sub> =	1	5.4.2.3.2-2
k <sub>ns</sub> =	1.44	5.4.2.3.3-2
k <sub>nc</sub> =	1.24	5.4.2.3.2-3
k <sub>r</sub> =	0.83	5.4.2.3.2-4
k <sub>td</sub> =	0.68	5.4.2.3.2-5
k <sub>tdr</sub> =	0.999	5.4.2.3.2-5
ε <sub>sh</sub> =	0.000394338	5.4.2.3.3-1
ψ(t, t <sub>i</sub> ) <sub>1</sub> =	1.34	5.4.2.3.2-1
ψ(t, t <sub>i</sub> ) <sub>27375</sub> =	1.96	5.4.2.3.2-1
K <sub>td</sub> =	0.97	5.9.5.4.2a-2
Δf <sub>psR</sub> =	10.89 ksi	5.9.5.4.2a-1
Δf <sub>psR</sub> =	3.52 ksi	5.9.5.4.2b-1
Relaxation (Between Transfer and Deck Installation)		
f <sub>pt</sub> =	199.8 ksi	
K <sub>L</sub> =	30 ksi	
Δf <sub>pr1</sub> =	1.81 ksi	5.9.5.4.2c-1

Table 6.6: Prestress losses at final age of the deck

Creep & Shrinkage (Between Deck Installation and Final Age)		
t =	27374	
k <sub>s</sub> =	1	5.4.2.3.2-2
k <sub>ns</sub> =	1.44	5.4.2.3.3-2
k <sub>nc</sub> =	1.24	
k <sub>r</sub> =	0.83	5.4.2.3.2-4
k <sub>td</sub> =	0.999	5.4.2.3.2-5
ε <sub>sh</sub> =	0.000575139	
ε <sub>ocr</sub> =	0.0001808	5.4.2.3.3-1
ψ <sub>0</sub> (t <sub>0</sub> , t <sub>i</sub> ) <sub>1</sub> =	1.34	5.4.2.3.2-1
ψ <sub>0</sub> (t <sub>0</sub> , t <sub>i</sub> ) <sub>27375</sub> =	1.96	5.4.2.3.2-1
K <sub>id</sub> =	0.97	5.4.2.3.2-5
Δf <sub>psD</sub> =	4.99 ksi	5.9.5.4.2a-1
Δf <sub>psD</sub> =	1.47 ksi	5.9.5.4.2b-1
Relaxation (Between Deck Installation and Final Age)		
Δf <sub>pr2</sub> =	1.81	5.9.5.4.2b-1
Total Losses at Transfer (Initial Losses)		
f <sub>ptransfer</sub> =	199.8 ksi	
P <sub>transfer</sub> =	366.8 k	
Total Losses at Final Age (Service)		
Δf <sub>plT</sub> =	24.50 ksi	5.9.5.1-1
f <sub>pefinal</sub> =	175.3 ksi	
P <sub>pe</sub> =	321.8 k	
0.8f <sub>py</sub> =	194.4 ksi	
Is f <sub>pe</sub> ≤ 0.8f <sub>py</sub>	Yes	If not, use 0.8f <sub>py</sub>
Total prestress loss, %	13.43%	

Next, the applied prestress force on the panel including all losses was used to calculate the panel capacity. The Service I moment was used to calculate the peak bending stresses with:

$$f_t = \frac{P_{pe}}{A} \pm \frac{M}{S}$$

Two compression limit states were considered; Case 1 = dead loads only and Case 2 = dead and live load. These compression stress limits were:

$$\text{Case 1: } 0.45f'_c = 0.45 * 6 \text{ ksi} = 2.7 \text{ ksi}$$

$$\text{Case 2: } 0.6f'_c = 0.6 * 6 \text{ ksi} = 3.6 \text{ ksi}$$

The peak compressive stress in the panel resulting from the combination of moment and prestress was calculated, and compared to the limits to ensure the maximum compressive stress did not exceed the allowable stress. These stress limits were checked twice for each case; once for positive moment and once for negative moment. In all four cases the applied stresses (as shown in Table 6.7) were less than the compression stress limits so the requirements were met. The tensile stress limit was  $\sigma_{allowable} = -0.465 \text{ ksi}$ . The tensile stress resulting from the combined moment due to Service III load combination and prestress was  $-0.327 \text{ ksi}$ , which satisfied the tensile stress limit.

Since all stresses were below the stress limits, the panel moment capacity was checked against the demand moment using a Strength I load combination. The initial estimate for the total tension force in the section  $T$  was calculated using Eq. (5.10), assuming the prestressing strand stress to be equal to the yield stress. The idealized depth of compression  $a$  was found using Eq. (5.11) and the neutral axis depth  $c$  using Eq. (5.12). The prestressing strand strains  $\varepsilon_p$  were calculated separately in each layer [Eq. (5.13)], which in turn were used to update the total stress  $f_{ps}$  in each prestressing layer [Eq. (5.14)]. The calculations were applied iteratively until the calculated prestress force in each layer converged to the assumed value. The calculations for the first iteration were:

$$T = \frac{n}{2} f_{py} A_{ps} + \frac{n}{2} f_{py} A_{ps} = \frac{12}{2} (243 \text{ ksi})(0.153 \text{ in}^2) + \frac{12}{2} (243 \text{ ksi})(0.153 \text{ in}^2) = 446 \text{ kips}$$

$$a = \frac{T}{0.85 * f'_c * b} = \frac{446 \text{ kips}}{0.85(6 \text{ ksi})(120 \text{ in})} = 0.729 \text{ in}$$

$$c = \frac{a}{\beta_1} = \frac{0.729 \text{ in}}{0.75} = 0.972 \text{ in}$$

The strain and stress in the top layer were calculated as:

$$\varepsilon_p = \frac{0.003(d - c)}{c} + \frac{f_{pe}}{E_p} = \frac{0.003(2.25 \text{ in} - 0.972 \text{ in})}{0.972 \text{ in}} + \frac{182 \text{ ksi}}{28500 \text{ ksi}} = 0.01$$

$$f_{ps} = \varepsilon_p E_p \left\{ Q + \frac{(1 - Q)}{\left[ 1 + \left( \frac{E_p \varepsilon_p}{K f_{py}} \right)^R \right]^{\frac{1}{R}}} \right\}$$

$$= 0.01(28500 \text{ ksi}) \left\{ 0.031 + \frac{(1 - 0.031)}{\left[ 1 + \left( \frac{28500 \text{ ksi}(0.01)}{1.04(243 \text{ ksi})} \right)^{7.36} \right]^{\frac{1}{7.36}}} \right\} = 244.9 \text{ ksi}$$

The strain and stress in the bottom layer were calculated as:

$$\varepsilon_p = \frac{0.003(d - c)}{c} + \frac{f_{pe}}{E_p} = \frac{0.003(5.75 \text{ in} - 0.972 \text{ in})}{0.972 \text{ in}} + \frac{182 \text{ ksi}}{28500 \text{ ksi}} = 0.021$$

$$f_{ps} = \varepsilon_p E_p \left\{ Q + \frac{(1 - Q)}{\left[ 1 + \left( \frac{E_p \varepsilon_p}{K f_{py}} \right)^R \right]^{\frac{1}{R}}} \right\}$$

$$= 0.017(28500 \text{ ksi}) \left\{ 0.031 + \frac{(1 - 0.031)}{\left[ 1 + \left( \frac{28500 \text{ ksi}(0.017)}{1.04(243 \text{ ksi})} \right)^{7.36} \right]^{\frac{1}{7.36}}} \right\}$$

$$= 263.5 \text{ ksi}$$

This process was repeated using the stress values from the previous iteration, until the prestress force in each layer did not change between iterations. Three iterations of the previous calculations were required to find the final capacity of the panel using Eq. (5.15), which was equal to 145.4 k-ft/panel. This capacity was sufficient to resist the maximum positive moment 123.9 k-ft/panel, and the maximum negative moment, -145.1 k-ft/panel. The panel capacity was also larger than 1.2 times the cracking moment (102.5 k-ft/panel), satisfying the minimum reinforcement limit. Tables 6.8, and 6.9 show the calculations for the moment capacity.

Table 6.7: Panel stress checks

Panel Capacity, 5.9.4.2			
	$P_{pe} =$	321.8 k	
<b>Compression Stress Limits: Service I</b>			
Case 1:	PS+DL: $0.45f'_c =$	2.7 ksi	
Case 2:	PS+DL+LL: $0.6f'_c =$	3.6 ksi	
	Tensile Stress Limit	-0.465 ksi	
	$M_1^+ =$	4.613 k-ft	
	$M_2^+ =$	72.013 k-ft	
	$M_1^- =$	-13.715 k-ft	
	$M_2^- =$	-85.65 k-ft	
	$f_{t1}^+ =$	0.38 ksi	<0.45f' <sub>c</sub> , Good
	$f_{t2}^+ =$	1.01 ksi	<0.6f' <sub>c</sub> , Good
	$f_{t1}^- =$	0.46 ksi	<0.45f' <sub>c</sub> , Good
	$f_{t2}^- =$	1.14 ksi	<0.6f' <sub>c</sub> , Good
<b>Tensile Stress Limits: Service III</b>			
	$f_b =$	-0.327 ksi	<σ <sub>allowed</sub> , Good

Table 6.8: Panel moment capacity iterations

Flexural Strength: Strength I			PCI Bridge Design Manual: 8.2.2.5
T=	446.1	k	
a=	0.729	in	
c=	0.972	in	
Top Layer			
d=	2.25	in	
$\epsilon_{pe}$ =	0.0064		
$\epsilon_p$ =	0.010		
$f_{ps}$ =	244.9	ksi	<270 ksi
Bottom Layer			
d=	5.75	in	
$\epsilon_p$ =	0.021		
$f_{ps}$ =	263.5	ksi	<270 ksi
Second Iteration			
T=	466.7	k	
a=	0.763	in	
c=	1.02	in	
Top Layer			
d=	2.25	in	
$\epsilon_p$ =	0.010		
$f_{ps}$ =	242.7	ksi	<270 ksi
Bottom Layer			
d=	5.75	in	
$\epsilon_p$ =	0.029		
$f_{ps}$ =	270.2	ksi	<270 ksi

Table 6.9 Panel moment capacity and minimum reinforcement limit

Third Iteration			
T=	470.9	k	
a=	0.769	in	
c=	1.03	in	
Top Layer			
d=	2.25	in	
$\epsilon_p$ =	0.010		
$f_{ps}$ =	242.3	ksi	<270 ksi
Bottom Layer			
d=	5.75	in	
$\epsilon_p$ =	0.028		
$f_{ps}$ =	270.0	ksi	<270 ksi
$\phi M_N$ =	145.4	k-ft/panel	
$M_{Strength I +}$ =	123.9	k-ft/panel	< $\phi M_N$
$M_{Strength I -}$ =	-145.1	k-ft/panel	< $\phi M_N$
<b>Minimum Reinforcement Limit</b>			
$f_{cpe}$ =	0.335	ksi	
$1.2M_{cr}$ =	102.5	k-ft	
$1.2M_{cr} < \phi M_N$ , Good			

### 6.3.3 Panel-to-Girder Connection Design

The panel-to-girder connection was designed according to the process explained in Section 5.2.4. Projected steel hooks from the prestressed concrete girders (connection detail shown in Figure 2.12), were assumed to develop the shear connection between the girders and the panels. Pockets in the panel were spaced 2 feet apart in the longitudinal direction along the girder lines; resulting in 4 pockets per panel. The design detailing included specifying the pocket width and length in addition to the number of steel bars per connection. For this example, an 8 inch wide by 10 inch long pocket with three projected rebar hooks was found to provide the required shear strength. The maximum factored shear demand for Strength I loads was determined to be 526 kips using the simple mechanics formula of  $V = \frac{wl}{2}$ . The required shear resistance was calculated according to the provisions in Section 5.2.4:

$$V_{h1} = \frac{V}{d_v \# \text{girders}} = \frac{526 \text{ kips}}{34 \text{ inches}(5)} = 3.9 \frac{k}{in}$$

$$V_u = \frac{V_{h1} w}{\phi} = \frac{3.9(120 \text{ in})}{0.9} = 515.7 \text{ kips.}$$

The area of concrete engaged in shear transfer was calculated by:

$$A_{cv} = w_{pocket} l_{pocket} (\# \text{ of pockets}) = 8 \text{ in} * 10 \text{ in} * 4 \text{ pockets} = 320 \text{ in}^2$$

The area of interface shear reinforcement crossing the shear plane was calculated with:

$$A_{vf} = 2 * \#_{U-bars} A_s (\# \text{ of pockets}) = 2 * 3 \text{ bars} * 0.31 \text{ in}^2 * 4 \text{ pockets} = 7.44 \text{ in}^2$$

The shear resistance was calculated according to Eq. (5.17):

$$V_n = cA_{cv} + \mu(A_{vf}f_y + P_c) = 0.24 \text{ ksi}(320 \text{ in}^2) + 1[7.44 \text{ in}^2(60 \text{ ksi}) + 0] = 523.2 \text{ kips.}$$

where  $c$  is the cohesion factor of 0.24 ksi,  $\mu$  is the friction factor of 1, and  $P_c$  is the permanent net compressive force normal to the shear plane which is zero for this example. The shear resistance exceeded the shear demand of 516 kips, with a final design ratio of 1.01. The intermediate calculations are summarized in Table 6.10. A drawing showing the plan view of one panel with the pockets is shown in Figure 6.6 with all dimensions listed in feet.

Table 6.10: Panel-to-girder connection design

Panel to Girder Connection Design		5.8.4
Pocket Width	8 in	
Pocket Length	10 in	
# Pockets per panel	4	
# U Bars per pocket	3	
$V_{n1} =$	3.87 k/in	C5.8.4.2-7
$V_U =$	515.7 k	PCI Bridge Design Manual: Chapter 9
$c =$	0.24 ksi	5.8.4.3
$\mu =$	1	5.8.4.3
$A_{cv} =$	320 in <sup>2</sup>	
$P_c =$	0 k	
$A_{vf} =$	7.44 in <sup>2</sup> /panel	
$V_N =$	523.2 k	5.8.4.1-3
$V_N/V_U =$	1.01	$V_U < V_n$ , Good

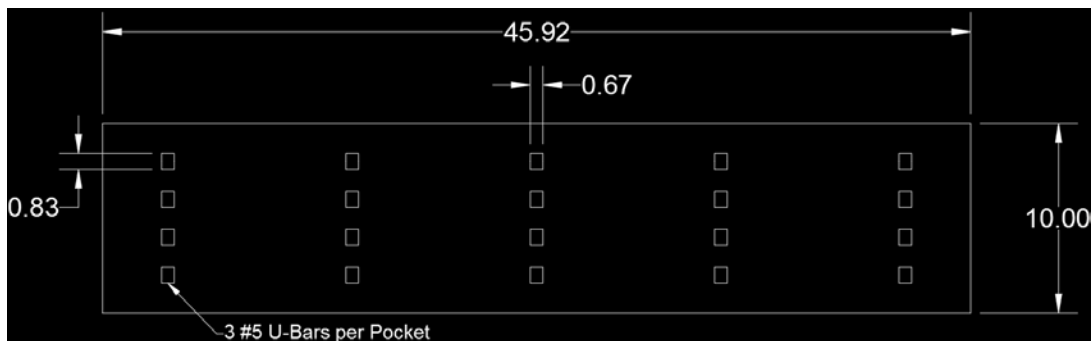


Figure 6.6: Pocket layout (dimensions in ft)

### 6.3.4 Post-Tensioning Design

AASHTO requires that transverse joints in prefabricated deck panels be subjected to a minimum of .25 ksi compression. To achieve this compression, post-tensioning was used. The strand properties are defined in Table 6.11; assumed values are similar to those for the prestressing strands. For this simplified design method the maximum tensile stress,  $\sigma_{tension}$ , was assumed to be 0 because the bridge was single span. This meant that additional post-tensioning due to tensile forces in the deck was not required. The only required post-tensioning force was the .25 ksi mandated by AASHTO (2012) for deck joints. The required number of post-tensioning strands was found by multiplying .25 ksi by the deck cross-sectional area in the longitudinal direction [Eq. (5.19)], leading to a required post-tensioning force of 1102 kips. The post-tensioning bars were assumed to be 0.6" diameter – 7 wire strand (Grade 270). The total force applied to one strand was calculated as:

$$F_{pe} = f_{pe}A_{PT} = 176 \text{ ksi} * 0.217 \text{ in}^2 = 38.1 \text{ kips}$$

where  $f_{pe}$  is the effective prestress force in the post-tensioning strand with assumed losses. Using these strands to apply the post-tensioning force, the total number of strands was:

$$n = \frac{F_{req}}{F_{pe}} = \frac{1102 \text{ kips}}{38.1 \frac{\text{kips}}{\text{strand}}} = 30 \text{ strands}$$

The post-tensioning calculations are shown in Table 6.12. (Note that the spreadsheet automatically accounts for the .250 ksi minimum required post-tensioning in addition to calculated tensile stresses, which in this case were 0.) The post-tensioning strands are distributed to 6 ducts with 5 strands per duct. The two exterior ducts are located 1.5 feet away from the edge of the panel. The four interior ducts are spaced such that one duct is halfway between each interior girder. Each duct was designed to be 2 inches in diameter along the center of the cross-section of the panels. Figure 6.7 shows the duct layout.

Table 6.11: Post-tensioning steel properties

Steel Properties - Post-tension Steel		
$f_{pu} =$	270	ksi
$f_{py} =$	203	ksi
$E_p =$	28500	ksi
$f_{pe} =$	176	ksi
0.6" diameter - 7 wire strands	0.6	in
A=	0.217	in <sup>2</sup>

Table 6.12: Post-tensioning steel calculations

Longitudinal Post-tensioning		
$f_t =$	0.0	psi
$F_{pe} =$	38.1	k
$F_{req} =$	1102	k
$n =$	28.9	strands

This value is the maximum tensile stress found in a transverse joint at any point along the bridge. This can be found through modeling or hand calculations.

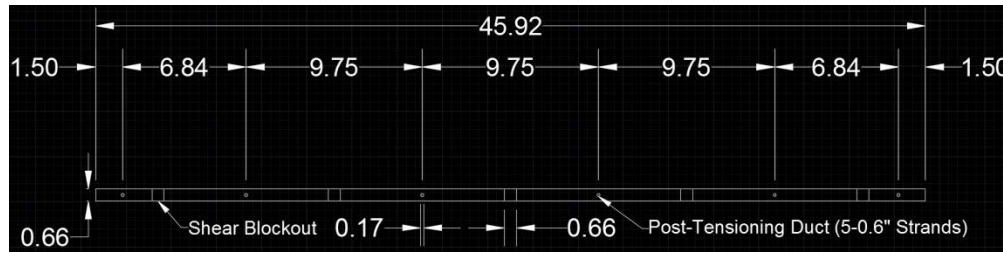


Figure 6.7: Mesquite Bridge duct layout (dimensions in ft)

Standard temperature and shrinkage reinforcement was added in addition to the post-tensioning. According to Eq. (5.20), the required amount of temperature and shrinkage reinforcement was:

$$Required A_s \geq \frac{1.3bh}{2(b+h)f_y} = \frac{1.3(120 \text{ in})(8 \text{ in})}{2(120 \text{ in} + 8 \text{ in})60 \text{ ksi}} = 0.11 \frac{\text{in}^2}{\text{ft}}$$

To satisfy this requirement, #3 bars were spaced 18 inches apart in two layers resulting in 0.15 in<sup>2</sup>/ft as shown below:

$$Actual A_s = 2 \text{ layers} * \frac{A_{bar}}{Spacing} = 2 * \frac{0.11 \text{ in}^2}{1.5 \text{ ft}} = 0.15 \frac{\text{in}^2}{\text{ft}}$$

The calculations are summarized in Table 6.13.

Table 6.13: Temperature and shrinkage reinforcement

Temperature and Shrinkage Reinforcement		
$A_s$ required=	0.11	in <sup>2</sup> /ft
Bar size	#3	
Bar area	0.11	in <sup>2</sup>
Spacing	18	in
$A_s$ actual=	0.15	in <sup>2</sup> /ft

Use two layers of reinforcement (mesh or rebar)  
<18 inches  
>  $A_s$  required

### 6.3.5 Overhang Design

Design of the barrier wall, which should be according to standard state procedures, was beyond the scope of this project. Thus, the properties used in the PCI design example (PCI, 2011b) were chosen as representative values and assumed to be the same for this design example. The design assumptions were: horizontal collision force = 147.03 kips, moment capacity at the base of the barrier wall  $M_{base} = 23.85$  k-ft/ft, and length of the wall failure mechanism = 13.589 ft. The height of the barrier wall = 3.5 ft, consistent with the original design of the Mesquite Interchange Bridge.

First, the moment capacity was checked for Case 1 (horizontal collision load combined with dead load) at Section 1-1 (inside edge of the barrier rail) and Section 2-2 (3 inches from the outside edge of the exterior girder). Sections 1-1 and 2-2 were located at  $l = 1.7$  feet (20.25 in) and  $l = 3.21$  feet (38.5 in) from the edge of the panel, respectively. The tension in the base per panel as a result of the vehicle collision was calculated according to [Eq. (5.21)]:

$$T_{base} = \frac{R_w}{L_c + 2H} = \frac{147.03 \text{ kips}}{13.589 \text{ ft} + 2(3.5 \text{ ft})} = 7.14 \frac{k}{ft}$$

$$T_{Extreme \text{ Event II}} = T_{base} * b = 7.14 \frac{k}{ft} * 10 \text{ ft} = 71.4 \frac{k}{panel}$$

For Section 1-1, the moments due to dead load of the parapet  $M_{DC \text{ Parapet}}$  and slab  $M_{DC \text{ Slab}}$ , were calculated as:

$$M_{DC \text{ Parapet}} = w_{parapet}(\text{width}_{parapet} - \text{centroid}_{parapet})$$

$$= 0.65 \frac{k}{ft} (1.7 \text{ ft} - 0.63 \text{ ft}) = 0.68 \frac{k-ft}{ft}$$

$$M_{DC \text{ Slab}} = \frac{DC_{Area \text{ Load}} l^2}{2} = \frac{0.1 \text{ ksf} * (1.7 \text{ ft})^2}{2} = 0.14 \frac{k-ft}{ft}$$

These moments combined with the barrier rail base moment capacity  $M_{base}$  (which is the maximum moment that could be transferred to the panel due to vehicle collision) according to Extreme Event II load combination:

$$M_{Extreme \text{ Event II}} = M_{base} + 1.25 * (M_{DC \text{ Parapet}} + M_{DC \text{ Slab}}) = 24.88 \frac{k-ft}{ft}$$

$$M_{Extreme \text{ Event II}} = M_{Extreme \text{ Event II}} * b = 26.32 \frac{k-ft}{ft} * 10 \text{ ft} = 263.2 \frac{k-ft}{panel}$$

The calculation resulted in a moment demand of 263 k-ft/panel at section 1-1. Using the design aid spreadsheet, the amount of reinforcement was adjusted until the capacity exceeded the demand, and the calculations below reflect the final design of 20 #7 bars per panel. First, the development length was calculated according to Eq. (5.22):

$$l_d = \frac{38d_b}{\sqrt{f'_c}} = \frac{38 * 0.875 \text{ in}}{\sqrt{6000 \text{ psi}}} = 16.29 \text{ in}$$

and the available strength of the rebar at the section being analyzed is found using Eq. (5.23):

$$\text{Available strength} = f_y \frac{(l - 2 \text{ in})}{l_d} \leq f_y = 60 \text{ ksi} \frac{(20.25 \text{ in} - 2 \text{ in})}{16.29 \text{ in}} = 60 \text{ ksi}$$

which indicates that the strength of the rebar was fully developed at section 1-1. Using the following calculations the capacity of the panel was determined:

$$A_s = 20 \text{ bars} * 0.6 \frac{\text{in}^2}{\text{bar}} = 12 \text{ in}^2$$

$$d = 5.7 \text{ in}$$

$$a = \frac{A_s f_y - T_{base}}{0.85 f'_c b} = \frac{12 \text{ in}^2 (60 \text{ ksi}) - 71.41 \text{ kips}}{0.85 (6 \text{ ksi}) (120 \text{ in})} = 1.06 \text{ in}$$

$$c = \frac{a}{\beta_1} = \frac{1.06 \text{ in}}{0.75} = 1.41 \text{ in}$$

The strain in the rebar  $\epsilon_s$  and moment capacity  $\phi M_N$  were determined per Eqs. (5.24) and (5.25).

$$\epsilon_s = 0.003 \frac{d - c}{c} = \frac{5.7 \text{ in} - 1.41 \text{ in}}{1.41 \text{ in}} = 0.009$$

$$\phi M_N = \phi A_s f_y \left( d - \frac{a}{2} \right) = \frac{0.9 (12 \text{ in}^2) (60 \text{ ksi}) \left( 5.7 \text{ in} - \frac{1.06 \text{ in}}{2} \right)}{12 \frac{\text{in}}{\text{ft}}} = 279.2 \text{ k-ft}$$

The capacity of 279.2 k-ft exceeded the applied moment of 263 k-ft, so the design was sufficient for Section 1-1. The calculations were repeated for section 2-2, except the moment due to the collision load was assumed to distribute outward at a 30° angle between Sections 1-1 and 2-2. The moment and tension force at Section 2-2 were calculated by multiplying the comparable values at Section 1-1 by the ratio of lengths  $L_c/(L_c+2H)$ :

$$\begin{aligned} M_{base @ 2-2} &= \frac{M_{base @ 1-1} L_c}{L_c + 2L[\text{Tan}(30^\circ)]} = \frac{23.85 \frac{\text{k-ft}}{\text{ft}} (13.589 \text{ ft})}{13.589 \text{ ft} + 2 * 1.55 \text{ ft}[\text{Tan}(30^\circ)]} \\ &= 21.12 \frac{\text{k-ft}}{\text{ft}} \end{aligned}$$

$$\begin{aligned} T_{base @ 2-2} &= \frac{T_{base @ 1-1}}{L_c + 2L[\text{Tan}(30^\circ)]} = \frac{7.14 \frac{\text{k-ft}}{\text{ft}}}{13.589 \text{ ft} + 2 * 1.55 \text{ ft}[\text{Tan}(30^\circ)]} \\ &= 0.32 \frac{\text{k}}{\text{ft}} \end{aligned}$$

where  $L$  is the distance between Section 1-1 and 2-2 and  $H = L \cdot \tan(30)$ . This led to an applied moment of 240 k-ft/panel at this section. The capacity at Section 2-2 was identical to that at Section 1-1 (279 k-ft/panel) so the design was adequate for both Sections 1-1 and 2-2.

Section 2-2 was also checked for Case 2, which uses the Strength 1 load combination for dead load and live load moment due to axle load. The moments  $M_{DC \text{ parapet}}$  and  $M_{DC \text{ slab}}$  remained the same as for Case 1. Since Section 2-2 was located over the exterior girder, additional moment resulted from the wearing surface between Section 2-2 and the edge of the parapet.

$$M_{DW} = \frac{DW_{Area \text{ load}}(width_{OH} - width_{parapet} - 0.25 \text{ ft})^2}{2} \\ = \frac{0.025 \text{ ksf}(3.5 \text{ ft} - 1.7 \text{ ft} - 0.25 \text{ ft})^2}{2} = 0.03 \frac{\text{k-ft}}{\text{ft}}$$

The live load moment in the section was calculated according to Eqs. (5.26) and (5.27) as follows:

$$X = width_{OH} - width_{parapet} - 1.25 \text{ ft} = 3.5 \text{ ft} - 1.7 \text{ ft} - 1.25 \text{ ft} \\ = 0.521 \text{ ft}$$

$$L = 45.0 + 10.0X = 45 + 10 * 0.521 \text{ ft} = 50.21 \text{ in}$$

$$M_{LL+IM} = \frac{16 \text{ IM} \cdot m \cdot X}{L} = \frac{16 (1.33)(1.2) \cdot 0.521 \text{ ft}}{\frac{50.21 \text{ in}}{12 \frac{\text{in}}{\text{ft}}}} = 3.18 \frac{\text{k-ft}}{\text{ft}}$$

and the overall moment was calculated as:

$$M_{strength I} = [1.25(M_{DC}) + 1.5(M_{DW}) + 1.75(M_{LL})] \\ = [1.25 * (1.67 + 0.6) + 1.5(0.03) + 1.75(3.18)] \frac{\text{k-ft}}{\text{ft}} * 10 \text{ ft} = 84.5 \frac{\text{k-ft}}{\text{panel}}$$

The moment demand due to this load combination was 84.5 k-ft/panel which was less than the capacity of 279 k-ft/panel. The intermediate design calculations are shown below in Tables 6.14 for Section 1-1 and 6.15 for Section 2-2.

Table 6.14: Overhang design for section 1-1

<b>Overhang Design</b>		
<b>Design Case I - Horizontal Vehicular Collision Load</b>		
<b>1-1 Inside Face of Parapet</b>		
$M_{base} =$	23.85	k-ft/ft
$R_W =$	147.03	k
$L_c =$	13.589	ft
$H =$	42	in
$T_{base} =$	7.14	k/ft
$M_{DC, Parapet} =$	0.68	k-ft/ft
$M_{DC, slab} =$	0.14	k-ft/ft
$M_{service I} =$	24.68	k-ft/ft
$M_{Extreme Event II} =$	24.88	k-ft/ft
$M_{Extreme Event II} =$	248.84	k-ft/panel
$T_{Extreme Event II} =$	71.41	k/panel
Hooked Bar Type	#7	
$l =$	1.7	ft
$d =$	0.875	in
$A_{bar} =$	0.6	in <sup>2</sup>
$I_G =$	16.29	in
Available Strength	60.0	ksi
# of bars	20	bars
$A_s =$	12	in <sup>2</sup>
$d =$	5.7	in
$a =$	1.06	in
$c =$	1.41	in
$\epsilon_s =$	0.009	Good
$\phi M_N =$	279.2	k-ft/panel

Table 6.15: Overhang design for section 2-2

<b>2-2 Edge of Exterior Girder</b>		
$M_{base@2-2} =$	21.12	k-ft/ft
$T_{base@2-2} =$	0.32	k/ft
$M_{DC, Parapet} =$	1.67	k-ft/ft
$M_{DC, Slab} =$	0.60	k-ft/ft
$M_{DW} =$	0.03	k-ft/ft
$M_{Extreme\ Event\ II} =$	240.03	k-ft/panel
$T_{Extreme\ Event\ II} =$	3.20	k/panel
$l =$	3.21	ft
Available Strength	60	ksi
$a =$	1.17	in
$c =$	1.56	in
$\epsilon_r =$	0.008	Good
$\phi M_N =$	276.2	k-ft/panel
<b>Design Case II - Dead and Live Load</b>		
<b>2-2 Edge of Exterior Girder</b>		
$M_{DC, Parapet} =$	1.67	k-ft/ft
$M_{DC, Slab} =$	0.60	k-ft/ft
$M_{DW} =$	0.03	k-ft/ft
$X =$	0.521	ft
$L =$	50.21	in
$m =$	1.2	
$IM =$	1.33	
$M_{LL+IM} =$	3.18	k-ft/ft
$M_{strength\ I} =$	84.5	k-ft/panel

## 6.4 Model Based Design Method

### 6.4.1 Overview

This section summarizes the modeling and analysis assumptions to apply the model-based design method to the Mesquite Bridge. The goal of this approach was to compare analysis results from the model to calculations used in the simplified design method. For this design example, comparisons were made between the simplified and model-based designs, especially with respect to skew since simplified calculations cannot capture most of the effects of skew. These comparisons were used to determine the applicability of the simplified method for highly skewed bridges.

The model used for the model based design was created using CSiBridge. This method was used in conjunction with the design aid spreadsheet discussed in Section 6.3, but refined the analysis to improve the accuracy of some of the input values to the spreadsheet. Figure 6.8 shows a 3-D view of the completed model. The purple elements are the shells used for the deck, the blue line elements represent the girders, and the green elements represent the girder prestressing strands and longitudinal post-tensioning. The coordinate system is as follows: x-direction refers to the longitudinal direction of the bridge, y-direction refers to the transverse direction, and z-direction refers to the direction of gravity.

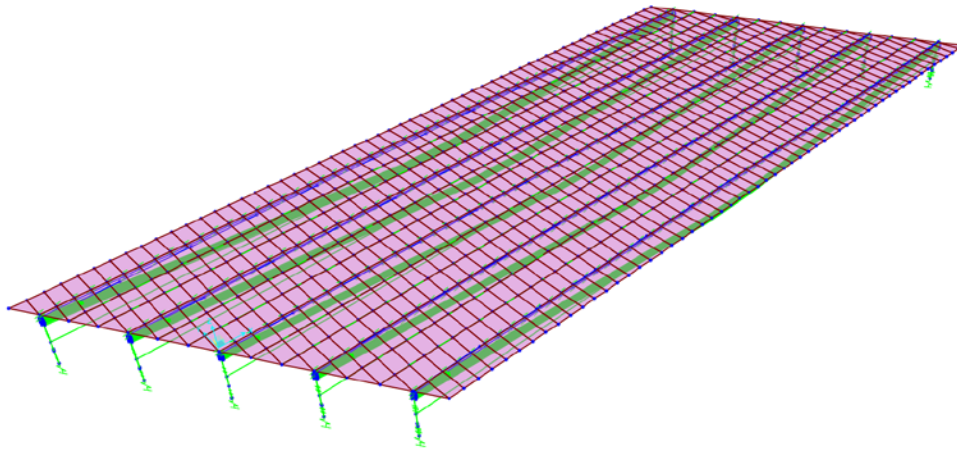


Figure 6.8: 3-D view of CSiBridge model

This model was not designed to be a stand-alone design tool, but rather to validate and determine applicability of simplified calculations used in the design aid spreadsheet to a bridge with a large amount of skew. The output from this model was then used to refine the input for the spreadsheet to achieve an improved design.

### 6.4.2 Material Definitions

All base materials used to define the various bridge elements were defined in CSiBridge. The properties of the deck concrete were: weight per unit volume  $\gamma_{dc} = 0.15$  kcf, Poisson's ratio  $\nu = 0.2$ , compressive strength  $f'_{dc} = 6$  ksi, and modulus of elasticity  $E_{dc} = 4415$  ksi. The girder concrete properties were: compressive strength  $f'_{gc} = 9$  ksi, and modulus of elasticity  $E_{gc} = 5407$  ksi. The deck concrete material was applied to the deck

(represented by shell elements) and the girder concrete material was applied to the girders (represented by frame elements). The tendon steel was defined with: weight per unit volume  $\gamma_{steel} = 0.49$  kcf, modulus of elasticity  $E_s = 28500$  ksi.

Link elements were used to connect the deck shell elements to the girder line elements. In lieu of material properties, the overall stiffness in each direction was defined. The links were assigned to be rigid for z-direction translation and rotations in all three directions. The stiffnesses in the x and y-directions were calculated using the following equation (Cheng, 2006):

$$K_{vf,45} = \frac{\rho_v}{1 + 4n\rho_v} E_s b_w d = \frac{0.00646}{1 + 4 * \frac{29000 \text{ ksi}}{4415 \text{ ksi}} (0.00646)} 29000 \text{ ksi} (12 \text{ in})(12 \text{ in})$$

$$= 23057 \frac{k}{in}$$

where  $\rho_v$  is the shear reinforcement ratio,  $n$  is the modular ratio of the reinforcing steel and concrete,  $E_s$  is the modulus of elasticity of the reinforcing steel, and  $b_w$  and  $d$  are the section widths perpendicular and parallel to the applied shear.

### 6.4.3 Geometric and Element Definitions

Bridge properties were input and an initial model was generated using the bridge wizard feature in CSiBridge. A layout line was created extending 111.5 feet in the x-direction from node (0, 0, 0), representing the length and centerline of the bridge. The model was created using frame elements for the girders, thin shell elements for the deck, link elements for deck-to-girder connections, and tendon elements for the post-tensioning steel. In this example, the transverse deck prestressing steel was not included in the model as it had already been designed using a structural analysis software in conjunction with the simplified method. Because a refined analysis had already been used for the transverse prestress steel design, the focus for this example was the post-tensioning stress.

The girders and deck were created by defining a bridge superstructure section, referred to as “deck section” by CSiBridge. The deck section was defined as a bridge object and used to automatically place the girder and deck elements based on the defined geometry and bridge centerline. The deck slab shell elements were assigned the deck concrete material, overall deck width = 45.917 feet, deck slab thickness = 8 inches, and left and right overhang width = 41.5 inches. The girder frame elements were assigned the girder concrete material, and dimensions as shown in Figures 6.3 and 6.9. The girders were placed with a constant spacing of 9.75 feet and a constant girder haunch thickness of 3 inches was added to the deck section. The output from the defined geometry is shown in Figure 6.10.

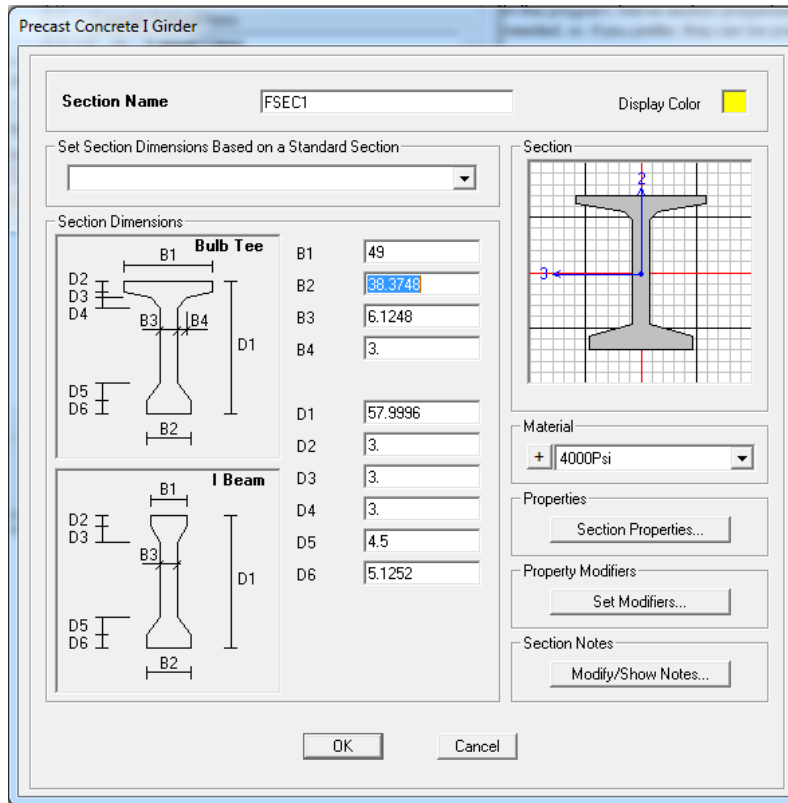


Figure 6.9: Girder properties

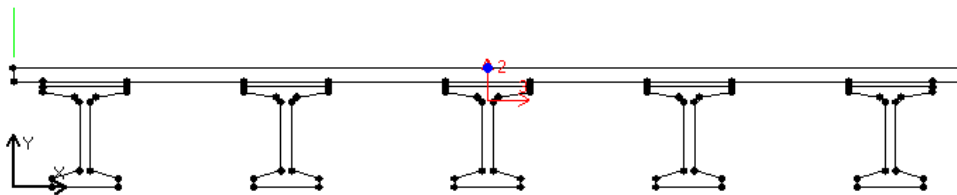


Figure 6.10: Model bridge deck cross-section

The geometric properties for the deck section were initially used to automatically generate a simple version of the bridge model. This initial model did not include any joints between the deck and the girder but assumed full composite action between the two systems. However, to check whether the deck to girder connection generated enough resistance to achieve full composite action, an additional refined model was created. This model used a manually discretized deck and girder elements to allow the deck and girder elements to be connected by links at nodal locations. The deck shell elements for the refined model were created using a mesh size of 2 feet in the longitudinal direction of the bridge and 3.25 feet in the transverse direction. As a result, the shells along the abutments were triangular and all shells between the abutments were rectangular. A plan view of the deck discretization is shown in Figure 6.11. The girder elements were also discretized every 2 feet to accommodate the link elements. Links were added to the model connecting the nodes along the girder line elements to the nodes in the deck shell

elements. These links were spaced every 2 feet along the girder line and were defined with the properties discussed in Section 6.4.2.

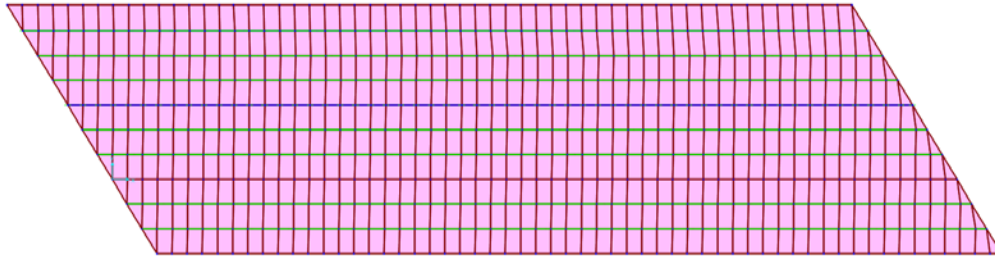


Figure 6.11: Discretization of the deck

To account for the prestressing force in the prestressed concrete girders, tendons following the tendon steel path defined in the Mesquite bridge plan set (Figure 6.4) were incorporated. The 10 harped prestressing strands for each girder were specified in five rows and two columns, with each strand spaced 2 inches apart. At the girder ends, the top of the strand group was placed 2 inches below the top of the girder; and at a distance 43% along the girder length, the bottom of the strand group was placed 4 inches from the bottom of the girder. The depth of each strand within the girder varied linearly between these two points as shown by the C.G. Harped Strands callout in Figure 6.12. Each strand was defined in the model using the tendon steel material described previously, as a 0.6 inch diameter tendon with a prestress force of 43.94 kips. The remaining straight strands at the bottom of the section were modeled as a single strand applied at the center of the prestress force, which was the center of the girder, 3.75 inches away from the bottom face. The strand was defined with cross-sectional area = 8.68 in<sup>2</sup> and a total jacking (prestress) force = 1757.7 kips. These properties were defined in the Mesquite Bridge plan set and the applied prestress forces accounted for all losses. The post-tensioning tendons were input into the model after the dead load analysis and completion of their design.

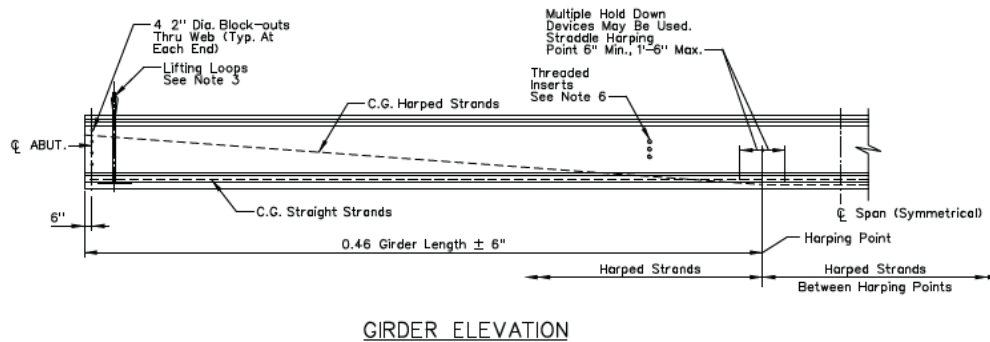


Figure 6.12: Girder prestress steel along girder

The ends of the bridge at the abutments were constrained by fixing the translation in each direction and leaving all rotations free. The girder support condition was set as “connect to girder bottom only”, representative of a non-integral girder connection or seat-type abutment. Each abutment was rotated 31.1° to set the skew.

#### **6.4.4 Loads and Analysis Assumptions**

The model was used mainly to check the stresses and moments in the deck and use these to design the post-tensioning. Three different load cases were defined, and combined using a load combination. The Dead Load case included the self-weight of the deck (shell elements) and girders (frame elements) each calculated by the program; girder prestressing force, and wearing surface conservatively applied as a 0.025 ksf area load to all shell elements. The Dead Load case was analyzed using a linear static analysis. The Live Load case included the effect of moving truck loads in each lane and was analyzed using a linear moving load analysis. Two 12 feet wide lanes were assigned, each with the lane centerline 6 feet from the bridge centerline. The lanes were adjacent to each other. The HL-93 truck load was applied to each lane by placing the truck load at different locations along the bridge in the longitudinal and transverse directions and determining the maximum effect. An “Other” load case was defined that included the prestressing force of the post-tensioning tendon elements. These load cases were all combined into a load combination named ACASE1, which represented the Strength I load combination (1.25 DC+1.5DW+1.75LL). Defining the different load types independently allowed the analysis results to be evaluated separately for each case or combined for a cumulative effect.

#### **6.4.5 Dead and Live Load Analysis and Post-Tensioning**

The model was initially analyzed with dead load only. Stresses due to dead load were compared in the simplified model without link elements and the refined model. Figures 6.13 and 6.14 show the maximum tensile stress in the longitudinal direction along the deck due to factored dead load for the refined and simplified models, respectively. This maximum stress represented the highest tensile stress through the depth of the deck cross-section. Both models developed a negative moment at the ends, resulting in tension in the deck. The refined model was subjected to a maximum tensile stress of 0.054 ksi, located along the abutment above the exterior girder. The simplified model was subjected to a maximum tensile stress of 0.051 ksi, located along the abutment between the exterior and interior girder. The forces transferred between the deck and girders were equal between the two models. All forces were transferred between the two elements so full composite action was being achieved with the spring connections. This meant that both the models would produce the same results as the assumption for the simplified model was full the deck and girders behaved compositely. Because the model results were similar, the simplified model was used to generate the moment diagrams as the refined model was limited in the force diagrams it could produce because it lacked an integral bridge object for the superstructure section. The simplified model was used for all calculations hereafter.

The moment diagram in the longitudinal direction due to factored dead load is shown in Figure 6.15. The analysis showed that the maximum positive moment was 4918 k-ft and largest magnitude negative moment was 2989 k-ft. The maximum positive moment was smaller than the 7136 k-ft calculated with the simplified method, but the negative moment was much higher than the assumed value of 0. Because the analysis predicted a negative moment in the deck, additional post-tensioning was required beyond what was used for the simplified method.

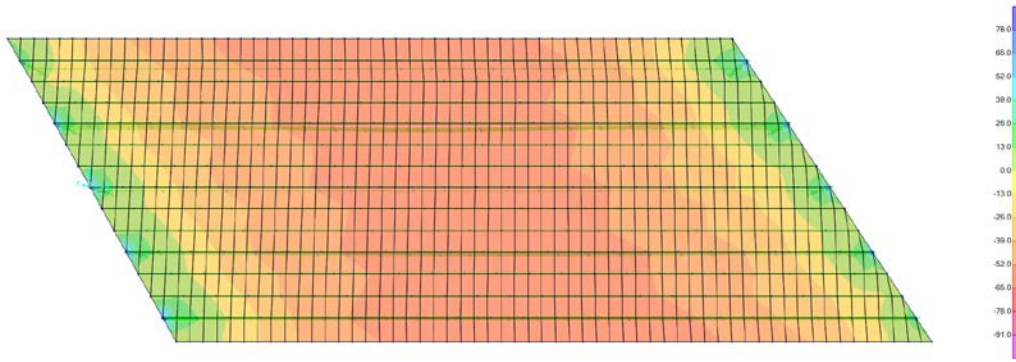


Figure 6.13 Deck stress for refined model subjected to dead load

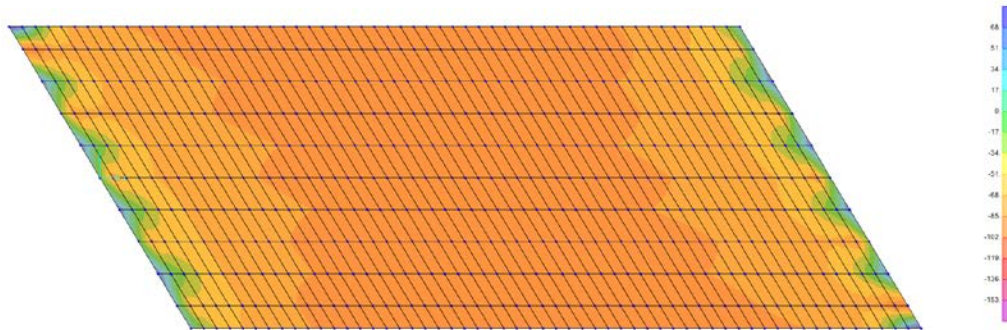


Figure 6.14 Deck stress for simplified model subjected to dead load

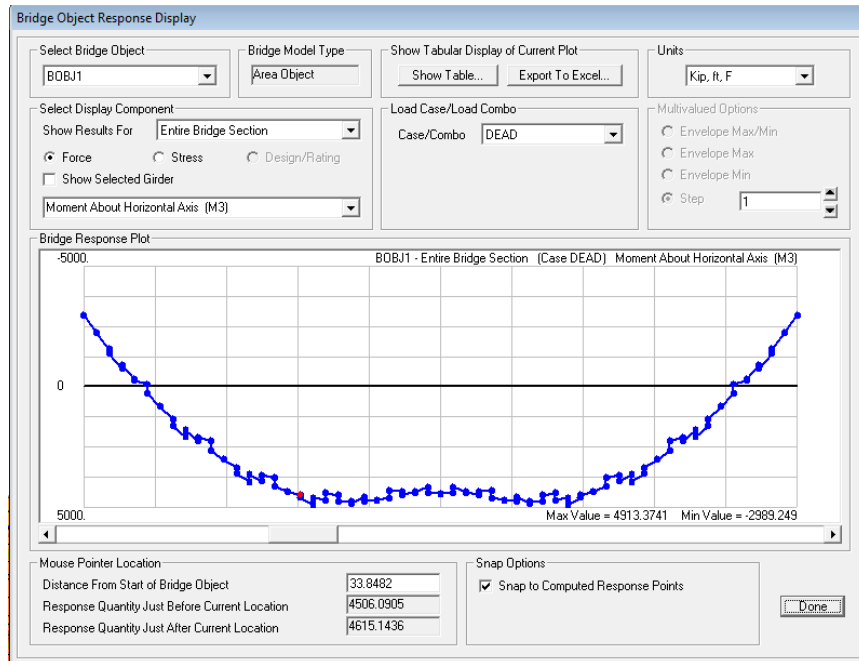


Figure 6.15: Moment diagram due to dead load

Live loads may also contribute to the tensile stresses in a skewed deck. A moving load analysis using the lanes and vehicle load was performed on the simplified model to determine additional tensile stresses that must be overcome by post-tensioning. The analysis results of the model subjected to combined factored dead and live loads showed that the maximum longitudinal tensile stress in the deck was equal to 0.090 ksi. The axial stress distribution resulting from live load is shown in Figure 6.16.

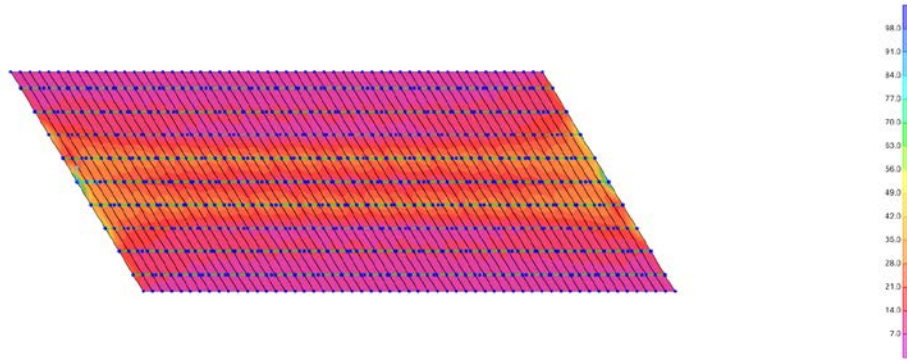


Figure 6.16: Stress due to live load

Post-tensioning was calculated based on the design stress of 0.090 ksi determined by the analysis and the additional 0.250 ksi minimum required compression. The required number of post-tensioning strands was calculated using the design aid spreadsheet with the same method described in Section 6.3.4. The spreadsheet calculated that 1498 kips of post-tensioning needed to be applied to the deck. The calculations are shown in Table 6.16.

Table 6.16 Post-tensioning calculations

Longitudinal Post-tensioning		
$f_t =$	90.0	psi
$F_{pe} =$	38.1	k
$F_{req} =$	1498.72	k
$n =$	39.4	strands

This value is the maximum tensile stress found in a transverse joint at any point along the bridge. This can be found through modeling or hand calculations.

### 6.4.6 Analysis with Post-Tensioning

The post-tensioning was designed according to the calculations shown in Section 6.4.5. The post-tensioning layout consisted of 10 ducts with four strands per duct. This differed from the design from the simplified method of 6 ducts with 5 strands per duct. Each duct carried a prestress force of 152 kips. The force was applied as a tendon element stressed from both ends. The tendons were input by connecting the element to nodes on each side of the bridge. The tendon layout is shown in Figure 6.17.

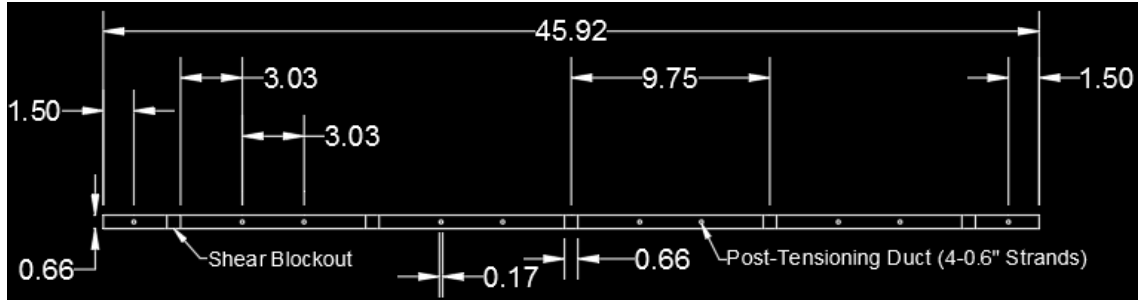


Figure 6.17: Post-tensioning layout for model based design (dimensions in ft)

The analysis was completed using a dead and live load analysis in addition to applying the post-tensioning force from the tendons. Applying each of these loads resulted in a residual maximum joint tensile stress of 0.02 ksi, meaning the prestress force was determined by the model to be insufficient to overcome the tension in the deck. The axial stress in the deck along the longitudinal direction is shown in Figure 6.18. The moment due to dead load in the longitudinal direction is shown in Figure 6.19. The tension in the joints could be removed in the model by adding additional post-tensioning beyond what was applied according to the calculations in Section 6.4.5. The amount of the post-tensioning force was iterated until there was 0.25 ksi compression in every joint. This force was much higher than what was predicted by the spreadsheet results that used the model tension values.

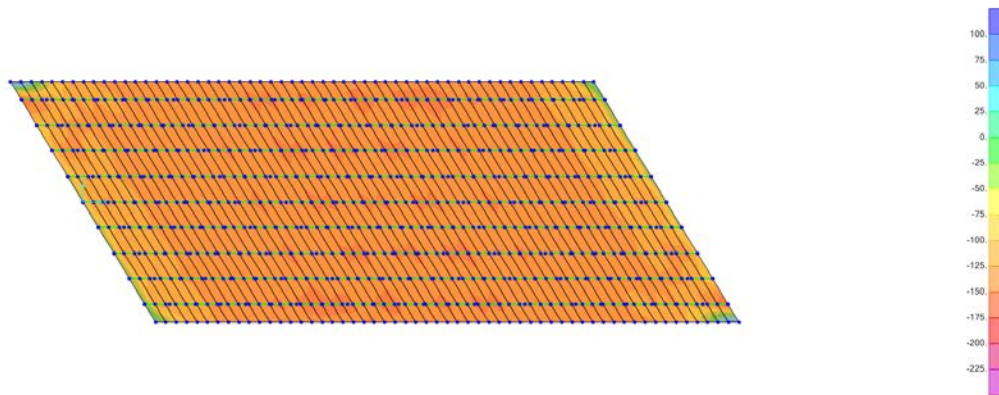


Figure 6.18: Stress in the deck after post-tensioning

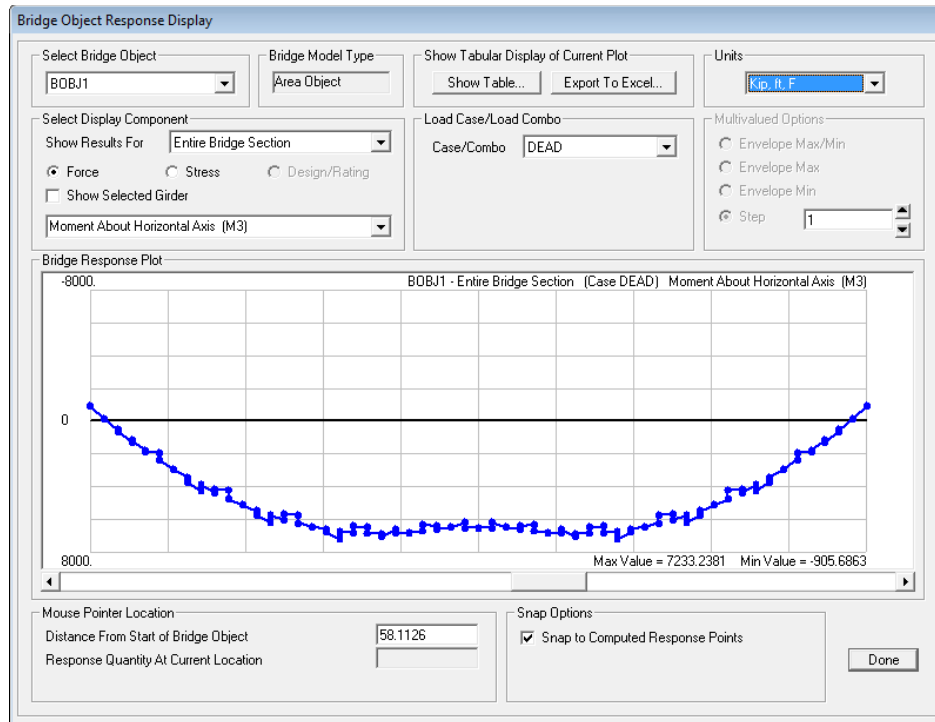


Figure 6.19: Moment due to dead load including post-tensioning

A review of the analysis results showed a discrepancy in how the post-tensioning was being applied to the model. In practice, application of the post-tensioning occurs prior to the connection of the deck to the girder. This causes all of the post-tensioning force to be applied directly to the deck. In the model, the post-tensioning was effectively applied to the composite deck-girder section. This resulted in the post-tensioning force being distributed to both the deck and the girders, which is a much larger cross-sectional area than the deck alone and requires a much higher post-tensioning force to achieve desired compressive stress. Because the post-tensioning force was not accounted for in the model as expected, the design that was calculated in Section 6.4.5 and shown in Figure 6.17 was considered to be the final design.

## 6.5 Validation and Comparison of Results

This section summarizes the differences between the simplified method and the model based method. Concerns regarding the methods are discussed and changes to the design procedure based on the findings are explored.

An initial observation from this design example was that a negative moment developed at the ends of the span, while the moment diagram is expected to be all positive in a non-skewed bridge. In the simplified design method, the negative moment was assumed to be zero because the bridge consisted of a single span. However, the analysis results predicted a significant negative moment (Figure 6.11). The shape of the moment diagram was similar to that predicted in the simplified method, but the diagram was shifted towards the negative moment region. This changed the post-tensioning design compared to the simplified method.

The model based method confirmed that the number and strength of shear connectors used in the simplified method was adequate. All shear stresses were transferred between the deck and girders. Full composite behavior was achieved and the deck panel system responded as would be expected from a conventional deck. Also, the modeling showed that if a model based method is used for design, the individual deck-to-girder connections need not be modeled explicitly. The bridge can be modeled more simplistically.

A main concern from the modeling procedure applied here is amount of post-tensioning required to negate the tensile forces in the joints. The predicted amount of post-tensioning based on the negative moment in the bridge was not adequate to remove the tension in the panel-to-panel joints. This was due to the deck being composite with the girders prior to application of the post-tensioning force. In actuality, the post-tensioning force is applied to the deck panels prior to being made composite with the girders. However, this behavior cannot be achieved in CSiBridge.

Based on the experiences gained from this design example, the recommendation is that all skewed bridges should be analyzed with a structural model. The model should be used to evaluate moments and stresses in the deck for use in the design aid spreadsheet. These forces should be used as the inputs for all load demands on the bridge as they describe the system behavior more accurately than what is achieved using simplified calculations. Because the change in stress in a post-tensioned section due to bending is linear in deck panel applications; the post-tensioning can be designed using the model loads, but a separate validation of the deck stresses with post-tensioning in the model is not needed. Therefore, the stresses are used to calculate the required post-tensioning force and the design aid spreadsheet is used to calculate the amount of post-tensioning required. The rest of the design including: the transverse prestress steel, flexural capacity, deck to girder connection, temperature and shrinkage reinforcement, and the overhang design can all be calculated with the design aid spreadsheet without requiring additional input.

## **Chapter 7: Design Example 2: SR 170 Bunkerville Road**

### **7.1 Introduction**

This chapter presents a second application of the design methods discussed in Chapter 5. The first design example for the Mesquite Bridge as described in Chapter 6, was limited to a single span bridge with significant skew. A multispan bridge was preferred for the second design example. Again, bridge plan sets provided by NDOT were evaluated to select a good example for incorporation of a prefabricated deck panel design. The second design example is a modified version of the SR 170 Bunkerville Road – Virgin River Bridge. The bridge has been reduced to three spans instead of five to simplify the design and modeling. The interior and exterior span lengths are selected to be consistent with the original design. The skew and superelevation are assumed to be 0, to simplify the focus to the multispan effects. Section 7.2 briefly describes the bridge geometry, and Sections 7.3 and 7.4 describe the implementation of the simplified design method and the model-based method, respectively, for the bridge. Section 7.5 discusses the findings from the Bunkerville Road design example and recommends changes to the design philosophy.

### **7.2 Bridge Description**

The Bunkerville Road Bridge is a three span bridge with exterior span lengths of 190 feet and an interior span length of 155 feet. The bridge is 39 feet wide with three steel girders spaced at 14 feet and 5.5 feet overhangs. The abutments are seat type, resting on spread footing with bearing pads. The intermediate piers are single column bents, each incorporating a 7 foot diameter column with a 34 foot wide cap beam that is non-integral with the girders. Figure 7.1 displays the bridge cross section at the pier location, and Figure 7.2 shows the elevation view. Figure 7.3 shows the girder dimensions.

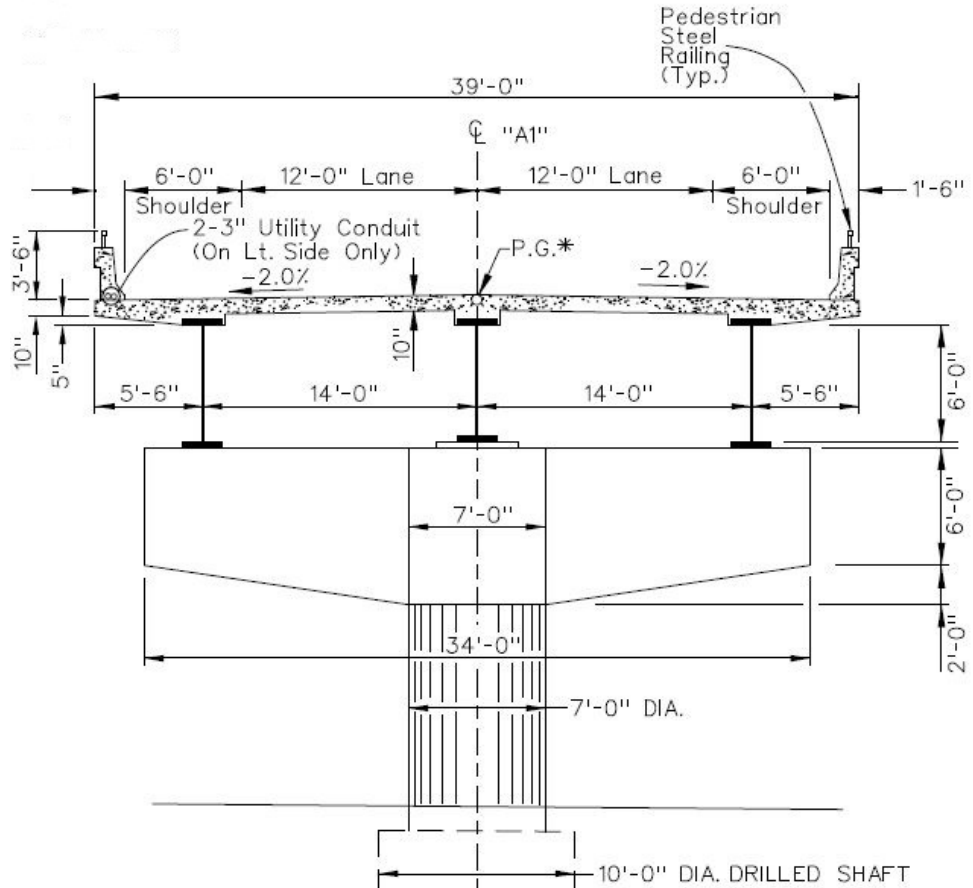


Figure 7.1: Bunkerville Road bridge cross-section

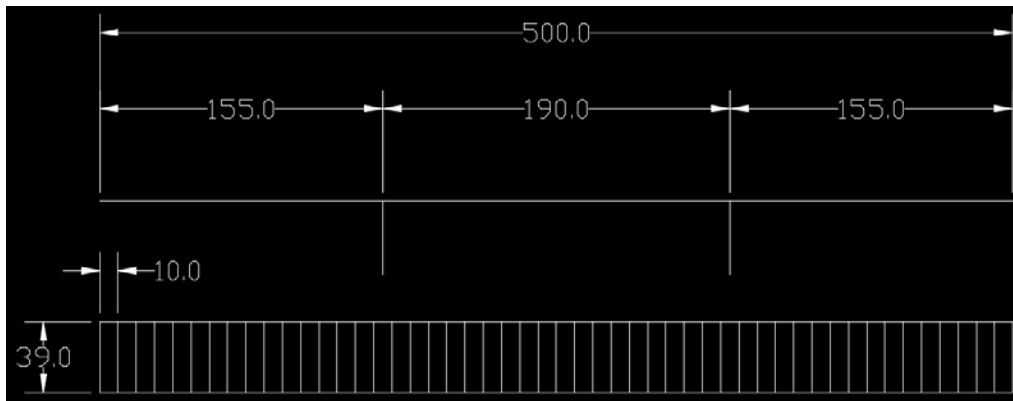


Figure 7.2: Bunkerville Road elevation view (dimensions in ft)

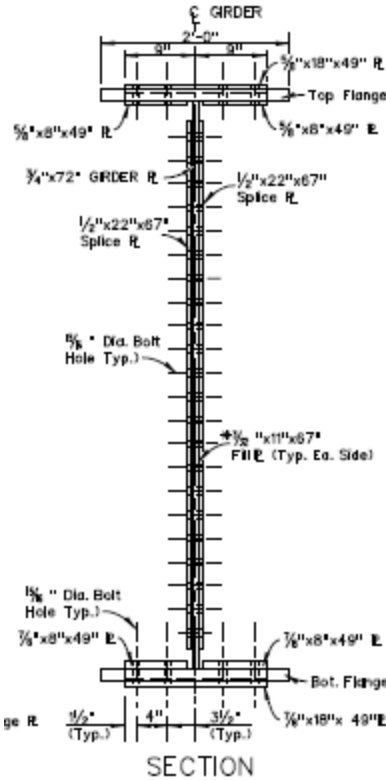


Figure 7.3: Bunkerville Road girder cross-section

Because the deck is 39 feet wide, less than the 50'-0" transportation limit, the panels are designed to span the entire width of the bridge with no longitudinal joint. For this example, because there is no skew, all panels are designed as rectangular. The panels are 39 feet long (equivalent to the bridge width) by 10 feet wide and 10 inches in depth. The concrete strength is specified as 6 ksi. Also, the bridge is assumed to have no overlay.

### 7.3 Simplified Design Method

The following sections describe the implementation of the simplified design method on the Bunkerville Road Bridge, supported by output from the design aid spreadsheet. For interpretation of the spreadsheet data, orange highlighted cells are user input values, while grey highlighted cells with orange text represent values calculated within the spreadsheet.

#### 7.3.1 Design Moments and Loads

Area loads and moments due to dead and live load were calculated first, and the output from the design aid spreadsheet is shown in Table 7.1. Assuming a 10-inch deck, the DC area load due to self-weight was calculated as:

$$DC = 0.15 \text{ kcf} * \frac{10 \text{ in}}{12 \frac{\text{in}}{\text{ft}}} = 0.125 \text{ ksf},$$

The DC load was then used to calculate the moment demand in a deck panel for the transverse and longitudinal directions. In this example, the transverse direction moments were calculated using two different methods to demonstrate alternative approaches. Method 1 estimates the moment using a simplified equation [Eq. (5.1)]. First, the distributed dead load (per unit length in the transverse direction) was calculated as:

$$w_{DC} = 0.125 \text{ ksf} * 1\text{ft} = 0.125 \text{ klf}$$

Then,  $w_{DC}$  was substituted for  $w$  in Eq. (5.1), with  $y = 10$ , and girder spacing  $l = 14$  ft, to compute the DC moments ( $M_{DC}$ ):

$$M_{DC} = \frac{0.125 \text{ klf} * (14 \text{ ft})^2}{10} = 2.45 \frac{\text{k-ft}}{\text{ft}}$$

This result, which applies to both positive and negative moment regions, is shown as Estimated  $M_{DC}$  in Table 7.1. For Method 2, the moments were computed the moments using a simple structural analysis model built from basic line elements with applied distributed loads  $w_{DC}$  as defined above. The results from this analysis are shown as transverse direction moments  $M_{DC}^+$  and  $M_{DC}^-$  in Table 7.1. Because the moments from Method 2 were calculated using a more accurate procedure, these moments were used for design.

The maximum positive and negative transverse moments due to live load were found using Table A4-1 in the AASHTO LRFD specifications (AASHTO, 2012), and are shown as  $M_{LL}^+$  and  $M_{LL}^-$  in Table 7.1. The live load calculation assumed a girder spacing of 14 feet and distance from the girder centerline to the design section of 0 inches for the negative moment.

Moments in the longitudinal direction were calculated using a simple structural analysis model, and the resulting values were entered into Table 7.1. The applied load in the model was equal to the DC load, calculated as:

$$w_{Deck-Long} = 0.125 \text{ ksf} * 39\text{ft} = 4.875 \text{ klf}$$

$$w_{Girder-Long} = \gamma_{steel} A_{girder} = 0.49 \text{ kcf} * 0.875\text{ft}^2 = 0.43 \text{ klf}$$

$$\begin{aligned} w_{DC-Long} &= w_{Deck-Long} + \#_{girder} w_{Girder-Long} = 4.875 \text{ klf} + 3 * 0.43 \text{ klf} \\ &= 6.2 \text{ klf} \end{aligned}$$

The maximum longitudinal moments for this combination were found to be equal for positive and negative moments,  $M_{DC}^+ = M_{DC}^- = 19020$  k-ft.

Table 7.1: Summary of transverse and longitudinal moments

Load Assignments 3.4.1			
DC:	0.125	kSF	
DW:	0	kSF	
LL:	HL-93 with lane load and multi presence factor		
Moments in transverse direction			
c =	10		
Estimated $M_{DC} +$	2.450	k-ft/ft	Calculated using estimate of $wl^2/c$
Estimated $M_{DW} +$	0.000	k-ft/ft	
$M_{DC} +$	1.5	k-ft/ft	Calculated using standard formulas or structural analysis program
$M_{DC} -$	-2.12	k-ft/ft	
$M_{DW} +$	0.0	k-ft/ft	
$M_{DW} -$	0.00	k-ft/ft	
$M_{LL} +$	9.02	k-ft/ft	
$M_{LL} -$	-12.24	k-ft/ft	
Moments in longitudinal direction			
$M_{DC} +$	10102	k-ft	
$M_{DC} -$	-18520	k-ft	
$M_{DW} +$	0	k-ft	
$M_{DW} -$	0	k-ft	

The transverse direction moments were combined according to the load combinations, Strength I, Service I and Service III. Each load combination is used for a different part of the design calculations. The moment demands for each load combination were calculated as:

$$M_{Strength I}^+ = \left( 1.5 \frac{k-ft}{ft} * 1.25 + 9.02 \frac{k-ft}{ft} * 1.75 \right) * 10 ft = 177 \frac{k-ft}{panel}$$

$$M_{Strength I}^- = \left( -2.12 \frac{k-ft}{ft} * 1.25 - 12.24 \frac{k-ft}{ft} * 1.75 \right) * 10 ft = -241 \frac{k-ft}{panel}$$

$$M_{Service I without LL}^+ = \left( 1.5 \frac{k-ft}{ft} * 1 \right) * 10 ft = 15 \frac{k-ft}{panel}$$

$$M_{Service I without LL}^- = \left( -2.12 \frac{k-ft}{ft} * 1 \right) * 10 ft = -21.2 \frac{k-ft}{panel}$$

$$M_{Service I with LL}^+ = \left( 1.5 \frac{k-ft}{ft} * 1 + 9.02 \frac{k-ft}{ft} * 1 \right) * 10 ft = 105.2 \frac{k-ft}{panel}$$

$$M_{Service I with LL}^- = \left( -2.12 \frac{k-ft}{ft} * 1 - 12.24 \frac{k-ft}{ft} * 1 \right) * 10 ft = -143.6 \frac{k-ft}{panel}$$

$$M_{Service III}^+ = \left( 1.5 \frac{k-ft}{ft} * 1 + 9.02 \frac{k-ft}{ft} * 0.8 \right) * 10 ft = 87.2 \frac{k-ft}{panel}$$

$$M_{Service III}^- = \left( -2.12 \frac{k-ft}{ft} * 1 - 12.24 \frac{k-ft}{ft} * 0.8 \right) * 10 ft = -119.1 \frac{k-ft}{panel}$$

### 7.3.2 Prestress Steel Design

The prestressing steel was designed using the process overviewed in Section 5.3.2. First, an initial amount of prestressing steel was estimated, and used to iterate toward final converged values for prestress loss and capacity of the section. Table 7.2 shows the prestress steel properties assumed for transverse panel reinforcement, which included 1/2" diameter 7-wire (Grade 270) prestressing strands. The ultimate stress,  $f_{pu}$ , of the strand was defined as 270 ksi, and other values assumed by the design aid spreadsheet were: strand yield stress  $f_{py} = 90\%$  of  $f_{pu}$ , initial prestress  $f_{pi} = 75\%$  of  $f_{pu}$ , and effective prestress  $f_{pe} = 90\%$  of  $f_{pi}$ .

Table 7.2: Prestressing steel properties

Steel Properties - Prestressing Steel		
$f_{pu} =$	270	ksi
$f_{py} =$	243	ksi
$E_p =$	28500	ksi
$f_{pi} =$	203	ksi
1/2" diameter - 7 wire strands	0.153	in <sup>2</sup>
$f_{pe} =$	182	ksi

The larger of the two Service III moments,  $M_{Service III} Max$ , was used to calculate an initial value for the number of prestressing strands per panel. The allowable tensile stress in the concrete,  $\sigma_{allowable}$ , was computed as:

$$\sigma_{allowable} = 0.19\sqrt{f'_c} = 0.19\sqrt{6 \text{ ksi}} = 0.465 \text{ ksi}.$$

The initial prestress force was calculated by rearranging Eq. (5.2) and solving for  $P_{pe}$ :

$$P_{pe} = \left( \sigma_{allowable} + \frac{M_{Service III}}{s} \right) * A = \left( -0.465 \text{ ksi} + \frac{119.1 \text{ k-ft} * 12 \frac{in}{ft}}{2000 \text{ in}^4} \right) * 1200 \text{ in}^2 = 299.2 \text{ kips}.$$

Note that compression is positive in the above calculation. The initial number of prestressing strands,  $n$ , rounded up to the nearest even number, was calculated per Eq. (5.3) as:

$$n = \frac{299.2 \text{ k}}{0.153 \frac{\text{in}^2}{\text{strand}} * 182 \text{ ksi}} = 12 \text{ strands}.$$

Thus, the required number of prestressing strands was initially estimated as 12. Table 7.3 shows the initial prestress steel calculations.

Next, the subsequent calculations and prestress design checks are described, which are based on the specified number of strands. As part of the design process, the number of strands was iteratively adjusted until all checks were satisfied. Application of this

iterative process led to a final calculation of 24 strands required to satisfy all design checks. All subsequent calculations are based on this final value (24 strands), shown as the highlighted orange input cell in Table 7.3. The strands were placed in two layers; each located 2.25 inches from the outside edge of the panel.

Table 7.3: Initial prestressing steel design

Prestress Steel Estimate			
$M_{service III} Max =$	119.12	k-ft	This uses the service moment to calculate a required number of strands based off of estimated properties. These calculations are checked in the following sections
$\sigma_{allowed} =$	-0.465	ksi	
$P_{pe} =$	299.2	k	
$n =$	10.7	strands	
Use	24	- 1/2" strands	
Try 2 layers	12	strands/layer	
$A_{ps} =$	3.672	in <sup>2</sup>	
$\beta_1 =$	0.75		

Losses were calculated for the prestress steel according to the equations found in Section 5.2.3. Elastic shortening loss was initially assumed to be 1%, and the actual loss was subsequently calculated. The initial prestress value,  $f_{pi}$ , was multiplied by 99% to reflect the prestress in the strand after elastic shortening loss,  $f_{pes}$ .

$$f_{pes} = 0.99 * 203 \text{ ksi} = 200.5 \text{ ksi}.$$

The updated total prestress force (with 24 bars) was computed as:

$$P_{pe} = nA_{ps}f_{pes} = 24 * 0.153 \text{ in}^2 * 200.5 \text{ ksi} = 736.1 \text{ kips}.$$

This prestress force was used to find the stress  $f_{cgp}$  in the concrete due to prestressing:

$$f_{cgp} = \frac{P_{pe}}{A} = \frac{736.1 \text{ k}}{1200 \text{ in}^2} = 0.613 \text{ ksi}.$$

Using Eq. (5.4) with  $E_p = 28500$  ksi and  $E_{ct} = 4031$  ksi, the losses due to elastic shortening were found to be 4.34 ksi, which is equivalent to a prestress loss of 2.14%. Because the calculated elastic shortening loss was not close to the assumed loss, the procedure was repeated using an assumed initial loss of 2.1%. This resulted in an elastic shortening loss of 4.3 ksi and a loss percentage of 2.12%, which was close enough to the assumed value to be considered converged. The elastic shortening loss calculations are shown in Table 7.4.

Table 7.4: Elastic shortening losses

Prestress Losses		
Elastic Shortening		
Try 1% initial loss	2.10%	
Assumed strand stress =	198.2	ksi
$P_i =$	728.0	k
$f_{cp} =$	0.607	ksi
$\Delta f_{pES} =$	4.290	ksi
% Loss =	2.12%	Should be close to assumed value, if not recalculate

After the calculation of short term losses (elastic shortening), long term losses due to shrinkage, creep, and relaxation were determined. Panel properties prior to deck installation differed from the properties after deck installation, so shrinkage and creep losses were calculated both before and after deck installation. The following input values were defined: volume-to-surface area ratio of one deck panel  $V/SA = 4.62$ , relative humidity  $H = 40\%$  for this bridge location (Figure 5.4.2.3.3-1 in AASHTO, 2012), time between curing and loading  $t = 89$  days, and the overall lifespan of the deck  $t_f = 75$  years or 27375 days. Based on these inputs, the following factors were calculated: volume-to-surface ratio factor  $k_s$ , humidity factor for shrinkage  $k_{hs}$ , humidity factor for creep  $k_{hc}$ , factor for the effect of concrete strength  $k_f$ , time development factor at time of transfer  $k_{td}$ , and time development factor at the end of the service life of the deck  $k_{tdf}$ , according to AASHTO 5.4.2.3.2-(2-5) and 5.4.2.3.3-2:

$$k_s = 1.45 - 0.13 \left( \frac{V}{SA} \right) \geq 1.0, 1.45 - 0.13(4.62): k_s = 1$$

$$k_{hs} = 2 - 0.014H = 2 - 0.014(40): k_{hs} = 1.44$$

$$k_{hc} = 1.56 - 0.008H = 1.56 - 0.008(40): k_{hc} = 1.24$$

$$k_f = \frac{5}{1 + f'_{ci}} = \frac{5}{1 + 5 \text{ ksi}}: k_f = 0.83$$

$$k_{td} = \frac{t}{61 - 4f'_{ci} + t} = \frac{89 \text{ days}}{61 - 4 * 5 \text{ ksi} + 89 \text{ days}}: k_{td} = 0.68$$

$$k_{tdf} = \frac{t_f}{61 - 4f'_{ci} + t_f} = \frac{27375 \text{ days}}{61 - 4 * 5 \text{ ksi} + 27375 \text{ days}}: k_{tdf} = 0.99$$

These factors were used to calculate the strain due to shrinkage,  $\epsilon_{sh}$  per AASHTO 5.4.2.3.3-1 (2012), and the creep coefficient at time of installation,  $\psi_b(t, t_i)$  and final service life of the deck,  $\psi_b(t_f, t_i)$  per AASHTO 5.4.2.3.2-1 (2012).

$$\varepsilon_{sh} = k_s k_{hs} k_f k_{td} 0.48 * 10^{-3} = 1(1.44)(0.83)(0.68)(0.48 * 10^{-3}) \\ = 0.000394$$

$$\psi_b(t, t_i) = 1.9 k_s k_{hc} k_f k_{td} t_i^{-0.118} = 1.9(1)(1.24)(0.83)(0.68)(89^{-0.118}) = 1.34$$

$$\psi_b(t_f, t_i) = 1.9 k_s k_{hc} k_f k_{td} t_f^{-0.118} = 1.9(1)(1.24)(0.83)(0.68)(27375^{-0.118}) = 1.96$$

The transformed section coefficient,  $K_{id}$  was found using AASHTO 5.9.5.4.2a-2 (2012):

$$K_{id} = \frac{1}{1 + \frac{E_p A_{ps}}{E_{ci} A_g} \left(1 + \frac{A_g e_{pg}^2}{I_g}\right) [1 + 0.7 \psi_b(t_f, t_i)]} = \frac{1}{1 + \frac{28500 \text{ ksi}}{4287 \text{ ksi}} \left(\frac{3.672 \text{ in}^2}{1200 \text{ in}^2}\right) (1 + 0) [1 + 0.7(1.96)]} \\ = 0.95$$

Each of the above factors were used to find the losses due to shrinkage and creep prior to deck installation using Eqs. (5.5) and (5.7):

$$\Delta f_{pSR} = \varepsilon_{sh} E_p K_{id} = 0.000394 * 28500 \text{ ksi} * 0.95 = 10.7 \text{ ksi}$$

$$\Delta f_{pCR} = \frac{E_p}{E_{ci}} f_{cgp} \psi_b(t, t_i) K_{id} = \frac{28500 \text{ ksi}}{4287 \text{ ksi}} 0.607 \text{ ksi} (1.34)(0.95) = 5.5 \text{ ksi}$$

Relaxation before deck installation was calculated according to Eq. (5.9):

$$\Delta f_{pR1} = \Delta f_{pR2} = \frac{f_{pt}}{K_L} \left( \frac{f_{pt}}{f_{py}} - 0.55 \right) = \frac{198.2 \text{ ksi}}{30} \left( \frac{198.2 \text{ ksi}}{243 \text{ ksi}} - 0.55 \right) = 1.8 \text{ ksi}$$

Shrinkage and creep losses at the end of the deck life were calculated as follows:

$$\varepsilon_{bif} = k_s k_{hs} k_f k_{tdf} 0.48 * 10^{-3} = 1(1.44)(0.83)(0.999)(0.48 * 10^{-3}) \\ = 0.000575$$

$$\varepsilon_{bdf} = \varepsilon_{bif} - \varepsilon_{sh} = 0.000575 - 0.000394 = 0.000181$$

$$\Delta f_{pSD} = \varepsilon_{bdf} E_p K_{id} = 0.000181 * 28500 \text{ ksi} * 0.95 = 4.9 \text{ ksi}$$

$$\Delta f_{pCD} = \frac{E_p}{E_c} f_{cgp} \psi_b[(t_f, t_i) - \psi_b(t_d, t_i)] K_{df} + \frac{E_p}{E_{ci}} \Delta f_{cd} \psi_b(t_f, t_d) K_{df} \\ = \frac{28500 \text{ ksi}}{4415 \text{ ksi}} 0.607 \text{ ksi} (1.96 - 1.34)(0.95) + 0 = 2.30 \text{ ksi}$$

The relaxation loss after deck placement was assumed to be identical to that before deck placement. Prestress loss calculations prior to deck installation and at the end of service

life are shown in Tables 7.5 and 7.6, respectively. The total long term prestress loss (26.9 ksi) was calculated by summing all individual losses before and after deck placement. This led to a final prestress value of 171.3 ksi with a net loss of 15.4% over the life of the deck.

Table 7.5: Prestress losses prior to deck installation

Creep & Shrinkage (Between Transfer and Deck Installation)			5.9.5.4
V/SA	4.62		
H	40		Relative Humidity
t =	89	days	Time between curing and loading
t <sub>r</sub> =	27375	days	Overall life of panels
k <sub>s</sub> =	1		5.4.2.3.2-2
k <sub>ns</sub> =	1.44		5.4.2.3.3-2
k <sub>nc</sub> =	1.24		5.4.2.3.2-3
k <sub>r</sub> =	0.83		5.4.2.3.2-4
k <sub>td</sub> =	0.68		5.4.2.3.2-5
k <sub>tdr</sub> =	0.999		5.4.2.3.2-5
E <sub>sh</sub> =	0.00039		5.4.2.3.3-1
ψ(t, t <sub>i</sub> ) <sub>1</sub> =	1.34		5.4.2.3.2-1
ψ(t, t <sub>i</sub> ) <sub>27375</sub> =	1.96		5.4.2.3.2-1
K <sub>td</sub> =	0.95		5.9.5.4.2a-2
Δf <sub>psR</sub> =	10.69	ksi	5.9.5.4.2a-1
Δf <sub>psCR</sub> =	5.48	ksi	5.9.5.4.2b-1
Relaxation (Between Transfer and Deck Installation)			
f <sub>pt</sub> =	198.2	ksi	
K <sub>L</sub> =	30	ksi	
Δf <sub>psR1</sub> =	1.76	ksi	5.9.5.4.2c-1

Table 7.6: Prestress losses at final age of the deck

Creep & Shrinkage (Between Deck Installation and Final Age)		
t =	27374	
k <sub>s</sub> =	1	5.4.2.3.2-2
k <sub>ns</sub> =	1.44	5.4.2.3.3-2
k <sub>nc</sub> =	1.24	
k <sub>r</sub> =	0.83	5.4.2.3.2-4
k <sub>td</sub> =	0.999	5.4.2.3.2-5
ε <sub>sh</sub> =	0.000575139	
ε <sub>sh</sub> =	0.0001808	5.4.2.3.3-1
ψ <sub>0</sub> (t <sub>0</sub> , t <sub>i</sub> ) <sub>1</sub> =	1.34	5.4.2.3.2-1
ψ <sub>0</sub> (t <sub>0</sub> , t <sub>i</sub> ) <sub>27375</sub> =	1.96	5.4.2.3.2-1
K <sub>td</sub> =	0.95	5.4.2.3.2-5
Δf <sub>psd</sub> =	4.90	ksi 5.9.5.4.2a-1
Δf <sub>pcd</sub> =	2.30	ksi 5.9.5.4.2b-1
Relaxation (Between Deck Installation and Final Age)		
Δf <sub>pr2</sub> =	1.76	5.9.5.4.2b-1
Total Losses at Transfer (Initial Losses)		
f <sub>transfer</sub> =	198.2	ksi
P <sub>transfer</sub> =	727.8	k
Total Losses at Final Age (Service)		
Δf <sub>plT</sub> =	26.88	ksi 5.9.5.1-1
f <sub>pefinal</sub> =	171.3	ksi
P <sub>pe</sub> =	629.1	k
0.8f <sub>py</sub> =	194.4	ksi
Is f <sub>pe</sub> ≤ 0.8f <sub>py</sub>	Yes	If not, use 0.8f <sub>py</sub>
Total prestress loss, %	15.39%	

Next, the applied prestress force on the panel including all losses was used to calculate the panel capacity. The Service I moment (Section 7.3.1) was used to calculate the peak bending stresses with:

$$f_t = \frac{P_{pe}}{A} \pm \frac{M}{S}$$

Two compression limit states were considered; Case 1 = dead loads only and Case 2 = dead and live load. These compression stress limits were:

$$\text{Case 1: } 0.45f'_c = 0.45 * 6 \text{ ksi} = 2.7 \text{ ksi}$$

$$\text{Case 2: } 0.6f'_c = 0.6 * 6 \text{ ksi} = 3.6 \text{ ksi}$$

The peak compressive stress in the panel resulting from the combination of moment and prestress was calculated, and compared to the limits to ensure the maximum compressive stress did not exceed the allowable stress. The stress limits were checked twice for each case; once for positive moment and once for negative moment. In all four cases the applied stresses (as shown in Table 7.7) were less than the compression stress limits so the requirements were met. The tensile stress limit was  $\sigma_{allowable} = 0.465 \text{ ksi}$ . The tensile stress resulting from the combined moment due to Service III load combination and prestress was 0.190 ksi, which satisfied the tensile stress limit.

Since all stresses were below the stress limits, the panel moment capacity was checked against the demand moment using a Strength I load combination. The initial estimate for the total tension in the section  $T$  was calculated using Eq. (5.10), assuming the prestressing strand stress to be equal to the yield stress. The idealized depth of compression  $a$  was found using Eq. (5.11) and the neutral axis depth  $c$  using Eq. (5.12). The prestressing strand strains  $\varepsilon_p$  were calculated separately in each layer [Eq. (5.13)], which in turn were used to update the total stress  $f_{ps}$  in each prestressing layer [Eq. (5.14)]. The calculations were applied iteratively until the calculated prestress force in each layer converged to the assumed value. The calculations for the first iteration were:

$$T = \frac{n}{2} f_{py} A_{ps} + \frac{n}{2} f_{py} A_{ps} = \frac{24}{2} (243 \text{ ksi})(0.153 \text{ in}^2) + \frac{24}{2} (243 \text{ ksi})(0.153 \text{ in}^2) = 892 \text{ kips}$$

$$a = \frac{T}{0.85 * f'_c * b} = \frac{892 \text{ kips}}{0.85(6 \text{ ksi})(120 \text{ in})} = 1.46 \text{ in}$$

$$c = \frac{a}{\beta_1} = \frac{0.972 \text{ in}}{0.75} = 1.94 \text{ in}$$

The strain and stress in the top layer were calculated as:

$$\varepsilon_p = \frac{0.003(d - c)}{c} + \frac{f_{pe}}{E_p} = \frac{0.003(2.25 \text{ in} - 1.94 \text{ in})}{1.94 \text{ in}} + \frac{182 \text{ ksi}}{28500 \text{ ksi}} = 0.007$$

$$f_{ps} = \varepsilon_p E_p \left\{ Q + \frac{(1 - Q)}{\left[ 1 + \left( \frac{E_p \varepsilon_p}{K f_{py}} \right)^R \right]^{\frac{1}{R}}} \right\}$$

$$= 0.007(28500 \text{ ksi}) \left\{ 0.031 + \frac{(1 - 0.031)}{\left[ 1 + \left( \frac{28500 \text{ ksi}(0.007)}{1.04(243 \text{ ksi})} \right)^{7.36} \right]^{\frac{1}{7.36}}} \right\}$$

$$= 192.1 \text{ ksi}$$

The strain and stress in the bottom layer were calculated as:

$$\varepsilon_p = \frac{0.003(d - c)}{c} + \frac{f_{pe}}{E_p} = \frac{0.003(5.75 \text{ in} - 1.94 \text{ in})}{1.94 \text{ in}} + \frac{182 \text{ ksi}}{28500 \text{ ksi}} = 0.012$$

$$f_{ps} = \varepsilon_p E_p \left\{ Q + \frac{(1 - Q)}{\left[ 1 + \left( \frac{E_p \varepsilon_p}{K f_{py}} \right)^R \right]^{\frac{1}{R}}} \right\}$$

$$= 0.012(28500 \text{ ksi}) \left\{ 0.031 + \frac{(1 - 0.031)}{\left[ 1 + \left( \frac{28500 \text{ ksi}(0.012)}{1.04(243 \text{ ksi})} \right)^{7.36} \right]^{\frac{1}{7.36}}} \right\}$$

$$= 252.8 \text{ ksi}$$

This process was repeated using the stress values from the previous iteration, until the prestress force in each layer did not change between iterations. Three iterations of the previous calculations were required to find the final capacity of the panel using Eq. (5.15), which was equal to 247 k-ft/panel. This capacity was sufficient to resist the maximum positive moment 177 k-ft/panel, and the maximum negative moment, -241 k-ft/panel. The panel capacity was also larger than 1.2 times the cracking moment, satisfying the minimum reinforcement limit. Tables 7.8, and 7.9 show the calculations for the moment capacity.

Table 7.7: Panel stress checks

Panel Capacity, 5.9.4.2			
	$P_{pe} =$	629.1 k	
Compression Stress Limits: Service I			
Case 1:	PS+DL: $0.45f'_c =$	2.7 ksi	
Case 2:	PS+DL+LL: $0.6f'_c =$	3.6 ksi	
	Tensile Stress Limit	-0.465 ksi	
	$M_1^+ =$	15 k-ft	
	$M_2^+ =$	105.2 k-ft	
	$M_1^- =$	-26.5 k-ft	
	$M_2^- =$	-143.6 k-ft	
	$f_{t1}^+ =$	0.61 ksi	<0.45f'c, Good
	$f_{t2}^+ =$	1.16 ksi	<0.6f'c, Good
	$f_{t1}^- =$	0.68 ksi	<0.45f'c, Good
	$f_{t2}^- =$	1.39 ksi	<0.6f'c, Good
Tensile Stress Limits: Service III			
	$f_o =$	-0.190 ksi	<σ <sub>allowed</sub> , Good

Table 7.8: Panel moment capacity iterations

Flexural Strength: Strength I			PCI Bridge Design Manual: 8.2.2.5
T=	892.3	k	
a=	1.458	in	
c=	1.944	in	
Top Layer			
d=	2.25	in	
$\epsilon_{ps}$ =	0.0064		
$\epsilon_p$ =	0.007		
$f_{ps}$ =	192.1	ksi	<270 ksi
Bottom Layer			
d=	5.75	in	
$\epsilon_p$ =	0.012		
$f_{ps}$ =	252.8	ksi	<270 ksi
Second Iteration			
T=	816.9	k	
a=	1.335	in	
c=	1.78	in	
Top Layer			
d=	2.25	in	
$\epsilon_p$ =	0.007		
$f_{ps}$ =	199.7	ksi	<270 ksi
Bottom Layer			
d=	5.75	in	
$\epsilon_p$ =	0.016		
$f_{ps}$ =	258.7	ksi	<270 ksi

Table 7.9 Panel moment capacity and minimum reinforcement limit

Third Iteration		
T=	841.7	k
a=	1.375	in
c=	1.83	in
Top Layer		
d=	2.25	in
$\epsilon_p$ =	0.007	
$f_{ps}$ =	197.1	ksi <270 ksi
Bottom Layer		
d=	5.75	in
$\epsilon_p$ =	0.016	
$f_{ps}$ =	258.2	ksi <270 ksi
$\phi M_N$ =	247	k-ft/panel
$M_{Strength I +}$ =	177	k-ft/panel < $\phi M_N$
$M_{Strength I -}$ =	-241	k-ft/panel < $\phi M_N$
<b>Minimum Reinforcement Limit</b>		
$f_{cpe}$ =	0.524	ksi
$1.2M_{cr}$ =	197.9	k-ft
	1.2M <sub>cr</sub> < $\phi M_N$ , Good	

### 7.3.3 Panel-to-Girder Connection Design

The panel-to-girder connection was designed according to the process explained in Section 5.2.4. Welded steel studs (connection detail shown in Figure 2.20), were assumed to develop the shear connection between the girders and the panels. Pockets in the panel were spaced 2 feet apart in the longitudinal direction along the girder lines; resulting in four connections per panel. The design detailing included specifying the pocket width and length in addition to the number of studs per connection. For this example, an 8 inch wide by 12 inch long pocket with four studs per pocket was found to provide the required shear strength. The maximum factored shear was found to be 746.2 kips using the Strength 1 load combination with a structural model. The required shear resistance was calculated according to the provisions in Section 4.2.4:

$$V_{h1} = \frac{V}{d_v \#_{girders}} = \frac{726.2 \text{ kips}}{49 \text{ in}(3)} = 5.1 \frac{k}{in}$$

$$V_u = \frac{5.1w}{\phi} = \frac{5.1(120 \text{ in})}{0.9} = 676.9 \text{ kips.}$$

The area of concrete engaged in shear transfer was calculated by:

$$A_{cv} = w_{pocket} l_{pocket} (\# \text{ of pockets}) = 10 \text{ in} * 12 \text{ in} * 4 \text{ pockets} = 480 \text{ in}^2$$

The area of interface shear reinforcement crossing the shear plane was calculated with:

$$A_{vf} = \#_{studs} A_{stud} (\# \text{ of pockets}) = 4 \text{ studs} * 0.60 \text{ in}^2 * 4 \text{ pockets} = 9.6 \text{ in}^2$$

The shear resistance was calculated according to Eq. (5.17):

$$V_n = cA_{cv} + \mu(A_{vf}f_y + P_c) = 0.24 \text{ ksi}(480 \text{ in}^2) + 1[9.6 \text{ in}^2(60 \text{ ksi}) + 0] = 692.5 \text{ kips.}$$

where  $c$  is the cohesion factor of 0.24 ksi,  $\mu$  is the friction factor of 1, and  $P_c$  is the permanent net compressive force normal to the shear plane which is zero for this example. The shear resistance exceeded the shear demand of 676.9 kips, with a final design ratio of 1.02. The intermediate calculations are summarized in Table 7.10. The plan view of a single panel with the pockets is shown in Figure 7.4, with all dimensions given in feet.

Table 7.10: Panel-to-girder connection design

Panel to Girder Connection Design		
Pocket Width	10	in
Pocket Length	12	in
# Pockets per panel	4	
# Studs per pocket	4	
V=	746.25	k
$d_v =$	49	in
$V_{n1} =$	5.08	k/in
$V_u =$	676.9	k
$c =$	0.24	ksi
$\mu =$	1	
$A_{cv} =$	480	$\text{in}^2$
$P_c =$	0	k
$A_{vf} =$	9.6	$\text{in}^2/\text{panel}$
$V_N =$	692.5	k
$V_N/V_u =$	1.02	$V_u < V_n$ , Good

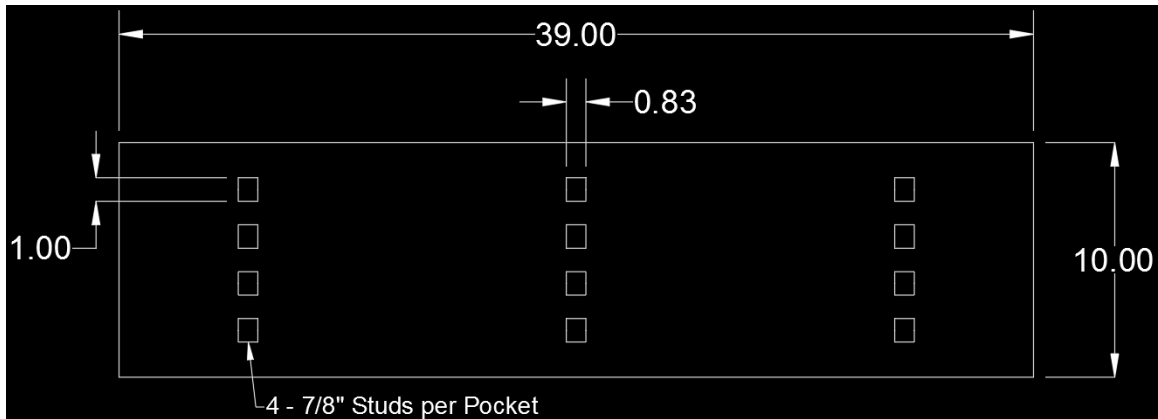


Figure 7.4: Pocket layout (dimensions in ft)

### 7.3.4 Post-Tensioning Design

AASHTO requires that transverse joints in prefabricated deck panels be subjected to a minimum of 0.250 ksi compression. To achieve this compression, post-tensioning was used. The strand properties are defined in Table 7.11; assumed values are similar to those for the prestressing strands. In this multi-span bridge example, the bridge experienced negative moment over the intermediate supports. The tension in the top of the deck panels was found by performing a composite section analysis of the deck cross-section using an effective deck width. The effective moment of inertia for one girder section was found to be  $1738389 \text{ in}^4$  with a centroid located 19.55 inches from the top of the deck. The stress in the deck was calculated as:

$$\sigma_{Top} = \frac{My}{I} = \frac{-19020 \text{ k-ft} * 12 \frac{\text{in}}{\text{ft}} * 19.55 \text{ in}}{3 \text{ girders} (1738389 \text{ in}^4)} = -0.83 \text{ ksi}$$

The required post-tensioning force for the deck was 1.08 ksi, which is the sum of 0.250 ksi mandated by AASHTO (2012) for deck joints and 0.83 ksi to balance the tensile stress from the moment demand. The required number of post-tensioning strands was found by multiplying 1.08 ksi by the deck cross-sectional area in the longitudinal direction [Eq. (5.19)] leading to a required post-tensioning force of 5068 kips. The post-tensioning bars were assumed to be 0.6" diameter – 7 wire strand (Grade 270). The total force applied to one strand was calculated as:

$$F_{pe} = f_{pe} A_{PT} = 176 \text{ ksi} * 0.217 \text{ in}^2 = 38.1 \text{ kips}$$

where  $f_{pe}$  is the effective prestress force in the post-tensioning strand with assumed losses. Using these strands to apply the post-tensioning force, the total number of strands was:

$$n = \frac{F_{req}}{F_{pe}} = \frac{5068 \text{ kips}}{38.1 \frac{\text{kips}}{\text{strand}}} = 136 \text{ strands}$$

To satisfy this requirement, 140 strands were distributed 7 strands per duct over 20 – 3 inch diameter ducts centered along the depth of the deck. Two ducts were spaced evenly between the edge of the deck and the exterior girder and 8 ducts were spaced evenly between each exterior and interior girder. This amount of post-tensioning provided 5640 kips of compression, which exceeded the required 5068 kips. The post-tensioning calculations are shown in Table 7.12. Figure 7.5 shows the duct layout.

Table 7.11: Post-tensioning steel properties

Steel Properties - Post-tension Steel		
$f_{pu} =$	270	ksi
$f_{py} =$	203	ksi
$E_p =$	28500	ksi
$f_{pe} =$	176	ksi
0.6" diameter - 7 wire strands	0.6	in
A=	0.217	in <sup>2</sup>

Table 7.12: Post-tensioning steel calculations

Longitudinal Post-tensioning		
Centroid =	19.55	in
$I_{section} =$	1738389.0	in <sup>4</sup>
$\sigma_{T,yy} =$	-0.833	ksi
$f_t =$	833.0	psi
$F_{pe} =$	38.1	k
$F_{req} =$	5068.44	k
n=	133.1	strands

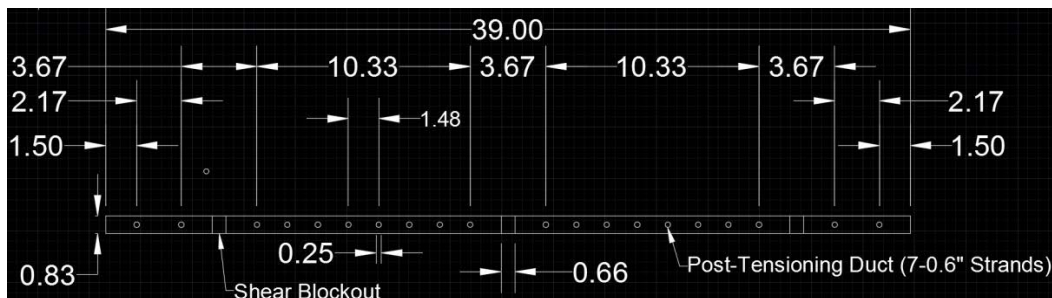


Figure 7.5: Bunkerville Road Bridge duct layout (dimensions in ft)

Standard temperature and shrinkage reinforcement was added in addition to the post-tensioning. According to Eq. (5.20), the required amount of temperature and shrinkage reinforcement was:

$$Required A_s \geq \frac{1.3bh}{2(b+h)f_y} = \frac{1.3(120 \text{ in})(10 \text{ in})}{2(120 \text{ in} + 10 \text{ in})60 \text{ ksi}} = 0.11 \frac{\text{in}^2}{\text{ft}}$$

To satisfy this requirement, #3 bars were spaced 18 inches apart in two layers resulting in  $0.15 \text{ in}^2/\text{ft}$  as shown below:

$$\text{Actual } A_s = 2 \text{ layers} * \frac{A_{bar}}{\text{Spacing}} = 2 * \frac{0.11 \text{ in}^2}{1.5 \text{ ft}} = 0.15 \frac{\text{in}^2}{\text{ft}}$$

The calculations are summarized in Table 7.13.

Table 7.13: Temperature and shrinkage reinforcement

Temperature and Shrinkage Reinforcement		
$A_s$ required=	0.11 $\text{in}^2/\text{ft}$	Use two layers of reinforcement (mesh or rebar)
Bar size	#3	
Bar area	0.11 $\text{in}^2$	
Spacing	18 in	<18 inches
$A_s$ actual=	0.15 $\text{in}^2/\text{ft}$	> $A_s$ required

### 7.3.5 Overhang Design

Design of the barrier wall, which should be according to standard state procedures, was beyond the scope of this project. Thus, the properties used in the PCI design example (PCI, 2011b) were chosen as representative values and assumed to be the same for this design example. The design assumptions were: horizontal collision force = 147.03 kips, moment capacity at the base of the barrier wall  $M_{base} = 23.85 \text{ k-ft/ft}$ , and length of the wall failure mechanism = 13.589 ft. The height of the barrier wall = 3.5 ft, consistent with the original design of the Bunkerville Road Bridge.

First, the moment capacity was checked for Case 1 (horizontal collision load combined with dead load) at Section 1-1 (inside edge of the barrier rail) and Section 2-2 (3 inches from the outside edge of the exterior girder). Sections 1-1 and 2-2 were located at  $l = 1.5$  feet (18 in) and  $l = 5.25$  feet (63 in) from the edge of the panel, respectively. The tension in the base per panel as a result of the vehicle collision was calculated according to [Eq. (5.21)]:

$$T_{base} = \frac{R_w}{L_c + 2H} = \frac{147.03 \text{ kips}}{13.589 \text{ ft} + 2(3.5 \text{ ft})} = 7.14 \frac{\text{k}}{\text{ft}}$$

$$T_{Extreme \text{ Event II}} = T_{base} * b = 7.14 \frac{\text{k}}{\text{ft}} * 10 \text{ ft} = 71.4 \frac{\text{k}}{\text{panel}}$$

For Section 1-1, the moments due to dead load of the parapet  $M_{DC \text{ Parapet}}$  and slab  $M_{DC \text{ Slab}}$ , were calculated as:

$$\begin{aligned} M_{DC \text{ Parapet}} &= w_{parapet} (\text{width}_{parapet} - \text{centroid}_{parapet}) \\ &= 0.65 \frac{\text{k}}{\text{ft}} (1.5 \text{ ft} - 0.63 \text{ ft}) = 0.56 \frac{\text{k-ft}}{\text{ft}} \end{aligned}$$

$$M_{DC\ Slab} = \frac{DC_{Area\ Load} l^2}{2} = \frac{0.1\ ksf * (1.5\ ft)^2}{2} = 0.14\ \frac{k-ft}{ft}$$

These moments combined with the barrier rail base moment capacity  $M_{base}$  (which is the maximum moment that could be transferred to the panel due to vehicle collision) according to Extreme Event II load combination:

$$M_{Extreme\ Event\ II} = M_{base} + 1.25 * (M_{DC\ Parapet} + M_{DC\ Slab}) = 24.73\ \frac{k-ft}{ft}$$

$$M_{Extreme\ Event\ II} = M_{Extreme\ Event\ II} * b = 26.32\ \frac{k-ft}{ft} * 10\ ft = 247.3\ \frac{k-ft}{panel}$$

The calculation resulted in a moment demand of 247 k-ft/panel at section 1-1. Using the design aid spreadsheet, the amount of reinforcement was adjusted until the capacity exceeded the demand, and the calculations below reflect the final design of 14 #7 bars per panel. First, the development length was calculated according to Eq. (5.22):

$$l_d = \frac{38d_b}{\sqrt{f'_c}} = \frac{38 * 0.875\ in}{\sqrt{6000\ psi}} = 16.29\ in$$

and the available strength of the rebar at the section being analyzed is found using Eq. (5.23):

$$Available\ strength = f_y \frac{(l - 2\ in)}{l_d} \leq f_y = 60\ ksi \frac{(18\ in - 2\ in)}{16.29\ in} = 59\ ksi$$

which indicates that the strength of the rebar was close to fully developed at Section 1-1. Using the following calculations the capacity of the panel was determined:

$$A_s = 14\ bars * 0.6\ \frac{in^2}{bar} = 8.4\ in^2$$

$$d = 7.7\ in$$

$$a = \frac{A_s f_y - T_{base}}{0.85 f'_c b} = \frac{8.4\ in^2 (59\ ksi) - 71.41\ kips}{0.85 (6\ ksi) (120\ in)} = 0.69\ in$$

$$c = \frac{a}{\beta_1} = \frac{0.69\ in}{0.75} = 0.92\ in$$

The strain in the rebar  $\epsilon_s$  and moment capacity  $\phi M_N$  were determined per Eqs. (5.24) and (5.25).

$$\epsilon_s = 0.003 \frac{d - c}{c} = \frac{7.7\ in - 0.92\ in}{0.92\ in} = 0.022$$

$$\phi M_N = \phi A_s f_y \left( d - \frac{a}{2} \right) = \frac{0.9(8.4 \text{ in}^2)(59 \text{ ksi}) \left( 7.7 \text{ in} - \frac{0.69 \text{ in}}{2} \right)}{12 \frac{\text{in}}{\text{ft}}} = 273 \text{ k-ft}$$

The capacity of 273 k-ft exceeded the applied moment of 247 k-ft, so the design was sufficient for Section 1-1. The calculations were repeated for Section 2-2, except the moment due to the collision load is assumed to distribute outwards at a 30° angle between Sections 1-1 and 2-2. The moment and tension force at Section 2-2 were calculated by multiplying the comparable values at Section 1-1 by the ratio of lengths  $L_c/(L_c+2H)$ :

$$\begin{aligned} M_{base @ 2-2} &= \frac{M_{base @ 1-1} L_c}{L_c + 2L[\text{Tan}(30^\circ)]} = \frac{23.85 \frac{\text{k-ft}}{\text{ft}} (13.589 \text{ ft})}{13.589 \text{ ft} + 2 * 3.75 \text{ ft}[\text{Tan}(30^\circ)]} \\ &= 18.1 \frac{\text{k-ft}}{\text{ft}} \end{aligned}$$

$$\begin{aligned} T_{base @ 2-2} &= \frac{T_{base @ 1-1}}{L_c + 2L[\text{Tan}(30^\circ)]} = \frac{7.14 \frac{\text{k-ft}}{\text{ft}}}{13.589 \text{ ft} + 2 * 3.75 \text{ ft}[\text{Tan}(30^\circ)]} \\ &= 0.29 \frac{\text{k}}{\text{ft}} \end{aligned}$$

where  $L$  is the distance between Section 1-1 and 2-2. This led to an applied moment of 242 k-ft/panel at this section. The capacity at Section 2-2 was equal to 275 k-ft/panel so the design was adequate for both Section 1-1 and 2-2.

Section 2-2 was also checked for Case 2, which uses the Strength 1 load combination for dead load and live load moment due to axle load. The moments  $M_{DC \text{ parapet}}$  and  $M_{DC \text{ slab}}$  remain the same as for Case 1. The live load moment in the section was calculated according to Eqs. (5.26) and (5.27) as follows:

$$X = \text{width}_{OH} - \text{width}_{parapet} - 1.25 \text{ ft} = 5.5 \text{ ft} - 1.5 \text{ ft} - 1.25 \text{ ft} = 2.75 \text{ ft}$$

$$L = 45.0 + 10.0X = 45 + 10 * 2.75 \text{ ft} = 72.5 \text{ in}$$

$$M_{LL+IM} = \frac{16 IM \cdot m \cdot X}{L} = \frac{16 (1.33)(1.2) \cdot 2.75 \text{ ft}}{\frac{72.5 \text{ in}}{12 \frac{\text{in}}{\text{ft}}}} = 11.62 \frac{\text{k-ft}}{\text{ft}}$$

and the overall moment was calculated as:

$$\begin{aligned}
 M_{strength I} &= [1.25(M_{DC}) + 1.5(M_{DW}) + 1.75(M_{LL})] \\
 &= [1.25 * (3.0 + 1.9) + 1.5(0) + 1.75(11.62)] \frac{k-ft}{ft} * 10 ft \\
 &= 264.5 \frac{k-ft}{panel}
 \end{aligned}$$

The moment demand due to this load combination was 264.5 k-ft/panel which was less than the capacity of 277 k-ft/panel. The intermediate design calculations are shown below in Tables 7.14 for Section 1-1 and 6.15 for Section 2-2.

Table 7.14: Overhang design for section 1-1

<b>Overhang Design</b>		
<b>Design Case I - Horizontal Vehicular Collision Load</b>		
<b>1-1 Inside Face of Parapet</b>		
$M_{base}$ =	23.85	k-ft/ft
$R_W$ =	147.03	k
$L_c$ =	13.589	ft
$H$ =	42	in
$T_{base}$ =	7.14	k/ft
$M_{DC, Parapet}$ =	0.56	k-ft/ft
$M_{DC, Slab}$ =	0.14	k-ft/ft
$M_{service I}$ =	24.55	k-ft/ft
$M_{Extreme Event II}$ =	24.73	k-ft/ft
$M_{Extreme Event II}$ =	247.29	k-ft/panel
$T_{Extreme Event II}$ =	71.41	k/panel
Hooked Bar Type	#7	
$l$ =	1.5	ft
$d$ =	0.875	in
$A_{bar}$ =	0.6	in <sup>2</sup>
$l_d$ =	16.29	in
Available Strength	58.9	ksi
# of bars	14	bars
$A_s$ =	8.4	in <sup>2</sup>
$d$ =	7.7	in
$a$ =	0.69	in
$c$ =	0.92	in
$\epsilon_r$ =	0.022	Good
$\phi M_N$ =	273.0	k-ft/panel

Table 7.15: Overhang design for section 2-2

<b>2-2 Edge of Exterior Girder</b>		
$M_{\text{base@2-2}} =$	18.09	k-ft/ft
$T_{\text{base@2-2}} =$	0.29	k/ft
$M_{\text{DC, Parapet}} =$	3.00	k-ft/ft
$M_{\text{DC, Slab}} =$	1.89	k-ft/ft
$M_{\text{DW}} =$	0.00	k-ft/ft
$M_{\text{Extreme Event II}} =$	242.00	k-ft/panel
$T_{\text{Extreme Event II}} =$	2.87	k/panel
$l =$	5.25	ft
Available Strength	60	ksi
$a =$	0.82	in
$c =$	1.09	in
$\epsilon_y =$	0.018	Good
$\phi M_N =$	275.6	k-ft/panel
<b>Design Case II - Dead and Live Load</b>		
<b>2-2 Edge of Exterior Girder</b>		
$M_{\text{DC, Parapet}} =$	3.00	k-ft/ft
$M_{\text{DC, Slab}} =$	1.89	k-ft/ft
$M_{\text{DW}} =$	0.00	k-ft/ft
$X =$	2.750	ft
$L =$	72.50	in
$m =$	1.2	
$IM =$	1.33	
$M_{\text{LL+IM}} =$	11.62	k-ft/ft
$M_{\text{strength I}} =$	264.5	k-ft/panel

## 7.4 Model Based Design Method

### 7.4.1 Overview

This section summarizes the modeling and analysis assumptions to apply the model-based design method to the Bunkerville Road Bridge. The goal of this approach is to compare analysis results from the model to calculations used in the simplified design method. For this design example, comparisons are made between the simplified and model-based designs, especially with respect to multi-span effects. These comparisons are used to determine the applicability of the simplified method for multi-span bridges.

The model used for the model based design was created using CSiBridge. This method was used in conjunction with the design aid spreadsheet discussed in Section 7.3, but refined the analysis to improve the accuracy of some of the input values to the spreadsheet. Figure 7.6 shows a 3-D view of the completed model. The red elements are the shells used for the deck, the blue line elements represent the girders, cap beams and columns, and the green elements represent the longitudinal post-tensioning and support springs. The coordinate system is as follows: x-direction refers to the longitudinal direction of the bridge, y-direction refers to the transverse direction, and z-direction refers to the direction of gravity.

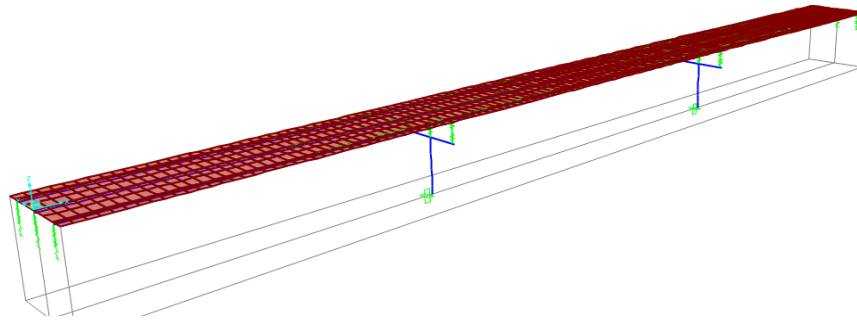


Figure 7.6: 3-D view of CSiBridge model

This model was not designed to be a stand-alone design tool, but rather to validate and determine applicability of simplified calculations used in the design aid spreadsheet to a bridge with a large amount of skew. The output from this model was then used to refine the input for the spreadsheet to achieve an improved design.

### 7.4.2 Material Definitions

All base materials used to define the various bridge elements were defined in CSiBridge. The properties of the deck concrete were: weight per unit volume  $\gamma_c = 0.15$  kcf, Poisson's ratio  $\nu = 0.2$ , compressive strength  $f'_{dc} = 6$  ksi, and modulus of elasticity  $E_{dc} = 4415$  ksi. The girder steel properties were: weight per unit volume  $\gamma_{steel} = 0.49$  kcf, yield strength  $f_y = 50$  ksi, and modulus of elasticity  $E_{gs} = 29000$  ksi. The structural concrete properties were:  $\gamma_c = 0.15$  kcf, Poisson's ratio  $\nu = 0.2$ , compressive strength  $f'_{dc} = 4.5$  ksi, and modulus of elasticity  $E_{dc} = 3824$  ksi. The deck concrete material was applied to the deck (represented by shell elements), the girder steel material was applied to the girders (represented by frame elements) and the structural concrete properties were applied to the cap beam and columns (represented by frame elements). The tendon steel was defined

with: weight per unit volume  $\gamma_{steel} = 0.49$  kcf, modulus of elasticity  $E_s = 28500$  ksi and the conventional reinforcement steel with: weight per unit volume  $\gamma_{steel} = 0.49$  kcf, yield strength  $f_y = 60$  ksi, modulus of elasticity  $E_s = 29000$  ksi.

### 7.4.3 Geometric and Element Definitions

Bridge properties were input and the model was generated using the bridge wizard feature in CSiBridge. A layout line was created extending 500 feet in the x-direction from node (0, 0, 0), representing the length and centerline of the bridge. The model was created using frame elements for the girders, thin shell elements for the deck, and tendon elements for the post-tensioning steel. In this example, the transverse deck prestressing steel was not included in the model as it had already been designed using a structural model used in the simplified method. The focus for this example was the post-tensioning stress.

The girders and deck were created by defining a bridge section. The bridge section was defined as a bridge object and used to automatically place the girder and deck elements based on the defined geometry and bridge centerline. The deck slab shell elements were assigned the deck concrete material, overall deck width = 39 feet, deck slab thickness = 10 inches, and left and right overhang width = 66 inches. The girder frame elements were assigned the girder steel material, and dimensions as shown in Figures 7.3 and 7.7. The girders were spaced with a constant spacing of 14 feet and a constant girder haunch thickness of 3 inches was added to the bridge section. The output from the defined geometry is shown in Figure 7.8.

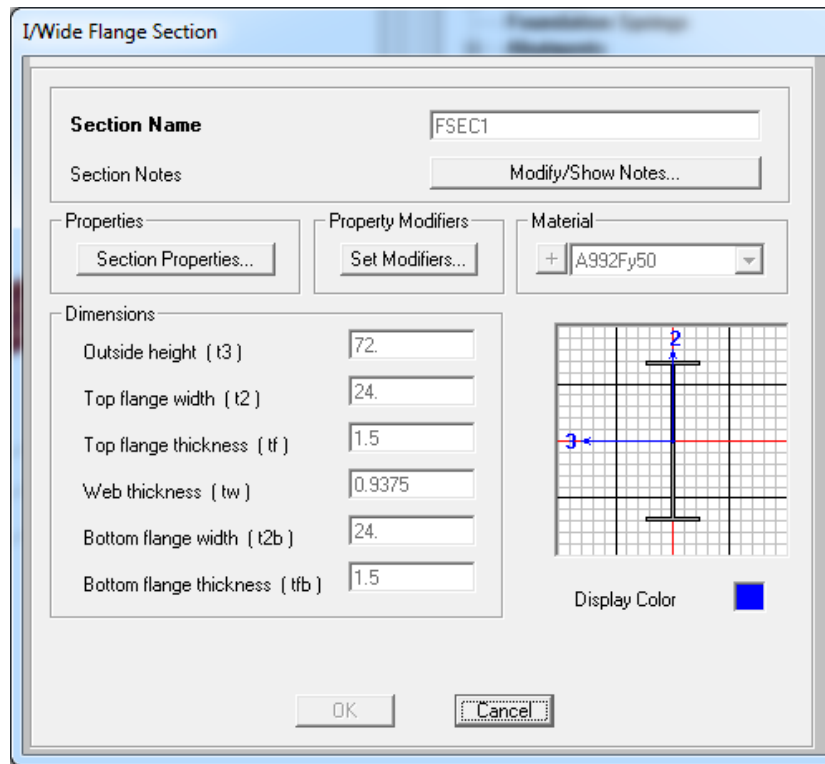


Figure 7.7: Girder properties

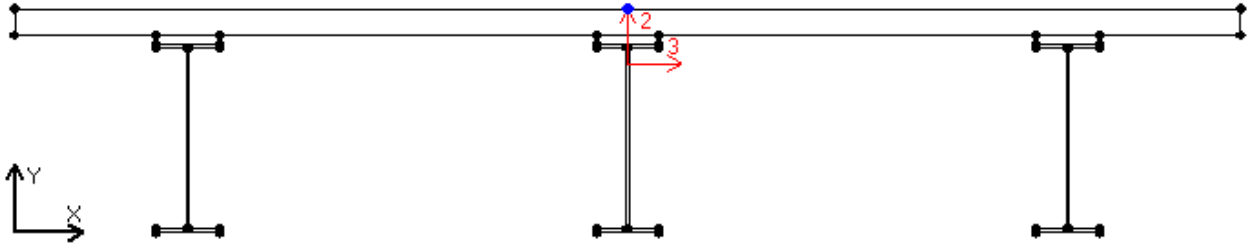


Figure 7.8: Model bridge cross-section

The geometric properties for the deck section were used to automatically generate the bridge model. As shown in Section 6.4, full composite action between the deck and girders is a reasonable assumption, so links representing the connection stiffness were not included in the model. The deck shell elements were defined as having a maximum mesh size of 2 feet in both the longitudinal or transverse directions of the bridge. In this example, all shell elements were rectangular. A plan view of the deck discretization is shown in Figure 7.9. The girder elements were also discretized every 2 feet.



Figure 7.9: Discretization of the deck

The columns were defined with a diameter of 7 feet and a height of 40 feet. The column longitudinal reinforcement was specified as 50 #11 bars placed in a circular pattern. The confining reinforcement was specified as a #6 spiral with a 4" pitch. Both sets of reinforcement used the conventional steel material. The cap beam was specified as a rectangular section that was 8 feet wide by 7 feet tall and 34 feet long. Both the column and the cap beam were assigned the structural concrete material.

The ends of the bridge at the abutments were constrained by fixing the translation in each direction and leaving all rotations free. The girder support condition was set as “connect to girder bottom only”, representative of a non-integral girder connection or seat-type abutment.

#### 7.4.4 Loads and Analysis Assumptions

The model was used mainly to check the stresses and moments in the deck for design of the post-tensioning. Three different load cases were defined, and combined using a load combination. The Dead Load case included the self-weight of the deck (shell elements), girders (frame elements), cap beams (frame elements), and columns (frame elements), each calculated by the program. The Dead Load case was analyzed using a linear static analysis. The Live Load case included the effect of moving truck loads in each lane and was analyzed using a linear moving load analysis. Two 12 feet wide lanes were assigned, each with the lane centerline 6 feet from the bridge centerline. The lanes were adjacent to each other. The HL-93 truck load was applied to each lane by placing the truck load at different locations along the bridge in the longitudinal and transverse directions and determining the maximum effect. An “Other” load case was defined that included the

prestressing force of the post-tensioning tendon elements. These load cases were all combined into a load combination named ACASE1, which represented the Strength I load combination (1.25 DC+1.5DW+1.75LL). Defining the different load types independently allowed the analysis results to be evaluated separately for each case or combined for a cumulative effect.

#### 7.4.5 Dead and Live Load Analysis and Post-Tensioning

The model was initially analyzed with factored dead load only. The results showed that the maximum axial stress in the longitudinal direction of the deck was 0.7 ksi. The axial stress distribution in the deck is shown in Figure 7.10. The moment diagram in the longitudinal direction due to factored dead load is shown in Figure 7.11. The analysis showed that the maximum positive moment was 10238 k-ft and largest magnitude negative moment was -18097 k-ft. The negative moment was comparable to what was calculated with the simplified method of 19020 k-ft.

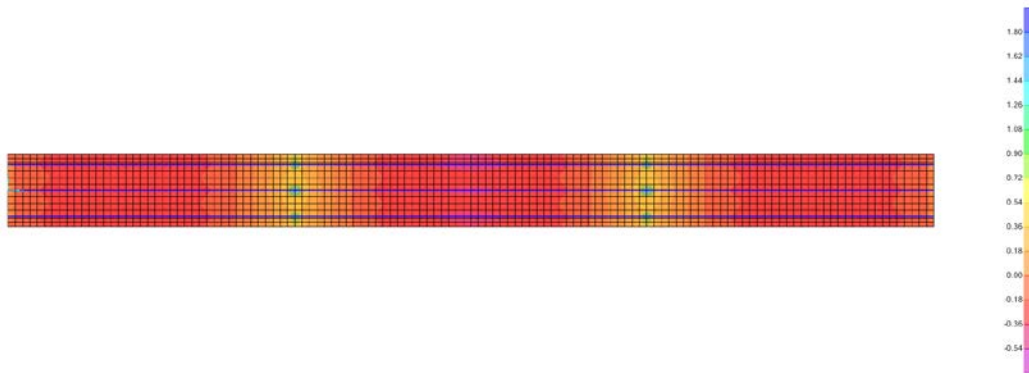


Figure 7.10 Deck stress for model subjected to dead load

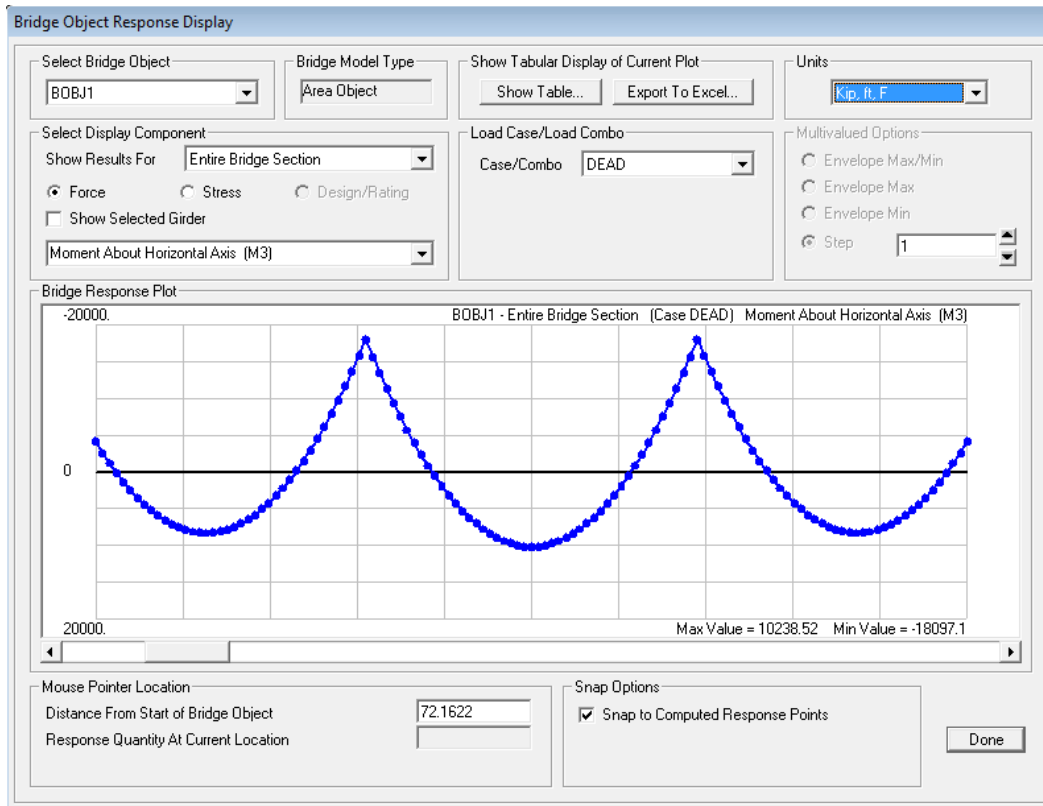


Figure 7.11: Moment diagram due to dead load

Live loads may also contribute to the tensile stresses in a deck on a multi-span bridge. A moving load analysis using the lanes and vehicle load was performed on the model to determine additional tensile stresses that must be overcome by post-tensioning. The combined analysis results of the factored dead and live load showed that the maximum longitudinal tensile stress in the deck was equal to 1.0 ksi. The resulting stress distribution is shown in Figure 7.12.

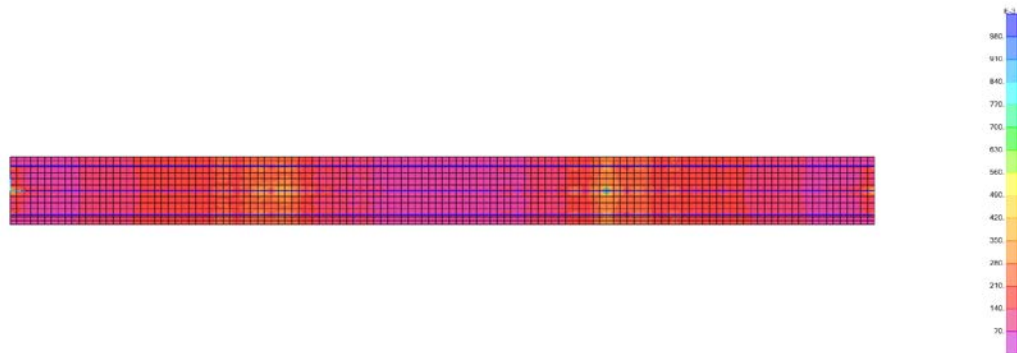


Figure 7.12: Stress due to live load

Post-tensioning was calculated based on the design stress of 1 ksi determined by the analysis and the additional 0.250 ksi minimum required compression. The required number of post-tensioning strands was calculated using the design aid spreadsheet with the same method described in Section 7.3.4. The spreadsheet calculated that 5850 kips of

post-tensioning needed to be applied to the deck which could be achieved using 154 strands. The calculations are shown in Table 7.16.

Table 7.16 Post-tensioning calculations

Longitudinal Post-tensioning		
Centroid =	19.55	in
$I_{section}$ =	1738389.0	$in^4$
$\sigma_{T_{ps}}$ =	-0.856	ksi
$f_t$ =	1000.0	psi
$F_{pe}$ =	38.1	k
$F_{req}$ =	5850	k
$n$ =	153.6	strands

#### 7.4.6 Analysis with Post-Tensioning

The results from Section 6.4 showed that longitudinal post-tensioning does not behave as desired in the model, because the post-tensioning is effectively applied to the composite deck-girder section rather than the deck alone. Post-tensioning was still applied to this example to compute approximate stresses including post-tensioning. The required 160 strands of post-tensioning was applied over 20 – 3 inch ducts with 8 strands per duct in the same duct configuration as shown in Figure 7.5. This configuration when applied to the model resulted in a residual maximum joint tensile stress of 0.03 ksi. The axial stress in the longitudinal direction due to dead and live load is shown in Figure 7.13

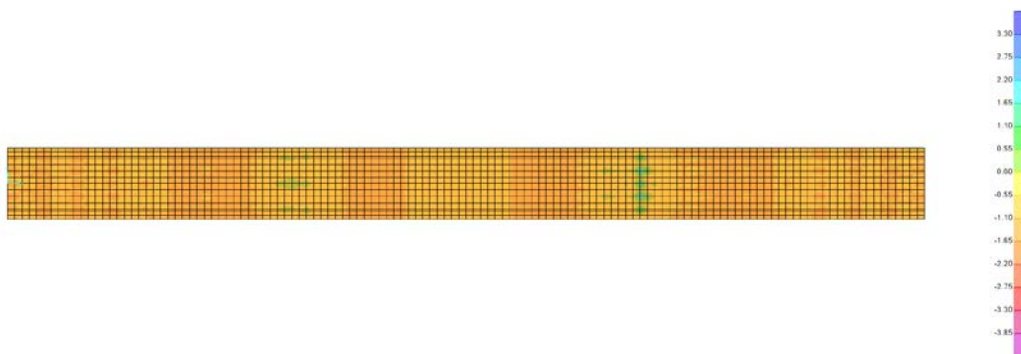


Figure 7.13: Stress in the deck after post-tensioning

#### 7.5 Validation and Comparison of Results

This section summarizes the differences between the simplified method and the model based method. Concerns regarding the methods are discussed and changes to the design procedure based on the findings are explored.

In this design example, the moments due to loading predicted by the model were similar to those computed by the design aid spreadsheet in the simplified method. The longitudinal negative moment due to dead load was -19030 k-ft for the simplified method and -18097 k-ft for the model based method. The maximum tensile stress in the deck due to dead load calculated with the two methods were also close, 0.85 ksi for the simplified method and 0.7 ksi for the model based method. In both cases the simplified method was

conservative. However, similar to the Mesquite Bridge, the model based method required a higher amount of post-tensioning than predicted by the simplified method because the composite action between the deck and the girder was applied prior to applying the post-tensioning force. Because the resulting forces from the two methods were close to each other, if the post-tensioning could be applied in the model prior to connecting the deck to the girder, the required amount of post-tensioning predicted by the model-based method is expected to be close to that calculated for the simplified method.

Based on the experiences gained from this design example, the recommendation is that simple multi-span bridges need not be analyzed with a finite element model. The simplified method was conservative for all loads and designs and would adequately represent the behavior that would be expected from a model. When a detailed model is used that includes stiffness of the supports, the resulting forces are expected to be smaller than those being generated with a simply supported model. If optimization of the design is desired, a model could be used to collect more accurate forces that may be lower than what is predicted in the simplified method. While the results from this design example do not encompass all bridges with differing numbers of spans or span lengths, similar behavior between the simplified method and model based method is expected because of the same assumptions used for the load inputs. The simplified method uses loads calculated with rigid models and the model based method uses loads and forces generated from a model that accounts for stiffness of the intermediate supports and superstructure. Full-depth deck panel systems may be designed for simple bridges without requiring a model, but it is recommended that bridges that contain complex features such as skew, curvature, or a combination of factors be designed with the design aid spreadsheet supplemented with results from a finite element model.

## **Chapter 8: Summary and Conclusions**

### **8.1 Project Summary**

The Nevada Department of Transportation has been interested in incorporating accelerated bridge construction (ABC) in the form of prefabricated deck panels and other bridge components. The purpose of this project was to study and recommend details and specifications that could be used as an implementation plan of prefabricated deck panels for Nevada. A literature review was completed on the experiences and standard design and construction practices of various states for prefabricated deck panels. Guidelines from PCI (2011a), ODOT (2015), UDOT (2015), TXDOT (2006) and NCHRP reports (2008) became primary sources for the current use of prefabricated deck panels in practice. In particular, PCI has developed connections and details for full-depth deck panels. The guidelines and details from all of the sources were used to develop a survey that was sent to all state DOTs regarding their experience with prefabricated deck panels. The literature review and survey results showed that prefabricated deck panels are commonly used in ABC. Based on the survey, 63% of respondents had at least experimented with prefabricated deck panels. DOT responses showed that full-depth deck panels have been more widely used and performed better than their partial depth counterparts. Because of the better performance and to take full advantage of the quicker construction time resulting from this ABC, the project subsequently focused on full-depth deck panels. Results from the survey also showed that many states have adopted details similar to those in the PCI guidelines.

Because the PCI full-depth deck panel guidelines and details were the most widely referenced in the survey results, these provisions have been recommended for adoption as the base standard specification for Nevada, with additional details from other sources for clarification or customization when needed. In conjunction with these guidelines, two design methods were developed. The first design method was a simplified method that used a design aid spreadsheet to design the reinforcement and connections of the panels according to AASHTO (2012) and PCI (2011a) guidelines. The second method was a model based method that used finite element modeling to determine the load effects on the deck. Each design method was applied to two example bridges: the Mesquite Interchange and a modified version of the SR 170 Bunkerville Road Bridge, to verify that the design procedures adequately accounted for all key design considerations and to determine any limitations that should be placed on the use of prefabricated deck panels. The Mesquite Bridge was chosen because it contained a high degree of skew but was single span. This allowed the effects of skew to be analyzed in an isolated context. The Bunkerville Road Bridge was chosen because it was a multispan bridge with no skew or curvature. Also, the Mesquite bridge had prestressed concrete girders while the Bunkerville Road Bridge had steel girders, such that the differences in design and detailing between the two were demonstrated.

## 8.2 Conclusions

The summary of current prefabricated deck panel practices, survey results, development of design specifications and procedures, and application of design specifications to example bridges led to the following conclusions:

- Based on survey results, full-depth deck panels have performed better than partial-depth deck panels for most states. Because of this, full-depth deck panels rather than partial depth panels are recommended for implementation. The connections proposed by PCI: the female-to-female shear key for the transverse panel-to-panel connection and the deck-to-girder joints were more commonly used and received higher ratings in the survey based on DOT responses. Based on these reviews, the PCI details are recommended as the foundation for the developed specifications. Survey results also revealed that either longitudinal post-tensioning or UHPC transverse joints are vital to maintaining deck integrity. Therefore, PCI's post-tensioning details or ODOT's UHPC connections are recommended for transverse joints.
- Based on the design examples, bridges without complex geometry can be designed with the simplified method with no extra modeling required. All loads are calculated in the spreadsheet and the capacity of the sections are designed to exceed the applied loads. Based on the results of the Mesquite Bridge, skewed bridges should be designed with the model based method using a structural model to determine external forces (i.e. shear, moment). The shear and moment are input into the spreadsheet and used for design. The amount of transverse prestressing steel, longitudinal post-tensioning force, panel-to-girder connection dimensions and steel area and steel reinforcement in the overhang section are then calculated using the forces from the model as the design values.
- Structural models should not incorporate the post-tensioning forces into the analysis of the entire composite section of the girders and deck panels. In practice, deck panels are post-tensioned before the grout pockets are filled and the deck is fully connected to the girders. However, in CSiBridge applications of the post-tensioning, the model assumes the deck is acting composite with the girder. This causes the post-tensioning force to be applied to the full section including the girder rather than just the deck and does not represent how the system functions. As a result, the model analysis should be limited to collecting the longitudinal axial stress for the calculation of the required post-tensioning force. If the contractor post-tensions the deck after application of the deck-to-girder grout, the model may incorporate the post-tensioning stress and be used to iterate towards a final design value where there is at least 0.25 ksi compression in every joint.
- Because each DOT creates its own design procedures and the design criteria is subject to change once the DOT has gained experience in the implementation of full-depth deck panels, the following recommendations have been made. If additional requirements are adopted beyond what AASHTO specifies, the spreadsheet should be updated accordingly. The optimal use for the spreadsheet

and the design of the full-depth deck panels is to incorporate the calculations performed in the spreadsheet with standard calculations for deck and bridge systems. If loads and capacity information are already calculated for the girders and other bridge components, this same information could be used to design the deck without requiring additional modeling. Optimally, the bridge is designed as a system, rather than designing the deck around an existing superstructure for new bridge construction. Using these recommendations in combination with the proposed specifications provides a good starting point for use of full-depth prefabricated deck panels.

## References

1. Accelerated Bridge Construction University Transportation Center (2016). “Development of Prefabricated Bridge Railings”, <https://abc-utc.fiu.edu/research-projects/development-of-prefabricated-bridge-railings/>
2. Ackerman, T. (2007). “Lessons Learned, Deck Replacement with Pre-cast Panels, Bridge at 800 N. Over I-15, Structure C-417”, <https://drive.google.com/folderview?id=0B2RsOp2Y3K9vMEFvYI9xSE9CQIU&usp=sharing&tid=0B2RsOp2Y3K9vNVRKbDVVY2FPMUK>
3. American Association of State Highway and Transportation Officials (AASHTO), (2012). AASHTO LRFD Bridge Design Specifications, 7<sup>th</sup> edition.
4. Badie, S. S, and Tadros, M. K, (2008). “Full-Depth Precast Concrete Bridge Deck Panel Systems”, Report 584 by National Cooperative Highway Research Program.
5. Bridge Grid Flooring Manufacturers Association, (BGFMA), (2015). “BGFMA Design Data for Steel Grid Decks”. <http://www.bgfma.org/grids.htm>
6. Cheng, Z et al. (2006). “Development of a Seismic Design Method for Reinforced Concrete Two-Way Bridge Column Hinges”, Report No. CCEER-06-01
7. Colorado Department of Transportation, (CODOT), (1991). “Prestressed Concrete Composite Bridge Deck Panels”. <https://www.codot.gov/library/bridge/bridge-manuals/bridge-design-manual/section-9-2-precast-prestressed-concrete-composite-bridges/view>
8. Colorado Department of Transportation, (CODOT), (2015). *Structural Worksheets*, pg. 78-81. <https://www.codot.gov/library/bridge/design-standards/structural-worksheets-pdfs>
9. CONTECH, (2012). “CONTECH Bride Plank”, Product manual for CONTECH bridge deck panels. [http://www.conteches.com/DesktopModules/Bring2mind/DMX/Download.aspx?Command=Core\\_Download&EntryId=1502&PortalId=0&TabId=144](http://www.conteches.com/DesktopModules/Bring2mind/DMX/Download.aspx?Command=Core_Download&EntryId=1502&PortalId=0&TabId=144)
10. Culmo, M. P. (2013). “Performance of Accelerated Bridge Construction Projects in Utah as of October 2013”, Report by CME Associates to Utah Department of Transportation, <https://drive.google.com/folderview?id=0B2RsOp2Y3K9vNVRKbDVVY2FPMUK>
11. Culmo, M. P. (2011). “Accelerated Bridge Construction, Experience in Design, Fabrication and Erection of Prefabricated Bridge Elements and Systems.” Report by Federal Highway Administration. Final Manual.
12. Deloy Dye, M. (2005). “Prefabricated Bridge Replacement Report, Lessons Learned During Construction, Located at I-215 East, 3760 S. & 3900 S.”, Report by MD2 to Utah Department of Transportation. <https://drive.google.com/folderview?id=0B2RsOp2Y3K9vMEFvYI9xSE9CQIU&usp=sharing&tid=0B2RsOp2Y3K9vNVRKbDVVY2FPMUK>
13. Graybeal, B. (2010). “Field-Cast UHPC Connections for Modular Bridge Deck Elements” Report No. FHWA-HRT-11-022.

14. Graybeal, B. (2011). “Ultra-High Performance Concrete”, Report No. FHWA-HRT-11-038.
15. Hieber, D. G. and Wacker, J. M. (2005). “State-of-the-Art Report on Precast Concrete Systems for Rapid Construction of Bridges”, Report for Washington State Transportation Center (TRAC)
16. Holt, J. M., Design Section Director of TxDOT Bridge Division (2015). Personal Communication.
17. Iowa DOT, (2014). “Overview of Keg Creek Bridge”, Presentation for 2014 ABC Workshop
18. Johnson, B. V. (2011). “Full-Depth Prefabricated Bridge Deck Options for Durability and Cost”, [http://abc-utc.fiu.edu/index.php/technology/monthly\\_webinar\\_archive/view/full-depth-prefabricated-bridge-deck-options-for-durability-and-cost](http://abc-utc.fiu.edu/index.php/technology/monthly_webinar_archive/view/full-depth-prefabricated-bridge-deck-options-for-durability-and-cost)
19. Merrill, B. D. (2002). “Texas’ Use of Precast Concrete Stay-In-Place Forms for Bridge Decks”, Proc., 2002 Concrete Bridge Conference.
20. Oregon Department of Transportation (ODOT), (2015). *Standard Details – Bridge Section, Bridge – Slabs & Boxes*  
[http://www.oregon.gov/odot/hwy/engservices/pages/details\\_bridge.aspx](http://www.oregon.gov/odot/hwy/engservices/pages/details_bridge.aspx)
21. Precast/Prestressed Concrete Institute (PCI), (2001). “Precast Deck Panel Guidelines”, Report No. PCINER-01-PDPG.
22. Precast Concrete Institute (PCI), (2011a). “Full Depth Deck Panels Guidelines for Accelerated Bridge Deck Replacement or Construction”, Report No. PCINER-11-FDDP, Second Edition.
23. Precast Concrete Institute (PCI), (2011b). “State-of-the-Art Report on Full-Depth Precast Concrete Bridge Deck Panels”. First Edition.
24. Scoles, J. et al. (2014). “Deck Replacement with Full Depth Precast Post-tensioned Panels: Challenges, Solutions, Prefabrication and Construction Performance”. Proceedings, 2014 National Accelerated Bridge Construction Conference.
25. Sullivan, S. (2007). “Construction and Behavior of Precast Bridge Deck Panel Systems”, Ph.D. Dissertation, Virginia Tech
26. Texas Department of Transportation (TXDOT), (2006), *Prestressed Concrete Panels Deck Details*.
27. URS (2004). “Lessons Learned After Construction, Bridge Country Road Over I-80 (1.9 Miles East of Wanship)”, Report by URS to Utah Department of Transportation, <https://drive.google.com/folderview?id=0B2RsOp2Y3K9vMEFvYI9xSE9CQIU&usp=sharing&tid=0B2RsOp2Y3K9vNVRKbDVVY2FPMUK>
28. Utah Department of Transportation (UDOT), (2014). *Supplemental Specifications for 2012 Standard Specifications for Road and Bridge Construction*. Supplemental Issue Eight, <http://www.udot.utah.gov/main/uconowner.gf?n=12689904088310884>

29. Utah Department of Transportation (UDOT), (2015a). *UDOT Structures Design and Detailing Manual*.  
<https://drive.google.com/file/d/0B8QRVMpaE6oYWTg3WU5ISDhkRGM>
30. Utah Department of Transportation (UDOT), (2015b). *Drawings*.  
<https://drive.google.com/folderview?id=0B2RsOp2Y3K9vVUhjSml5RG9MY2s>
31. Wood, S. L. et al. (2008). “Recommendations for the Use of Precast Deck Panels at Expansion Joints”, Report No. FHWA/TX-09/0-5367-1, Prepared for Texas Department of Transportation.

## **Appendix A: NCHRP Report 584 DOT Survey**

**Q1: Has your organization used any full-depth precast concrete deck panel systems in**

**highway bridges during the last 10 years?**

Yes \_\_\_\_\_

No \_\_\_\_\_ (please, give reasons):

Incremental cost

Lack of specifications or guidelines

Unsatisfactory performance in the past

Other (specify)

**Q2: Approximately, how many bridges, utilizing full-depth precast concrete panels, have**

**you constructed during the last 10 years? \_\_\_\_\_**

**Q3: Approximately, how many square feet of full-depth precast concrete panels have you**

**constructed in the past 10 years? \_\_\_\_\_ sq. ft**

**Q4: Of the bridges listed in answer to Questions 3 & 4, please, indicate the type of transverse (normal to traffic direction) reinforcement.**

Pretensioned in the precast yard %

Post-tensioned in the field %

Conventionally reinforced %

Partially pretensioned and partially conventionally reinforced %

Other (specify) %

**Q5: How were the panels connected in the longitudinal direction (parallel to the traffic direction)?**

Using longitudinal post-tensioning %

Splicing reinforcing bars using commercial mechanical couplers %

Using special mechanical devices %

Other (please specify)%

**Q6: What is the percentage of the systems built compositely with the supporting girders? %**

**Q7: Did you use an overlay?**

Yes \_\_\_\_\_ (if Yes, please, provide the overlay type and percent of decks)

Asphalt % Thickness

Concrete % Thickness

Other (specify) % Thickness

No \_\_\_\_\_ (If No, did you provide special treatment to the top surface of the precast panels to provide for ride-ability?)

Yes No

If yes, what type? Roughening in the precast plant during production  
Grooving in the precast plant during production  
Grinding in the field after construction  
Sand blasting in the field after construction  
Other (specify)

**Q8: What is your overall evaluation of the performance of full-depth precast concrete deck panels?**

Excellent  
Good  
Fair  
Poor

Please comment and indicate whether or not you will use full depth precast deck panel systems again in future projects:

**Q9: Have you developed guidelines or specifications for design, fabrication or construction of full depth precast concrete panel systems?**

Yes (please, attach a copy of the specifications)  
No

**Q10: Successful grouting of the panel-to-panel and the deck-girder joints is considered one of the key elements of having a durable and high performance deck. Have you developed specifications for the grout properties and the grouting process?**

Yes (please, attach a copy of the specifications)  
No

**Q11: In order to simplify the connection between the concrete deck and the steel girders and to facilitate deck removal in the future, the state of Nebraska has used 1¼ in. diameter steel studs successfully. One 1¼ in. steel stud is equivalent to two 7/8 in. studs. Do you see any problems with use of individual or clustered 1¼ in. steel studs with full depth precast deck panels.**

Yes  
No (please, give reasons)

**Q12: AASHTO Specifications stipulate a maximum spacing of the shear connectors between the girder and the deck of 24 inches. Relaxing this limit could simplify deck placement and removal. Do you see a need for research on the performance of shear connectors at 4, 6 or even 8 feet?**

Yes No  
Please comment:

**Q13: Please, provide the name, phone number and e-mail address of one person on your**

**staff who can help in answering questions on issues related to design and construction with precast concrete deck panels.**

Name:

Title:

Phone:

E-mail:

**Q14: Are you interested in receiving a copy of the findings of this survey?**

Yes No

## Appendix B: NDOT Prefabricated Deck Panel Survey

Please tell us who is filling out this survey:

Name:

E-mail address:

Phone number:

Title:

State department of transportation or organization represented:

- 1. Has your state constructed bridges or performed deck replacement projects with prefabricated deck panels in the past 10 years?**  
 Yes  
 No
- 2. In the past 10 years, how many new bridges have been constructed using prefabricated deck panels?**  
List number: \_\_\_\_\_
- 3. In the past 10 years, how many bridge deck replacement projects have been completed using prefabricated deck panels?**  
List number: \_\_\_\_\_
- 4. Please indicate approximately how many of each of the following types of projects have been completed in the past 10 years.**

New bridges with full depth precast deck panels and steel girders

New bridges with full depth precast deck panels and prestressed concrete girders

New bridges with partial depth precast deck panels and steel girders

New bridges with partial depth precast deck panels and prestressed concrete girders

Bridge deck replacement with full depth precast deck panels and steel girders

Bridge deck replacement with full depth precast deck panels and prestressed concrete girders  
panels and steel girders

Bridge deck replacement with partial depth precast deck panels and prestressed concrete girders

5. **Considering all projects in the past 10 years (new bridges and bridge deck replacements) that used full-depth precast deck panels, please indicate approximately how many applied each of the following LONGITUDINAL connection details (provide continuity across transverse joints):**

Longitudinal post-tensioning with UHPC

Longitudinal post-tensioning with standard grout

Splicing reinforcing bars with UHPC

Splicing reinforcing bars with standard grout

Other type of longitudinal connection (please specify both connection type and number of applications)

Not applicable

6. **Considering all projects in the past 10 years (new bridges and bridge deck replacements) that used full-depth precast deck panels, please indicate approximately how many applied each of the following TRANSVERSE connection details (provide continuity across longitudinal joints):**

Transverse post-tensioning with UHPC

Transverse post-tensioning with standard grout

Splicing reinforcing bars with UHPC

Splicing reinforcing bars with standard grout

Other type of transverse connection (please specify both connection type and number of applications)

Not applicable

7. **Considering all projects in the past 10 years (new bridges and bridge deck replacements) that used partial-depth precast deck panels, please indicate approximately how many applied each of the following reinforcement types:**

Conventional longitudinal and transverse reinforcement

Conventional longitudinal and transverse reinforcement with transverse prestressing

Conventional longitudinal reinforcement with transverse prestressing

8. **In general, are deck overlays used for full depth prefabricated bridge deck construction?**

Yes

No

9. **Which of the following overlay options most closely represents standard practice for full depth panels?**

- Asphalt
- 3/8" Multilayer
- 3/4" Polymer concrete
- Other: \_\_\_\_\_

10. **In general, are deck overlays used for partial depth prefabricated bridge deck construction?**

Yes

No

11. **Which of the following overlay options most closely represents standard practice for partial depth panels?**

- Asphalt
- 3/8" Multilayer
- 3/4" Polymer concrete
- Other: \_\_\_\_\_

12. **Does your department prefer using partial depth or full depth precast deck panels over the alternative and if so, why?**

---

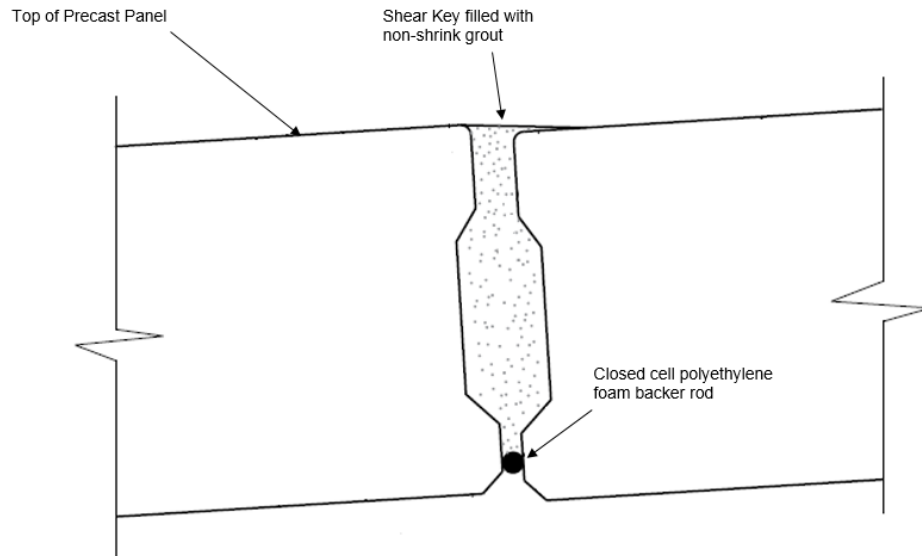
---

---

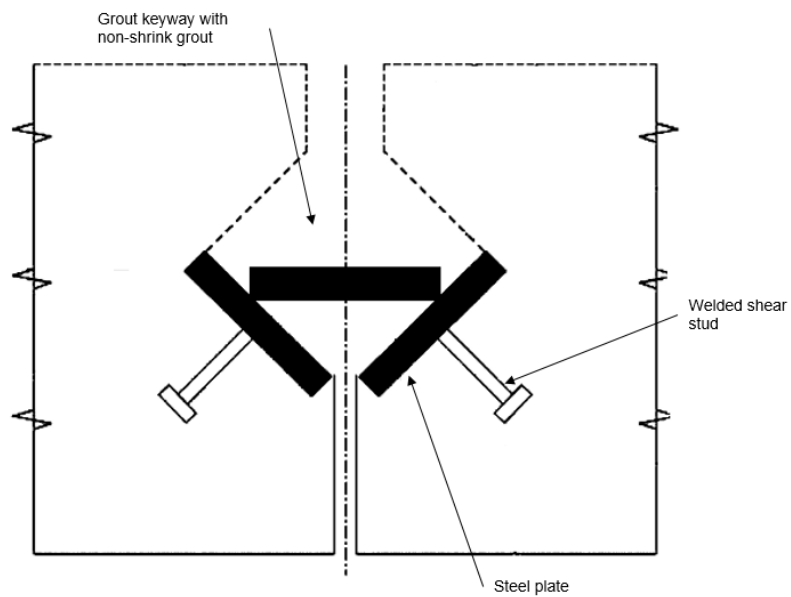
13. **We have compiled a menu of details for full-depth panel-to-panel joint details based on information found in publicly available documents. For each of the details shown, please indicate which statement best represents your state's position.**

- a. We use a detail similar to this regularly
- b. We have applied a similar detail but it is not considered regular practice
- c. We have applied a similar detail but would not use it again
- d. We have NOT applied a similar detail

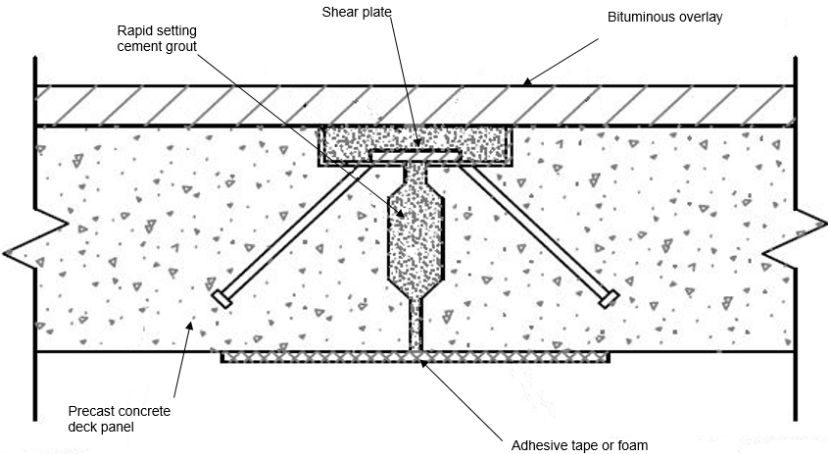
**i. Female-to-female shear key \_\_\_\_\_**



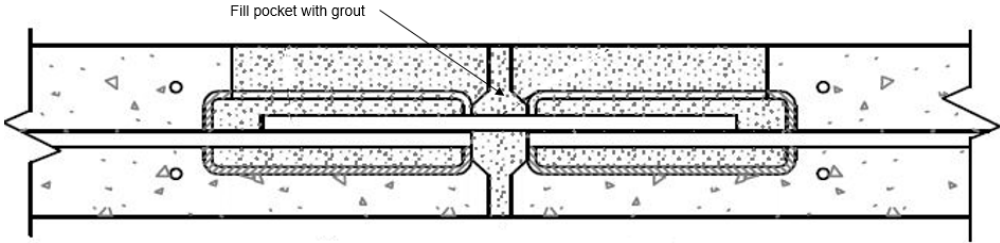
**ii. Female to female shear key with welded steel plate \_\_\_\_\_**



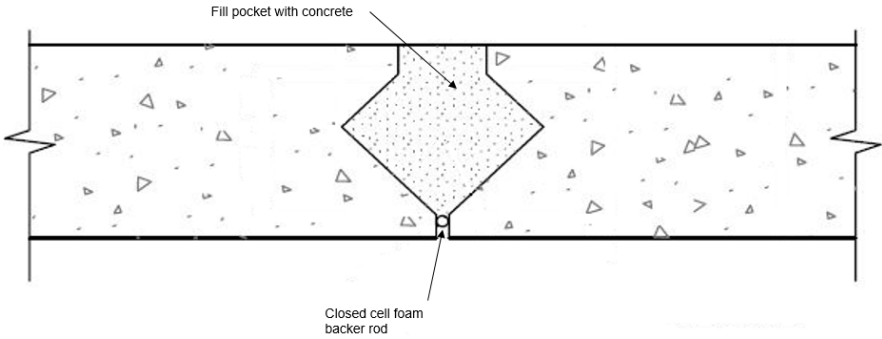
**iii. Transverse Shear Key with Shear Plate** \_\_\_\_\_



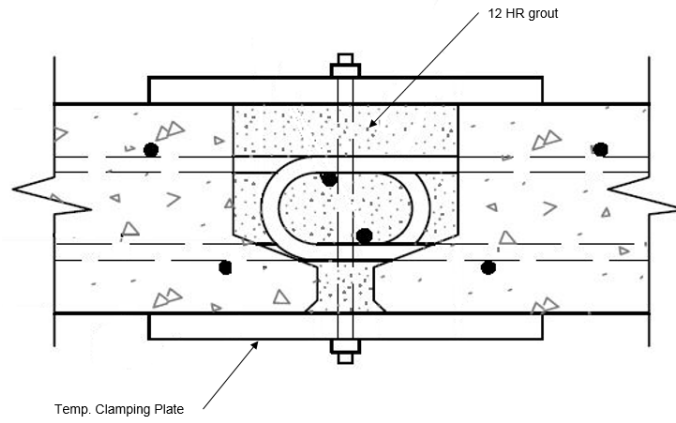
**iv. Female to Female Shear Key with HSS** \_\_\_\_\_



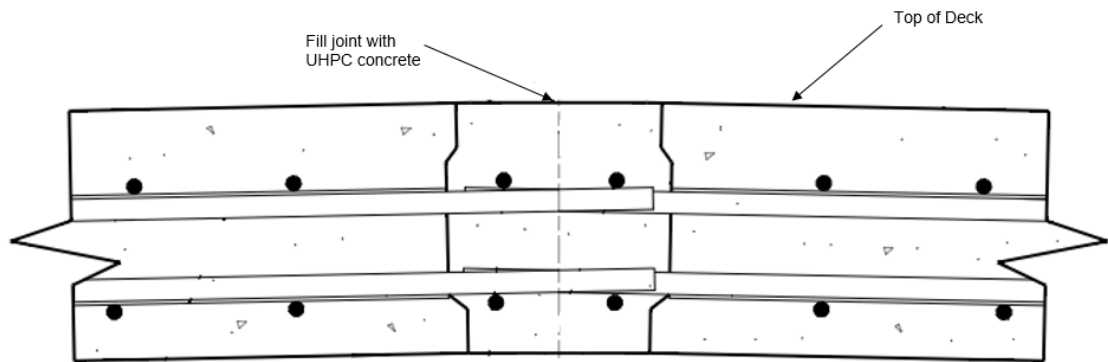
**v. Female to female diamond shear key** \_\_\_\_\_



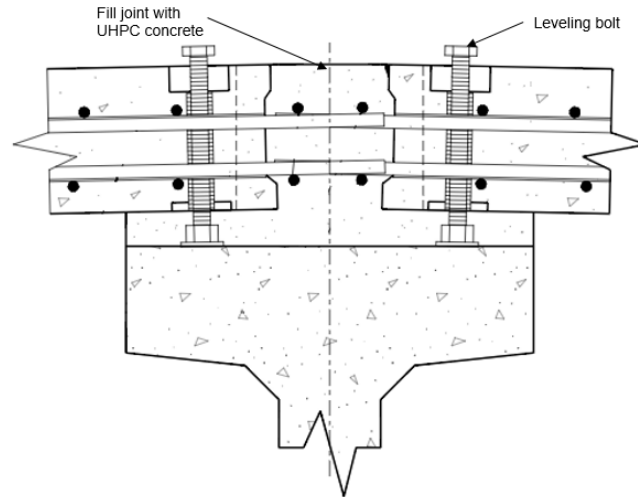
**vi. Female to Female Shear Key with Bent Reinforcement**



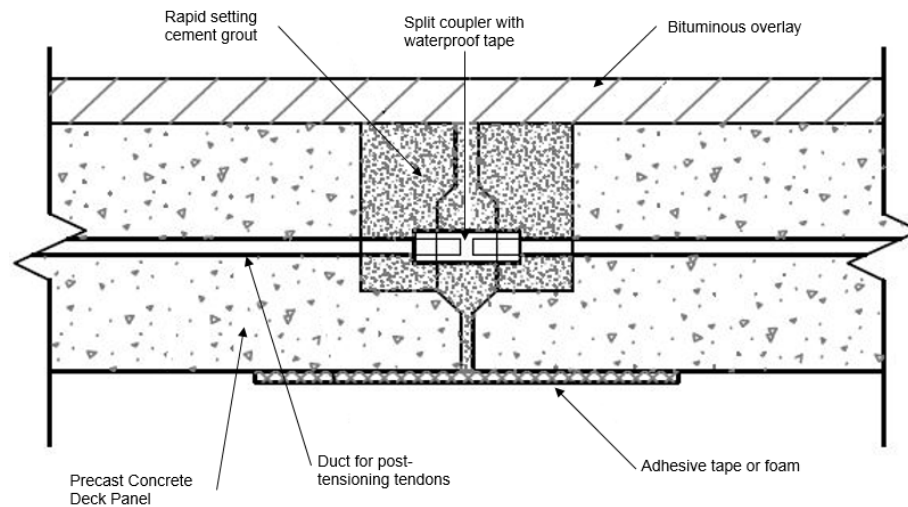
**vii. Longitudinal cast-in-place joint**



viii. Longitudinal cast-in-place joint over girder \_\_\_\_\_



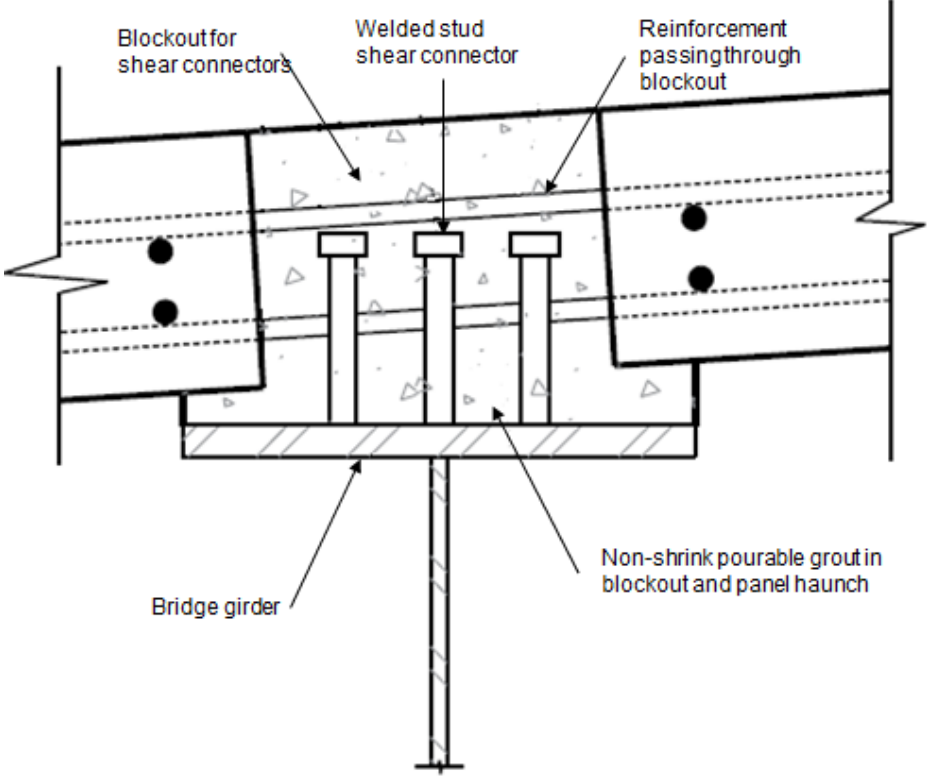
ix. Longitudinal Joint with spliced reinforcement \_\_\_\_\_



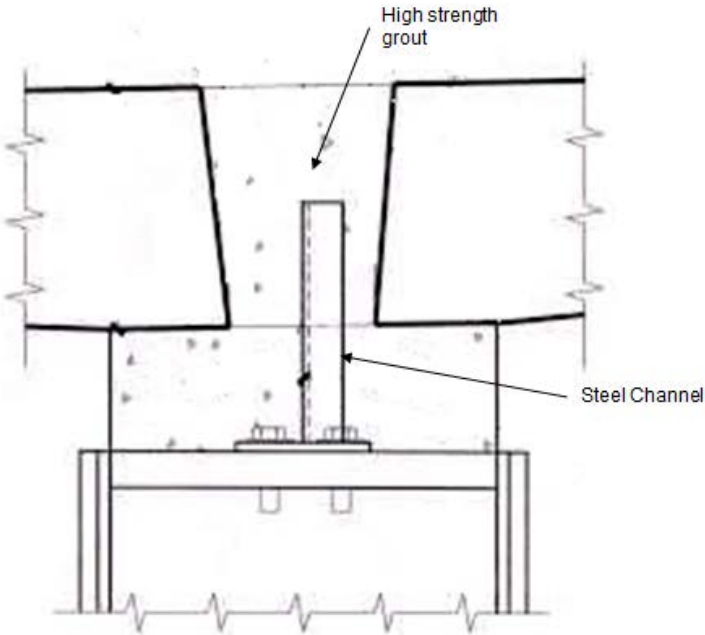
14. We have compiled a menu of details for full-depth panels deck-to-girder details based on information found in publicly available documents. For each of the details shown, please indicate which statement best represents your state's position.

- a. We use a detail similar to this regularly
- b. We have applied a similar detail but it is not considered regular practice
- c. We have applied a similar detail but would not use it again
- d. We have NOT applied a similar detail

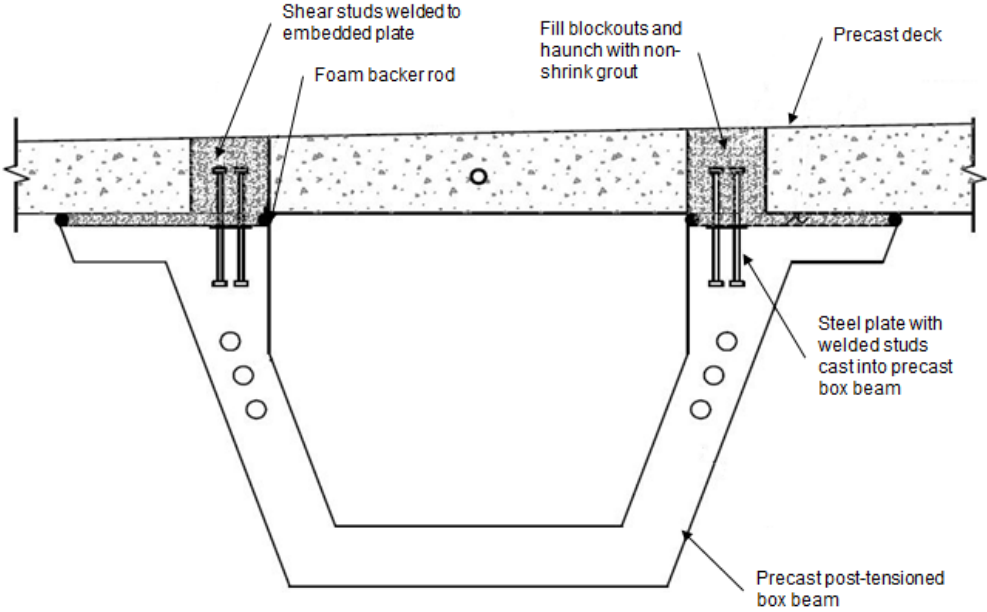
i. Steel girder with shear studs and grouted haunch \_\_\_\_\_



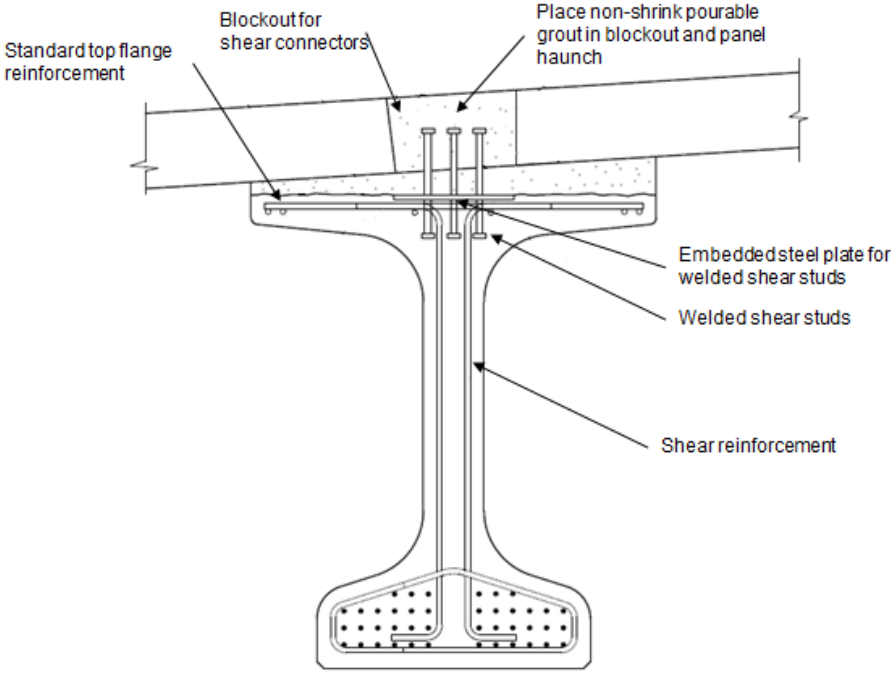
ii. Steel girder with welded C-channel \_\_\_\_\_



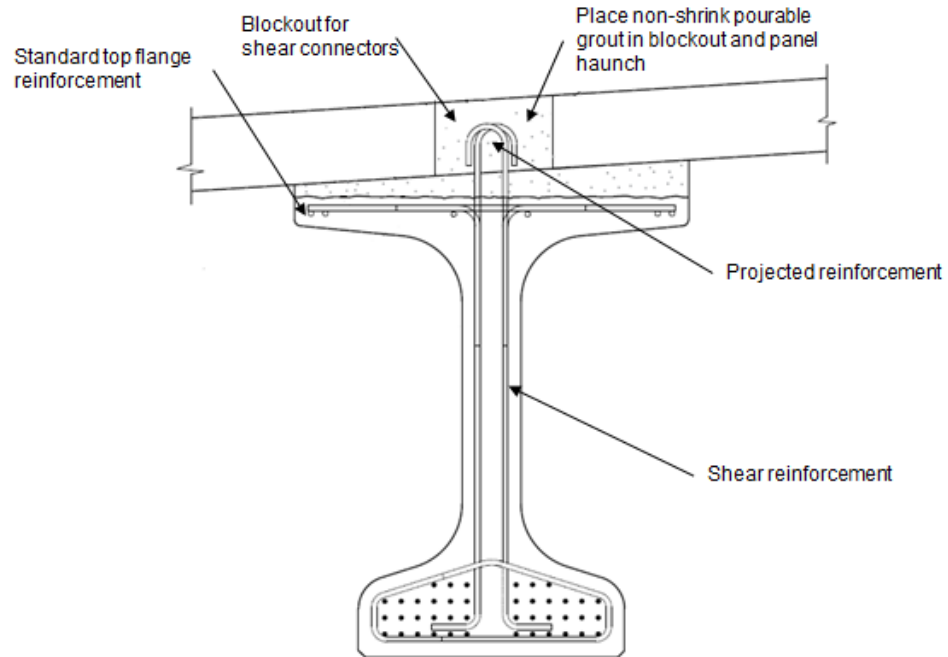
**iii. Tub Girder to Deck Connection \_\_\_\_\_**



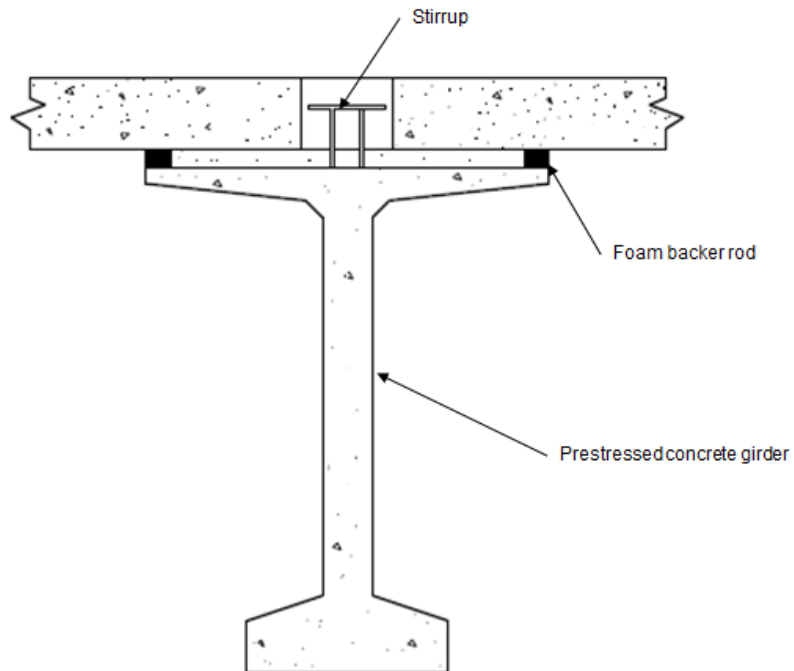
**iv. Prestressed concrete girder with shear studs \_\_\_\_\_**



**v. Prestressed concrete girder with projected reinforcement**



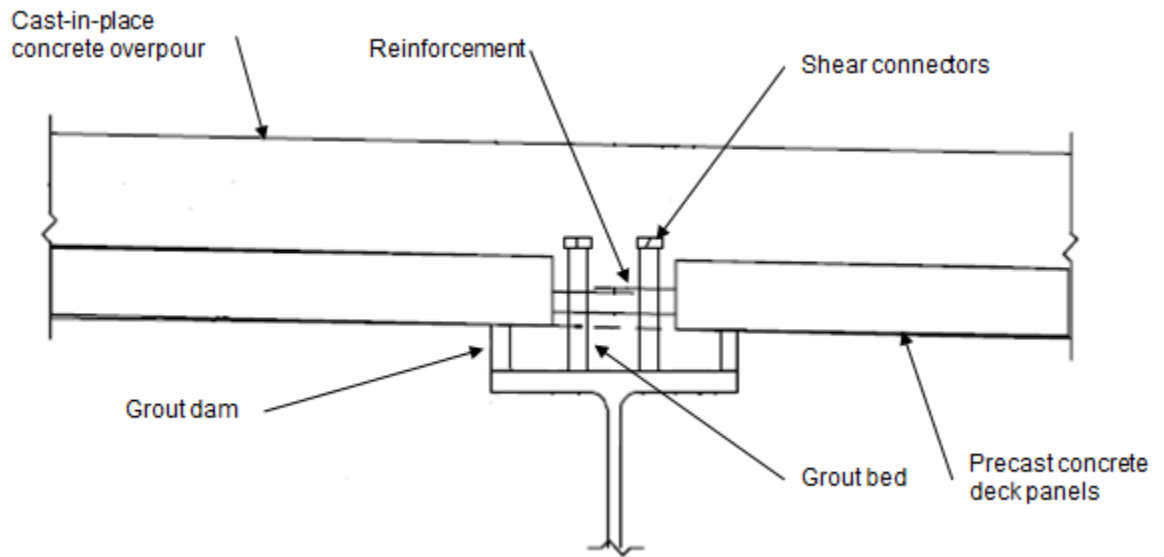
**vi. Prestressed concrete girder with stirrups**



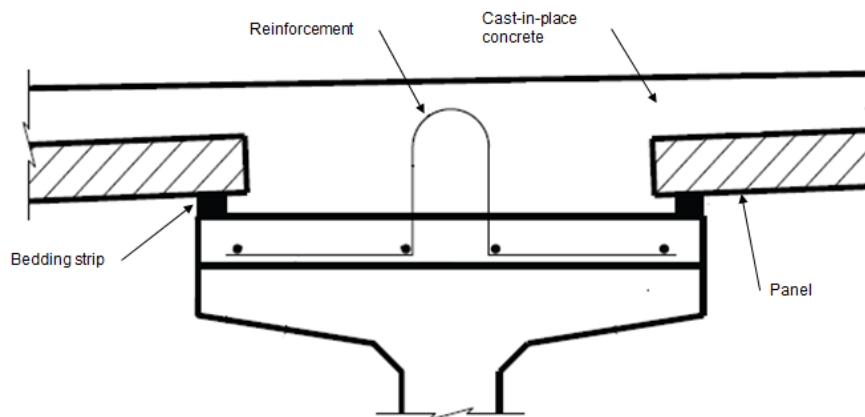
15. We have compiled a menu of details for partial-depth panels deck-to-girder details based on information found in publicly available documents. For each of the details shown, please indicate which statement best represents your state's position.

- a. We use a detail similar to this regularly
- b. We have applied a similar detail but it is not considered regular practice
- c. We have applied a similar detail but would not use it again
- d. We have NOT applied a similar detail

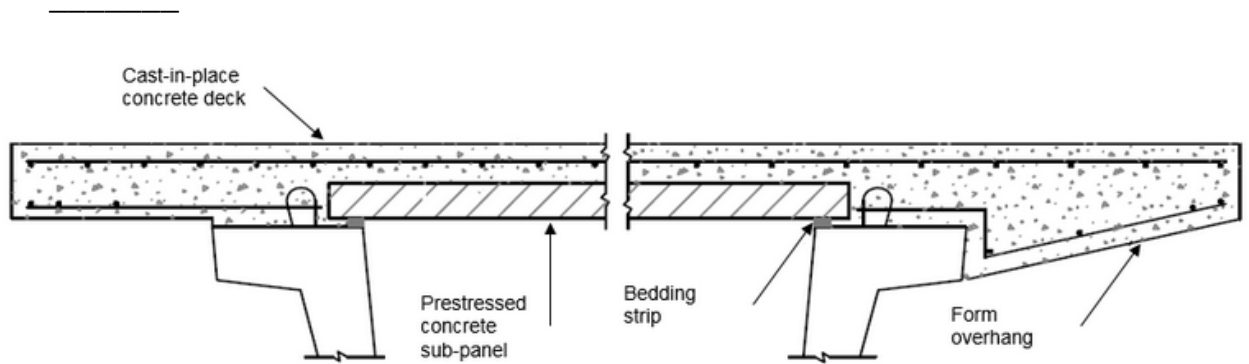
**i. Steel girder with welded steel studs \_\_\_\_\_**



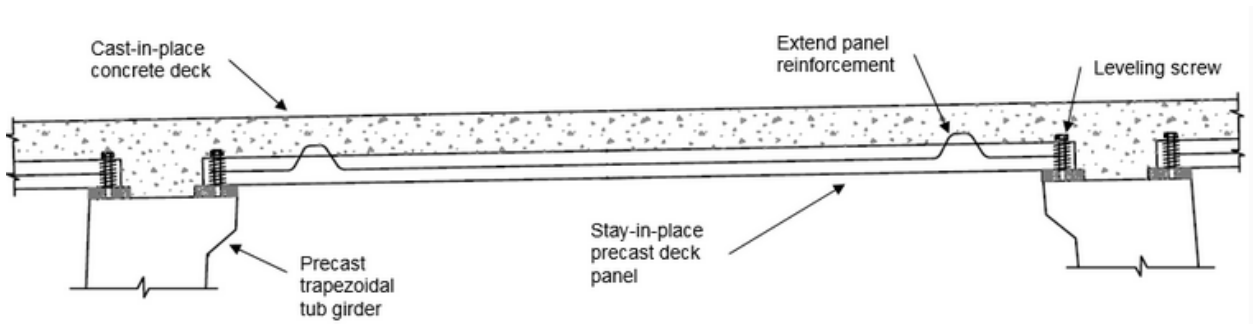
**ii. Prestressed concrete girder with partial depth panels \_\_\_\_\_**



iii. Prestressed concrete tub girder with partial depth panels



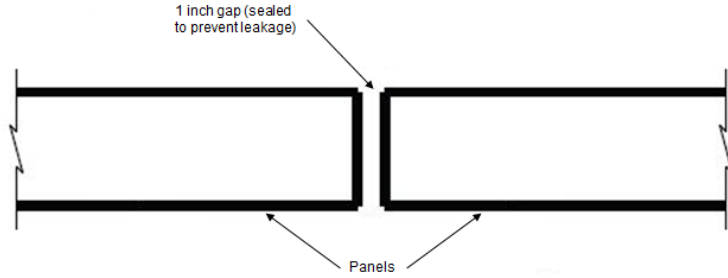
iv. Prestressed concrete tub girder with partial depth panels and leveling screws



16. The following represents a standard detail for partial-depth panels panel-to-panel connection based on information found in publicly available documents. Please indicate which statement best represents your state's position regarding this particular detail.

- a. We use a detail similar to this regularly
- b. We have applied a similar detail but it is not considered regular practice
- c. We have applied a similar detail but would not use it again
- d. We have NOT applied a similar detail

## Partial Depth Transverse Panel Connection



If your state's detailing for the partial depth panel-to-panel connection varies from the sample detail shown, please explain:

---

---

---

17. The following questions contain full-depth deck panel problems that have been reported by DOT's and research studies. Please indicate for each problem which statement best describes the frequency of occurrence for your state

- We frequently observe this problem*
- We have observed this problem in the past but it is not common*
- We have never observed this problem*

Joint leakage

Excessive surface wear

Concrete spalling

Closure pour cracking

Reflective cracking

Differential panel movement

Other full-depth deck panel issue (please specify the issue)

---

---

---

---

18. The following questions contain partial-depth deck panel problems that have been reported by DOT's and research studies. Please indicate for each problem which statement best describes the frequency of occurrence for your state.

- a. *We frequently observe this problem*
- b. *We have observed this problem in the past but it is not common*
- c. *We have never observed this problem*

Joint leakage

Excessive surface wear

Concrete spalling

Closure pour cracking

Reflective cracking

Differential panel movement

Other full-depth deck panel issue (please specify the issue)

---

---

---

---

19. Please indicate limitations that have been imposed by the state on the use of full-depth prefabricated deck panels for bridges with skew.

- Not permitted
- Permitted up to a maximum skew angle
- No limit

If applicable, what is the maximum skew angle (in degrees) permitted for the use of full-depth prefabricated deck panels?

20. Please indicate limitations that have been imposed by the state on the use of full-depth prefabricated deck panels for bridges with curvature.

- Not permitted

- Permitted up to a maximum curvature
- No limit

**If applicable, what is the minimum radius (ft) permitted for the use of full-depth prefabricated deck panels?**

**21. Please indicate limitations that have been imposed by the state on the use of full-depth prefabricated deck panels for bridges with superelevation.**

- Not permitted
- Permitted up to a maximum superelevation
- No limit

**If applicable, what is the maximum superelevation (%) permitted for the use of full-depth prefabricated deck panels?**

**22. Please indicate limitations that have been imposed by the state on the use of partial-depth prefabricated deck panels for bridges with skew.**

- Not permitted
- Permitted up to a maximum skew angle
- No limit

**If applicable, what is the maximum skew angle (in degrees) permitted for the use of partial-depth prefabricated deck panels?**

**23. Please indicate limitations that have been imposed by the state on the use of partial-depth prefabricated deck panels for bridges with curvature.**

- Not permitted
- Permitted up to a maximum curvature
- No limit

**If applicable, what is the minimum radius (ft) permitted for the use of partial-depth prefabricated deck panels?**

**24. Please indicate limitations that have been imposed by the state on the use of partial-depth prefabricated deck panels for bridges with superelevation.**

- Not permitted
- Permitted up to a maximum superelevation
- No limit

**If applicable, what is the maximum superelevation (%) permitted for the use of partial-depth prefabricated deck panels?**

**25. Please indicate limitations on maximum panel size that have been imposed by the state for transporting the panels**

Panel length

- No limit
- Specified limit

If applicable, specify a length limit (in ft)

Panel width

- No limit
- Specified limit

If applicable, specify a width limit (in ft)

Panel depth

- No limit
- Specified limit

If applicable, specify a depth limit (in ft)

**26. Which statement best represents the department's use of site casting for the following pre-fabricated bridge components?**

- a. Site casting is used regularly*
- b. Site casting is used sometimes depending on the project details*
- c. Site casting has been attempted only once or twice*
- d. Site casting has NEVER been attempted*

Girders

Columns

Pier caps

Footings

Abutments

Deck Panels (Full)

Deck Panels (Partial)

**27. If your department uses site casting of prefabricated deck panels, please answer each of the following:**

Please comment on the ease of construction and overall performance in comparison to panels manufactured in a certified precast contractor facility.

---

---

---

---

Are site cast specifications different than factory cast specifications? If so, how?

---

---

---

---

If your department uses site casting of prefabricated deck panels, please answer each of the following: What are the prequalification or certification requirements for the contractors in order to do site casting?

---

---

---

---

**28. Is there a bridge project that represents the general practices of your department? If so, would you indicate below so that we may follow-up to get more information?**

---

---

---

**29. Is there a bridge project that presented a unique challenge to your department? If so, would you indicate below so that we may follow-up to get more information?**

---

---

---

**30. Does your state have standards and specifications for the design, fabrication and construction of prefabricated deck panel systems? If so, would you indicate below so that we may follow-up to get more information?**

---

---

---

**31. Which statement best represents your department perception of the overall performance of the full depth prefabricated deck panel systems that have been used in your projects?**

- Excellent (Panel installation had no problems, only standard upkeep has been needed...)
- Good (Panel installation only had minor issues, and/or minor maintenance needed...)
- Fair (Panel installation had multiple problems, significant repairs needed...)

Poor (Panel installation had major issues, major renovations required during bridge life...)

**32. Which statement best represents your department perception of the overall performance of the partial depth prefabricated deck panel systems that have been used in your projects?**

Excellent (Panel installation had no problems, only standard upkeep has been needed...)

Good (Panel installation only had minor issues, and/or minor maintenance needed...)

Fair (Panel installation had multiple problems, significant repairs needed...)

Poor (Panel installation had major issues, major renovations required during bridge life...)

## **Appendix C: NDOT Design Specifications**

### **Introduction**

As part of a research project titled “Toward Successful Implementation of Prefabricated Deck Panels to Accelerate the Bridge Construction Process”, the authors have assembled for Nevada Department of Transportation (NDOT) the following guidelines pertaining to the design and construction of full-depth prefabricated deck panels. Full-depth deck panels are used as an accelerated bridge construction technique to decrease or eliminate the cure time required for the deck. The basis for the development of the guidelines was a review of existing national and state-adopted guidelines, as well as a survey of current practices by state DOTs. The results of the survey indicated that specifications and drawings from the PCI Northeast Full Depth Deck Panel Guidelines (PCI, 2011a) were the most widely used, and have been evaluated favorable by most agencies that have adopted them. As a result, the authors are recommending adoption of the PCI Northeast Guidelines. The guidelines presented here represent the PCI Northeast Guidelines with supplemental information as needed from other sources. Sources of supplemental information include: 1) the State of the Art Report on Full-Depth Deck Panels (PCI, 2011b), 2) Oregon Department of Transportation (ODOT) prefabricated deck panel guidelines (ODOT, 2015), 3) Utah Department of Transportation (UDOT) deck guidelines (UDOT, 2015), 4) results from the survey of DOT current practices.

The guidelines are formatted as follows: the main numbered sections (e.g. 1.1) and corresponding commentary sections preceded by C (e.g. C1.1) are exact replications of the PCI Northeast Full Depth Deck Panel Guidelines (PCI, 2011a). Supplemental commentary sections that correspond to the numbered sections are preceded by SC (e.g. SC1.1). Appendix A contains the drawings from Appendix A of PCI (2011a). An example illustrating the design of full-depth deck panels taken from PCI (2011b) can be found in Appendix B.

## **SECTION 1 General**

Precast Full Depth Deck Panels (FDDP) may be used for new construction or for replacement of existing deck slabs.

### **Commentary**

This guideline is not for use on partial depth precast deck panels that are intended to be overtopped with a reinforced concrete pour. Please refer to additional guidance on partial depth deck panels at [www.pcine.org](http://www.pcine.org).

### **1.1 Structure Types**

Precast FDDP can be used on virtually any structure that is currently designed with a cast in place deck. The following is a list of typical structure types that can be designed with Precast Prestressed Concrete Full Depth Deck Panels:

- Prestressed Concrete Stringers
- Steel Stringers
- Steel Girder/Floorbeam Systems
- Steel Truss Systems
- Long Span Suspension and Cable Stayed Systems

#### **C1.1**

FDDP can be used on straight, skewed and curved bridges.

## **SECTION 2 Materials**

### **2.1 Concrete**

All mild reinforcement shall conform to the requirements of ASTM A615 and shall be epoxy coated in accordance with ASTM D3963.

#### **C2.1**

Normal deck slab concrete may be used; however, this limits the use of prestressing in the pieces. The designer should take advantage of high strength and high quality concrete that is normally used in a precast plant.

## SC2.1

Section 2.1 text, copied directly from PCI (2011a), does not seem to apply here. To provide further guidance on the development and selection of a suitable concrete mix, the following information is included from PCI (2011b):

“The slab mix should be high-performance concrete with sufficient strength and durability parameters. The deck panels may be shipped to the bridge site when their strength is adequate to resist the shipping and handling stresses. This concrete strength will depend on support and rigging conditions for handling and erection respectively and may be well below the 28 day strength. Although the required strength can be achieved in as little as one day with HPC mixes, it is common practice to install the panels at a concrete age of 28 days or greater to ensure that a significant amount of the shrinkage deformation (and creep for pretensioned members has occurred prior to panel installation.

State practices vary in using performance-based and prescriptive specifications for concrete mixes. The following is an example mix developed for the Wacker Drive project in Chicago that was shown to have worked well:”

Cement Type I	525 lb/yd <sup>3</sup>
Natural Sand (FA-2)	1140 lb/yd <sup>3</sup>
Coarse Aggregate	1800 lb/yd <sup>3</sup>
Densified Silica	27 lb/yd <sup>3</sup> (5% by cement wt.)
Slag	79 lb/yd <sup>3</sup> (15% by cement wt.)
Flyash	53 lb/yd <sup>3</sup> (10% by cement wt.)
W/CM Ratio	0.37
Air Entraining Admixture	(as Required)
Water-Reducing Admixture	(as Required)

(Table 3.3.5-1 of PCI, 2011b)

## 2.2 Mild Reinforcement

All mild reinforcement shall conform to the requirements of ASTM A615 and shall be epoxy coated in accordance with ASTM D3963.

## **C2.2**

FDDP systems have been built with transverse prestressing (prestressed); however, some mild reinforcement will be required within the panel (distribution steel, slab overhang steel, etc.). FDDP systems may also be designed with only mild reinforcement.

### **2.3 Prestressing Strand**

The seven wire strand for pre-tensioning shall conform to the requirements of ASTM A416, Grade 270, low relaxation, and shall be tensioned to the allowable stresses outlined in the AASHTO specifications.

## **C2.3**

Prestressing strand may be used for flexural resistance of the deck panels. A maximum of four 0.6 inch or 0.5 inch diameter strand is typically used with a 2 inch nominal post tensioning duct. If flat slab ducts are used, it is recommended that a maximum of four ½ inch strand be used.2.3

### **2.4 Post-Tensioning Duct**

The use of 2 inch nominal diameter duct is recommended.

## **C2.4**

2 inch diameter duct provides ample room for the recommended post-tensioning strand and erection tolerances at the duct connections. Flat duct can also be used provided that mandrels are used during casting to maintain the geometry of the duct.

### **2.5 Post Tensioning Anchorage Devices**

Anchorage devices should be selected to provide the required concrete cover. The anchorage device should normally be placed at mid-depth of the panel. Anchorage devices should normally be kept a minimum horizontal distance of 18 inch from panel edges and shear connector blockouts.

## **C2.5**

For most deck panels, a four-strand flat anchorage assembly will provide the proper cover. This assembly can be used with the 2 inch nominal ducts. In cases where the top cover cannot be achieved, the anchorage device can be lowered slightly to provide the required cover. Smaller dimensions can be used provided that the anchorage forces are accounted for in the design of the panel.

## **2.6 Grout for Transverse Shear Keys, Shear Connector Pockets, and Beam Haunches**

Grout for transverse shear keys, shear connector pockets and beam haunches should meet the following general requirements:

- Non-shrink
- Flowable
- Moderate strength (5ksi)
- Low permeability

Field mixed grouts should not be used. The use of pre-qualified pre-bagged grouts is preferred.

### **C2.6**

Proportioned mixed grouts in general do not provide adequate quality and durability. State agency prequalified grouts should be used if required.

### **SC2.6**

Grout properties have been a source of problems for full-depth deck panel joints. UDOT reported joint cracking due to grout shrinkage because grout quality standards were not met. CME, which performed a detailed assessment of the performance of various ABC details in Utah bridges, made the following recommendations regarding grout specifications (Culmo, 2013):

“CME recommends modifying the existing grout specification used in ABC construction to include pre-qualified products. There are many “non-shrink” grouts in the market that meet common specifications. The performance of proprietary grouts varies significantly, with the higher priced grouts performing the best. Simply specifying “non-shrink” grout in a low bid environment will most likely lead to the use of an inexpensive, poor performing grout. The Department should establish a prequalification procedure, evaluate different grouts for performance such as the potential for shrinkage cracking, and develop a pre-qualified list.”

PCI (2011b) identified an example bridge with grouted deck panel connections that performed very well. The specifications of the grout for that application were as follows:

Compressive Strength	1,200 ksi @ 6 hrs 4,500 ksi @ 1 day 6,500 ksi @ 28 days
Flexural Strength (ASTM C78, air cured)	0.550 ksi @ 1 day 0.600 ksi @ 28 days
Slant Shear Bond (ASTM C882)	2,500 ksi @ 28 days
Freeze-Thaw Resistance (ASTM C666, A modified)	RDF of 80%
Scaling Resistance (ASTM C672, 25 cycles)	0 scaling rating
Shrinkage (ASTM C596)	0.03% @ 28 days
Sulfate Resistance (ASTM C1012)	0.10% @ 28 weeks

Table 3.3.5-1 of PCI (2011b)

## 2.7 Grout for Post-Tensioning Ducts

Grout for post tensioning ducts shall be specifically formulated to fill post tensioning systems. Pre-bagged grouts should be used.

## SECTION 3 Design Requirements

### 3.1 General

In general, the design of full depth deck panels should follow the requirements of the AASHTO LRFD Bridge Design Specifications.

A. The empirical design method outlined in Section 9.7.2 is not applicable to precast deck panels.

B. The design of transverse shear keys and longitudinal post-tensioning shall conform to Section 9.7.5

### **3.2 Framing Geometry and Layout**

Panels should be laid out perpendicular to the main supporting members. The main reinforcement (herein referred to as transverse reinforcement) should run along the length of the panel, generally transverse to the main supporting members. Distribution reinforcement shall consist of post-tensioning strand running the length of the deck, generally parallel to the main supporting members.

Deck panels can be set to match the cross slope of the finished roadway. For crowned roadways, a small closure pour should be incorporated into the design at the crown. For narrow roadways, it may be possible to install the panels level and crown the wearing surface.

For bridges with minor skews as shown in the details, the panels can be designed to follow the skew of the bridge. For larger skews, the panels should be laid out in a squared pattern.

#### **C3.2**

The terminology for this document is based on construction of typical stringer bridges where the FDDP are installed perpendicular to the stringers. Construction of other systems such as floorbeam bridges may result in panels that are running parallel with the roadway. In this case, the designer should account for the adjustment in the terminology.

Most states layout bridge framing along the cross slope of the roadway, which leads to a sloped deck panel. Roadway crowns are always an issue in precast FDDP bridges. It is very difficult to construct precast FDDP with a built-in crown, especially if pretensioned prestressing is used. A small closure pour has proven to be a very effective means of accommodating the crown of the deck without adding significant time to the construction of the bridge. Often, this closure pour is completed at the same time as the end closure pours or parapet placement.

#### **SC3.2**

Appendix A presents two different panel configurations for skewed bridges depending on the level of skew, one for skew angles between 0 and 15° (referred to as “minor skews” in Section 3.2), and the second for skew angles > 15° (referred to as larger skews in Section 3.2). In the best practices survey of state DOTs, several states have limited the maximum skew angle to 30° for application of full-depth deck panels.

Section 3.2 discusses using a longitudinal closure pour to accommodate roadway crown. This option is used only if the panel layout requires a longitudinal joint. In general, PCI (2011b) recommends avoiding longitudinal joints and makes the following additional recommendations:

“Avoid longitudinal construction joints in bridge decks. Only use longitudinal construction joints when unavoidable (e.g., widenings, phased construction, very wide structures). The following applies to longitudinal construction joints. For deck widths greater than 120 ft (i.e., where the finishing machine span width must exceed 120 ft), make provisions to permit placing the deck in practical widths. If a longitudinal construction joint is necessary, avoid locating the joint underneath a wheel line. Closure pours are not required but can be useful for phased construction projects. A closure pour serves two useful purposes:

- Defers final connection of the phases until after the deflection from deck slab weight has occurred
- Provides the width needed to provide a smooth transition between differences in final grades that result from differential deflection between the phases

Cross slopes can be created by either varying the elevation of the girders or by varying the haunch depth across the girder lines. Crowns can be created in several ways. One approach is to screed the top panel surface to the required crown alignment. This is only suitable for relatively narrow bridge widths. The deck panel can be significantly thicker at the crown than at its ends. Another approach is to form the crown in the plant by creating an internal hinge in the panel that enables the panel to rotate under its self-weight. In bridges with a longitudinal joint, the crown is preferably formed utilizing flat panels with the crown at the joint.”

An additional parameter that can cause difficulties in the incorporation of full-depth deck panels is superelevation. According to the best practices survey of DOTs, some states have opted to limit application of prefabricated deck panels in bridges with superelevation. Among states that applied a limit, the maximum allowed superelevation ranged from 2% to 4%. Other states reported no limitations for superelevation.

### **3.3 Concrete Design Strength**

The design of deck panels without prestressing should be based on a minimum concrete compressive strength ( $f'c$ ) of not less than 5 ksi. For designs with prestressing, the recommended concrete compressive strength is 6 ksi. The compressive strength of the concrete at the time of transfer ( $f'ci$ ) should not be less than 4 ksi.

### **3.4 Strand Pattern**

Typical strand patterns are laid out with zero eccentricity in order to resist the positive and negative moments in bridge decks.

#### **C3.4**

This is based on typical design equations for slabs in the AASHTO specifications where the maximum positive moment is equal to the maximum negative moment. Concentric prestress is also desirable in order to minimize the cambering of the panel after casting.

### **3.5 Allowable Concrete Stresses**

The allowable stresses in the deck panels shall conform to the AASHTO specifications.

### **3.6 Transverse Flexure Design**

Deck panels may be designed with mild reinforcement, prestressing strand, bonded post-tensioning strand, or combinations of each. Moments for design shall be based on the AASHTO specifications for concrete deck slabs.

#### **C3.6**

In many cases, the design of interior bays can be handled with mild reinforcing and/or prestressing. Some projects have been completed with post-tensioning systems; however, costs for large amounts of transverse stressing and grouting can be prohibitive. In general, panels with spans of 10 feet or less can be designed with only mild reinforcement resisting the flexural moments. Prestressing may be used for longer spans.

#### **SC3.6**

The following text expands upon the transverse flexure design methods discussed in the main specification and presents information on how the full-depth deck panel should be designed in the transverse direction (PCI, 2011b):

“The precast deck panel system is designed using the strip design method, where a transverse strip of the deck is analyzed as a continuous beam supported by the bridge girders. The girders are considered rigid supports with no settlement. The strip method concept results in providing the main reinforcement in the transverse direction of the deck. Once the flexural effects due to dead and live loads are determined the transverse strip is designed as a pretensioned or conventionally-reinforced concrete member, where service stresses at critical sections are checked against the AASHTO LRFD allowable stresses and then the nominal flexural resistance and reinforcement limits are checked. Proper AASHTO LRFD load combinations should be used for various checks. For example in a pretensioned panel, SERVICE I and SERVICE III limit states should be

used for checking allowable compressive and tensile stresses, respectively; and STRENGTH I limit state should be used for checking the nominal flexural resistance.

The strength design procedure of a prestressed concrete member is essentially the same as that for a conventionally-reinforced concrete member. However, some differences in behavior occur in the stress-strain relationship between the prestressing steel and the mild reinforcement. It is highly recommended to utilize the strain compatibility concept in determining the nominal flexural resistance of the deck for the following reasons:

- Variation of the stress-strain relationship between the prestressing and mild steel non-prestressed reinforcement
- To accurately account for the effect of various tensile reinforcement layers especially those that are close to neutral axis of the section”

### **3.7 Panel Overhang Design**

The design of the panel overhangs shall be in accordance with the AASHTO specifications. Special attention should be given to the design of the panel overhang with regard to the development of prestressing strand. If the strand cannot be developed within the panel overhang, a design using mild reinforcement or post-tensioning in conjunction with prestressing may be necessary in order to accommodate the overhang moments.

#### **C3.7**

The barrier weight and impact loads have a significant effect on the overhang design. The panel reinforcing needs to be designed to accommodate these forces. It is not desirable to have a large bending moment applied within the transfer and development zone of the prestressed component. In many cases, the maximum slab moment in the overhang occurs at the face of the curb, which is usually very close to the end of the precast panel. Mild reinforcement is often used to handle the slab overhang moments near the ends of the panels.

#### **SC3.7**

PCI (2011b) provides the following additional guidance on designing barriers and overhangs:

“As a general rule, the overhang length should not be more than half the girder spacing with 4 ft. 3 in. a recommended maximum.”

and

“Precast bridge deck design should account for a barrier crash load.”

Specific details on designing the overhang to withstand the impact of a vehicle crash load are given in a design example in Appendix B of these guidelines.

### **3.8 Design for Handling**

Design lifting hardware and panel reinforcement according to the provisions in Chapter 5 of the PCI Design Handbook (seventh edition). The criteria for “no discernable cracking” should be followed. The panels shall also be checked for placement stresses assuming that the panel is supported on every other girder. The design of the prestress for handling will be the responsibility of the contractor.

#### **C3.8**

This provision is based on the fact that during erection, every other leveling device will be in contact with the girders prior to the leveling of the panels. Fabricators and contractors normally determine lifting points based on their handling equipment. The amount of prestress will vary based on the lifting methods employed. The design and review of this prestressing should be treated as a working drawing submission since the prestress is being used for a temporary condition.

#### **SC3.8**

Clarification about prestressed reinforcement calculations is discussed in ODOT (2015):

“Prestressed reinforcement is typically used on the long side of deck panels that span between the bridge girders. This is the main reinforcement that provides flexural strength for resisting applied loads during shipment, erection, superimposed dead load, and vehicular live load. Panel thickness may be increased to accommodate final surface grinding and reinforcement detailing.”

Several states have imposed panel dimension limits because of transportation requirements. Oregon DOT has set the length limit at 50 feet and the width limit at 10 feet because of shipping weight and maximum shipping width (ODOT, 2015). Utah DOT has not set length or width limits but has specified a minimum depth limit of 8.75 inches (UDOT, 2015). The recent survey of DOTs on the use of deck panels asked DOTs if transportation limits had been applied for length, width, or depth. The range of response from each DOT for each of the three dimensions is shown below.

Transportation Limits Range Among States	
Length (maximum allowed)	10 to 41 ft.
Width (maximum allowed)	6 to 12 ft.
Depth (minimum allowed)	3.5 in. to 8.75 in.

The authors recommend that dimension limits be set based on local transportation limitations. Common transportation vehicles used by the state should be evaluated to set specific guidelines.

### **3.9 Longitudinal Distribution Design within each FDDP**

Reinforcement for distribution shall be comprised of mild reinforcement. The design of distribution reinforcement should be according to the AASHTO specifications based on a slab with mild reinforcement. The mild reinforcement does not need to pass through the joints between the deck panels.

#### **C3.9**

This steel is to be placed within each panel. The spacing of the steel will need to be adjusted to avoid blockouts and provide proper cover around blockouts. The designer should detail a bar layout for each panel.

#### **SC3.9**

The following section clarifies how longitudinal reinforcement should be designed (PCI, 2011b):

“Typically, conventional longitudinal reinforcement is provided in the deck slab to: (1) control shrinkage cracking, and (2) distribute the live load in the longitudinal direction. However, the design engineer may opt to utilize longitudinal post-tensioning conforming to LRFD Specifications 9.7.5.3 to provide live load distribution across panel joints and secure the joint against leakage.”

and

“The longitudinal bars in the top and bottom of the slab may be sized for temperature and shrinkage requirements per LRFD Specifications 5.10.8, or it may be accommodated through handling and transportation reinforcement. In slabs where longitudinal post-tensioning is not used, LRFD Specifications 9.7.3.2 requires reinforcement in the bottom of slabs.”

Section 2.4.3 of PCI (2011b) contains further information.

### **3.10 Longitudinal Post-Tensioning**

The design of transverse joints and longitudinal post-tensioning shall be in accordance with AASHTO Section 9.7.5. Post-tensioning combined with a grouted shear key should be used to provide continuity between deck panels. This post-tensioning should be located at mid-depth in the units and should run the entire length of the bridge or between closure pours. For continuous spans, the designer should design for additional prestress to overcome the service load tensile stress due to negative composite dead load and live load moments to achieve an effective minimum prestress of 0.250 ksi under all service loading conditions. The minimum final post-tensioning force per duct and the minimum effective prestress shall be shown on the plans, as well as a sequence for stressing the ducts (generally starting at the center and working to the outside). The plans should note the assumptions used to develop the post-tensioning force including the assumptions used for loss calculations. The project specifications should include requirements for submission of calculations for the design of the post-tensioning system. These calculations should account for the actual system and ducts that are proposed.

#### **C3.10**

Research has shown that moderate post-tensioning combined with a grouted shear key is the best way to provide continuity between full depth panels.

#### **SC3.10**

Oregon DOT lists CIP joints as an option for transverse joint connections. ODOT uses UHPC and CIP joints as their default construction type for full-depth decks. The following information from ODOT (2015) implies they use their own non-proprietary UHPC mix.

“Two possible types of transverse joint connections are CIP reinforced concrete and longitudinal posttensioning along the length of the bridge. Each connection type has its own advantages and disadvantages.

For CIP joint connections, Ultra High Performance Concrete (UHPC) is the preferred material due to its superior bond properties, durability, compressive strength, and tensile strength. There are a number of proprietary UHPC products on the global market, such as BCV®, BSI®, CRC®, Densit®. The only satisfactory UHPC joint material available on the domestic market is Ductal® JS1000 by Lafarge North America, Inc. Since use of this material would be considered a “sole source”, a finding of public interest letter (with approval from FHWA) must be secured before going to bid. In the past there was also an issue with steel fibers used in the Ductal® JS1000 product since the steel fibers were

manufactured in Europe and therefore did not meet the “Buy America” provisions for steel. Based on an FHWA Policy Memorandum published on February 12, 2014, steel fiber reinforcement, as used in the Ductal® JS1000 product, is now produced by Bekaert Corporation at a production facility in Rome, GA and commercially available to all potential purchasers. For other UHPC products made outside the USA, they would be able to meet the “Buy America” requirements as long as they used the steel fibers from the Rome, GA facility.

Note also that there are other types of steel fiber reinforcement that are made in the USA. However, at this time only those from the Rome, GA are thought to meet the size and shape needed for the UHPC application.

Due to the nature of new superior materials, UHPC is much more expensive than conventional concrete. Based on an FHWA publication, FHWA-HRT-13-100 published October 2013, the commercially available product by Lafarge is sold for about \$2000/yd<sup>3</sup>. This price includes material cost of the proprietary blend and fiber reinforcement, as well as costs associated with development and delivery. The same publication also reveals that there are a number of researchers, who have conducted testing programs to develop non-proprietary cost-effective UHPC mixes, which meet all the requirements for UHPC. All materials used in the research project were locally available in three regions across the U.S. One of the material sources is from the Pacific Northwest area. The result shows that it is possible to produce UHPC under \$1000/yd<sup>3</sup> using these domestic materials with a non-proprietary blend. Note that the fiber reinforcement is responsible for one half the total cost.

With the excellent bond behavior provided by UHPC, a non-contact splice length for rebar extending out from deck panels is significantly shorter than that required in conventional concrete. To ensure good bonding against precast deck panels, pre-wetting the interface and an exposed aggregate finish is recommended. FHWA Research, Development, and Technology published FHWA-HRT-14-084 in October 2014. This document provides substantial information regarding design and construction of UHPC.”

### **3.10.1 Losses in Post Tensioning**

Losses due to elastic shortening, anchorage set and friction in the ducts should be accounted for in the design of the post-tensioning. Long-term losses in longitudinal post-tensioning stress due to creep and shrinkage need not be accounted for in the design.

#### **C3.10.1**

Most designers do not account for long-term losses in the deck panel on steel beam bridges. This is due to several reasons:

A. The amount of post-tensioning stress specified is considered to be somewhat arbitrary and high; therefore, minor losses in post-tensioning are considered acceptable and insignificant.

B. The design of composite beams accounts for some creep by using a modified modular ratio for long-term loads.

### **3.10.2 Anchorage Zone Design**

The design of the reinforcement in the anchorage zones shall conform to the AASHTO specifications. The design of the local zone reinforcement is the responsibility of the anchorage device manufacturer. The design of the general zone reinforcement is the responsibility of the designer.

#### **C3.10.2**

The local zone reinforcement is highly dependent on the geometry of the anchorage device, which is under the control of the device manufacturer. The general zone reinforcement is affected by the geometry of the panel, which is under the control of the designer.

### **3.11 Composite Deck Design**

Deck panels should be made composite with the supporting members. Composite action is achieved with shear connectors placed in blockouts in the panel. Shear connectors shall consist of welded studs or hooked reinforcing steel on concrete girders. Spacing of shear connector blockouts shall be kept at approximately 2 feet on center where possible. The design for variable horizontal shear can be accommodated by varying the number of shear connectors per blockout. Special panels with larger reinforced blockouts may be required for continuous girder bridges. These special panels should only be used where necessary. They can be combined with regular panels with nominally spaced shear connector blockouts.

#### **C3.11**

The effectiveness of using welded stud shear connectors on steel beams has been verified through several research projects. The design of the shear connectors can be based on the requirements for cast-in-place slabs. A embedded steel plate can be used in concrete beams to achieve the same effect. This has also been verified through research. The use of hooked reinforcing steel for shear transfer has also been studied. The AASHTO provisions for horizontal shear design are appropriate for this design. The 2 foot maximum shear connector spacing has been in the AASHTO specifications for many years. Recent research has shown that the spacing can be increased to 4 feet without any reduction in composite action. This can only be achieved if a confinement pocket is

provided such as a steel tube or confinement reinforcement. Larger diameter shear studs have been tested and been found to perform adequately; however, they may not be readily available. Large spacing of shear connectors will require a large number of shear connectors per pocket, which may become problematic. In most cases, limiting the knockout spacing to 2 foot maximum will limit the number of shear connectors to a reasonable number. The design of short span and continuous steel girders for ultimate flexural strength typically requires a significant amount of shear connectors from the points of maximum moment to the adjacent supports. The number of studs is primarily controlled by the beam spacing (not the necessarily the beam size). On short span bridges, this distance can be very short, which will necessitate very close shear connector spacing. Large pockets can disrupt the spacing of panel reinforcement. Therefore it is desirable to run the reinforcement through the large pockets (see typical details).

### **3.12 Closure Pours**

In order to account for increased length of the overall deck due to build-up of tolerance effects, small closure pours may be necessary. Closure pours can also be used to accommodate cross slope changes in the deck.

#### **C3.12**

A cast-in-place concrete closure pour has been used at the end of the bridge deck to account for construction tolerances and varying field conditions. This closure pour can also accommodate the complex geometry that often occurs between the panel, end cross-frames and bridge joints. It may be possible to increase the width of the joints between the pieces in order to accommodate the buildup of tolerances. In this case, the connection to the end cross-frames would need to be investigated. There is a concern with this approach since the post-tensioning anchor head will be located directly under a deck joint. For this reason, most designers have opted for the small closure pour at the end of the deck. The accommodation of deck cross slope in a precast panel needs to be addressed. Casting a piece with a crown can be done; however, this will have an effect on the transverse prestressing design (if used). Casting a piece with an angle point at the crown is also problematic for the same reasons. Small longitudinal closure pours have been successfully used. The reinforcing can be projected from each piece and forming support can be provided by inserts in the precast panels.

#### **SC3.12**

Although UDOT avoids closure pours they have provided the following list as guidelines for closure pours if they are needed. (UDOT, 2015)

“When a closure pour is used, the following applies:

- Use a minimum closure pour width of 3 ft.
- Locate lap splices in the transverse reinforcing within the longitudinal closure pour. Allow transverse shrinkage of the deck concrete to occur by leaving the joint open as long as the construction schedule permits.
- Do not tie contact lap splices or couple reinforcing between different phases until placing adjacent phases of the deck.
- Consider the deflections of the bridge on either side of the closure pour to ensure proper transverse fit up.
- Do not rigidly connect diaphragms/cross frames in the closure pour bay of structural steel girders or prestressed concrete girders until after placing adjacent phases of the deck. If concrete diaphragms are used for prestressed girders, construct the concrete diaphragms in the closure pour bay of prestressed concrete girders after adjacent portions of the bridge are complete. Pour the diaphragms as part of the closure pour.
- Support the finishing machine on an overhang jack connected to the girder loaded by the deck pour. Do not place one edge of the finishing machine on a previously poured deck. Indicate in the plan sheets or the project specifications that this method of constructing the closure pour is not allowed.”

### **3.13 Curved Bridge Issues**

The post-tensioning ducts on curved bridges should follow the curvature of the roadway. The design of the longitudinal post-tensioning should take into account the losses due to friction in the post-tensioning ducts due to curvature.

#### **C3.13**

For curved bridges, the pieces can be cast in a trapezoidal shape so that the joints between deck panels are radial. The post-tensioning can be run along the curve. For large radius curves, it is acceptable to run the post-tensioning duct straight within each panel combined with small angle points at the hand hole splice locations. The amount of friction losses in a curved duct can become significant. It may be necessary to specify jacking the post-tensioning strand from each end in order to overcome the friction losses in the ducts.

### **SC3.13**

Because of the complexities associated with deck panel design for bridges with curvature, the authors recommend that full-depth deck panels for curved bridges only be attempted once experience has been gained in the use of full-depth deck panels. ODOT guidance for limitations on use of full-depth deck panels is summarized as follows (ODOT, 2015):

“Deck panels can accommodate skew, superelevation, slight horizontal curve, and vertical roadway profile. For a mild vertical roadway profile, a flat layout of deck panels constructed on bridge girders is adequate and makes the construction of joint connections easier. When the vertical roadway profile is significant, chorded deck panels are recommended to fit the profile with CIP reinforced concrete joints connecting the deck panels. Reinforcement and anchor bolts for bridge railing can be cast into the deck panels as well.”

## **SECTION 4 Construction**

### **4.1 Construction Sequence**

In order to avoid inducing undesirable stresses in the girders, the sequence of construction for precast concrete deck panels shall be such that the longitudinal post-tensioning is accomplished after the transverse panel joints have been grouted and before the panel has been made composite with the girders.

The following sequence of construction should be included on the plans:

1. Clean surfaces of shear keys.
2. Preset leveling bolts to anticipated height
3. Place all precast deck panels on girders in a span.
4. Adjust leveling devices on deck panels to bring panels to grade.
5. All leveling bolts shall be torqued to approximately the same value (20 percent maximum deviation).
6. Install longitudinal post-tensioning strand (un-tensioned) in ducts and seal joints in ducts between deck panels.
7. Place a flowable non-shrink grout in all transverse joints. The grout shall be rodded or vibrated to ensure all voids are filled.
8. After the grout in the transverse joints has attained a strength of 1000 psi (based on grout manufacturers' recommendations), the longitudinal posttensioning strands may be stressed. The contractor shall determine the

jacking force required to achieve the minimum final post-tensioning force shown on the plans accounting for all losses.

9. Grout post-tensioning ducts.
10. Install shear connectors in all blockouts.
11. Form haunches between the top of the girders and the bottom of the deck panels.
12. Grout all haunches and shear connector blockouts with a flowable non-shrink grout.
13. Cast end closure pours.
14. Cast parapets and/or sidewalks.
15. Place overlay (if required) and open Bridge

#### **C4.1**

If the post-tensioning is applied after the deck is made composite with the beams, the post-tensioning will induce a positive moment into the beam. The construction sequence outlined in the detail sheets ensures that this will not occur. Follow State specifications. High-pressure water blasting can be used for this cleaning. Sand blasting should be avoided if there is coated projecting reinforcement. Setting of the panels high and lowering them into position will require less torque. The FHWA manual entitled “Post-Tensioning Tendon Installation and Grouting Manual” should be followed for this operation. The interim strength of the transverse joint grout may need to be adjusted based on the level of post-tensioning stress specified. The FHWA manual entitled “Post-Tensioning Tendon Installation and Grouting Manual” should be followed for this operation. Haunch forms can be set before setting panels. Closure pours can be designed for lower initial concrete strength, which would allow for earlier opening of the bridge. Final strength of the closure pour concrete should follow State standards for deck panels. No vehicles or heavy equipment should be allowed on the panels until the installation sequence is complete and all materials have achieved adequate strength.

#### **4.2 Deck Elevations**

The plans should include the elevations of each panel (generally each corner of each panel) based on the required elevation of the panels after all panels are placed on a span. The following equation can be used to determine the deck elevations:

$$A = B - W + C$$

A = Deck Elevation shown on plans

B = Finished Elevation of Deck

W = Thickness of Wearing Surface

C = Deflection due to Composite Loads

#### **C4.2**

These elevations are the anticipated elevations just after the erection of the panels. The deflection due to composite loads shall account for all loads applied after the deck panels have been placed, including, but not limited, to the wearing surface, parapets, sidewalks and railings.

#### **4.3 Casting Tolerances**

Tolerances for casting panels shall be shown on the plans or in the specifications. Special attention should be given to the location of the longitudinal post-tensioning ducts. The ducts should be oversized in order to accommodate the specified tolerances.

#### **C4.3**

Recommended tolerances for precast deck panels have been developed by the committee. It is very important to have many of the tolerances measured from a common working point. Center-to-center measurements can lead to a buildup of measuring errors and unacceptable results. The location of the post-tensioning ducts requires the most stringent tolerances. Misalignment of the ducts can cause significant problems in the field. It is common for post-tensioning ducts to flex during concrete placement. For this reason, it is recommended that the duct be properly secured to the deck reinforcing or stiffened by a reinforcing bar. Mandrels can also be used to position the duct and prevent deformation during casting.

#### **SC4.3**

Because of the absence of a certified precast plant in the state of Nevada, site casting of full-depth deck panels may be a more viable form of construction for full-depth deck panels.

The survey of current practice requested information from other DOT's about the frequency of site casting in other areas. The findings of the survey showed that site casting has not been commonly implemented around the United States for full-depth deck panels. If the use of site casting is desired, interim guidelines should be developed for the manufacture and use of site-cast full-depth deck panels.

#### **4.4 Vertical Adjustment**

Leveling bolts should be used to adjust the grade of the deck panels after placement. The design of leveling devices is typically accomplished by the designer. If bolts are used, each bolt should be able to resist two times the tributary dead load of the panel. The design of the bolts should also account for the cross slope of the roadway. The plans or specifications should note that each bolt should be torqued to approximately the same value so that there is approximately equal load on each leveling bolt.

#### **C4.4**

The most common size of leveling bolt is 1 inch diameter. The bolts should be detailed so that they can be removed easily after grout placement. The device should also be recessed so that the top surface can be sealed with grout after bolt removal. The details included in this guide are the most common type used. Designers should show this detail, but allow the contractor to substitute alternate devices, provided they can meet the criteria described in this section. The cross slope of the roadway will induce bending in the bolts. In this case, the bolts should be designed for the bending or canted to match the cross slope of the road. These bolts serve two purposes. They allow for grade adjustment in the field after deck placement, and they also provide proper dead load distribution to each girder. For this reason, there should be the same number of leveling bolts over each beam (typically two per beam). The amount of torque on each bolt should be within 20% of an average torque that is determined in the field. This value offers sufficient uniform distribution. Minor variation in each bolt load can be overcome by distribution through the beam cross-frames.

#### **4.5 Horizontal Adjustment**

The transverse joints between deck panels should have a nominal width of  $\frac{1}{2}$  inch. The width of this joint may be adjusted in the field by  $+\frac{3}{8}$  inch to account for casting tolerances.

#### **C4.5**

Casting tolerances such as panel width and sweep can lead to a build-up of deck length. This buildup of length has been referred to as dimensional growth. If ten panels that are exactly 8 feet wide are laid side by side, the overall deck length would measure somewhat over 80 feet due to the uneven seating of the panels. The width of the joints between each deck panel can be used to account for this effect. For this reason, the allowable width of the panel joints should be closely related to the specified fabrication tolerances. The value of  $\frac{1}{2}$  inch  $+\frac{3}{8}$  inch has been found to be an adequate joint width variation to account for these effects. It is not necessary to design the deck layout to account for dimensional growth of the panels. If the variation in joint width does not

adequately account for the tolerance, the closure pours at the ends of the spans can be used to make up any minor differences.

#### **4.6 Parapets, Curbs, and Railings**

Cast-in-place parapets or curbs combined with railings should normally be used for the final traffic barrier.

##### **C4.6**

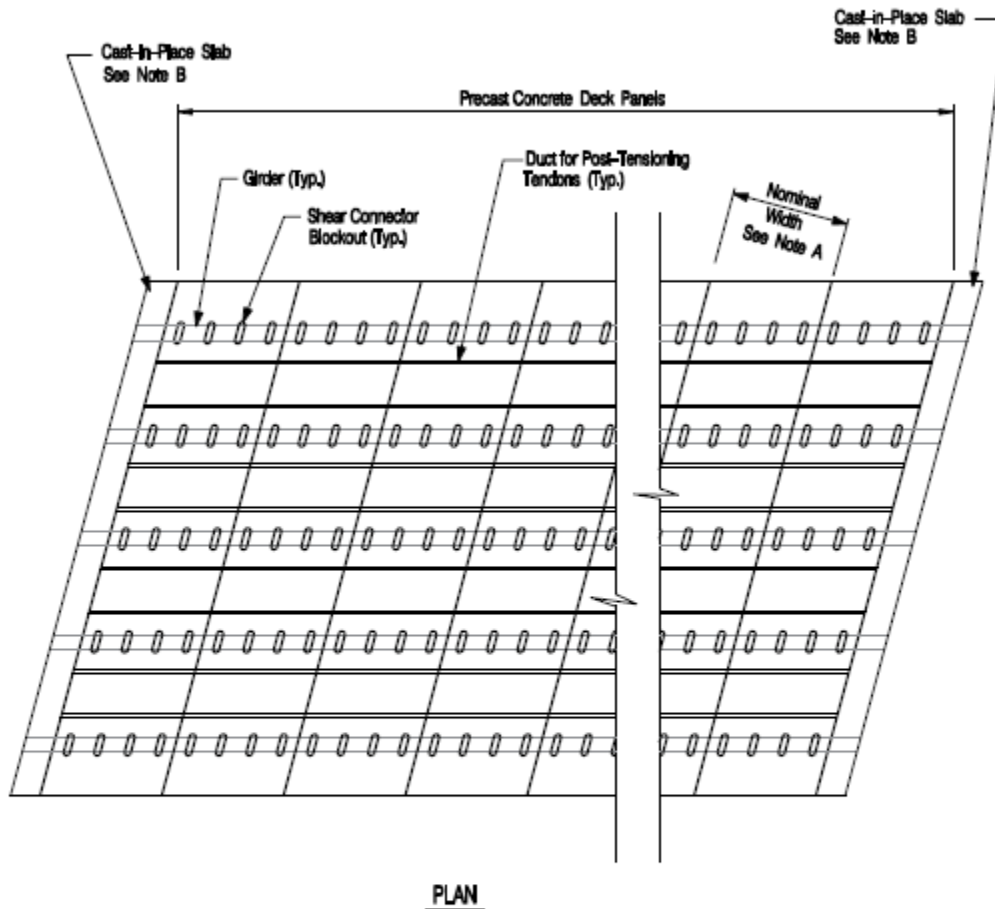
Cast-in-place parapets and curbs offer a number of benefits to the finished structure:

- They assist with connecting the adjacent deck panels in the deck overhang region.
- They provide a means of sealing the gutterline and prevent water leakage through the parapet.
- Most cast-in-place barriers are crash-tested. There are very few crash-tested precast barrier systems.
- The cast-in-place parapet or curb can be used to encase the ends of the deck panels.

There have been concerns from several agencies that the construction of a cast-in-place barrier system will increase the time for construction. This is true; however, for very rapid deck placement projects, the final barrier can be constructed after the bridge is opened to traffic. Temporary precast concrete barriers can be used in the shoulders. The permanent barrier can then be constructed behind the temporary barrier. Encasing the edge of the deck panels offers a number of benefits. If the panels are prestressed transversely, the edge of the panels will have numerous locations where the prestressing strand are cut and patched. Long-term deterioration of the patched strand ends is a concern. The ends of the panels can also be uneven due to casting tolerances. By casting a concrete curb or parapet over the deck end, a uniform deck edge can be produced that will enhance the appearance of the completed deck.

## Specifications Appendix A (Details)

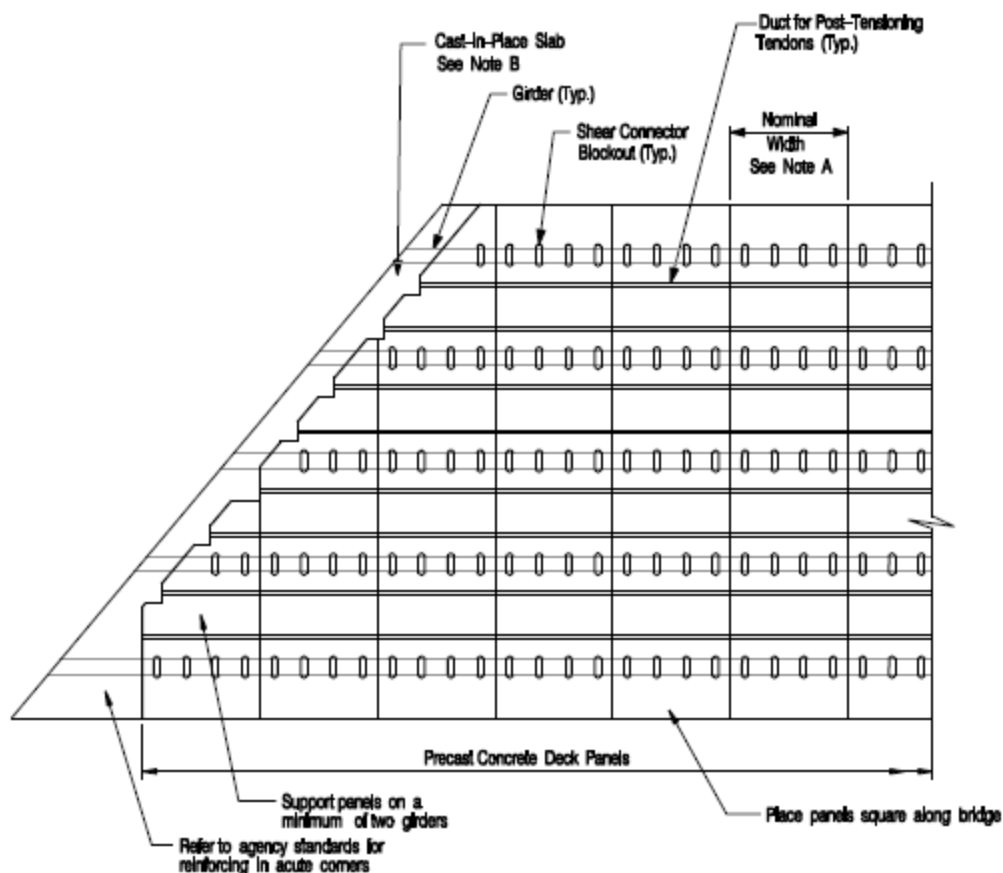
### Full Depth Deck Panels Guidelines—Appendix A



**Note A:** The nominal width of panel should normally be set in two foot increments. The maximum nominal width should be 12 feet in order to facilitate shipping. Panels shall be placed to the nominal spacing shown. Actual width of panels will be 1/2" narrower than the nominal width in order to account for the width of the transverse shear key.

**Note B:** Cast-in-place closure pours shall be used to provide attachment to end bearing diaphragms. See Detail FDDP-14.

**Typical Layout Plan  
Skew Between 0 and 15 Degrees  
Detail FDDP – 1**



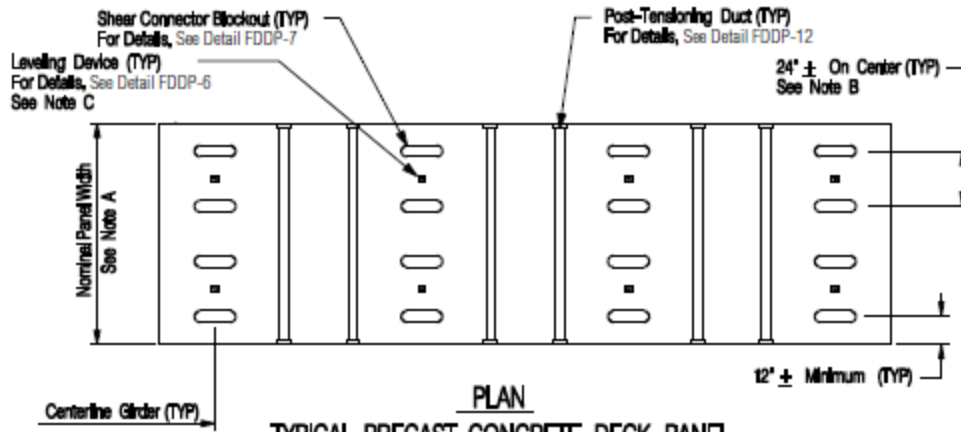
PLAN

Note A: The nominal width of panels should normally be set in two foot increments. The maximum nominal width should be 12 feet in order to facilitate shipping. Panels shall be placed to the nominal spacing shown. Actual width of panels will be 1/2" narrower than the nominal width in order to account for the width of the transverse shear key.

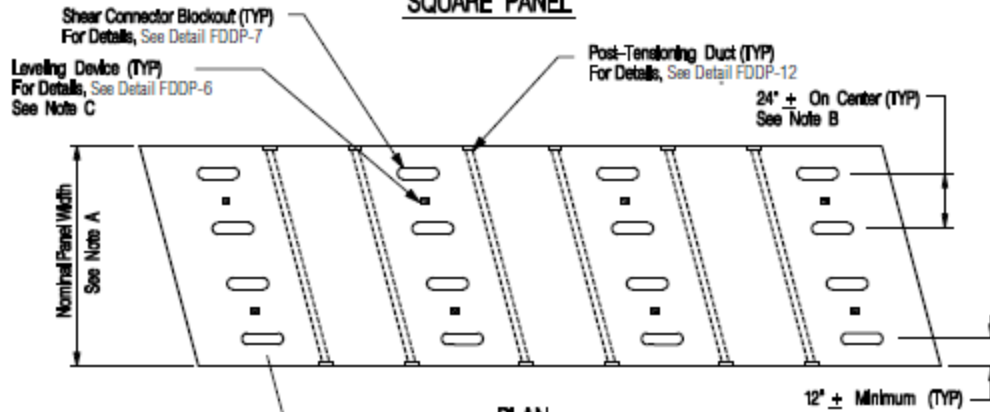
Note B: Cast-in-place closure pours shall be used to provide attachment to end bearing diaphragms. See Detail FDDP-14.

Note C: This layout is shown for information only. The layout will vary with different skews, panel widths, and beam spacings.

**Typical Layout Plan  
Skew Greater Than 15 Degrees  
Detail FDDP - 2**



**PLAN**  
**TYPICAL PRECAST CONCRETE DECK PANEL**  
**SQUARE PANEL**



**PLAN**  
**TYPICAL PRECAST CONCRETE DECK PANEL**  
**SKewed PANEL**

**Note A:** The nominal width of panels should normally be set in two foot increments. The maximum nominal width should be 12 feet in order to facilitate shipping. Panels shall be placed to the nominal spacing shown. Actual width of panels will be 1/2" narrower than the nominal width in order to account for the width of the transverse shear key.

**Note B:** Blockouts for shear connectors shall generally be spaced at two feet on center. For special designs, this dimension may be changed.

**Note C:** At least two leveling devices shall be used at each girder in order to achieve proper dead load distribution. For details, see Detail FDDP-6.

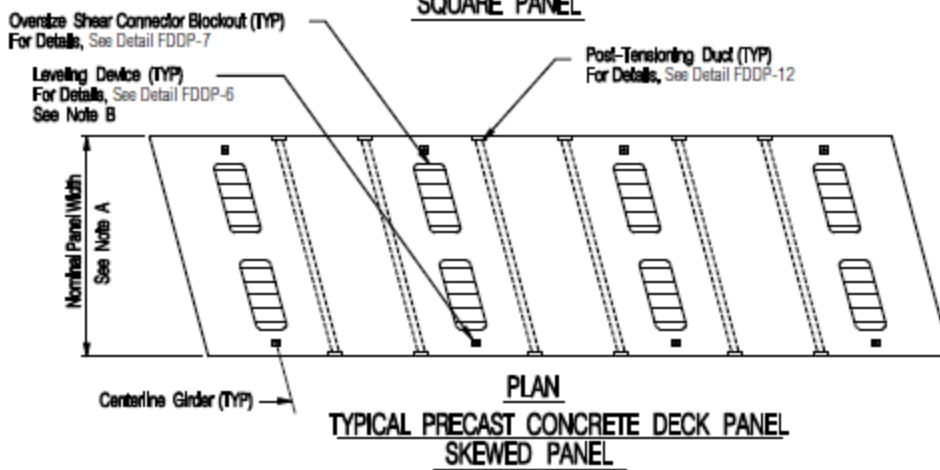
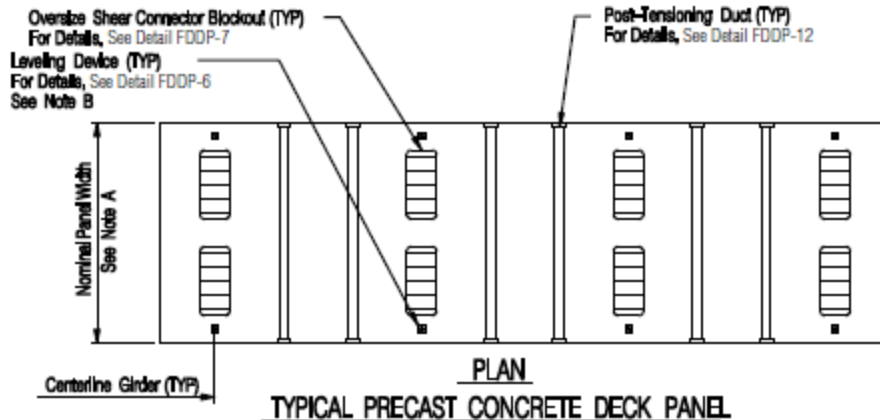
**Note D:** Post-tensioning may be placed in overhang regions. See Detail FDDP-13 for details.

Typical Panel Plan  
Detail FDDP - 3



Report Number  
PCINER-11-FDDP

Date Issued  
April 26, 2011



**Note A:** The nominal width of panels should normally be set in two foot increments. The maximum nominal width should be 12 feet in order to facilitate shipping. Panels shall be placed to the nominal spacing shown. Actual width of panels will be 1/2" narrower than the nominal width in order to account for the width of the transverse shear key.

**Note B:** At least two leveling devices shall be used at each girder in order to achieve proper dead load distribution. For details, see Detail FDDP-6.

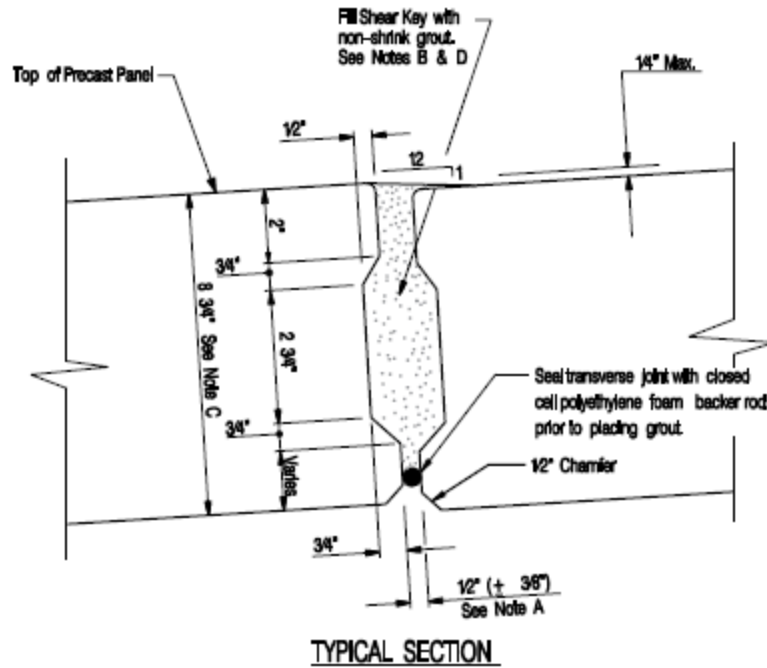
**Note C:** Post-tensioning may be placed in overhang regions. See Detail FDDP-12 for details.

**Note D:** The size of the pockets should be kept to a minimum.

**Note E:** Minor cracking projecting from the corners of the blockouts may occur. Round corners to minimize this potential.

**Note F:** Large packets may require special handling rigging (8 point sling, or spreader beam) in order to control cracking during handling.

**Typical Panel Plan**  
**Enlarge Blockout**  
**Detail FDDP - 4**



NOTE A: The variation indicated is due to fabrication tolerances for sweep and camber of the panels. The designer should add the following note to the plans:

"The panels shall be placed at the nominal spacing shown on the plans with a 12" wide gap between the panels. The width of this gap can vary due to tolerances of the panels."

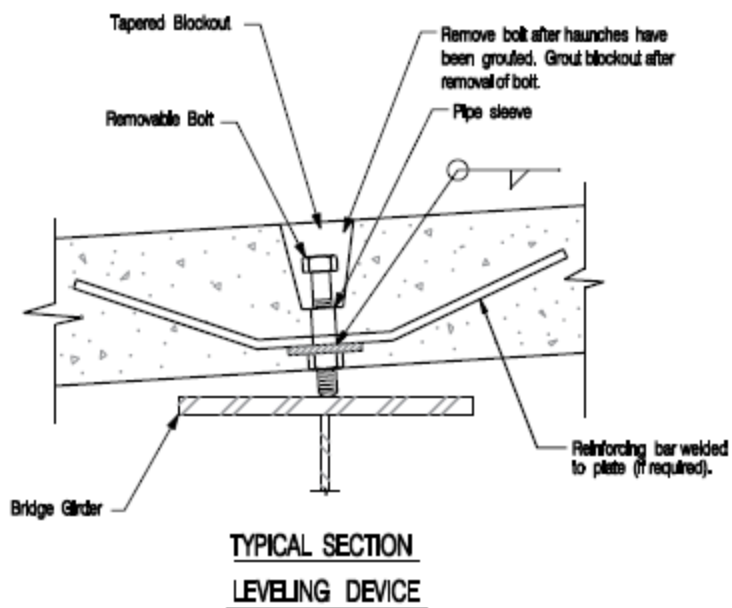
NOTE B: The designer should add the following note to the plans:

"Grout for shear keys shall be rodded or vibrated to ensure that all voids in the shear keys are filled."

NOTE C: Different panel thicknesses are permitted. Coordinate vertical location of PT ducts with slab reinforcing to avoid conflicts. Thicker panels can be used to accommodate increased reinforcing cover and the required design strength (large beam spacing or large overhangs).

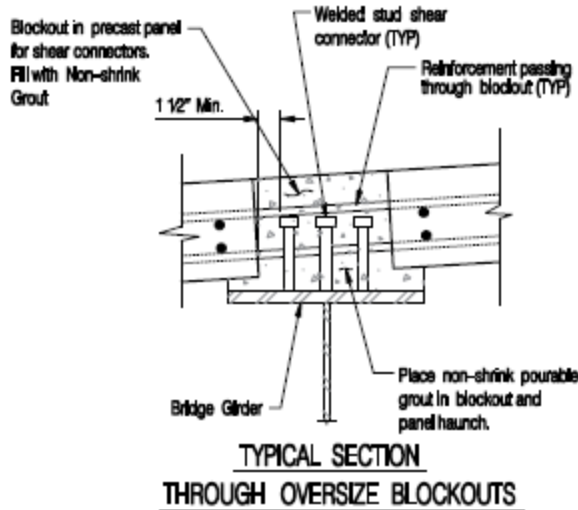
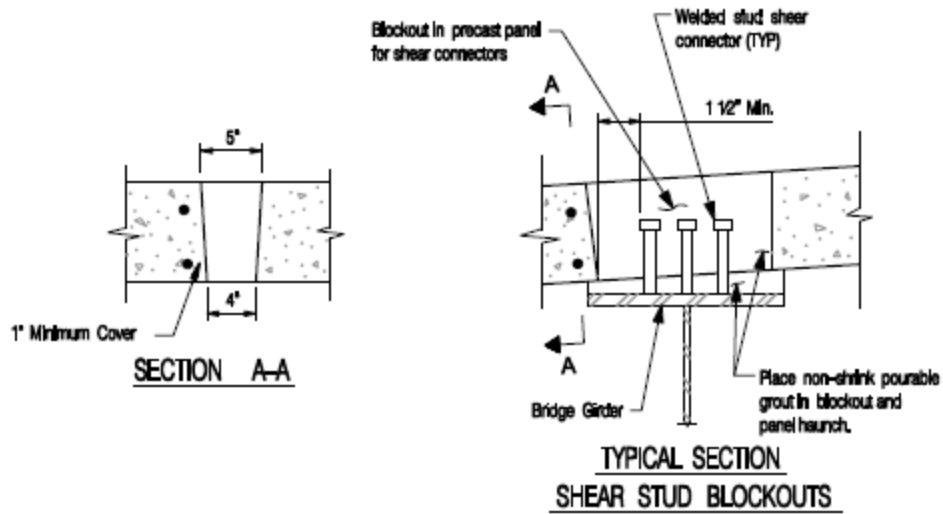
NOTE D: The face of the shear keys should be treated to improve the bond of the grout. Sand or water blasting of the surface in the shop combined with water cleaning prior to installation is recommended.

Transverse Shear Key Details  
Detail FDDP - 5



Note A: The contractor is responsible for the design of the leveling device based on the weight of the panels and the number of devices.

Note B: Alternate devices may be substituted with approval from the Engineer.

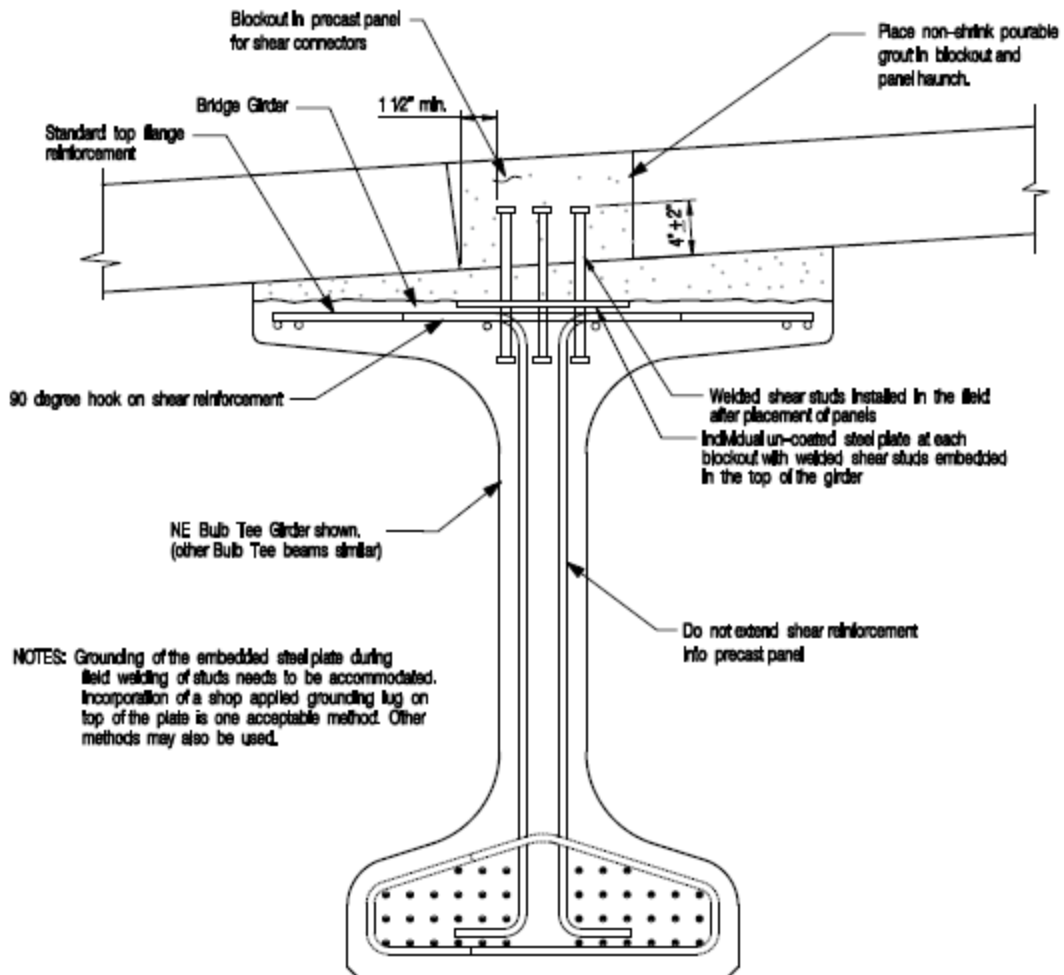


Note A: Shear connector blockouts may be either rectangular with rounded corners or oval.

Note B: Larger blockouts can be used if proper spacing of panel reinforcing can be provided (gaps in reinforcing spacing are required at blockouts)

Note C: Use oversize blockouts if reinforcing spacing gets too large.

Shear Connector  
Blockout Details  
Detail FDDP - 7



NOTES: Grounding of the embedded steel plate during field welding of studs needs to be accommodated. Incorporation of a shop applied grounding lug on top of the plate is one acceptable method. Other methods may also be used.

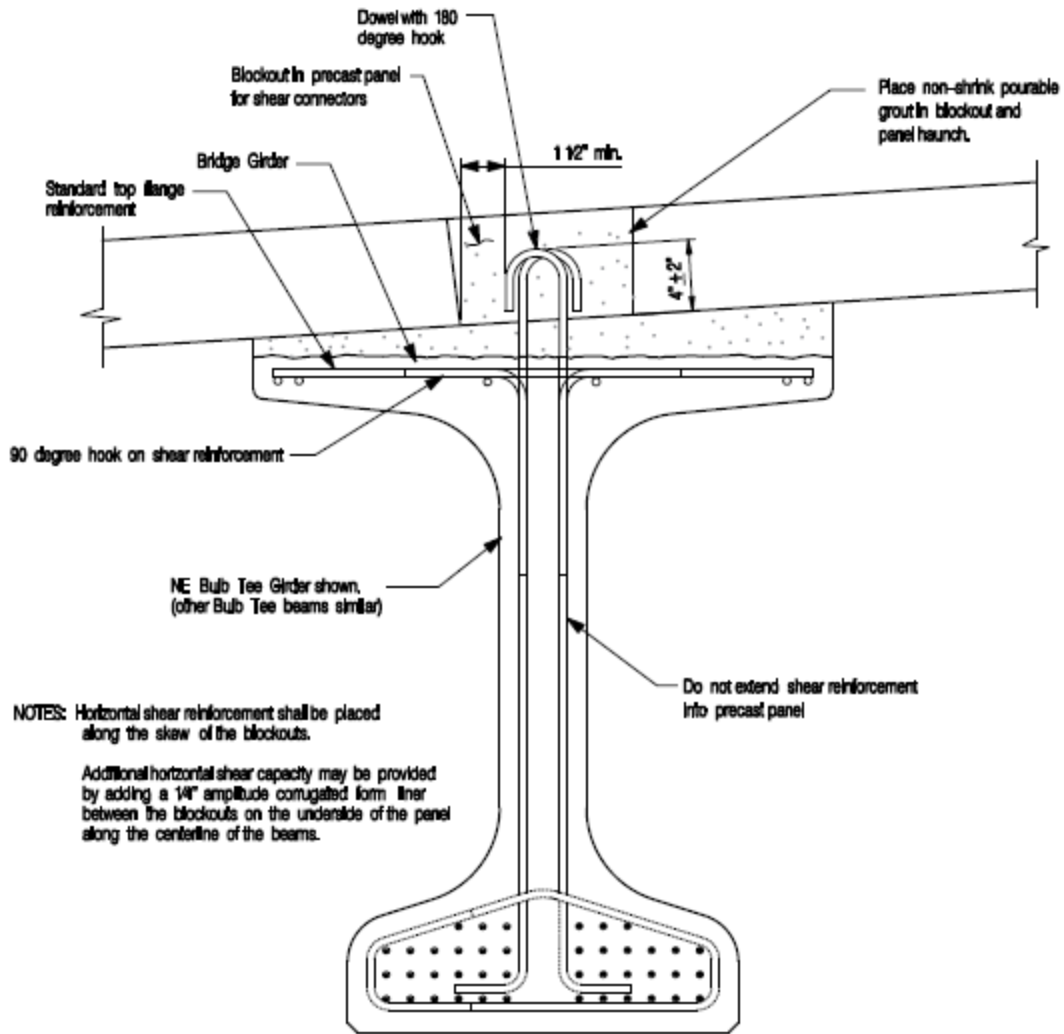
**TYPICAL SECTION – BULB TEE BEAMS**

**NEW CONSTRUCTION WITH WELDED STUD CONNECTION**

**Bulb Tee Beam Attachment  
Details 1  
Detail FDDP – 8**



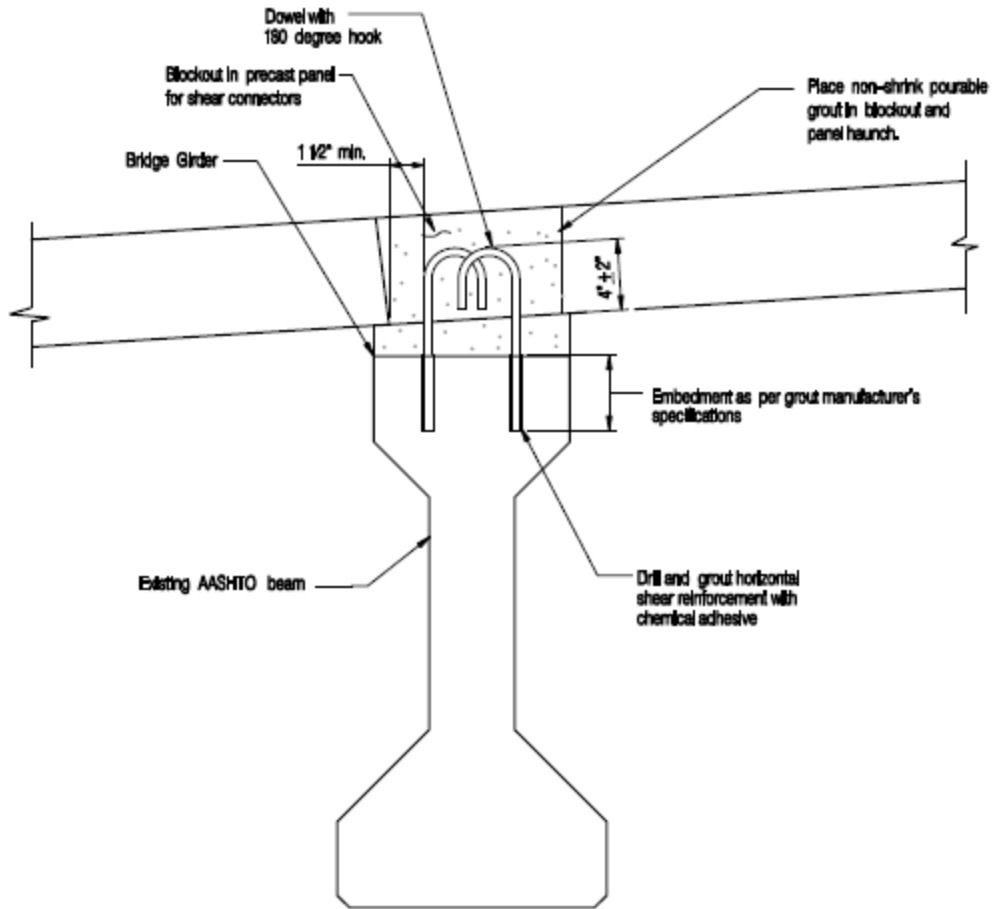
Report Number PCINER-11-FDDP | Date Issued April 26, 2011



**TYPICAL SECTION - BULB TEE BEAMS**

**NEW CONSTRUCTION WITH PROJECTING REINFORCING CONNECTION**

**Bulb Tee Beam Attachment  
Details 2  
Detail FDDP - 9**

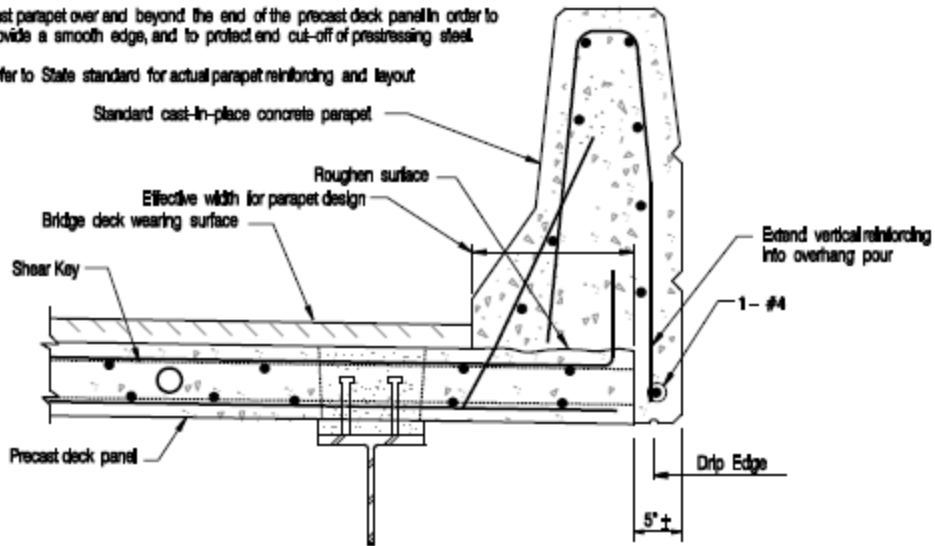


**TYPICAL SECTION – EXISTING AASHTO BEAMS**

**DECK REPLACEMENT**

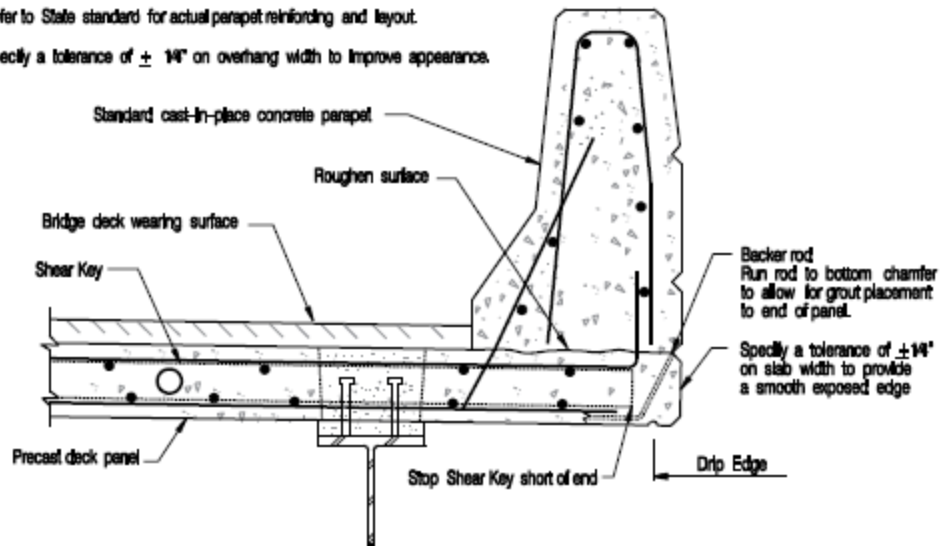
**Deck Replacement  
Attachment Details  
Detail FDDP – 10**

NOTES: Cast parapet over end beyond the end of the precast deck panel in order to provide a smooth edge, and to protect end cut-off of prestressing steel.  
Refer to State standard for actual parapet reinforcing and layout



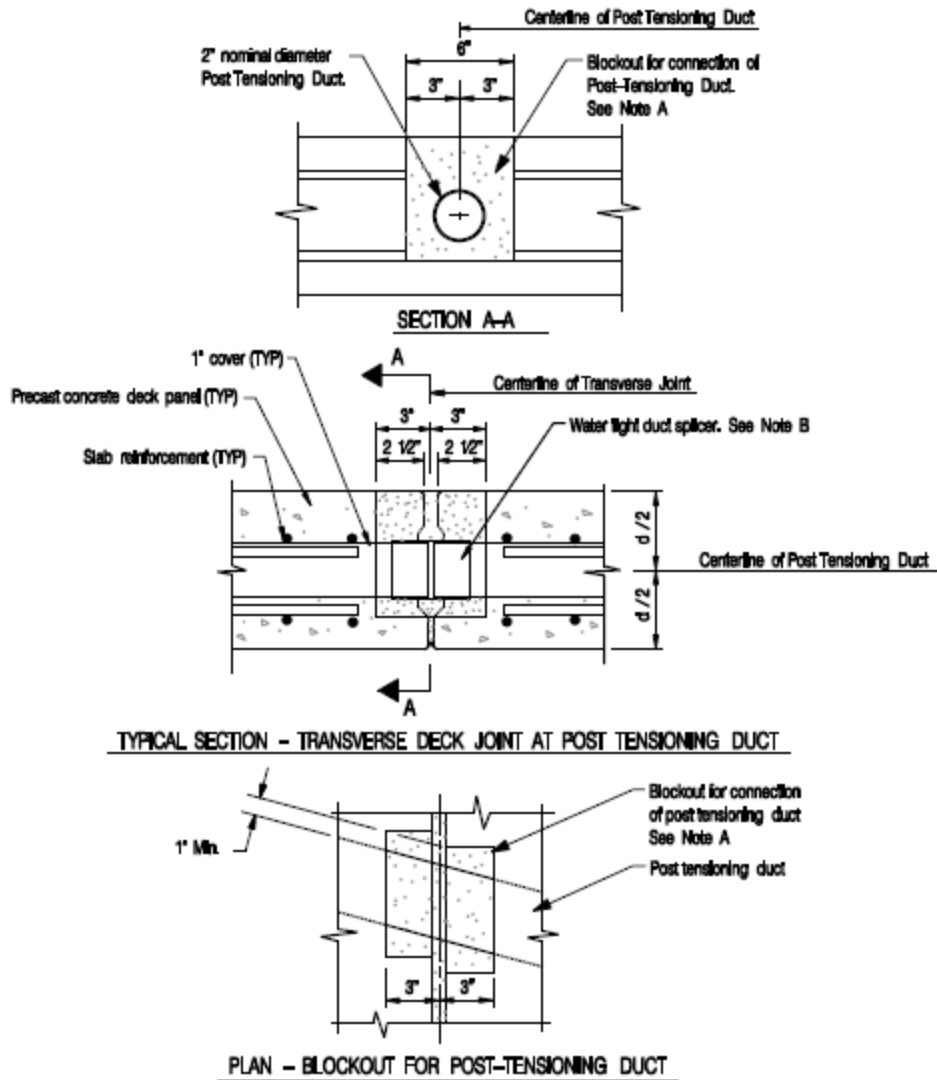
TYPICAL SECTION - PARAPET DETAILS COVERING EDGE

NOTES: Refer to State standard for actual parapet reinforcing and layout.  
Specify a tolerance of  $\pm 1/4"$  on overhang width to improve appearance.



TYPICAL SECTION - PARAPET DETAILS WITH EXPOSED EDGE

Deck Overhang & Parapet Details  
Detail FDDP - 11

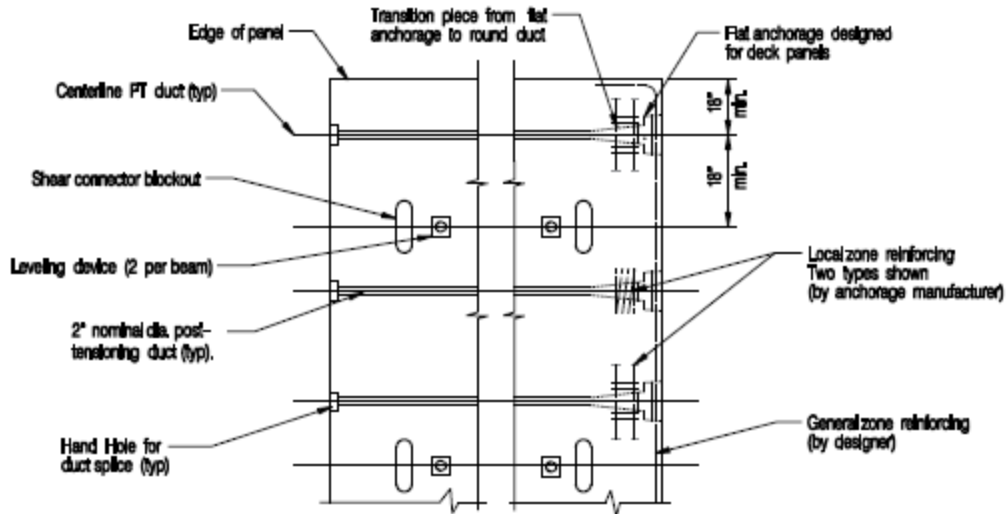


**Note A:** Fill handhole with non-shrink grout simultaneously with the transverse shear keys.

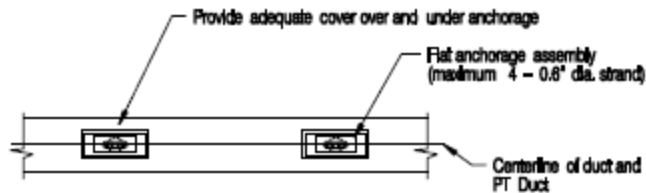
**Note B:** Add the following note to the plans:  
 It is of extreme importance to make these connections 100% water-tight in order to prevent mortar entering the post-tensioning ducts when it is placed in the transverse joints as well as to avert mortar from escaping the ducts during their subsequent grouting with mortar.

**Post Tensioning Duct Details  
 Detail FDDP - 12**

Note: For short overhangs, the exterior duct may be omitted

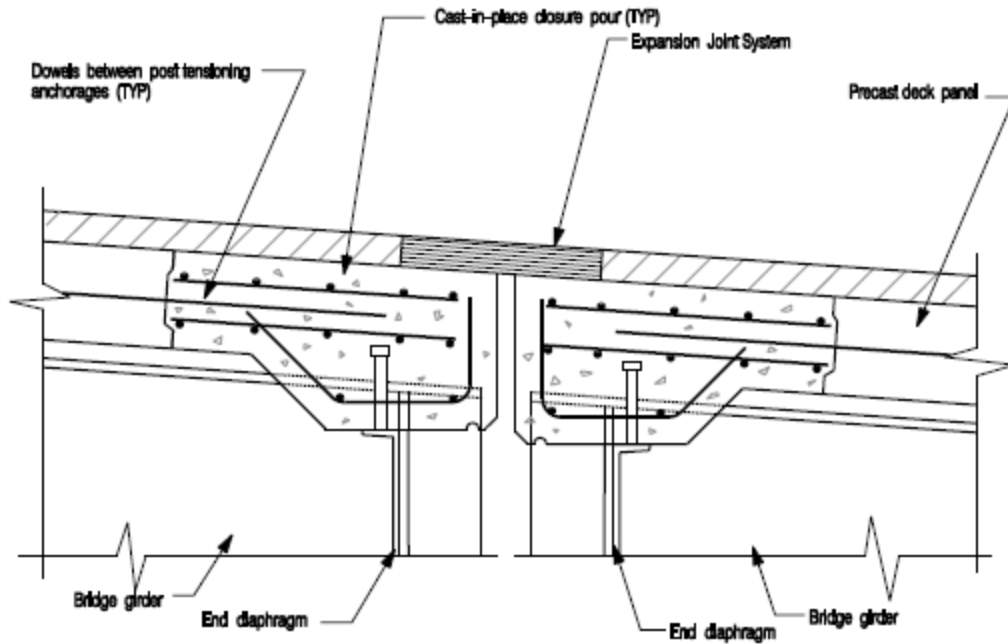


**PLAN - POST TENSION ANCHORAGE DETAILS**



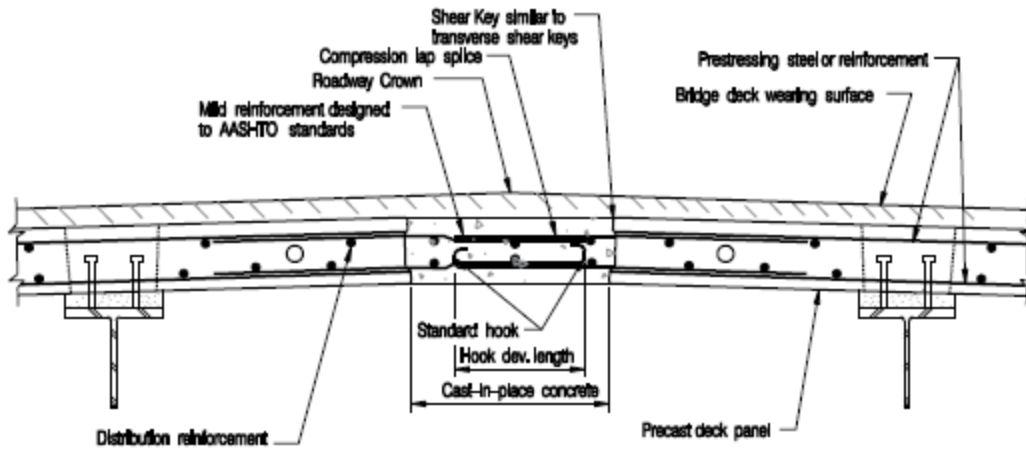
**END ELEVATION - POST TENSION ANCHORAGE DETAILS**

Post Tensioning Anchorage Details  
Detail FDDP - 13



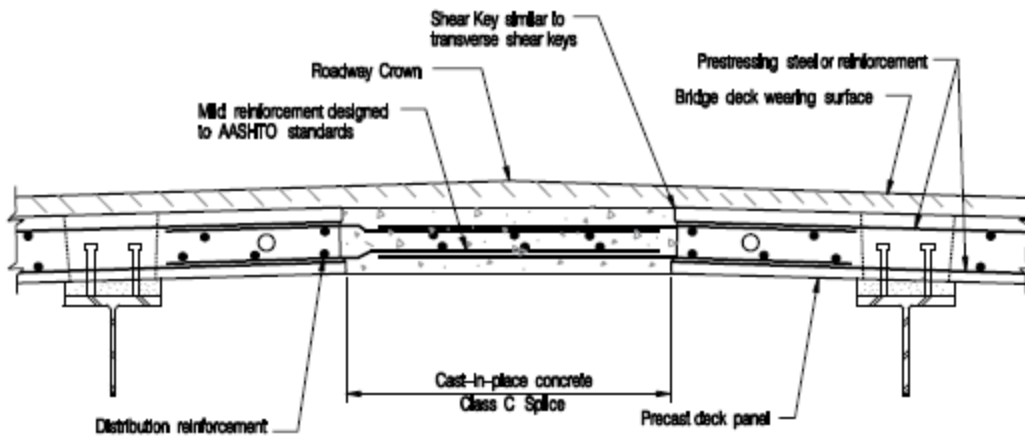
**TYPICAL SECTION – CLOSURE POURS AT DECK ENDS**

- NOTES: Closure pours shown at a pier. Closure pours at abutments similar.  
Closure pour details may vary based on design of bridge joint.  
Reinforcement for closure pours shall be designed by the engineer.



Note: Rotate hook bar to provide adequate top cover.

**TYPICAL SECTION – ROADWAY CROWN DETAILS WITH A NARROW CLOSURE POUR**



**TYPICAL SECTION – ROADWAY CROWN DETAILS WITH A LAP SPLICE**

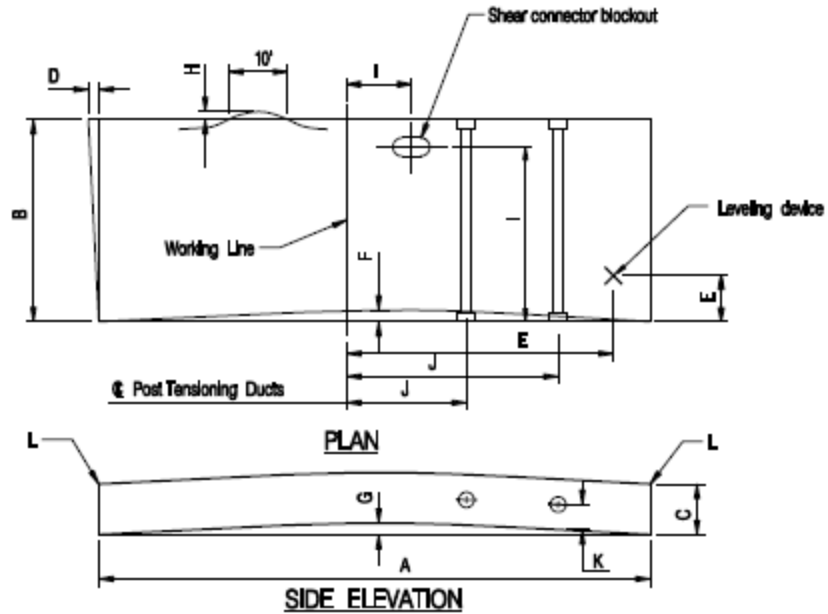
Notes: This closure pour can be used to adjust the horizontal location of panel to improve fit-up.  
Coordinate location of bars to avoid conflicts with lapped bars

Roadway Crown Detail  
Detail FDDP – 15



Report Number  
PCINER-11-FDDP

Date Issued  
April 26, 2011



ITEM	DESCRIPTION	RECOMMENDED TOLERANCE
A	LENGTH	$\pm 1/4"$
B	WIDTH	$\pm 1/4"$
C	DEPTH	$\pm 1/4"$
D	VARIATION FROM SPECIFIED PLAN SKEW	$\pm 1/4"$
E	LOCATION OF LEVELING DEVICE	$\pm 1"$
F	SWEEP	$\pm 3/8"$
G	CAMBER VARIATION FROM DESIGN CAMBER	$\pm 1/4"$
H	LOCAL SMOOTHNESS OF ANY SURFACE	1/4" IN 10 FEET
I	LOCATION OF SHEAR CONNECTOR BLOCKOUT	$\pm 1/2"$
J	DISTANCE FROM COMMON WORKING POINT TO $\phi$ OF ANY PT DUCT	$\pm 3/16"$
K	$\phi$ OF PT DUCT AT EDGE OF SLAB MEASURED FROM PANEL BOTTOM	$\pm 3/16"$
L	DEVIATION FROM SPECIFIED ELEVATION	$\pm 1/8"$

Note: Owners may allow contractors to deviate from the recommended tolerances provided that the contractor can properly install the panels within the overall bridge limits.

**Recommended Tolerances  
Detail FDDP - 16**

## Specifications Appendix B (Design Example)

### **ACKNOWLEDGEMENT**

This example was originally developed by the following team of George Washington University, Washington D.C.: Sameh S. Badie, Ph.D., PE, Associate Professor, Nghi Nguyen, D.Sc., and Parul Patel, M.Sc., Former Graduate Students.

The prestress loss calculations were updated according to the 2008 Interim Revisions to the *LRFD Specifications* by Sameh S. Badie, Ph.D., PE, Associate Professor, George Washington University, and Kromel Hanna, Ph.D., Post-Doctoral Associate, University of Nebraska-Lincoln.

### **DESIGN EXAMPLE OUTLINE**

#### D.1 DESIGN CRITERIA

#### D.2 DESIGN OF THE PRECAST DECK PANEL SYSTEM

##### D.2.1 Design of the Positive Moment Areas between Girder Lines

###### D.2.1.1 Estimate Required Prestress Force

###### D.2.1.2 Estimate Prestress Losses

###### D.2.1.3 Check of Concrete Stresses at Service Loads at the Positive Moment Area

###### D.2.1.4 Check of flexural strength

###### D.2.1.5 Check of maximum reinforcement limit

###### D.2.1.6 Check of Minimum Reinforcement Limit

##### D.2.2 Design of Panel-to-Girder Connection for Full Composite Action

##### D.2.3 Design of the Negative Moment Areas over Interior Girder Lines

##### D.2.4 Design of the Overhang (negative moment section at exterior girder line)

###### D.2.4.1 Case I: Due to Transverse Vehicular Collision Loads Using Extreme Event Limit State II

###### D.2.4.2 Case 2: Due Dead and Live Loads

##### D.2.5 Design of Longitudinal Reinforcement

##### D.2.6 Miscellaneous Design Issues

###### D.2.6.1 Check of Concrete Stresses at Time of Transferring the Prestressing Force

###### D.2.6.2 Check of Concrete Stresses during Lifting the Panel from the Prestressing Bed

#### D.3 DETAILS OF THE PRECAST DECK PANEL SYSTEM

## D.1 DESIGN CRITERIA

Design specifications AASHTO *LRFD Specifications* (2008 Interim Revisions)

Bridge type Single span, slab/girder system

Span length 120 ft

Total width 44 ft (two-lane, undivided two-way bridge)

Superstructure Four steel girders spaced at 12 ft with top flange width of the steel girders = 12 in. with a 4 ft cantilever at each end for support of side barriers.

OR

Four BT-72 recast, prestressed concrete girders space at 12 ft.

Deck slab Precast prestressed full-depth concrete panel system

Structural slab thickness = 8 in.

- Article 9.7.5.1 of the *LRFD Specifications* states that the depth of a precast concrete slab excluding any provisions for grinding, grooving, and sacrificial surface, should not be less than 7.0 in.
- Minimum clear concrete cover on top and bottom reinforcement shall be in accordance with the provisions of Article 5.12.3 of *LRFD Specifications*, which are 2.0 and 1.0 in., respectively.

Panel dimensions: 44 ft × 8 ft × 8 in. thick

Geometrical properties of the panel cross section:

$$A = (8 \text{ in.})(8 \text{ ft})(12 \text{ in./ft}) = 768 \text{ in}^2$$

$$I = \frac{(8 \times 12)(8^3)}{12} = 4096 \text{ in}^4$$

$$S_b = S_t = \frac{(8 \times 12)(8^2)}{6} = 1024 \text{ in}^3$$

Concrete properties:

Normal weight concrete, density = 0.150 kcf

Concrete compressive strength at 28-day,  $f'_c = 6.0$  ksi

$E_c$  = modulus of elasticity of panel at 28 days [*LRFD Specifications* 5.4.2.4]

$$= 33,000(0.150)^{1.5} \sqrt{6.0} = 4696 \text{ ksi} \text{ [LRFD Eq. 5.4.2.4-1]}$$

Concrete strength at release,  $f'_{ci} = 5.0$  ksi

$E_{ci}$  = modulus of elasticity of slab at release

$$= 33,000(0.150)^{1.5} \sqrt{5.0} = 4287 \text{ ksi}$$

Reinforcement type: The precast panel system is transversely pretensioned and longitudinally post-tensioned

Pretensioning reinforcement:

½ in. diameter, 270 ksi, low relaxation, 7 wire strands

Prestress force is released at 1 day

$E_p$  = modulus of elasticity of prestressing strands = 28,500 ksi

Ultimate tensile strength  $f_{pu} = 270$  ksi

Yield strength  $f_{py} = 0.9 f_{pu} = 0.9 \times 270 = 243$  ksi

Initial prestress just before detensioning the strands =

$$0.75 f'_{pu} = (0.75)(270) = 202.5 \text{ ksi}$$

Post-tensioning reinforcement:

1 in. diameter high strength rods, 150 ksi

Conventional reinforcement:

ASTM A615 Grade 60

Curing: Relative humidity ( $H$ ) = 70%

Steam curing for 1 day

Shear pockets are filled with a non-shrink grout that yields  $f'_c = 6.0$  ksi

Composite system: The precast panel is made composite with the supporting girders. Two cases are considered as follows:

1. Steel girders; where composite action is created by welding 1¼ in. diameter steel studs on the top surface of the girders. The studs are embedded in the panel in prefabricated shear pockets.

Shear studs used in composite steel bridge construction are typically ¾ in. or 1 in. in diameter. A recent development is the 1¼ in. diameter studs.<sup>47, 48</sup> The 1¼ in. diameter stud has about twice the strength of a ¾ in. diameter stud and higher fatigue capacity. Using the 1¼ in. diameter studs will result in the following benefits:

- reduced labor as fewer studs will be welded
  - higher construction speed
  - reduced possibility of damage to the studs and the top flange of the girder during future deck removal
  - smaller shear pockets and lesser amount of grouting material
2. Concrete girders: The web shear reinforcement is extended into the deck as shear connectors.

Time of installation of the precast deck panels on the supporting girders

= 90 days.

Future wearing surface: 2 in. of concrete wearing surface, 0.150 kcf

Side barriers: NJ Barriers, 420 plf, the barrier is 16 in. wide at bottom and 42 in. high. The center of gravity of the barrier is at 5.2 in. from the exterior face.

## **D.2 DESIGN OF THE PRECAST DECK PANEL SYSTEM**

In order to develop the precast deck panel system, the following elements of the system need to be designed in the following order:

1. Design of the positive moment areas between girder lines
2. Design of the panel-to-girder connection for full composite action
3. Design of the negative moment areas over interior girder lines
4. Design of overhang part of the panel
5. Design of the longitudinal reinforcement
6. Miscellaneous issues

Final details of the precast deck panel system are given in **Figures D.2.4.1-1 to D.3-5**.

### **D.2.1 Design of the Positive Moment Areas between Girder Lines**

Article 4.6.2.1.1 of the *LRFD Specifications* states that the deck slab can be analyzed by subdividing it into strips perpendicular to the supporting girders. This method is called the "Strip Method." Also, Article 4.6.2.1.1 states that wherever the strip method is used, the extreme positive moment in any section between girder lines shall be taken to apply to all positive moment regions. Similarly, the extreme negative moment over any interior girder line shall be taken to apply to the negative moment regions at all interior girder lines.

The deck slab is then analyzed as a continuous beam supported by the girders. The girders are considered as rigid supports with zero settlement and their width is taken equal to zero.

#### Loads applied on the deck slab:

A 12-in. wide strip is considered in the following calculations.

*DC:* Dead loads due to:

Panel self weight =  $(8/12)(0.150) = 0.100$  k/ft<sup>2</sup> (uniformly distributed load)

Barrier self weight = 0.420 k/ft/side (concentrated load)

*DW:* Dead load due to:

2 in. concrete wearing surface =  $(2/12)(0.150) = 0.025$  k/ft<sup>2</sup>

*LL:* Live load HL-93 due to truck load and lane load with dynamic allowance and multipresence factor

#### Design Limit States and Load Factors (2008 Interim Revisions 3.4.1):

##### 1. STRENGTH I:

Strength I limit state shall be taken to ensure that strength and stability, both local and global, are provided to resist the specified statically significant load combination relating to the normal vehicular use of the bridge without wind.

*DC:* Minimum = 0.90, Maximum = 1.25

*DW:* Minimum = 0.65, Maximum = 1.50

*LL:* 1.75

2. SERVICE I:

Service I limit state shall be used for checking deflection and to control crack width in reinforced concrete structures.

*DC*: 1.00

*DW*: 1.00

*LL*: 1.00

3. SERVICE III:

Service III limit state shall be used for checking tension in prestressed concrete structures with the objective of crack control. (2008 Interim Revisions 3.4.1)

*DC*: 1.00

*DW*: 1.00

*LL*: 0.80

Figure D.2-1 shows the service load moment due to *DC* and *DW* for a 1 ft strip.

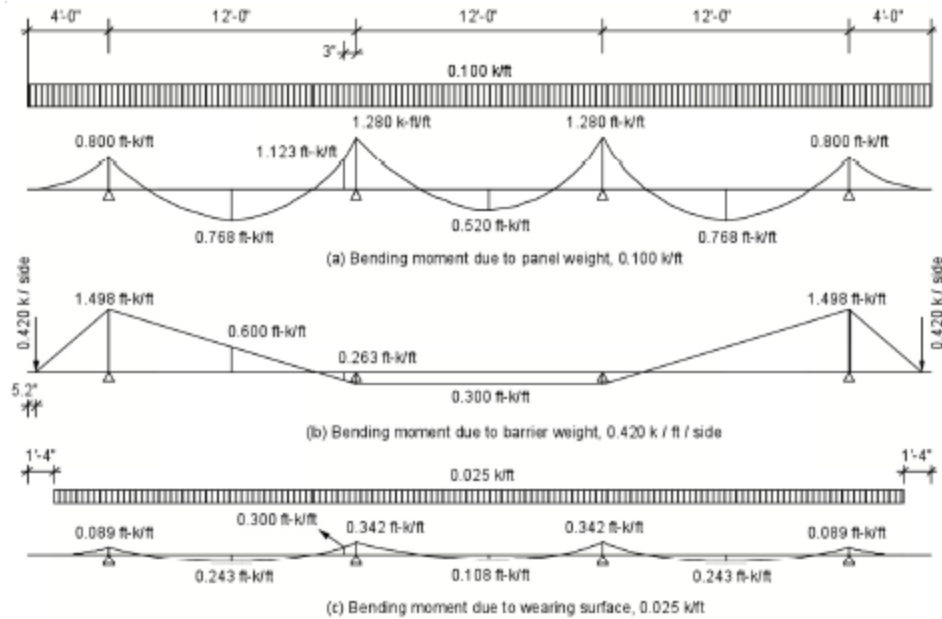


Figure D.2-1. Service load bending moment.

### D.2.1.1 Estimate Required Prestress Force

Assume that the tensile stresses at SERVICE III limit state at bottom surface of the panel,  $f_b$ , controls the design. The strand group is made concentric with the panel cross-section in order to avoid having the panel deflected upward or downward after releasing of the prestress force, i.e. strand eccentricity  $e_p = \text{zero}$ , therefore:

$$f_b = \frac{P_{pe}}{A} - \frac{(M_{SERVICE\ III})}{S_b}$$

Investigation of the bending moment (**Figure D.2-1**) shows that the midspan section of the center span controls the design, where:

$$\text{Panel wt. (DC)} \quad M_{panel} \quad = 0.520 \text{ ft-kip/ft}$$

$$\text{Barrier wt. (DC)} \quad M_{barrier} \quad = 0.300 \text{ ft-kip/ft}$$

$$\text{Wearing surface (DW)} \quad M_{ws} \quad = 0.108 \text{ ft-kip/ft}$$

Moment due to live load can be determined using the equivalent strip on which the wheels of the 32-kip axle of the design truck will be used. In this case, various combinations of one, two or three trucks with the proper multi-presence factor should be considered to get the maximum moment effects. However, Table A4-1 of the *LRFD Specifications* gives the maximum moment effect based on girder spacing.

Refer to Articles 3.6.1.3.3, 4.6.2.1.2 and Appendix A4 of the *LRFD Specifications*.

Live load,  $M_{LL+IM} = 8.01 \text{ ft-kips/ft}$

Therefore, at SERVICE III limit state:

$$\begin{aligned} M_{SERVICE\ III} &= 1.0 M_{DC} + 1.0 M_{DW} + 0.8 M_{LL+IM} \\ &= 1.0 (0.520 + 0.3) + 1.0 (0.108) + 0.8 (8.01) \\ &= 7.336 \text{ ft-kips/ft} \\ &= (7.336 \text{ ft-kips/ft}) (8 \text{ ft/panel}) \\ &= 58.688 \text{ ft-kips/panel} \end{aligned}$$

Assume  $\frac{1}{2}$  in. diameter, seven-wire, 270 ksi, low relaxation strands are used

Initial prestress just before detensioning the strands  $= 0.75f_{pu} = (0.75)(270) = 202.5 \text{ ksi}$

Assume that the total prestressed losses (i.e. elastic shortening, creep, shrinkage, and prestress loss) at service = 10%. Therefore, the effective prestress in the strands at service,  $f_{pe} = (202.5 \text{ ksi}) (1-0.10) = 182.250 \text{ ksi}$

Effective prestress force  $P_{pe} = A_{pe} (182.250) \text{ kips/strand}$

Allowable tensile stress in pretensioned members, for components with bonded prestressing tendons or reinforcement that are subjected to not worse than moderate corrosion conditions, (*LRFD Specifications 5.9.4.2*)

$$= 0.19\sqrt{f'_c} = 0.19\sqrt{6.0} = 0.465 \text{ ksi}$$

The tensile stress at bottom fiber of the section at SERVICE III limit state is:

$$-0.465 = \frac{P_{pe}}{768} - \frac{(58.688)(12)}{1024}$$

$P_{pe} = 171.072$  kips =  $n$  (0.153 in<sup>2</sup>/strand) (182.250 ksi), where  $n$  = number of strands per panel

Therefore,  $n = 6.135$  strands

Try (8) ½-in. diameter, 270 ksi strands per panel, placed on two layers, four strands per layer. For each layer, provide 2 in. clear concrete cover to satisfy the minimum clear concrete cover requirements of Article 5.12.3 of the *LRFD Specifications*.

Since this estimate is based on only satisfying the service tensile stresses in concrete and on estimated prestress losses, the following steps are required to finalize the design of the maximum positive moment section:

1. Determine the exact prestress losses
2. Check concrete stresses
3. Check flexural capacity
4. Check reinforcement limits

### D.2.1.2 Estimate Prestress Losses

*LRFD Specifications* provides two methods to calculate the prestress losses, which are the approximate method (Article 5.9.5.3) and the refined method (Article 5.9.5.4). The refined method is used here as it provides a more accurate measure of prestress losses.

Total prestress losses is:

$$\Delta f_{pT} = \Delta f_{pES} + \Delta f_{pLT} \quad \text{[LRFD Eq. 5.9.5.1-1]}$$

Where,

$\Delta f_{pES}$  = sum of all losses or gains due to elastic shortening

$\Delta f_{pLT}$  = losses due to long-term shrinkage and creep of concrete, and relaxation of steel

$$= (\Delta f_{pSR} + \Delta f_{pCR} + \Delta f_{pR1})_{id} + (\Delta f_{pSD} + \Delta f_{pCD} + \Delta f_{pR2})_{af} \quad \text{[LRFD Eq. 5.9.5.4.1-1]}$$

$(\Delta f_{pSR} + \Delta f_{pCR} + \Delta f_{pR1})_{id}$  = sum of time-dependent losses between transfer and deck placement

$(\Delta f_{pSD} + \Delta f_{pCD} + \Delta f_{pR2})_{af}$  = sum of time-dependent losses after deck placement (to final age)

Article 5.9.5.4.4 of the *LRFD Specifications* states that for precast elements with no topping, which is the case for full-depth precast deck panel systems, the value for time of “deck placement” may be taken as the value of time of installation of the precast element. In this example, the time of installation of the precast deck is taken 90 days, and the final age is taken 75 years (27,375 days).

The following losses are from transfer to time of installation of the precast deck:

$\Delta f_{pSR}$  = prestress loss due to shrinkage of concrete

$\Delta f_{pCR}$  = prestress loss due to creep of concrete

$\Delta f_{pR1}$  = prestress loss due to relaxation of steel

The following losses are from time of installation of the precast deck to final age:

$\Delta f_{pSD}$  = prestress loss due to shrinkage of concrete

$\Delta f_{pCD}$  = prestress loss due to creep of concrete

$\Delta f_{pR2}$  = prestress loss due to relaxation of steel

The gross section area of the concrete section is used in the prestress losses calculations.

**Elastic shortening loss:**

$$\Delta f_{pES} = (E_p / E_{ci}) f_{cgp} \quad \text{[LRFD Eq. 5.9.5.2.3a-1]}$$

Where,

$E_p$  = modulus of elasticity of prestressing strands = 28,500 ksi

$f'_{ci}$  = concrete strength at release = 5.0 ksi

$E_{ci}$  = modulus of elasticity of panel at transfer = 4287 ksi (Note that  $E_{ci}$  is the same as  $E_c$ )

$f_{cgp}$  = the concrete stress at the center of gravity of the prestressing strands due to the prestressing force immediately after transfer and self-weight of the member at the section of maximum moment.

The Commentary to Article 5.9.5.2.3a of the *LRFD Specifications* states that  $f_{cgp}$  may be assumed to be 90 percent of the initial prestress before transfer and the analysis iterated until acceptable accuracy is achieved. However, in this example, 1% initial loss is assumed and then checked later.

Strand stress immediately after release = 202.5 (1.00-0.01) = 200.475 ksi

Since the strand group is concentric with the panel cross section,  $f_{cgp} = \frac{P_i}{A}$

$P_i$  = total prestressing force at release = (8 strands)(0.153 in<sup>2</sup>/strand)(200.475 ksi) = 245.38 kips

$$f_{cgp} = \frac{245.381}{768} = 0.320 \text{ ksi}$$

Therefore, loss due to elastic shortening:

$$\Delta f_{pES} = \frac{28,500}{4,287} (0.320) = 2.127 \text{ ksi}$$

$$\text{Initial prestress loss} = \frac{2.127}{202.5} \times 100 = 1.05\%$$

The initial prestress loss is very close to the assumed value, so a second iteration is not necessary.

**Time-dependent losses between transfer and time of deck installation:**

Shrinkage of concrete loss:

$$\Delta f_{pSR} = \epsilon_{bid} E_p K_{id} \quad [\text{LRFD Eq. 5.9.5.4.2a-1}]$$

Where,  $\epsilon_{bid}$  = concrete shrinkage strain of panel between transfer and deck placement

$$\epsilon_{bid} = k_s \cdot k_{hs} \cdot k_f \cdot k_{td} \cdot (0.48 \times 10^{-3}) \quad [\text{LRFD Eq. 5.4.2.3.3-1}]$$

$k_s$  = factor for effect of the volume-to-surface ratio of the component

$$= 1.45 - 0.13(V/S) \geq 1.000 \quad [\text{LRFD Eq. 5.4.2.3.2-2}]$$

$$\text{Where } (V/S) = \text{volume-to-surface ratio (in.)} = \frac{(8)(8)(12)}{2[8 + (8)(12)]} = 3.692 \text{ in.}$$

$$k_s = 1.45 - 0.13(3.692) = 0.970 < 1.000, \text{ therefore use } k_s = 1.000$$

$$k_{hs} = \text{humidity factor for shrinkage} = (2.00 - 0.014H) \quad [\text{LRFD Eq. 5.4.2.3.3-2}]$$

Where  $H$  = relative humidity (assume 70%)

Relative humidity varies significantly from one area of the country to another; see **Figure 5.4.2.3.3-1** in the *LRFD Specifications*.

$$k_{hs} = 2.00 - 0.014(70) = 1.020$$

$$k_f = \text{factor for the effect of concrete strength} = \frac{5}{1 + f'_{ci}} \quad [\text{LRFD Eq. 5.4.2.3.2-4}]$$

$$k_f = \frac{5}{1 + 5} = 0.833$$

$$k_{td} = \text{time development factor} = \frac{t}{61 - 4f'_{ci} + t} \quad [\text{LRFD Eq. 5.4.2.3.2-5}]$$

Where  $t$  = maturity of concrete, defined as age of concrete between time of loading for creep calculations, or end of curing for shrinkage calculations, and time being considered for analysis of creep or shrinkage effects = 90 - 1 = 89 days

$$k_{td} = \frac{89}{61 - 4(5) + 89} = 0.685$$

$$\epsilon_{bid} = (1.000)(1.020)(0.833)(0.685)(0.48 \times 10^{-3}) = 2.794 \times 10^{-4}$$

$K_{id}$  = transformed section coefficient that accounts for time-dependent interaction between concrete and bonded steel in the section being considered for the time period between transfer and deck placement

$$K_{id} = \frac{1}{1 + \frac{E_p}{E_{ci}} \frac{A_{ps}}{A_g} \left( 1 + \frac{A_g e_{pg}^2}{I_g} \right) [1 + 0.7\psi_b(t_f, t_i)]} \quad [\text{LRFD Eq. 5.9.5.4.2a-2}]$$

Where,

$e_{pg}$  = eccentricity of prestressing force = zero

$\psi_b(t_f, t_i)$  = creep coefficient at final time due to loading introduced at transfer

$$= (1.9) k_s \cdot k_{hc} \cdot k_f \cdot k_{td} \cdot t_i^{-0.118} \quad [\text{LRFD Eq. 5.4.2.3.2-1}]$$

$t_f$  = final age = 27,375 days

$t_i$  = age at transfer = 1 day

$$k_{hc} = \text{humidity factor for creep} = (1.56 - 0.008f) \quad [\text{LRFD Eq. 5.4.2.3.2-3}]$$

$$= 1.56 - 0.008(70) = 1.000$$

$$k_{td} = \text{time development factor} = \frac{t}{61 - 4f'_{ci} + t} \quad [\text{LRFD Eq. 5.4.2.3.2-5}]$$

$$= \frac{(27,375 - 1)}{61 - 4(5) + (27,375 - 1)} = 0.999$$

$$\psi_b(t_f, t_i) = (1.9)(1.000)(1.000)(0.833)(0.999)(1)^{-0.118} = 1.581$$

$$k_{td} = \frac{1}{1 + \left(\frac{28,500}{4287}\right) \left(\frac{8(0.153)}{768}\right) (1+0) [1 + 0.7(1.581)]} = 0.978$$

$$\Delta f_{pSR} = (2.794 \times 10^{-4})(28,500)(0.978) = 7.788 \text{ ksi}$$

Creep of concrete loss:

$$\Delta f_{pCR} = \frac{E_p}{E_{ci}} \cdot f_{cp} \cdot \psi_b(t_d, t_i) \cdot K_{td} \quad [\text{LRFD Eq. 5.9.5.4.2b-1}]$$

$$\psi_b(t_d, t_i) = \text{creep coefficient} = (1.9) k_s \cdot k_{hc} \cdot k_f \cdot k_{td} \cdot t_i^{-0.118} \quad [\text{LRFD Eq. 5.4.2.3.2-1}]$$

$$= (1.9)(1.000)(1.000)(0.833)(0.685)(1)^{-0.118} = 1.084$$

$$\Delta f_{pCR} = \left(\frac{28,500}{4287}\right) (0.320)(1.084)(0.978) = 2.255 \text{ (ksi)}$$

Relaxation of strands loss:

$$\Delta f_{pRI} = \frac{f_{pr}}{K_L} \left( \frac{f_{pr}}{f_{py}} - 0.55 \right) \quad [\text{LRFD Eq. 5.9.5.4.2c-1}]$$

Where:

$f_{pr}$  = stress in prestressing strands immediately after transfer, taken not less than  $0.55f_{py}$

$$= 202.5 - 2.127 = 200.373 \text{ ksi} > 0.55(243) = 133.650 \text{ ksi}$$

$K_L$  = 30 ksi for low relaxation strands

$$\Delta f_{pRI} = \frac{200.373}{30} \left( \frac{200.373}{243} - 0.55 \right) = 1.834 \text{ (ksi)}$$

**Time-dependent losses between time of installation of the precast deck and final age:**

Shrinkage of concrete loss:

$$\Delta f_{pSD} = \epsilon_{bdf} E_p K_{df} \quad [\text{LRFD Eq. 5.9.5.4.3a-1}]$$

Where,  $\epsilon_{bdf}$  = concrete shrinkage strain of panel between deck installation and final age

$$= \epsilon_{bjf} - \epsilon_{bid}$$

$\epsilon_{bjf}$  = concrete shrinkage strain of panel between initial and final age

$$\epsilon_{bjf} = k_s \cdot k_{hs} \cdot k_f \cdot k_{td} (0.48 \times 10^{-3}) \quad [\text{LRFD Eq. 5.4.2.3.3-1}]$$

$$k_s = 1.000 \text{ (from above)} \quad [\text{LRFD Eq. 5.4.2.3.2-2}]$$

$$k_{hs} = 1.020 \text{ (from above)} \quad [\text{LRFD Eq. 5.4.2.3.3-2}]$$

$$k_f = 0.833 \text{ (from above)} \quad [\text{LRFD Eq. 5.4.2.3.2-4}]$$

$$k_{td} = \text{time development factor} = \frac{t}{61 - 4 f'_{ci} + t} \quad [\text{LRFD Eq. 5.4.2.3.2-5}]$$

Where  $t$  = maturity of concrete, defined as age of concrete between time of loading for creep calculations, or end of curing for shrinkage calculations, and time being considered for analysis of creep or shrinkage effects  
 $= 27,375 - 1 = 27,374$  days

$$K_{td} = \frac{27,374}{61 - 4(5) + 27,374} = 0.999 \text{ (same as above)}$$

$$\epsilon_{bjf} = (1.000)(1.020)(0.833)(0.999)(0.48 \times 10^{-3}) = 4.074 \times 10^{-4}$$

$$\epsilon_{bdf} = \epsilon_{bjf} - \epsilon_{bid} = 4.074 \times 10^{-4} - 2.794 \times 10^{-4} = 1.280 \times 10^{-4}$$

$K_{df}$  = transformed section coefficient that accounts for time-dependent interaction between concrete and bonded steel in the section being considered for the time period between deck installation and final time

$$K_{df} = \frac{1}{1 + \frac{E_p}{E_{ci}} \frac{A_{ps}}{A_c} \left( 1 + \frac{A_c e_{pc}^2}{I_c} \right) [1 + 0.7 \psi_s(t_f, t_i)]} \quad [\text{LRFD Eq. 5.9.5.4.2a-2}]$$

Where,

$A_c$  = gross area of the composite section

$e_{pc}$  = eccentricity of prestressing force with respect to the composite section

$I_c$  = Moment of inertia of the composite section

Since the precast panel has no composite topping,  $K_{df} = K_{td} = 0.978$

$$\Delta f_{pSD} = (1.280 \times 10^{-4})(28,500)(0.978) = 3.568 \text{ ksi}$$

Creep of concrete loss:

$$\Delta f_{pCD} = \frac{E_p}{E_c} \cdot f_{sp} \cdot \psi_b[(t_f, t_i) - \psi_b(t_d, t_i)] \cdot K_{df} + \frac{E_p}{E_c} \cdot \Delta f_{cd} \cdot \psi_b(t_f, t_d) \cdot K_{df} \quad [\text{LRFD Eq. 5.9.5.4.3b-1}]$$

Where  $\Delta f_{cd}$  = change of stresses at centroid of prestressing strands due to long-term losses between transfer and deck installation combined with deck weight and superimposed loads. Since the strand group is concentric with the panel cross section,  $\Delta f_{cd}$  = zero

$$\psi_b(t_f, t_i) = (1.9) k_s \cdot k_{hc} \cdot k_f \cdot k_{td} \cdot t_i^{-0.118} \quad [\text{LRFD Eq. 5.4.2.3.2-1}]$$

$$= (1.9)(1.000)(1.000)(0.833)(0.999)(1)^{-0.118} = 1.581$$

$$\psi_b(t_d, t_i) = (1.9) k_s \cdot k_{hc} \cdot k_f \cdot k_{td} \cdot t_i^{-0.118} \quad [\text{LRFD Eq. 5.4.2.3.2-1}]$$

$$= (1.9)(1.000)(1.000)(0.833)(0.685)(1)^{-0.118} = 1.084$$

$$\Delta f_{pCD} = \left( \frac{28,500}{4287} \right) (0.320)(1.581 - 1.084)(0.978) + (\text{zero}) = 1.034 \text{ (ksi)}$$

Relaxation of strands loss:

$$\Delta f_{pR2} = \Delta f_{pR1} = 1.834 \text{ ksi} \quad [\text{LRFD Eq. 5.9.5.4.3c-1}]$$

**Total losses at transfer (initial losses):**

$$\Delta f_{pES} = 2.127 \text{ ksi}$$

$$\text{Stress in tendons after transfer} = 202.5 - 2.127 = 200.373 \text{ ksi}$$

$$\text{Prestressing force immediately after transfer} = (200.373)(8)(0.153) = 245.257 \text{ kips}$$

**Total losses at final age (service):**

*Time-dependent losses,*

$$\Delta f_{pLT} = (\Delta f_{pSR} + \Delta f_{pCR} + \Delta f_{pR1})_{id} + (\Delta f_{pSD} + \Delta f_{pCD} + \Delta f_{pR2})_{df} \quad [\text{LRFD Eq. 5.9.5.4.1-1}]$$

$$= (7.788 + 2.255 + 1.834) + (3.568 + 1.034 + 1.834) = 18.313 \text{ ksi}$$

$$\text{Total prestress losses} = \Delta f_{pES} + \Delta f_{pLT} = 2.127 + 18.313 = 20.440 \text{ ksi}$$

$$\text{Stress in tendons after all losses, } f_{pe} = 202.5 - 20.440 = 182.060 \text{ ksi}$$

Check prestressing stress limit at service limit state: Table 5.9.3-1 of the *LRFD Specifications* states that  $f_{pe} \leq 0.8 f_{py}$ , therefore:

$$f_{pe} = 182.060 \text{ ksi} \leq 0.8 f_{py} = 0.8(243) = 194.4 \text{ ksi} \quad \mathbf{OK}$$

$$\text{Total prestress losses, \%} = \frac{(20.440)(100)}{(202.5)} = 10.094 \%$$

Since the calculated total prestress losses (10.094%) is close enough to the assumed total losses (10%) used in estimating the required number of strands, no refinement of the required number of strands is done

Prestressing force at service,  $P_{pe} = (182.060)(8)(0.153) = 222.841$  kips

### D.2.1.3 Check of Concrete Stresses at Service at the Positive Moment Area

Prestressing force at service,  $P_{pe} = 222.841$  kips

Stress limits for concrete:

[LRFD Art. 5.9.4.2]

- Compression stress limits: at SERVICE I limit state:
  - Due to live load and 50% of the sum of effective prestress and permanent loads
 
$$= 0.40 f'_c = (0.40)(6.0) = + 2.4 \text{ ksi}$$
  - Due to sum of effective prestress and permanent loads
 
$$= 0.45 f'_c = (0.45)(6.0) = + 2.7 \text{ ksi}$$
  - Due to effective prestress, permanent loads, and transient loads
 
$$= 0.6 f'_c = (0.6)(6.0) = + 3.6 \text{ ksi}$$
- Tensile stress limits: For components with bonded prestressing tendons, limit state Service III

$$= -0.19\sqrt{f'_c} = -0.19\sqrt{6.0} = -0.465 \text{ ksi}$$

Concrete stress at the top fiber of the deck, SERVICE I:

Under permanent and transient loads, SERVICE I:

$$f_t = + \frac{P_{pe}}{A} + \frac{(M_{SERVICE I})}{S_t}$$

	Due to live load and 50% of the sum of effective prestress and permanent loads	Due to sum of effective prestress and permanent loads	Due to effective prestress, permanent loads, and transient loads
$M_{SERVICE I}$ =			
$(1.0)M_{DC}$ +	$(1.0)(0.520 + 0.3)(0.5) +$	$(1.0)(0.520 + 0.3) +$	$(1.0)(0.520 + 0.3) +$
$(1.0)M_{DW}$ +	$(1.0)(0.108)(0.5) +$	$(1.0)(0.108)$	$(1.0)(0.108)$
$(1.0)M_{LL+IM}$	$(1.0)(8.01)$		$+ (1.0)(8.01)$
	= 8.47 ft-kips/ft ×8 ft = 67.8 ft-kips/panel	= 0.93 ft-kips/ft ×8 ft = 7.44 ft-kips/panel	= 8.94 ft-kips/ft ×8 ft = 71.52 ft-kips/panel
$f_i$	$0.5 \left( \frac{222.841}{768} \right) + \frac{(67.8)(12)}{1024}$ + 0.940 ksi	$\frac{222.841}{768} + \frac{(7.44)(12)}{1024} =$ + 0.377 ksi	$\frac{222.841}{768} + \frac{(71.52)(12)}{1024} =$ + 1.128 ksi
Stress limit	+ 2.4 ksi	+ 2.7 ksi	+ 3.6 ksi
Check	O.K.	O.K.	O.K.

Concrete stress at the bottom fiber of the deck, SERVICE III:

$$f_b = \frac{P_{pe}}{A} - \frac{(M_{SERVICE III})}{S_b}$$

$M_{SERVICE III} = 58.688$  ft-k/panel (see Section D2.1-1 of this example)

$$f_b = \frac{222.841}{768} - \frac{(58.688)(12)}{1024} = -0.398 \text{ ksi}$$

Tensile stress limit: -0.465 ksi

**OK**

#### D.2.1.4 Check of Flexural Strength

Moment due to STRENGTH I Limit State (LRFD, Art. 3.4.1),

$$\begin{aligned}M_{STRENGTH I} &= 1.25 M_{DC} + 1.5 M_{DW} + 1.75 M_{LL+IM} \\ &= 1.25 (0.520 + 0.300) + 1.5 (0.108) + 1.75 (8.010) \\ &= 15.205 \text{ ft-kips/ft} \\ &\times 8 \text{ ft/panel} = 121.640 \text{ ft-kips/panel}\end{aligned}$$

The design procedure given by the *LRFD Specifications* (Art. 5.7.3.1.1) cannot be used with this case because the LRFD procedure assumes that the strand group is lumped at the center of gravity of the group. In this example, there are two layers of strands that are far away from each other, one layer is close to the top fiber and the second layer is close to the bottom layer. Therefore, the *LRFD Specifications* procedure will significantly under-estimate the flexural strength.

In this example, the flexural strength is determined using the strain compatibility approach and the power stress-strain formula for all types of reinforcement. The analysis procedure of the strain compatibility approach can be found in Section 8.2.2.5 of the *PCI Bridge Design Manual*.<sup>49</sup> The analysis uses an iterative process, where the stress in every layer of reinforcement is assumed and the depth of the equivalent compression block is determined based on the assumed values. Then, the stress in every layer of reinforcement is determined and checked against the assumed values. If the assumed and calculated values do not match, a second iteration is required using the values of the reinforcement stresses determined from the previous round of calculations.

Assume that net stress in the top and bottom layer of strands at ultimate is 243 ksi tension. Note that this value is chosen arbitrary and will be checked later.

From equilibrium of forces,  $T = C$

Where:  $T =$  Tension force in strands  $= A_{ps} (f_{ps})$

$C =$  Compression force in concrete  $= 0.85(f'_c)(b)(a)$

$b =$  Width of section  $= (8)(12) = 96 \text{ in.}$

$[(4)(0.153)(243)] + [(4)(0.153)(243)] = (0.85)(6)(96)(a)$

Depth of rectangular stress block,  $a = 0.608 \text{ in.}$

Distance from top of section to neutral axis,  $c = a/\beta_1$

$\beta_1 = 0.85 - 0.05(f'_c - 4) = 0.85 - 0.05(6 - 4) = 0.75$

$c = 0.608/0.75 = 0.811 \text{ in.}$

#### Check the assumed stresses in each layer of strands:

- *Top layer:*

Depth of top layer  $= 2.25 \text{ in.}$

Decompression stress,  $f_{ps} = 182.060 \text{ ksi (tension)}$

Decompression strain  $= \frac{182.060}{28,500} = 6.388 \times 10^{-3}$

$$\text{Total strain, } \epsilon_p = 0.003 \left( \frac{2.25 - 0.811}{0.811} \right) + 6.388 \times 10^{-3} = 5.323 \times 10^{-3} + 6.388 \times 10^{-3} = 11.711 \times 10^{-3}$$

Based on the power stress-strain formula developed by Devalapura and Tadros [Section 8.2.2.5 in the *PCI Bridge Design Manual*<sup>69</sup>]

$$f_{ps} = \epsilon_p E_p \left[ Q + \frac{(1-Q)}{\left\{ 1 + \left( \frac{E_p \epsilon_p}{K f_{py}} \right)^R \right\}^{1/R}} \right] \leq 270 \text{ ksi}$$

Where:

Q is a calibration factor used in the power equation.

$$f_{ps} = (11.711 \times 10^{-3})(28,500) \left[ 0.031 + \frac{(1-0.031)}{\left\{ 1 + \left( \frac{(28,500)(11.711 \times 10^{-3})}{(1.04)(243)} \right)^{7.36} \right\}^{1/7.36}} \right] = 251.223 \text{ ksi} < 270 \text{ ksi}$$

Therefore,  $f_{ps} = 251.223 \text{ ksi}$

- *Bottom layer:*

Depth of bottom layer = 5.75 in.

$$\epsilon_p = 0.003 \left( \frac{5.75 - 0.811}{0.811} \right) + 6.388 \times 10^{-3} = 18.270 \times 10^{-3} + 6.388 \times 10^{-3} = 24.658 \times 10^{-3}$$

$$f_{ps} = (24.658 \times 10^{-3})(28,500) \left[ 0.031 + \frac{(1-0.031)}{\left\{ 1 + \left( \frac{(28,500)(24.658 \times 10^{-3})}{(1.04)(243)} \right)^{7.36} \right\}^{1/7.36}} \right] = 266.653 \text{ ksi} < 270 \text{ ksi}$$

Therefore,  $f_{ps} = 266.653 \text{ ksi}$

Since the calculated stresses do not match the assumed values, a second round of calculations is required. In this round of calculations, assume that the stress at the top layer of strands = 251.223 ksi and at the bottom layer of strands = 266.653 ksi. This iterative process should be continued

until the calculated values match the assumed values. Results of the final round of calculations are as follow:

Depth of rectangular stress block,  $a = 0.644$  in.

Depth of the neutral axis,  $c = 0.859$  in

Strain in top layer of strands =  $11.250 \times 10^{-3}$  (tension)

Stress in top layer of strands = 249.579 ksi (tension)

Strain in bottom layer of strands =  $23.470 \times 10^{-3}$  (tension)

Since the total strain in this layer is  $> 0.005$ , the strength reduction factor according to Article 5.5.4.2.1 of the *LRFD Specifications* = 1.0

Stress in bottom layer of strands = 265.597 ksi (tension)

The flexural capacity of the section:

$$\begin{aligned}\phi M_n &= \phi \sum \left[ A_p(f_{ps}) \left( d_p - \frac{a}{2} \right) + A_s(f_s) \left( d_s - \frac{a}{2} \right) \right] \\ &= 1.0 \left[ (4)(0.153)(249.579) \left( 2.25 - \frac{0.644}{2} \right) + (4)(0.153)(265.597) \left( 5.75 - \frac{0.644}{2} \right) \right] \\ &= 1,176.777 \text{ in-kips/panel} \\ &= 98.065 \text{ ft-kips/panel} < M_{STRENGTH1} = 121.640 \text{ ft-kips/panel} \quad \mathbf{NG}\end{aligned}$$

- Since the flexural capacity is not safe, add two layers of Grade 60 bars. The first layer close to the top fiber of the section and the second layer close to the bottom fiber of the section. Each layer consists of 4 No. 5, Grade 60 steel, with a 2 in. clear concrete cover. Assume that the decompression stress in both layers = 25 ksi (compression). Using the strain compatibility procedure, results of the final round of calculations are as follows:

Depth of rectangular stress block,  $a = 0.906$  in.

Depth of the neutral axis,  $c = 1.208$  in.

Strain in top layer of strands =  $8.976 \times 10^{-3}$  (tension)

Stress in top layer of strands = 232.053 ksi (tension)

Strain in top layer of No. 5 bars =  $1.880 \times 10^{-3}$  (tension)

Stress in top layer of No. 5 bars = 54.546 ksi (tension)

Strain in bottom layer of strands =  $17.670 \times 10^{-3}$  (tension)

Since the total strain in this layer is  $> 0.005$ , the strength reduction factor according to Article 5.5.4.2.1 of the *LRFD Specifications* = 1.0

Stress in bottom layer of strands = 260.306 ksi (tension)

Strain in bottom layer of No. 5 bars =  $10.260 \times 10^{-3}$  (tension)

Stress in bottom layer of No. 5 bars = 60.000 ksi (tension)

The flexural capacity of the section:

$$\begin{aligned} \phi M_n &= 1.0 \left[ (4)(0.153)(232.053) \left( 2.25 - \frac{0.906}{2} \right) + (4)(0.153)(260.306) \left( 5.75 - \frac{0.906}{2} \right) \right] \\ &\quad + 1.0 \left[ (4)(0.31)(54.546) \left( 2.3125 - \frac{0.906}{2} \right) + (4)(0.31)(60) \left( 5.6875 - \frac{0.906}{2} \right) \right] \\ &= 1,614.171 \text{ in-kips/panel} \\ &= 134.514 \text{ ft-kips/panel} > M_{\text{STRENGTH1}} = 121.6 \text{ ft-kips/panel} \quad \mathbf{OK} \end{aligned}$$

#### D.2.1.5 Check of Maximum Reinforcement Limit (*LRFD Specifications 5.7.3.3.1*)

The maximum reinforcement limit is already incorporated in the strength reduction factor, as shown in Section D.2.1.4 of this example.

In editions of and interims to the *LRFD Specifications* prior to 2005, Article 5.7.3.3.1 limited the tension reinforcement quantity to a maximum amount such that the ratio ( $c/d_e$ ) did not exceed 0.42, where  $c$  = the neutral axis depth and  $d_e$  is effective depth of the steel reinforcement.

$$d_e = \frac{A_{ps}f_{ps}d_p + A_s f_y d_s}{A_{ps}f_{ps} + A_s f_y} = 4.0 \text{ in. (due to symmetry of reinforcement)}$$

$$\frac{c}{d_e} = \frac{1.208}{4.00} = 0.302 \leq 0.42 \quad \mathbf{OK}$$

### D.2.1.6 Check of Minimum Reinforcement Limit (LRFD Specifications 5.7.3.3.2)

Article 5.7.3.3.2 states that the amount of prestressed and nonprestressed tensile reinforcement shall be adequate to develop a factored flexural resistance,  $M_r$ , at least equal to  $1.2 M_{cr}$ , where:

$$M_{cr} = S_c(f_r + f_{cpe}) - M_{dnc} \left( \frac{S_c}{S_{nc}} - 1 \right) \quad [\text{LRFD Eq. 5.7.3.3.2-1}]$$

Where,

$S_c$  = section modulus for the extreme fiber of the composite section where tensile stress is caused by externally applied loads ( $\text{in}^3$ )

$S_{nc}$  = section modulus for the extreme fiber of the monolithic or non-composite section where tensile stress is caused by externally applied loads ( $\text{in}^3$ )

Since there is no composite topping,  $S_c = S_{nc} = 1024 \text{ in}^3$

$f_{cpe}$  = compressive stress in concrete due to effective prestress forces only (after allowance for all prestress losses) at extreme fiber of section where tensile stress is caused by externally applied loads (ksi) =  $\frac{222.841}{768} = 0.290 \text{ ksi}$

$f_r$  = Allowable tensile stress in pretensioned members (LRFD Table 5.9.4.2.2-1)

$$= 0.19\sqrt{f'_c} = 0.19\sqrt{6.0} = 0.465 \text{ ksi}$$

$M_{dnc}$  = total unfactored dead load moment

$$1.2 M_{cr} = 1.2 [ 1024 (0.465+0.290) - \text{zero} ] = 927.744 \text{ in-kips}$$

$$= 77.312 \text{ ft-kips}$$

$$< \phi M_n = 134.514 \text{ ft-kips} \quad \text{OK}$$

### D.2.2 Design of Panel-to-Girder Connection for Full Composite Action

Shear connectors that are fully anchored with the girder are extended into the deck panel to create full composite action between the deck panels and the girders. Typically, this is achieved by creating shear pockets in the panel over girder lines to accommodate the shear connectors. The shear connectors have to be clustered in groups to match the locations of these shear pockets. As a rule of thumb, the fewer the number of shear pockets that a precast panel has, the less expensive the panel will be due to savings on time and labor associated with forming of these pockets.

The *LRFD Specifications* do not provide any guidelines on the maximum spacing between the stud clusters. It has been a common practice to limit the maximum spacing to 24 in. based on the recommendations given by the LRFD specifications for shear connectors used with cast-in-place deck slabs. Recently, the idea of extending the maximum spacing to 48 in. for clustered studs has been investigated in the NCHRP 12-65.<sup>1</sup> The investigation has shown that extending the spacing between clusters of studs to 48 in. has no detrimental effect on the composite action. In this example, 48 in. spacing is considered.

In order to determine the size of the shear pockets of the precast panel, either for use with steel or precast concrete girders, it is required to determine the amount of shear connector reinforcement

that is required. Two cases are considered in this example: (1) steel girders, and (2) concrete girders.

More information on the design of cluster of studs at 48 in. can be found in references 50 and 51.

The calculations provided in this section are for illustration purposes only and are not to be used for all bridge projects. It is the responsibility of the design engineer to design the horizontal shear reinforcement in lieu of the design of the composite slab/girder system of the bridge being considered. Since the design parameters of the composite slab/girder system are not given in this example, an empirical approach, developed based on a parametric study conducted in NCHRP 12-41<sup>3</sup>, is used here to estimate the number and size of the required shear connectors.

#### Steel girder bridges:

As stated in the design criteria, 1¼ in. diameter studs<sup>46, 47</sup> are used as the shear connectors. The use of this large size studs is advantageous for precast deck panel systems because one 1¼ in. diameter stud replaces two 7⁄8 in. diameter studs, which will reduce the size of the shear pockets and the amount of grouting material needed to fill them.

In a study conducted in NCHRP 12-41,<sup>3</sup> the researchers conducted a parametric study for the horizontal shear requirement for a wide range of simply supported bridges, where the span length ranged from 40 to 130 ft and the girder spacing ranged from 6 to 12 ft. The researchers found that using 1¼ in. studs uniformly spaced at 6 in. throughout the span of the bridge would sufficiently satisfy the horizontal shear requirements.

Therefore, for the precast panel system in this example, if the clusters of studs are spaced at 48 in., each cluster will have (8) 1¼-in. studs. Using two studs per row, and the stud rows spaced at 6 in., the shear pocket will be 12 in. wide (in the transverse direction) and 24 in. long (in the longitudinal direction). Note, that the 6 in. stud spacing satisfies the LRFD specifications that set the minimum stud spacing to four times the stud diameter.

#### Concrete girder bridges:

For precast concrete girders, typically, the vertical shear reinforcement is extended above the top flange to provide the required horizontal shear reinforcement. The vertical shear reinforcement usually takes an L-shape or an inverted U-shape to provide for anchorage and fully develop the yield strength of the reinforcement. Although this detail provides an inexpensive way to provide for the composite action, it is not convenient for the production of the precast concrete girders. This is because the locations of the shear pockets have to be pre-determined, and only the shear reinforcement within these locations should extend outside the top flange. For this reason, it is recommended to separate the vertical shear reinforcement of the precast girder from the horizontal shear reinforcement required for full composite action. This can be done by providing for the horizontal shear reinforcement in the form of separate inverted U-shape bars that are installed only in the shear pocket locations.

To determine the amount of reinforcement required per shear pocket, the design examples provided in Chapter 9 of the PCI-Bridge Design Manual<sup>48</sup> were studied. Four design examples of slab/I-girder bridge systems are given in this reference, where the bridge structures range from simply supported span to three continuous span structures, with a span length up to 120 ft and girder spacing from 9 to 12 ft. Studying these examples reveals that the maximum horizontal factored shear force at the interface between the deck slab and the precast concrete girders is about 3.7 kip/in. of the girder length.

Therefore, the required horizontal nominal shear strength per panel

$$= 3.7(w)/\phi$$

Where  $\phi = 0.9$

$w$  = panel length

$$V_n = (3.7 \text{ kip/in.})(96 \text{ in.})/(0.9) = 395 \text{ kips}$$

The shear connector system consists of individual inverted No. 5 U-bars that are embedded in the top flange of the girder and extended into the panel shear pockets. The inverted U-bars are clustered at 48 in. This detail has been successfully used on bridges in Nebraska.

Using (6) No. 5 U-bars per pocket spaced at 7 in., two U-bars per row, the pocket will be 12 in. wide (in the transverse direction) and 24 in. long (in the longitudinal direction).

The nominal shear resistance of the interface plane is:

$$V_n = c A_{cv} + \mu (A_{vf} f_y + P_c) \quad \text{[LRFD Eq. 5.8.4.1-3]}$$

Where:

$c$  = cohesion factor = 0.24 ksi for concrete placed against clean, hardened concrete with surface intentionally roughened to an amplitude of 0.25 in. (LRFD Sect. 5.8.4.3)

$\mu$  = friction factor = 1.0 for concrete placed against clean, hardened concrete with surface intentionally roughened to an amplitude of 0.25 in. [LRFD Sect. 5.8.4.3]

$A_{cv}$  = area of concrete engaged in shear transfer

$$= (12 \text{ in.})(24 \text{ in.})(2 \text{ pockets}) = 576 \text{ in}^2$$

(Note: the width of the pocket has to be less than the width of the top flange of the concrete girder)

$f_y$  = shear reinforcement strength = 60 ksi

$P_c$  = permanent net compressive force normal to the shear plane; if force is tensile,  $P_c = 0$

(Note:  $P_c = \text{zero}$  because the panel weight is ignored)

$A_{vf}$  = area of shear reinforcement crossing the shear plane

$$= [(6 \text{ No. 5 U-bars} \times 2 \text{ legs} \times 0.31 \text{ in}^2/\text{leg})](2 \text{ pockets}) = 7.44 \text{ in}^2/\text{panel}$$

$V_n = (0.24 \text{ ksi})(576 \text{ in}^2) + 1.0(7.44)(60 \text{ ksi})$

$$= 584.64 \text{ kips/panel} > 396 \text{ kips/panel} \quad \text{OK}$$

### D.2.3 Design of the Negative Moment Areas over Interior Girder Lines

The design of the negative moment section provided in this section is conducted on the precast panel after the shear pockets are grouted. It is assumed in these calculations that the grout material has the same concrete strength as the precast concrete panel, i.e. 6.0 ksi.

The reader should note that the negative moment section should also be checked at time of prestress release and at time of installing the panel on the bridge. At these stages, the cross section of the panel after subtracting the shear pockets should be used as the effective concrete area. These calculations are given in Section 2.6 of this example.

Article 4.6.2.1.6 of the *LRFD Specifications* states that the critical section for flexural design at the negative moment area should be at a specific distance from the centerline of the support. This distance is defined as follows:

- For slabs supported on concrete I-shape girders: The least of 15 in. or  $\frac{1}{2}$  of the width of the flange of the concrete girder
- For slabs supported on steel girders:  $\frac{1}{4}$  the width of the flange of the steel girder from centerline of the support

In this section, the precast deck panels are assumed to be supported on steel girders because this type of support provides higher flexural effects in the slab compared to any concrete girders.

Assume that the minimum width of steel girder top flange is 12 in., therefore at  $12/4 = 3$  in. from the centerline of the support, the bending moment is as follows:

Slab wt.	$M_{slab} = -1.123$ ft-kips/ft
Barrier wt.	$M_{barrier} = +0.263$ ft-kips/ft
Wearing surface	$M_{ws} = -0.300$ ft-kips/ft
Live load	$M_{LL+IM} = -9.400$ ft-kips/ft [Table A4.1, <i>LRFD Specifications</i> ]
$M_{STRENGTH}$	$= 1.25 (DC) + 1.5 (DW) + 1.75 (LL+IM)$
	$= 1.25(-1.123+0.263) + 1.5(-0.300) + 1.75(-9.40)$
	$= -17.98$ ft-kips/ft
$\times 8$ ft/panel	$= -143.84$ ft-kips/panel

Try two layers of reinforcement, each layer has (4)  $\frac{1}{2}$ -in. strands and (6) No.5 bars. Provide a 2.0 in. clear concrete cover over each layer. The decompression stress in the strands,  $f_{pc} = 182.060$  ksi (tension), and in the No. 5 bars = 25 ksi (compression), are shown in Section D.2.1.2 and D.2.1.4 of this example respectively. Using the Strain Compatibility analysis in conjunction with the power formula,<sup>48</sup> the final round of calculations yields the following results:

Depth of the rectangular stress block,  $a = 0.988$  in.

Depth of the neutral axis,  $c = 1.317$  in

Strain in top layer of strands =  $16.490 \times 10^{-3}$  (tension)

Stress in top layer of strands = 259.080 ksi (tension)

Strain in top layer of No. 5 bars =  $9.094 \times 10^{-3}$  (tension)

Stress in top layer of No. 5 bars = 60.000 ksi (tension)

Strain in bottom layer of strands =  $8.513 \times 10^{-3}$  (tension)

Since the total strain in this layer is  $> 0.005$ , the strength reduction factor according to Article 5.5.4.2.1 of the *LRFD Specifications* = 1.0

Stress in bottom layer of strands = 225.620 ksi (tension)

Strain in bottom layer of No. 5 bars =  $1.406 \times 10^{-3}$  (tension)

Stress in bottom layer of No. 5 bars = 40.762 ksi (tension)

The flexural capacity of the section:

$$\phi M_n = \phi \sum \left[ A_{ps}(f_{ps}) \left( d_p - \frac{a}{2} \right) + A_s(f_s) \left( d_s - \frac{a}{2} \right) \right]$$

$$= 1,793.473 \text{ in.-kips./panel} = 149.456 \text{ ft-kips/panel}$$

$$> M_{strength I} = 143.84 \text{ ft-kips/panel} \quad \text{OK}$$

Since the maximum negative moment at the interior supports dies very quickly, provide two of the (6) No. 5 bars on each layer for 3 ft (i.e. one-fourth of the girder spacing) on each side of the girder line. This distance is adequate to cover the negative moment area over the interior supports and to fully develop these bars. The rest of the No. 5 bars (four No. 5 bars on each layer) are provided for the full length of the panel. This is because they are serving both the positive and negative moment areas.

#### **D.2.4 Design of the Overhang (negative moment section at exterior girder line)**

Most of the highway agencies have their own policies regarding the design of the overhang. This section provides the design of overhang according to the guidelines given in Article A13.4.1 of the *LRFD Specifications*, where the overhang should be designed for the following cases separately.

##### **D.2.4.1 Case I: Due to Transverse Vehicular Collision Loads Using Extreme Event Limit State II**

Since the New Jersey Barrier adopted in this example is crash tested, and since the LRFD states that the deck should be stronger than the railing system used, the collision moment and the horizontal collision force will be determined based on the reinforcement and geometry of the New Jersey Barrier as follows:

The base of the NJ Barrier is 16 in. wide and reinforced with No. 5 closed stirrups at 12 in. spacing. One leg of the stirrup is close to the inner face of the barrier and the other leg is close to the exterior face of the barrier. Using a 2 in. clear concrete cover over each layer and using the strain compatibility analysis,<sup>48</sup> the nominal flexural capacity of the section = 286.2 in.-kips/ft.

Article 1.3.2.1 of the *LRFD Specifications* states that the strength reduction factor for the Extreme Event Limit State,  $\phi = 1.0$ . Therefore, the flexural capacity of the base section is:

$$M_{base} = 1.0 \times 286.2 \text{ in.-kips/ft} = 23.85 \text{ ft-kips/ft}$$

In order to complete the design of the overhang, it is required to determine the total transverse resistance of the barrier,  $R_B$ , and the critical length of the wall failure,  $L_c$ , at the top surface of the barrier. Typically, these parameters depend on the barrier dimensions and failure mechanisms. Since the calculations of these parameters are beyond the scope of this document, they are taken from the following publication:

National Highway Institute. *Load and Resistance Factor Design of Highway Bridges*, NHI Course No 13061, Publication No FHWA HI-95. Federal Highway Administration.<sup>52</sup>

In lecture 16 of this publication, a NJ Barrier identical to the NJ Barrier used in this example is considered, and the values for  $R_w$  and  $L_c$  are as follow:

$$R_w = 147.03 \text{ kips}, L_c = 13.589 \text{ ft}$$

To determine the tensile force at the base of the barrier,  $T_{base}$ , assume that  $R_w$  is distributed over a distance of  $(L_c + 2H)$  at the barrier base, where  $H$  is the height of the barrier,  $H = 42$  in.

$$T_{base} = R_w / (L_c + 2H) = 147.03 / [13.589 + (2)(42/12)] = 7.14 \text{ kips/ft}$$

Therefore, due to the collision force, the following straining actions are transferred to the precast panel at the inner face of the barrier:

$$M_{base} = 23.85 \text{ ft-kips/ft and } T_{base} = 7.14 \text{ kips/ft (tension force)}$$

Two sections of the overhang need to be checked. The first section is at the inner face of the barrier (Section 1-1, **Figure D.2.4.1-1**) and the second section is at 3 in. from the centerline of the exterior girder line (Section 2-2, **Figure D.2.4.1-1**).

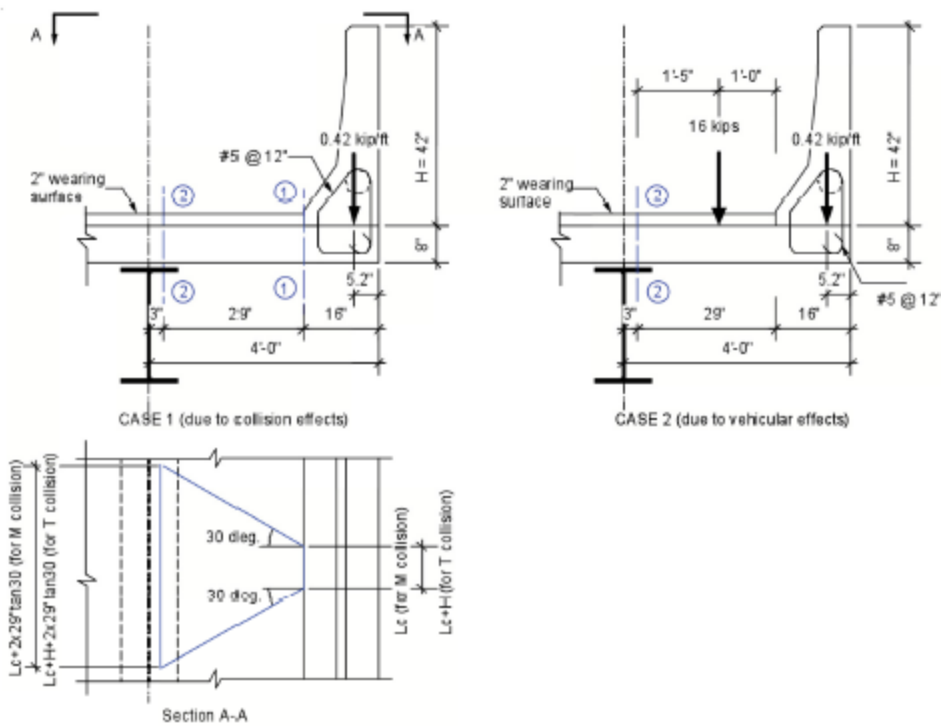


Figure D.2.4.1-1. Overhang design parameters.

Check capacity of section 1-1:

$$\begin{aligned}M_{base} &= 23.850 \text{ ft-kips/ft} \\T_{base} &= 7.14 \text{ kips/ft} \\M_{barrier} &= (0.420)(16-5.2)/12 = 0.378 \text{ ft-kips/ft} \\M_{slab} &= (0.100)(16/12)^2/2 = 0.089 \text{ ft-kips/ft} \\M_{SERVICE I} &= 23.850 + 0.378 + 0.089 = 24.317 \text{ ft-kips} \\M_{EXTREME EVENT II} &= 1.25DC + 1.5DW + 1.0CT \\&= 1.25(0.378+0.089) + 1.0(23.85) \\&= 24.434 \text{ ft-kips/ft} = 195.472 \text{ ft-kips /panel} \\T_{EXTREME EVENT II} &= (1.0)(7.14) = 7.14 \text{ kips/ft} = 57.12 \text{ kips /panel}\end{aligned}$$

As a starting point, assume that this section is reinforced with the same amount of reinforcement provided at the interior girder lines, which is: two layers of Grade 270 strands, each layer has (4) ½ in. strands, and two layers of Grade 60 steel, each layer has (2) No. 5 bars.

Since section (1-1) is 16 in. away from the edge of the panel, it is required to check the maximum strength that can be provided by the reinforcement based on the available embedment length.

For the ½ in. strands, the development length is,

$$\begin{aligned}\ell_d &= \kappa[f_{ps} - (2/3)f_{pc}] d_b && \text{[LRFD Eq. 5.11.4.2-1]} \\&= \left(259.080 - \frac{(2)(182.060)}{3}\right)(0.5) \\&= 68.9 \text{ in.}/12 = 5.74 \text{ ft}\end{aligned}$$

Where:

$\kappa = 1.0$  for pretensioned panels with depth equal to or less than 24 in.

The value of  $f_{ps}$  is taken from the calculations of the negative moment section over the interior girder lines.

$$\text{Available strength} = 259.080 \left( \frac{16-2}{68.9} \right) = 52.643 \text{ ksi}$$

It is assumed that the strands are recessed 2 in. from the edge of the panel to satisfy the corrosion protection requirements. It is clear that the strands can develop only a small amount of their tensile strength. Therefore, they will be ignored in the analysis of this section.

The development length for the No.5 Grade 60 straight bars,

$$\begin{aligned} \ell_d &= \text{greater} \left\{ \begin{array}{l} \frac{1.25 A_b f_y}{\sqrt{f_c}} \\ 0.4 d_b f_y \end{array} \right\} && \text{[LRFD Art. 5.11.2]} \\ &= \text{greater} \left\{ \begin{array}{l} \frac{(1.25)(0.31)(60)}{\sqrt{6.0}} = 9.5 \\ (0.4)\left(\frac{5}{8}\right)(60) = 15.0 \end{array} \right\} = 15 \text{ in.} \end{aligned}$$

Assume that the No.5 bars are epoxy coated. Since the concrete cover is  $> 3 d_b$  and the bar spacing is  $> 6 d_b$ , (LRFD, Article 5.11.2.1.2) therefore,

$$\ell_d = (1.2)(15) = 18 \text{ in.}$$

$$\text{Available strength, } f_s = 60 \left( \frac{16-2}{18} \right) = 46.7 \text{ ksi}$$

It is assumed that a 2 in. clear concrete cover is provided from the edge of the panel to the No. 5 bars to satisfy the corrosion protection requirements.

Based on the available strength of the strands, it is clear that section 1-1 should be designed as a partially pretensioned section. However, to simplify the calculations, this section is designed as a conventionally-reinforced section, ignoring the prestressed strands.

In addition to the (4) No. 5 bars, provide (17) No. 7 bars close to the top surface of the deck with 2 in. clear. In order to make the maximum benefit of these bars, provide them with a 90-degree standard hook where the tail of the standard hook will be embedded in the barrier. This detail is selected because the thickness of the panel and the required concrete cover do not provide enough distance to provide for a 180-degree standard hook within the panel thickness.

The development length of the No. 7 bar standard hook is:

$$\ell_d = \frac{38.0 d_b}{\sqrt{f_c}} = \frac{(38.0)\left(\frac{7}{8}\right)}{\sqrt{6.0}} = 13.6 \text{ in.} > (8 d_b \text{ and } 6.0 \text{ in.}) \quad \text{[LRFD Eq. 5.11.2.4.1-1]}$$

For epoxy coated bars,  $\ell_d = (1.2)(13.6) = 16.3 \text{ in.}$  [LRFD, Sect. 5.11.2.4.2]

$$\text{Available strength, } f_s = 60 \left( \frac{16-2}{16.3} \right) = 51.5 \text{ ksi}$$

Therefore, the total reinforcement provided at this section (ignoring the strands) is as follows:

Layers	Type	Area (in <sup>2</sup> )	Depth from bottom fiber (in.), $d_s$	Maximum developed strength (ksi)
(2) No. 5 top	Straight bar	2(0.31) = 0.62	8-2-0.5(5/8) = 5.6875	46.7
(17) No. 7 top	90-degree standard hook	17(0.60) = 10.2	8-2-0.5(7/8) = 5.5625	51.5
(2) No. 5 bottom	Straight bar	2(0.31) = 0.62	2+0.5(5/8) = 2.3125	46.7

Depth of the plastic center of the cross section (measured from bottom fiber) =

$$= \frac{[46.7 - (0.85)(6)][(0.62)(5.6875) + (0.62)(2.3125)] + [51.5 - (0.85)(6)][(10.2)(5.5625)] + (0.85)(6)(96)(8)(4)}{[46.7 - (0.85)(6)](0.62 + 0.62) + [51.5 - (0.85)(6)](10.2) + (0.85)(6)(96)(8)}$$

$$= 4.167 \text{ in.}$$

Assume that the three layers of reinforcement are on the tension side of the neutral axis, and that the stress in these layers equal to the maximum developed strength, therefore:

$$\begin{aligned} T_{EXTREME \text{ EVENT II}} &= T - C \\ 57.12 &= (46.7)(0.62+0.62) + (51.5)(10.2) - (0.85)(6)(96)(a) \\ a &= 1.075 \text{ in.} \\ c &= (a/\beta_1) = 1.075/0.75 = 1.433 \text{ in.} \end{aligned}$$

The assumption, that all layers of reinforcement are on the tension side of the neutral axis, is valid.

Check the stress in each layer:

$$(2) \text{ No. 5 top: } \epsilon_s = 0.003 \frac{(d_s - c)}{c} = 0.00891 > 0.002,$$

Therefore,  $f_s$  = lesser of 60.0 or 46.7 ksi.; use 46.7 ksi (tension)

Since  $\epsilon_s = \epsilon_t = 0.00891 > 0.005$ , therefore,  $\phi = 0.9$

$$(17) \text{ No. 7 top: } \epsilon_s = 0.003 \frac{(d_s - c)}{c} = 0.00864 > 0.002,$$

Therefore,  $f_s$  = lesser of 60.0 or 51.5 ksi; use 51.5 ksi (tension)

$$(2) \text{ No. 5 bottom: } \epsilon_s = 0.003 \frac{(d_s - c)}{c} = 0.00184 < 0.002,$$

Therefore,  $f_s$  = lesser of  $29,000 \times 0.00184 = 53.4$  or 46.7 ksi; use = 46.7 ksi (tension)

The assumed values of stress are valid.

Taking the moment about the plastic center:

$$\begin{aligned}\phi M_n &= \phi \{ (0.62 \times 46.7)(5.6875 - 4.167) + (10.2 \times 51.5)(5.5625 - 4.167) + (0.62 \times 46.7)(2.3125 - 4.167) + (0.85 \times 6)(96 \times 1.075)(4.167 - 0.5 \times 1.075) \} \\ &= 0.9 (2633.7) = 2370.3 \text{ in.-kips} \\ &= 197.5 \text{ ft-kips} > M_{EXTREME EVENT II} = 195.472 \text{ ft-kips/panel} \quad \text{OK}\end{aligned}$$

Check capacity of section 2-2:

At the inside face of the barrier (section 1-1), the collision effects,  $M_{base}$  and  $T_{base}$ , are distributed over  $L_c$  and  $(L_c + 2H)$ , respectively. Assume that these effects will spread between sections 1-1 and 2-2 at a  $30^\circ$  angle. Therefore the collision effects at section 2-2 are:

$$\begin{aligned}M_{base@2-2} &= (M_{base@1-1} \times L_c) / [L_c + (2 \times \frac{29}{12} \tan 30)] \\ &= (23.38 \times 13.589) / (13.589 + 2 \times \frac{29}{12} \times \tan 30) \\ &= 19.40 \text{ ft-kips/ft}\end{aligned}$$

Note that the distance between section 1-1 and 2-2 = 29 in.

$$\begin{aligned}T_{base@2-2} &= R_W / (L_c + 2H + 2 \times 29 \tan 30) \\ &= 147.03 / [13.589 + (2 \times \frac{42}{12}) + (2 \times \frac{29}{12}) \tan 30] \\ &= 6.29 \text{ kips/ft}\end{aligned}$$

$$M_{slab} = (8/12 \times 0.150) (3.75^2/2) = 0.70 \text{ ft-kip/ft}$$

$$M_{barrier} = 0.42 [(45 - 5.2)/(12)] = 1.40 \text{ ft-kips/ft}$$

$$M_{ws} = [(2/12) \times 0.150] (2.417^2/2) = 0.073 \text{ ft-kip/ft}$$

$$\begin{aligned}M_{EXTREME EVENT II} &= 1.25DC + 1.5DW + 1.0CT \\ &= 1.25(0.70 + 1.40) + 1.25(0.073) + 1.0(19.40) \\ &= 22.17 \text{ ft-kips/ft} \times 8 = 177.36 \text{ ft-kips/panel}\end{aligned}$$

$$T_{EXTREME EVENT II} = 1.0(6.29) = 6.29 \text{ kips/ft} = 50.32 \text{ kips/panel}$$

At section 2-2, the strands are still not fully developed, but the three layers of reinforcing bars, (2) No. 5 top, (17) No. 7 top and (2) No. 5 bottom, are fully developed. To simplify the calculations, the strands are ignored. Running the flexural analysis similar to section 1-1, the axial and corresponding flexural design capacity of the section are:

$$\phi T_n = 50.32 \text{ kips/panel, and}$$

$$\phi M_n = 229.3 \text{ ft-kips/panel} > M_{EXTREME EVENT II} = 177.36 \text{ ft-kips/panel} \quad \text{OK}$$

### D.2.4.2 Case 2: Due Dead and Live Loads

Due to combined dead and live load, the flexural capacity of section 2-2 should be checked. Load effects at section 2-2 are as follows:

$$\begin{aligned}M_{slab} &= (8/12 \times 0.150) (3.75^2/2) = 0.70 \text{ ft-kip/ft} \\M_{barrier} &= 0.42 [(45-5.2)/(12)] = 1.40 \text{ ft-kips/ft} \\M_{ws} &= [(2/12) (0.150) (2.417^2/2)] = 0.073 \text{ ft-kips/ft}\end{aligned}$$

Live load effects:

Article 3.6.1.3 of the *LRFD Specifications* states that where primary strips are transverse and their span does not exceed 15.0 ft, the transverse strips should be designed for the wheels of the 32.0 kip axle. Also, the center of the outside 16.0-kip wheel must be positioned 1 ft from the curb face for the design of the deck overhang.

Article 4.6.2.1.3 of the *LRFD Specifications* states that the live load effects should be distributed over a distance,  $L$  (in.) =  $45.0 + 10.0(X)$ , where  $X$  (in.) = distance from the wheel load to the section under consideration = 17 in.

$$\text{Live load moment, } M_{LL+IM} = (IM)(m) (16)(X) / L$$

Where,  $m$  = multiple presence factor (one loaded lane)

$$= 1.20 \quad \text{[LRFD Specifications, Table 3.6.1.1.2-1]}$$

$IM$  = dynamic load allowance

$$= 1.33 \quad \text{[LRFD Specifications, Table 3.6.2.1-1]}$$

$$M_{LL+IM} = 1.33 \times 1.2 \frac{(16) \left( \frac{17}{12} \right)}{\left[ 45 + (10) \left( \frac{17}{12} \right) \right] \frac{1}{12}} = 7.34 \text{ ft-kips/ft}$$

$$\begin{aligned}M_{STRENGTH1} &= 1.25DC + 1.5DW + 1.75(LL+IM) \\&= 1.25(0.70 + 1.40) + 1.5(0.073) + 1.75(7.34) \\&= 15.58 \text{ ft-kips/ft} = 124.6 \text{ ft-kips/panel}\end{aligned}$$

At section 2-2, the pure flexural design capacity (ignoring the strands) is:

$$\phi M_n = 229.3 \text{ ft-kips/panel} > M_{Strength1} = 124.6 \text{ ft-kips/panel} \quad \text{OK}$$

## D.2.5 Design of Longitudinal Reinforcement

Longitudinal post-tensioning is provided for the following reasons:

- (1) to put the panel-to-panel joints in compression
- (2) to help in distributing the live load in the longitudinal direction
- (3) to provide for the shrinkage and temperature reinforcement

Try high-strength, 150 ksi, 1.0 in. diameter, threaded bars. Assume that the effective prestress,  $f_{pe}$ , after seating, anchorage, and time dependent losses is 65% of the maximum tensile capacity.

$$f_{pe} = 0.65(0.785)(150) = 76.5 \text{ kips}$$

Article 9.7.5.3 of the *LRFD Specifications* states that a minimum effective stress of 0.25 ksi on concrete should be provided on precast components joined together by longitudinal post-tensioning.

$$\text{Required effective post-tensioning force} = (0.25 \text{ ksi})(8 \text{ in.})(44 \times 12 \text{ in.}) = 1056 \text{ kips}$$

$$\text{Required number of post-tensioning bars} = 1056/76.5 = 13.8 \text{ bars}$$

Use (14) 1.0 in. diameter, 150 ksi bars across the full width of the bridge as follows: 3 bars at 36 in. per girder spacing and one bar per each cantilever at mid distance of the cantilever.

Article 5.10.8 of the *LRFD Specifications* states that the longitudinal post-tensioning reinforcement can be used as shrinkage and temperature reinforcement if it provides a minimum stress of 0.11 ksi on the gross concrete area, which is already satisfied in this example. Articles 5.10.8.2 and 5.10.3.4 of the *LRFD Specifications* state that if maximum spacing of post-tensioning tendons does not exceed 72 in. or four times the slab thickness, 32 in., or 18 in., no additional conventional reinforcement should be provided between the post-tensioning tendons. However, in order to protect the panel from shrinkage cracking before the post-tensioning reinforcement is added, conventional welded wire reinforcement is provided.

Article 5.10.8 of the *LRFD Specifications* states that for bars or welded wire reinforcement, the area of shrinkage reinforcement per foot,  $A_s$ , on each face and in each direction, shall satisfy:

$$A_s \geq \frac{1.30bh}{2(b+h)f_y} \quad [\text{LRFD Eq. 5.10.8-1}]$$

$$0.11 \leq A_s \leq 0.60 \quad [\text{LRFD Eq. 5.10.8-2}]$$

Where,  $b$  = least width of component section (in.)

$h$  = least thickness of component section (in.)

$$A_s = \frac{(1.3)(12)(8)}{(2)(12+8)(60)} = 0.052 \text{ in}^2/\text{ft} < 0.11 \text{ in}^2/\text{ft}$$

Therefore,  $A_s = 0.11 \text{ in}^2/\text{ft}$

Use two layers of D4.5 at 6 in. (top and bottom layers), therefore, provided shrinkage and

$$\text{temperature reinforcement} = 2(0.045 \times \frac{12}{6}) = 0.180 \text{ in}^2$$

### **D.2.6 Miscellaneous Design Issues**

The previous sections presented detailed design calculations of the proposed system under service conditions, i.e. after the deck panel system is installed, connected with the supporting girders, and opened for traffic. However, during the life span of the precast panels from the time of fabrication to the time of opening the bridge to traffic, there are some other stages where the stresses of the deck panel have to be checked. These stages typically result from the fact that the panel is a pretensioned concrete member. For this type of member, the pretension force is usually released between 18 and 24 hours after casting the concrete. At that age, the concrete does not have its full design strength and the prestressing force is at its maximum value. This stage is typically called "At Transfer" or "At Release." At this stage the critical section is at the girder lines where there are ungrouted shear pockets that reduce the size of the concrete cross section that will resist the applied prestressing force.

After the prestressing force is released, the panel will be lifted and moved to a temporary storage location. The locations of the lifting points on the panel have to be pre-determined by the design engineer in order to make sure that the stresses, due to the weight of the panel combined with the prestressing force, will not cause any damage to the panel.

The design engineer also has to check the stresses in the panel at time of installation on the supporting girders. At this stage, the concrete has reached its full design strength and all the creep and shrinkage deformation has been attained. Also, the prestressing strands have had almost all the relaxation deformation. The loads that should be used at this stage are the panel weight, the prestressing force after all losses, and any construction load. The construction loads can be concentrated loads due to a fork lift that will be used to carry the panels and install them in place or a uniform live load that represents the crew and equipment that are used during installation of the panels. Typically, the construction loads vary in magnitude and nature from one project to another depending on the way the precast panels are installed. Therefore, it is the contractor's responsibility to provide the design engineer with the construction plan, and it is the design engineer's responsibility to check the stresses in the panel to accommodate this plan. The design engineer must state clearly on the plans that the construction plan of the panels must be checked and approved by him/her prior to construction. Check of stresses in the panel for the above discussed stages are given in the next sections.

### D.2.6.1 Check of Concrete Stresses at Time of Transferring the Prestressing Force

$$f'_{ci} = 5.0 \text{ ksi}$$

$$f_{pi} = \text{strand stress after initial elastic shortening losses} = 200.373 \text{ ksi} \quad [\text{See Sect. D.2.1.2}]$$

$$P_i = (200.373)(8)(0.153) = 245.257 \text{ kips}$$

Stress limits for concrete:

[LRFD Art. 5.9.4.1]

- Compression:

[LRFD Art. 5.9.4.1.1]

$$0.6 f'_{ci} = 0.6 \times 5.0 = +3.0 \text{ ksi}$$

- Tension:

[LRFD Art. 5.9.4.1.2]

In areas with bonded reinforcement sufficient to resist 120% of the tension force in the cracked concrete computed on the basis of an uncracked section:

$$0.24\sqrt{f'_{ci}} = 0.24\sqrt{5.0} = -0.537 \text{ ksi}$$

Stresses at top or bottom fibers of the slab:

$$f_t \text{ or } f_b = P_i / A = 245.257 / 768 = +0.319 \text{ ksi}$$

Compressive stress limit for concrete: +3.0 ksi

**OK**

### D.2.6.2 Check of Concrete Stresses During Lifting the Panel from the Prestressing Bed

The following assumptions are used to check the stresses during lifting the panel from the prestressing bed:

1. The time elapsed between releasing the strands and lifting up the panel is very short. Therefore the concrete strength  $f'_{ci}$  and strand stress  $f_{pi}$  used to check stresses at release will be used at this stage.
2. The panel will be lifted at every girder line.

Check of stresses at mid span section of the exterior span:

$$\begin{aligned} f_t &= (P_i / A) + (M_{slab} / S_t) \\ &= (245.257 / 768) + (0.768)(8)(12) / (1024) \\ &= +0.391 \text{ ksi} \end{aligned}$$

Compressive stress limit for concrete: +3.0 ksi

**OK**

$$\begin{aligned} f_b &= (P_i / A) - (M_{slab} / S_b) \\ &= (245.257 / 768) - (0.768)(8)(12) / (1024) \\ &= +0.247 \text{ ksi} \end{aligned}$$

Compressive stress limit for concrete: +3.0 ksi

**OK**

Check of stresses at first interior girder line:

$$\begin{aligned}f_i &= (P_i / A) - (M_{slab} / S_i) \\ &= (245.257 / 768) - (1.28)(8)(12) / (1024) \\ &= + 0.199 \text{ ksi} \\ \text{Compressive stress limit for concrete: } &+3.0 \text{ ksi} \quad \mathbf{OK}\end{aligned}$$

$$\begin{aligned}f_b &= (P_i / A) + (M_{slab} / S_b) \\ &= (245.257 / 768) + (1.28)(8)(12) / (1024) \\ &= + 0.439 \text{ ksi} \\ \text{Compressive stress limit for concrete: } &+3.0 \text{ ksi} \quad \mathbf{OK}\end{aligned}$$

### **D.3 DETAILS OF THE PRECAST DECK PANEL SYSTEM**

Details of the precise deck panel system are given in **Figures D.3-1 to D.3-5**.

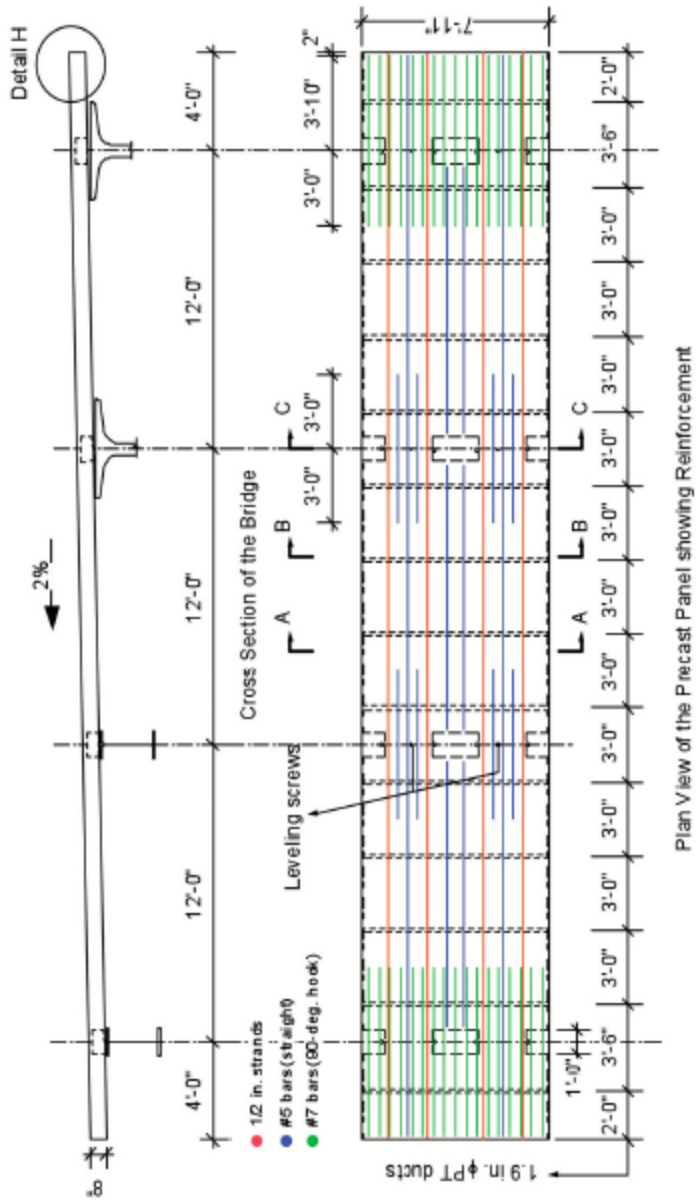


Figure D.3-1. Cross section and plan view of the precast panel.

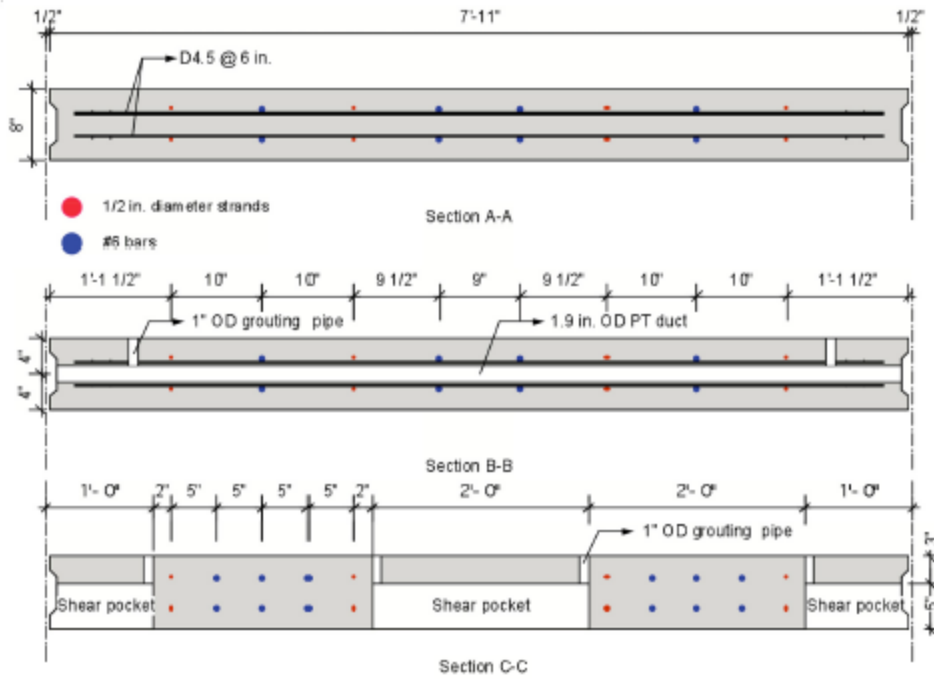


Figure D.3-2. Sections A – A, B – B, and C – C.

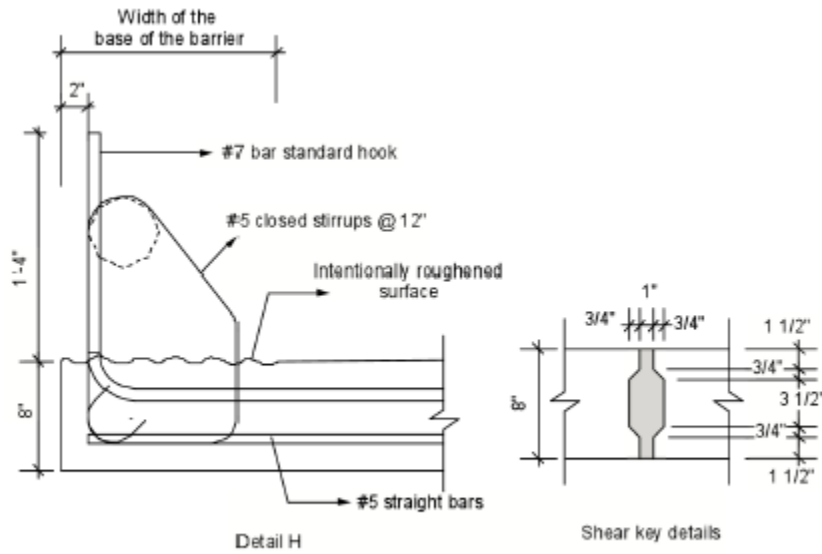


Figure D.3-3. Barrier and shear key details.

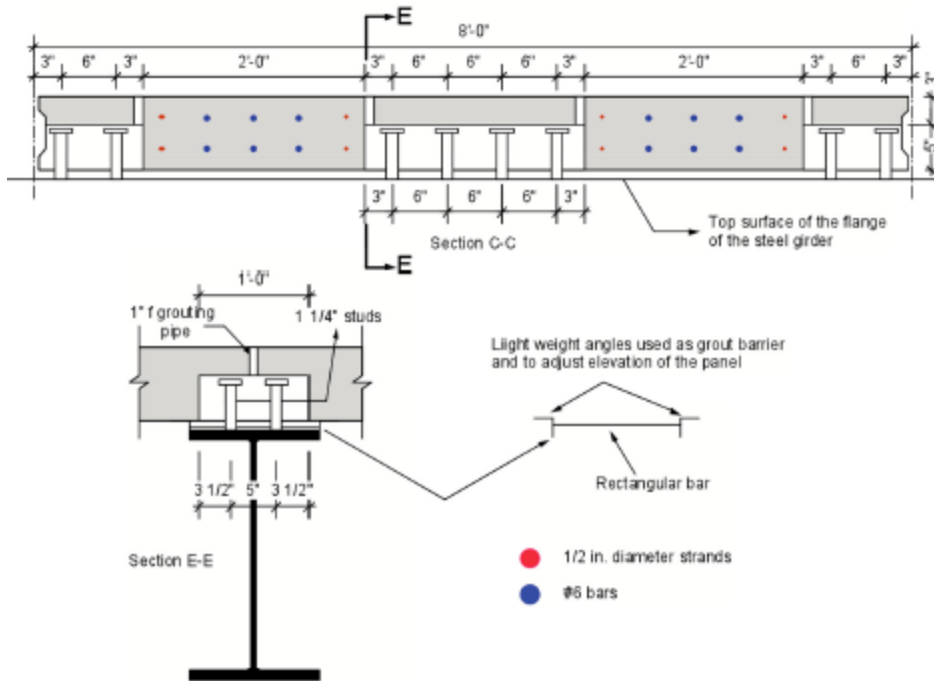


Figure D.3-4. Sections C – C and E – E for steel girders.

## LIST OF CCEER PUBLICATIONS

<b>Report No.</b>	<b>Publication</b>
CCEER-84-1	Saiidi, M., and R. Lawver, "User's Manual for LZAK-C64, A Computer Program to Implement the Q-Model on Commodore 64," Civil Engineering Department, Report No. CCEER-84-1, University of Nevada, Reno, January 1984.
CCEER-84-1	Douglas, B., Norris, G., Saiidi, M., Dodd, L., Richardson, J. and Reid, W., "Simple Bridge Models for Earthquakes and Test Data," Civil Engineering Department, Report No. CCEER-84-1 Reprint, University of Nevada, Reno, January 1984.
CCEER-84-2	Douglas, B. and T. Iwasaki, "Proceedings of the First USA-Japan Bridge Engineering Workshop," held at the Public Works Research Institute, Tsukuba, Japan, Civil Engineering Department, Report No. CCEER-84-2, University of Nevada, Reno, April 1984.
CCEER-84-3	Saiidi, M., J. Hart, and B. Douglas, "Inelastic Static and Dynamic Analysis of Short R/C Bridges Subjected to Lateral Loads," Civil Engineering Department, Report No. CCEER-84-3, University of Nevada, Reno, July 1984.
CCEER-84-4	Douglas, B., "A Proposed Plan for a National Bridge Engineering Laboratory," Civil Engineering Department, Report No. CCEER-84-4, University of Nevada, Reno, December 1984.
CCEER-85-1	Norris, G. and P. Abdollahiaee, "Laterally Loaded Pile Response: Studies with the Strain Wedge Model," Civil Engineering Department, Report No. CCEER-85-1, University of Nevada, Reno, April 1985.
CCEER-86-1	Ghusn, G. and M. Saiidi, "A Simple Hysteretic Element for Biaxial Bending of R/C in NEABS-86," Civil Engineering Department, Report No. CCEER-86-1, University of Nevada, Reno, July 1986.
CCEER-86-2	Saiidi, M., R. Lawver, and J. Hart, "User's Manual of ISADAB and SIBA, Computer Programs for Nonlinear Transverse Analysis of Highway Bridges Subjected to Static and Dynamic Lateral Loads," Civil Engineering Department, Report No. CCEER-86-2, University of Nevada, Reno, September 1986.
CCEER-87-1	Siddharthan, R., "Dynamic Effective Stress Response of Surface and Embedded Footings in Sand," Civil Engineering Department, Report No. CCEER-86-2, University of Nevada, Reno, June 1987.
CCEER-87-2	Norris, G. and R. Sack, "Lateral and Rotational Stiffness of Pile Groups for Seismic Analysis of Highway Bridges," Civil Engineering Department, Report No. CCEER-87-2, University of Nevada, Reno, June 1987.
CCEER-88-1	Orie, J. and M. Saiidi, "A Preliminary Study of One-Way Reinforced Concrete Pier Hinges Subjected to Shear and Flexure," Civil Engineering Department, Report No. CCEER-88-1, University of Nevada, Reno, January 1988.
CCEER-88-2	Orie, D., M. Saiidi, and B. Douglas, "A Micro-CAD System for Seismic Design of Regular Highway Bridges," Civil Engineering Department, Report No. CCEER-88-2, University of Nevada, Reno, June 1988.

- CCEER-88-3 Orie, D. and M. Saiidi, "User's Manual for Micro-SARB, a Microcomputer Program for Seismic Analysis of Regular Highway Bridges," Civil Engineering Department, Report No. CCEER-88-3, University of Nevada, Reno, October 1988.
- CCEER-89-1 Douglas, B., M. Saiidi, R. Hayes, and G. Holcomb, "A Comprehensive Study of the Loads and Pressures Exerted on Wall Forms by the Placement of Concrete," Civil Engineering Department, Report No. CCEER-89-1, University of Nevada, Reno, February 1989.
- CCEER-89-2 Richardson, J. and B. Douglas, "Dynamic Response Analysis of the Dominion Road Bridge Test Data," Civil Engineering Department, Report No. CCEER-89-2, University of Nevada, Reno, March 1989.
- CCEER-89-2 Vrontinos, S., M. Saiidi, and B. Douglas, "A Simple Model to Predict the Ultimate Response of R/C Beams with Concrete Overlays," Civil Engineering Department, Report NO. CCEER-89-2, University of Nevada, Reno, June 1989.
- CCEER-89-3 Ebrahimpour, A. and P. Jagadish, "Statistical Modeling of Bridge Traffic Loads - A Case Study," Civil Engineering Department, Report No. CCEER-89-3, University of Nevada, Reno, December 1989.
- CCEER-89-4 Shields, J. and M. Saiidi, "Direct Field Measurement of Prestress Losses in Box Girder Bridges," Civil Engineering Department, Report No. CCEER-89-4, University of Nevada, Reno, December 1989.
- CCEER-90-1 Saiidi, M., E. Maragakis, G. Ghusn, Y. Jiang, and D. Schwartz, "Survey and Evaluation of Nevada's Transportation Infrastructure, Task 7.2 - Highway Bridges, Final Report," Civil Engineering Department, Report No. CCEER 90-1, University of Nevada, Reno, October 1990.
- CCEER-90-2 Abdel-Ghaffar, S., E. Maragakis, and M. Saiidi, "Analysis of the Response of Reinforced Concrete Structures During the Whittier Earthquake 1987," Civil Engineering Department, Report No. CCEER 90-2, University of Nevada, Reno, October 1990.
- CCEER-91-1 Saiidi, M., E. Hwang, E. Maragakis, and B. Douglas, "Dynamic Testing and the Analysis of the Flamingo Road Interchange," Civil Engineering Department, Report No. CCEER-91-1, University of Nevada, Reno, February 1991.
- CCEER-91-2 Norris, G., R. Siddharthan, Z. Zafir, S. Abdel-Ghaffar, and P. Gowda, "Soil-Foundation-Structure Behavior at the Oakland Outer Harbor Wharf," Civil Engineering Department, Report No. CCEER-91-2, University of Nevada, Reno, July 1991.
- CCEER-91-3 Norris, G., "Seismic Lateral and Rotational Pile Foundation Stiffnesses at Cypress," Civil Engineering Department, Report No. CCEER-91-3, University of Nevada, Reno, August 1991.
- CCEER-91-4 O'Connor, D. and M. Saiidi, "A Study of Protective Overlays for Highway Bridge Decks in Nevada, with Emphasis on Polyester-Styrene Polymer Concrete," Civil Engineering Department, Report No. CCEER-91-4, University of Nevada, Reno, October 1991.
- CCEER-91-5 O'Connor, D.N. and M. Saiidi, "Laboratory Studies of Polyester-Styrene Polymer Concrete Engineering Properties," Civil Engineering Department, Report No. CCEER-91-5, University of Nevada, Reno, November 1991.

- CCEER-92-1 Straw, D.L. and M. Saiidi, "Scale Model Testing of One-Way Reinforced Concrete Pier Hinges Subject to Combined Axial Force, Shear and Flexure," edited by D.N. O'Connor, Civil Engineering Department, Report No. CCEER-92-1, University of Nevada, Reno, March 1992.
- CCEER-92-2 Wehbe, N., M. Saiidi, and F. Gordaninejad, "Basic Behavior of Composite Sections Made of Concrete Slabs and Graphite Epoxy Beams," Civil Engineering Department, Report No. CCEER-92-2, University of Nevada, Reno, August 1992.
- CCEER-92-3 Saiidi, M. and E. Hutchens, "A Study of Prestress Changes in A Post-Tensioned Bridge During the First 30 Months," Civil Engineering Department, Report No. CCEER-92-3, University of Nevada, Reno, April 1992.
- CCEER-92-4 Saiidi, M., B. Douglas, S. Feng, E. Hwang, and E. Maragakis, "Effects of Axial Force on Frequency of Prestressed Concrete Bridges," Civil Engineering Department, Report No. CCEER-92-4, University of Nevada, Reno, August 1992.
- CCEER-92-5 Siddharthan, R., and Z. Zafir, "Response of Layered Deposits to Traveling Surface Pressure Waves," Civil Engineering Department, Report No. CCEER-92-5, University of Nevada, Reno, September 1992.
- CCEER-92-6 Norris, G., and Z. Zafir, "Liquefaction and Residual Strength of Loose Sands from Drained Triaxial Tests," Civil Engineering Department, Report No. CCEER-92-6, University of Nevada, Reno, September 1992.
- CCEER-92-6-A Norris, G., Siddharthan, R., Zafir, Z. and Madhu, R. "Liquefaction and Residual Strength of Sands from Drained Triaxial Tests," Civil Engineering Department, Report No. CCEER-92-6-A, University of Nevada, Reno, September 1992.
- CCEER-92-7 Douglas, B., "Some Thoughts Regarding the Improvement of the University of Nevada, Reno's National Academic Standing," Civil Engineering Department, Report No. CCEER-92-7, University of Nevada, Reno, September 1992.
- CCEER-92-8 Saiidi, M., E. Maragakis, and S. Feng, "An Evaluation of the Current Caltrans Seismic Restrainer Design Method," Civil Engineering Department, Report No. CCEER-92-8, University of Nevada, Reno, October 1992.
- CCEER-92-9 O'Connor, D., M. Saiidi, and E. Maragakis, "Effect of Hinge Restrainers on the Response of the Madrone Drive Undercrossing During the Loma Prieta Earthquake," Civil Engineering Department, Report No. CCEER-92-9, University of Nevada, Reno, February 1993.
- CCEER-92-10 O'Connor, D., and M. Saiidi, "Laboratory Studies of Polyester Concrete: Compressive Strength at Elevated Temperatures and Following Temperature Cycling, Bond Strength to Portland Cement Concrete, and Modulus of Elasticity," Civil Engineering Department, Report No. CCEER-92-10, University of Nevada, Reno, February 1993.
- CCEER-92-11 Wehbe, N., M. Saiidi, and D. O'Connor, "Economic Impact of Passage of Spent Fuel Traffic on Two Bridges in Northeast Nevada," Civil Engineering Department, Report No. CCEER-92-11, University of Nevada, Reno, December 1992.
- CCEER-93-1 Jiang, Y., and M. Saiidi, "Behavior, Design, and Retrofit of Reinforced Concrete One-way Bridge Column Hinges," edited by D. O'Connor, Civil Engineering Department, Report No. CCEER-93-1, University of Nevada, Reno, March 1993.

- CCEER-93-2 Abdel-Ghaffar, S., E. Maragakis, and M. Saiidi, "Evaluation of the Response of the Aptos Creek Bridge During the 1989 Loma Prieta Earthquake," Civil Engineering Department, Report No. CCEER-93-2, University of Nevada, Reno, June 1993.
- CCEER-93-3 Sanders, D.H., B.M. Douglas, and T.L. Martin, "Seismic Retrofit Prioritization of Nevada Bridges," Civil Engineering Department, Report No. CCEER-93-3, University of Nevada, Reno, July 1993.
- CCEER-93-4 Abdel-Ghaffar, S., E. Maragakis, and M. Saiidi, "Performance of Hinge Restrainers in the Huntington Avenue Overhead During the 1989 Loma Prieta Earthquake," Civil Engineering Department, Report No. CCEER-93-4, University of Nevada, Reno, June 1993 (in final preparation).
- CCEER-93-5 Maragakis, E., M. Saiidi, S. Feng, and L. Flournoy, "Effects of Hinge Restrainers on the Response of the San Gregorio Bridge during the Loma Prieta Earthquake," (in final preparation) Civil Engineering Department, Report No. CCEER-93-5, University of Nevada, Reno.
- CCEER-93-6 Saiidi, M., E. Maragakis, S. Abdel-Ghaffar, S. Feng, and D. O'Connor, "Response of Bridge Hinge Restrainers during Earthquakes -Field Performance, Analysis, and Design," Civil Engineering Department, Report No. CCEER-93-6, University of Nevada, Reno, May 1993.
- CCEER-93-7 Wehbe, N., Saiidi, M., Maragakis, E., and Sanders, D., "Adequacy of Three Highway Structures in Southern Nevada for Spent Fuel Transportation," Civil Engineering Department, Report No. CCEER-93-7, University of Nevada, Reno, August 1993.
- CCEER-93-8 Roybal, J., Sanders, D.H., and Maragakis, E., "Vulnerability Assessment of Masonry in the Reno-Carson City Urban Corridor," Civil Engineering Department, Report No. CCEER-93-8, University of Nevada, Reno, May 1993.
- CCEER-93-9 Zafir, Z. and Siddharthan, R., "MOVLOAD: A Program to Determine the Behavior of Nonlinear Horizontally Layered Medium Under Moving Load," Civil Engineering Department, Report No. CCEER-93-9, University of Nevada, Reno, August 1993.
- CCEER-93-10 O'Connor, D.N., Saiidi, M., and Maragakis, E.A., "A Study of Bridge Column Seismic Damage Susceptibility at the Interstate 80/U.S. 395 Interchange in Reno, Nevada," Civil Engineering Department, Report No. CCEER-93-10, University of Nevada, Reno, October 1993.
- CCEER-94-1 Maragakis, E., B. Douglas, and E. Abdelwahed, "Preliminary Dynamic Analysis of a Railroad Bridge," Report CCEER-94-1, January 1994.
- CCEER-94-2 Douglas, B.M., Maragakis, E.A., and Feng, S., "Stiffness Evaluation of Pile Foundation of Cazenovia Creek Overpass," Civil Engineering Department, Report No. CCEER-94-2, University of Nevada, Reno, March 1994.
- CCEER-94-3 Douglas, B.M., Maragakis, E.A., and Feng, S., "Summary of Pretest Analysis of Cazenovia Creek Bridge," Civil Engineering Department, Report No. CCEER-94-3, University of Nevada, Reno, April 1994.
- CCEER-94-4 Norris, G.M., Madhu, R., Valceschini, R., and Ashour, M., "Liquefaction and Residual Strength of Loose Sands from Drained Triaxial Tests," Report 2, Vol. 1&2, Civil Engineering Department, Report No. CCEER-94-4, University of Nevada, Reno, August 1994.

- CCEER-94-5 Saiidi, M., Hutchens, E., and Gardella, D., "Prestress Losses in a Post-Tensioned R/C Box Girder Bridge in Southern Nevada," Civil Engineering Department, CCEER-94-5, University of Nevada, Reno, August 1994.
- CCEER-95-1 Siddharthan, R., El-Gamal, M., and Maragakis, E.A., "Nonlinear Bridge Abutment , Verification, and Design Curves," Civil Engineering Department, CCEER-95-1, University of Nevada, Reno, January 1995.
- CCEER-95-2 Ashour, M. and Norris, G., "Liquefaction and Undrained Response Evaluation of Sands from Drained Formulation," Civil Engineering Department, Report No. CCEER-95-2, University of Nevada, Reno, February 1995.
- CCEER-95-3 Wehbe, N., Saiidi, M., Sanders, D. and Douglas, B., "Ductility of Rectangular Reinforced Concrete Bridge Columns with Moderate Confinement," Civil Engineering Department, Report No. CCEER-95-3, University of Nevada, Reno, July 1995.
- CCEER-95-4 Martin, T., Saiidi, M. and Sanders, D., "Seismic Retrofit of Column-Pier Cap Connections in Bridges in Northern Nevada," Civil Engineering Department, Report No. CCEER-95-4, University of Nevada, Reno, August 1995.
- CCEER-95-5 Darwish, I., Saiidi, M. and Sanders, D., "Experimental Study of Seismic Susceptibility Column-Footing Connections in Bridges in Northern Nevada," Civil Engineering Department, Report No. CCEER-95-5, University of Nevada, Reno, September 1995.
- CCEER-95-6 Griffin, G., Saiidi, M. and Maragakis, E., "Nonlinear Seismic Response of Isolated Bridges and Effects of Pier Ductility Demand," Civil Engineering Department, Report No. CCEER-95-6, University of Nevada, Reno, November 1995.
- CCEER-95-7 Acharya, S., Saiidi, M. and Sanders, D., "Seismic Retrofit of Bridge Footings and Column-Footing Connections," Civil Engineering Department, Report No. CCEER-95-7, University of Nevada, Reno, November 1995.
- CCEER-95-8 Maragakis, E., Douglas, B., and Sandirasegaram, U., "Full-Scale Field Resonance Tests of a Railway Bridge," A Report to the Association of American Railroads, Civil Engineering Department, Report No. CCEER-95-8, University of Nevada, Reno, December 1995.
- CCEER-95-9 Douglas, B., Maragakis, E. and Feng, S., "System Identification Studies on Cazenovia Creek Overpass," Report for the National Center for Earthquake Engineering Research, Civil Engineering Department, Report No. CCEER-95-9, University of Nevada, Reno, October 1995.
- CCEER-96-1 El-Gamal, M.E. and Siddharthan, R.V., "Programs to Computer Translational Stiffness of Seat-Type Bridge Abutment," Civil Engineering Department, Report No. CCEER-96-1, University of Nevada, Reno, March 1996.
- CCEER-96-2 Labia, Y., Saiidi, M. and Douglas, B., "Evaluation and Repair of Full-Scale Prestressed Concrete Box Girders," A Report to the National Science Foundation, Research Grant CMS-9201908, Civil Engineering Department, Report No. CCEER-96-2, University of Nevada, Reno, May 1996.
- CCEER-96-3 Darwish, I., Saiidi, M. and Sanders, D., "Seismic Retrofit of R/C Oblong Tapered Bridge Columns with Inadequate Bar Anchorage in Columns and Footings," A Report to the Nevada Department of Transportation, Civil Engineering Department, Report No. CCEER-96-3, University of Nevada, Reno, May 1996.

- CCEER-96-4 Ashour, M., Pilling, R., Norris, G. and Perez, H., "The Prediction of Lateral Load Behavior of Single Piles and Pile Groups Using the Strain Wedge Model," A Report to the California Department of Transportation, Civil Engineering Department, Report No. CCEER-96-4, University of Nevada, Reno, June 1996.
- CCEER-97-1-A Rimal, P. and Itani, A. "Sensitivity Analysis of Fatigue Evaluations of Steel Bridges," Center for Earthquake Research, Department of Civil Engineering, University of Nevada, Reno, Nevada Report No. CCEER-97-1-A, September, 1997.
- CCEER-97-1-B Maragakis, E., Douglas, B., and Sandirasegaram, U. "Full-Scale Field Resonance Tests of a Railway Bridge," A Report to the Association of American Railroads, Civil Engineering Department, University of Nevada, Reno, May, 1996.
- CCEER-97-2 Wehbe, N., Saiidi, M., and D. Sanders, "Effect of Confinement and Flares on the Seismic Performance of Reinforced Concrete Bridge Columns," Civil Engineering Department, Report No. CCEER-97-2, University of Nevada, Reno, September 1997.
- CCEER-97-3 Darwish, I., M. Saiidi, G. Norris, and E. Maragakis, "Determination of In-Situ Footing Stiffness Using Full-Scale Dynamic Field Testing," A Report to the Nevada Department of Transportation, Structural Design Division, Carson City, Nevada, Report No. CCEER-97-3, University of Nevada, Reno, October 1997.
- CCEER-97-4-A Itani, A. "Cyclic Behavior of Richmond-San Rafael Tower Links," Center for Civil Engineering Earthquake Research, Department of Civil Engineering, University of Nevada, Reno, Nevada, Report No. CCEER-97-4, August 1997.
- CCEER-97-4-B Wehbe, N., and M. Saiidi, "User's Manual for RCMC v. 1.2 : A Computer Program for Moment-Curvature Analysis of Confined and Unconfined Reinforced Concrete Sections," Center for Civil Engineering Earthquake Research, Department of Civil Engineering, University of Nevada, Reno, Nevada, Report No. CCEER-97-4, November, 1997.
- CCEER-97-5 Isakovic, T., M. Saiidi, and A. Itani, "Influence of new Bridge Configurations on Seismic Performance," Department of Civil Engineering, University of Nevada, Reno, Report No. CCEER-97-5, September, 1997.
- CCEER-98-1 Itani, A., Vesco, T. and Dietrich, A., "Cyclic Behavior of "as Built" Laced Members With End Gusset Plates on the San Francisco Bay Bridge," Center for Civil Engineering Earthquake Research, Department of Civil Engineering, University of Nevada, Reno, Nevada Report No. CCEER-98-1, March, 1998.
- CCEER-98-2 G. Norris and M. Ashour, "Liquefaction and Undrained Response Evaluation of Sands from Drained Formulation," Center for Civil Engineering Earthquake Research, Department of Civil Engineering, University of Nevada, Reno, Nevada, Report No. CCEER-98-2, May, 1998.
- CCEER-98-3 Qingbin, Chen, B. M. Douglas, E. Maragakis, and I. G. Buckle, "Extraction of Nonlinear Hysteretic Properties of Seismically Isolated Bridges from Quick-Release Field Tests," Center for Civil Engineering Earthquake Research, Department of Civil Engineering, University of Nevada, Reno, Nevada, Report No. CCEER-98-3, June, 1998.
- CCEER-98-4 Maragakis, E., B. M. Douglas, and C. Qingbin, "Full-Scale Field Capacity Tests of a Railway Bridge," Center for Civil Engineering Earthquake Research, Department of Civil Engineering, University of Nevada, Reno, Nevada, Report No. CCEER-98-4, June, 1998.

- CCEER-98-5 Itani, A., Douglas, B., and Woodgate, J., "Cyclic Behavior of Richmond-San Rafael Retrofitted Tower Leg," Center for Civil Engineering Earthquake Research, Department of Civil Engineering, University of Nevada, Reno. Report No. CCEER-98-5, June 1998
- CCEER-98-6 Moore, R., Saiidi, M., and Itani, A., "Seismic Behavior of New Bridges with Skew and Curvature," Center for Civil Engineering Earthquake Research, Department of Civil Engineering, University of Nevada, Reno. Report No. CCEER-98-6, October, 1998.
- CCEER-98-7 Itani, A and Dietrich, A, "Cyclic Behavior of Double Gusset Plate Connections," Center for Civil Engineering Earthquake Research, Department of Civil Engineering, University of Nevada, Reno, Nevada, Report No. CCEER-98-5, December, 1998.
- CCEER-99-1 Caywood, C., M. Saiidi, and D. Sanders, "Seismic Retrofit of Flared Bridge Columns with Steel Jackets," Civil Engineering Department, University of Nevada, Reno, Report No. CCEER-99-1, February 1999.
- CCEER-99-2 Mangoba, N., M. Mayberry, and M. Saiidi, "Prestress Loss in Four Box Girder Bridges in Northern Nevada," Civil Engineering Department, University of Nevada, Reno, Report No. CCEER-99-2, March 1999.
- CCEER-99-3 Abo-Shadi, N., M. Saiidi, and D. Sanders, "Seismic Response of Bridge Pier Walls in the Weak Direction," Civil Engineering Department, University of Nevada, Reno, Report No. CCEER-99-3, April 1999.
- CCEER-99-4 Buzick, A., and M. Saiidi, "Shear Strength and Shear Fatigue Behavior of Full-Scale Prestressed Concrete Box Girders," Civil Engineering Department, University of Nevada, Reno, Report No. CCEER-99-4, April 1999.
- CCEER-99-5 Randall, M., M. Saiidi, E. Maragakis and T. Isakovic, "Restrainer Design Procedures For Multi-Span Simply-Supported Bridges," Civil Engineering Department, University of Nevada, Reno, Report No. CCEER-99-5, April 1999.
- CCEER-99-6 Wehbe, N. and M. Saiidi, "User's Manual for RCMC v. 1.2, A Computer Program for Moment-Curvature Analysis of Confined and Unconfined Reinforced Concrete Sections," Civil Engineering Department, University of Nevada, Reno, Report No. CCEER-99-6, May 1999.
- CCEER-99-7 Burda, J. and A. Itani, "Studies of Seismic Behavior of Steel Base Plates," Civil Engineering Department, University of Nevada, Reno, Report No. CCEER-99-7, May 1999.
- CCEER-99-8 Ashour, M. and G. Norris, "Refinement of the Strain Wedge Model Program," Civil Engineering Department, University of Nevada, Reno, Report No. CCEER-99-8, March 1999.
- CCEER-99-9 Dietrich, A., and A. Itani, "Cyclic Behavior of Laced and Perforated Steel Members on the San Francisco-Oakland Bay Bridge," Civil Engineering Department, University, Reno, Report No. CCEER-99-9, December 1999.
- CCEER 99-10 Itani, A., A. Dietrich, "Cyclic Behavior of Built Up Steel Members and their Connections," Civil Engineering Department, University of Nevada, Reno, Report No. CCEER-99-10, December 1999.
- CCEER 99-10-A Itani, A., E. Maragakis and P. He, "Fatigue Behavior of Riveted Open Deck Railroad Bridge Girders," Civil Engineering Department, University of Nevada, Reno, Report No. CCEER-99-10-A, August 1999.

- CCEER 99-11 Itani, A., J. Woodgate, "Axial and Rotational Ductility of Built Up Structural Steel Members," Civil Engineering Department, University of Nevada, Reno, Report No. CCEER-99-11, December 1999.
- CCEER-99-12 Sgambelluri, M., Sanders, D.H., and Saiidi, M.S., "Behavior of One-Way Reinforced Concrete Bridge Column Hinges in the Weak Direction," Department of Civil Engineering, University of Nevada, Reno, Report No. CCEER-99-12, December 1999.
- CCEER-99-13 Laplace, P., Sanders, D.H., Douglas, B, and Saiidi, M, "Shake Table Testing of Flexure Dominated Reinforced Concrete Bridge Columns", Department of Civil Engineering, University of Nevada, Reno, Report No. CCEER-99-13, December 1999.
- CCEER-99-14 Ahmad M. Itani, Jose A. Zepeda, and Elizabeth A. Ware "Cyclic Behavior of Steel Moment Frame Connections for the Moscone Center Expansion," Department of Civil Engineering, University of Nevada, Reno, Report No. CCEER-99-14, December 1999.
- CCEER 00-1 Ashour, M., and Norris, G. "Undrained Lateral Pile and Pile Group Response in Saturated Sand," Civil Engineering Department, University of Nevada, Reno, Report No. CCEER-00-1, May 1999. January 2000.
- CCEER 00-2 Saiidi, M. and Wehbe, N., "A Comparison of Confinement Requirements in Different Codes for Rectangular, Circular, and Double-Spiral RC Bridge Columns," Civil Engineering Department, University of Nevada, Reno, Report No. CCEER-00-2, January 2000.
- CCEER 00-3 McElhaney, B., M. Saiidi, and D. Sanders, "Shake Table Testing of Flared Bridge Columns With Steel Jacket Retrofit," Civil Engineering Department, University of Nevada, Reno, Report No. CCEER-00-3, January 2000.
- CCEER 00-4 Martinovic, F., M. Saiidi, D. Sanders, and F. Gordaninejad, "Dynamic Testing of Non-Prismatic Reinforced Concrete Bridge Columns Retrofitted with FRP Jackets," Civil Engineering Department, University of Nevada, Reno, Report No. CCEER-00-4, January 2000.
- CCEER 00-5 Itani, A., and M. Saiidi, "Seismic Evaluation of Steel Joints for UCLA Center for Health Science Westwood Replacement Hospital," Civil Engineering Department, University of Nevada, Reno, Report No. CCEER-00-5, February 2000.
- CCEER 00-6 Will, J. and D. Sanders, "High Performance Concrete Using Nevada Aggregates," Civil Engineering Department, University of Nevada, Reno, Report No. CCEER-00-6, May 2000.
- CCEER 00-7 French, C., and M. Saiidi, "A Comparison of Static and Dynamic Performance of Models of Flared Bridge Columns," Civil Engineering Department, University of Nevada, Reno, Report No. CCEER-00-7, October 2000.
- CCEER 00-8 Itani, A., H. Sedarat, "Seismic Analysis of the AISI LRFD Design Example of Steel Highway Bridges," Civil Engineering Department, University of Nevada, Reno, Report No. CCEER 00-08, November 2000.
- CCEER 00-9 Moore, J., D. Sanders, and M. Saiidi, "Shake Table Testing of 1960's Two Column Bent with Hinges Bases," Civil Engineering Department, University of Nevada, Reno, Report No. CCEER 00-09, December 2000.

- CCEER 00-10 Asthana, M., D. Sanders, and M. Saiidi, "One-Way Reinforced Concrete Bridge Column Hinges in the Weak Direction," Civil Engineering Department, University of Nevada, Reno, Report No. CCEER 00-10, April 2001.
- CCEER 01-1 Ah Sha, H., D. Sanders, M. Saiidi, "Early Age Shrinkage and Cracking of Nevada Concrete Bridge Decks," Civil Engineering Department, University of Nevada, Reno, Report No. CCEER 01-01, May 2001.
- CCEER 01-2 Ashour, M. and G. Norris, "Pile Group program for Full Material Modeling a Progressive Failure," Civil Engineering Department, University of Nevada, Reno, Report No. CCEER 01-02, July 2001.
- CCEER 01-3 Itani, A., C. Lanaud, and P. Dusicka, "Non-Linear Finite Element Analysis of Built-Up Shear Links," Civil Engineering Department, University of Nevada, Reno, Report No. CCEER 01-03, July 2001.
- CCEER 01-4 Saiidi, M., J. Mortensen, and F. Martinovic, "Analysis and Retrofit of Fixed Flared Columns with Glass Fiber-Reinforced Plastic Jacketing," Civil Engineering Department, University of Nevada, Reno, Report No. CCEER 01-4, August 2001
- CCEER 01-5 Not Published
- CCEER 01-6 Laplace, P., D. Sanders, and M. Saiidi, "Experimental Study and Analysis of Retrofitted Flexure and Shear Dominated Circular Reinforced Concrete Bridge Columns Subjected to Shake Table Excitation," Civil Engineering Department, University of Nevada, Reno, Report No. CCEER 01-6, June 2001.
- CCEER 01-7 Reppi, F., and D. Sanders, "Removal and Replacement of Cast-in-Place, Post-tensioned, Box Girder Bridge," Civil Engineering Department, University of Nevada, Reno, Report No. CCEER 01-7, December 2001.
- CCEER 02-1 Pulido, C., M. Saiidi, D. Sanders, and A. Itani, "Seismic Performance and Retrofitting of Reinforced Concrete Bridge Bents," Civil Engineering Department, University of Nevada, Reno, Report No. CCEER 02-1, January 2002.
- CCEER 02-2 Yang, Q., M. Saiidi, H. Wang, and A. Itani, "Influence of Ground Motion Incoherency on Earthquake Response of Multi-Support Structures," Civil Engineering Department, University of Nevada, Reno, Report No. CCEER 02-2, May 2002.
- CCEER 02-3 M. Saiidi, B. Gopalakrishnan, E. Reinhardt, and R. Siddharthan, "A Preliminary Study of Shake Table Response of A Two-Column Bridge Bent on Flexible Footings," Civil Engineering Department, University of Nevada, Reno, Report No. CCEER 02-03, June 2002.
- CCEER 02-4 Not Published
- CCEER 02-5 Banghart, A., Sanders, D., Saiidi, M., "Evaluation of Concrete Mixes for Filling the Steel Arches in the Galena Creek Bridge," Civil Engineering Department, University of Nevada, Reno, Report No. CCEER 02-05, June 2002.
- CCEER 02-6 Dusicka, P., Itani, A., Buckle, I. G., "Cyclic Behavior of Shear Links and Tower Shaft Assembly of San Francisco – Oakland Bay Bridge Tower," Civil Engineering Department, University of Nevada, Reno, Report No. CCEER 02-06, July 2002.

- CCEER 02-7 Mortensen, J., and M. Saiidi, "A Performance-Based Design Method for Confinement in Circular Columns," Civil Engineering Department, University of Nevada, Reno, Report No. CCEER 02-07, November 2002.
- CCEER 03-1 Wehbe, N., and M. Saiidi, "User's manual for SPMC v. 1.0 : A Computer Program for Moment-Curvature Analysis of Reinforced Concrete Sections with Interlocking Spirals," Center for Civil Engineering Earthquake Research, Department of Civil Engineering, University of Nevada, Reno, Nevada, Report No. CCEER-03-1, May, 2003.
- CCEER 03-2 Wehbe, N., and M. Saiidi, "User's manual for RCMC v. 2.0 : A Computer Program for Moment-Curvature Analysis of Confined and Unconfined Reinforced Concrete Sections," Center for Civil Engineering Earthquake Research, Department of Civil Engineering, University of Nevada, Reno, Nevada, Report No. CCEER-03-2, June, 2003.
- CCEER 03-3 Nada, H., D. Sanders, and M. Saiidi, "Seismic Performance of RC Bridge Frames with Architectural-Flared Columns," Civil Engineering Department, University of Nevada, Reno, Report No. CCEER 03-3, January 2003.
- CCEER 03-4 Reinhardt, E., M. Saiidi, and R. Siddharthan, "Seismic Performance of a CFRP/ Concrete Bridge Bent on Flexible Footings," Civil Engineering Department, University of Nevada, Reno, Report No. CCEER 03-4, August 2003.
- CCEER 03-5 Johnson, N., M. Saiidi, A. Itani, and S. Ladhany, "Seismic Retrofit of Octagonal Columns with Pedestal and One-Way Hinge at the Base," Center for Civil Engineering Earthquake Research, Department of Civil Engineering, University of Nevada, Reno, Nevada, and Report No. CCEER-03-5, August 2003.
- CCEER 03-6 Mortensen, C., M. Saiidi, and S. Ladhany, "Creep and Shrinkage Losses in Highly Variable Climates," Center for Civil Engineering Earthquake Research, Department of Civil Engineering, University of Nevada, Reno, Report No. CCEER-03-6, September 2003.
- CCEER 03-7 Ayoub, C., M. Saiidi, and A. Itani, "A Study of Shape-Memory-Alloy-Reinforced Beams and Cubes," Center for Civil Engineering Earthquake Research, Department of Civil Engineering, University of Nevada, Reno, Nevada, Report No. CCEER-03-7, October 2003.
- CCEER 03-8 Chandane, S., D. Sanders, and M. Saiidi, "Static and Dynamic Performance of RC Bridge Bents with Architectural-Flared Columns," Center for Civil Engineering Earthquake Research, Department of Civil Engineering, University of Nevada, Reno, Nevada, Report No. CCEER-03-8, November 2003.
- CCEER 04-1 Olaegbe, C., and Saiidi, M., "Effect of Loading History on Shake Table Performance of A Two-Column Bent with Infill Wall," Center for Civil Engineering Earthquake Research, Department of Civil Engineering, University of Nevada, Reno, Nevada, Report No. CCEER-04-1, January 2004.
- CCEER 04-2 Johnson, R., Maragakis, E., Saiidi, M., and DesRoches, R., "Experimental Evaluation of Seismic Performance of SMA Bridge Restrainers," Center for Civil Engineering Earthquake Research, Department of Civil Engineering, University of Nevada, Reno, Nevada, Report No. CCEER-04-2, February 2004.

- CCEER 04-3 Moustafa, K., Sanders, D., and Saiidi, M., "Impact of Aspect Ratio on Two-Column Bent Seismic Performance," Center for Civil Engineering Earthquake Research, Department of Civil Engineering, University of Nevada, Reno, Nevada, Report No. CCEER-04-3, February 2004.
- CCEER 04-4 Maragakis, E., Saiidi, M., Sanchez-Camargo, F., and Elfass, S., "Seismic Performance of Bridge Restrainers At In-Span Hinges," Center for Civil Engineering Earthquake Research, Department of Civil Engineering, University of Nevada, Reno, Nevada, Report No. CCEER-04-4, March 2004.
- CCEER 04-5 Ashour, M., Norris, G. and Elfass, S., "Analysis of Laterally Loaded Long or Intermediate Drilled Shafts of Small or Large Diameter in Layered Soil," Center for Civil Engineering Earthquake Research, Department of Civil Engineering, University of Nevada, Reno, Nevada, Report No. CCEER-04-5, June 2004.
- CCEER 04-6 Correal, J., Saiidi, M. and Sanders, D., "Seismic Performance of RC Bridge Columns Reinforced with Two Interlocking Spirals," Center for Civil Engineering Earthquake Research, Department of Civil Engineering, University of Nevada, Reno, Nevada, Report No. CCEER-04-6, August 2004.
- CCEER 04-7 Dusicka, P., Itani, A. and Buckle, I., "Cyclic Response and Low Cycle Fatigue Characteristics of Plate Steels," Center for Civil Engineering Earthquake Research, Department of Civil Engineering, University of Nevada, Reno, Nevada, Report No. CCEER-04-7, November 2004.
- CCEER 04-8 Dusicka, P., Itani, A. and Buckle, I., "Built-up Shear Links as Energy Dissipaters for Seismic Protection of Bridges," Center for Civil Engineering Earthquake Research, Department of Civil Engineering, University of Nevada, Reno, Nevada, Report No. CCEER-04-8, November 2004.
- CCEER 04-9 Sureshkumar, K., Saiidi, S., Itani, A. and Ladkany, S., "Seismic Retrofit of Two-Column Bents with Diamond Shape Columns," Center for Civil Engineering Earthquake Research, Department of Civil Engineering, University of Nevada, Reno, Nevada, Report No. CCEER-04-9, November 2004.
- CCEER 05-1 Wang, H. and Saiidi, S., "A Study of RC Columns with Shape Memory Alloy and Engineered Cementitious Composites," Center for Civil Engineering Earthquake Research, Department of Civil Engineering, University of Nevada, Reno, Nevada, Report No. CCEER-05-1, January 2005.
- CCEER 05-2 Johnson, R., Saiidi, S. and Maragakis, E., "A Study of Fiber Reinforced Plastics for Seismic Bridge Restrainers," Center for Civil Engineering Earthquake Research, Department of Civil Engineering, University of Nevada, Reno, Nevada, Report No. CCEER-05-2, January 2005.
- CCEER 05-3 Carden, L.P., Itani, A.M., Buckle, I.G, "Seismic Load Path in Steel Girder Bridge Superstructures," Center for Civil Engineering Earthquake Research, Department of Civil Engineering, University of Nevada, Reno, Nevada, Report No. CCEER-05-3, January 2005.
- CCEER 05-4 Carden, L.P., Itani, A.M., Buckle, I.G, "Seismic Performance of Steel Girder Bridge Superstructures with Ductile End Cross Frames and Seismic Isolation," Center for Civil Engineering Earthquake Research, Department of Civil Engineering, University of Nevada, Reno, Nevada, Report No. CCEER-05-4, January 2005.

- CCEER 05-5 Goodwin, E., Maragakis, M., Itani, A. and Luo, S., "Experimental Evaluation of the Seismic Performance of Hospital Piping Subassemblies," Center for Civil Engineering Earthquake Research, Department of Civil Engineering, University of Nevada, Reno, Nevada, Report No. CCEER-05-5, February 2005.
- CCEER 05-6 Zadeh M. S., Saiidi, S, Itani, A. and Ladkany, S., "Seismic Vulnerability Evaluation and Retrofit Design of Las Vegas Downtown Viaduct," Center for Civil Engineering Earthquake Research, Department of Civil Engineering, University of Nevada, Reno, Nevada, Report No. CCEER-05-6, February 2005.
- CCEER 05-7 Phan, V., Saiidi, S. and Anderson, J., "Near Fault (Near Field) Ground Motion Effects on Reinforced Concrete Bridge Columns," Center for Civil Engineering Earthquake Research, Department of Civil Engineering, University of Nevada, Reno, Nevada, Report No. CCEER-05-7, August 2005.
- CCEER 05-8 Carden, L., Itani, A. and Laplace, P., "Performance of Steel Props at the UNR Fire Science Academy subjected to Repeated Fire," Center for Civil Engineering Earthquake Research, Department of Civil Engineering, University of Nevada, Reno, Nevada, Report No. CCEER-05-8, August 2005.
- CCEER 05-9 Yamashita, R. and Sanders, D., "Shake Table Testing and an Analytical Study of Unbonded Prestressed Hollow Concrete Column Constructed with Precast Segments," Center for Civil Engineering Earthquake Research, Department of Civil Engineering, University of Nevada, Reno, Nevada, Report No. CCEER-05-9, August 2005.
- CCEER 05-10 Not Published
- CCEER 05-11 Carden, L., Itani, A., and Peckan, G., "Recommendations for the Design of Beams and Posts in Bridge Falsework," Center for Civil Engineering Earthquake Research, Department of Civil Engineering, University of Nevada, Reno, Nevada, Report No. CCEER-05-11, October 2005.
- CCEER 06-01 Cheng, Z., Saiidi, M., and Sanders, D., "Development of a Seismic Design Method for Reinforced Concrete Two-Way Bridge Column Hinges," Center for Civil Engineering Earthquake Research, Department of Civil Engineering, University of Nevada, Reno, Nevada, Report No. CCEER-06-01, February 2006.
- CCEER 06-02 Johnson, N., Saiidi, M., and Sanders, D., "Large-Scale Experimental and Analytical Studies of a Two-Span Reinforced Concrete Bridge System," Center for Civil Engineering Earthquake Research, Department of Civil Engineering, University of Nevada, Reno, Nevada, Report No. CCEER-06-02, March 2006.
- CCEER 06-03 Saiidi, M., Ghasemi, H. and Tiras, A., "Seismic Design and Retrofit of Highway Bridges," Proceedings, Second US-Turkey Workshop, Center for Civil Engineering Earthquake Research, Department of Civil Engineering, University of Nevada, Reno, Nevada, Report No. CCEER-06-03, May 2006.
- CCEER 07-01 O'Brien, M., Saiidi, M. and Sadrossadat-Zadeh, M., "A Study of Concrete Bridge Columns Using Innovative Materials Subjected to Cyclic Loading," Center for Civil Engineering Earthquake Research, Department of Civil Engineering, University of Nevada, Reno, Nevada, Report No. CCEER-07-01, January 2007.
- CCEER 07-02 Sadrossadat-Zadeh, M. and Saiidi, M., "Effect of Strain rate on Stress-Strain Properties and Yield Propagation in Steel Reinforcing Bars," Center for Civil Engineering Earthquake Research, Department of Civil Engineering, University of Nevada, Reno, Nevada, Report No. CCEER-07-02, January 2007.

- CCEER 07-03 Sadrossadat-Zadeh, M. and Saiidi, M., "Analytical Study of NEESR-SG 4-Span Bridge Model Using OpenSees," Center for Civil Engineering Earthquake Research, Department of Civil Engineering, University of Nevada, Reno, Nevada, Report No. CCEER-07-03, January 2007.
- CCEER 07-04 Nelson, R., Saiidi, M. and Zadeh, S., "Experimental Evaluation of Performance of Conventional Bridge Systems," Center for Civil Engineering Earthquake Research, Department of Civil Engineering, University of Nevada, Reno, Nevada, Report No. CCEER-07-04, October 2007.
- CCEER 07-05 Bahen, N. and Sanders, D., "Strut-and-Tie Modeling for Disturbed Regions in Structural Concrete Members with Emphasis on Deep Beams," Center for Civil Engineering Earthquake Research, Department of Civil Engineering, University of Nevada, Reno, Nevada, Report No. CCEER-07-05, December 2007.
- CCEER 07-06 Choi, H., Saiidi, M. and Somerville, P., "Effects of Near-Fault Ground Motion and Fault-Rupture on the Seismic Response of Reinforced Concrete Bridges," Center for Civil Engineering Earthquake Research, Department of Civil Engineering, University of Nevada, Reno, Nevada, Report No. CCEER-07-06, December 2007.
- CCEER 07-07 Ashour M. and Norris, G., "Report and User Manual on Strain Wedge Model Computer Program for Files and Large Diameter Shafts with LRFD Procedure," Center for Civil Engineering Earthquake Research, Department of Civil Engineering, University of Nevada, Reno, Nevada, Report No. CCEER-07-07, October 2007.
- CCEER 08-01 Doyle, K. and Saiidi, M., "Seismic Response of Telescopic Pipe Pin Connections," Center for Civil Engineering Earthquake Research, Department of Civil Engineering, University of Nevada, Reno, Nevada, Report No. CCEER-08-01, February 2008.
- CCEER 08-02 Taylor, M. and Sanders, D., "Seismic Time History Analysis and Instrumentation of the Galena Creek Bridge," Center for Civil Engineering Earthquake Research, Department of Civil Engineering, University of Nevada, Reno, Nevada, Report No. CCEER-08-02, April 2008.
- CCEER 08-03 Abdel-Mohti, A. and Pekcan, G., "Seismic Response Assessment and Recommendations for the Design of Skewed Post-Tensioned Concrete Box-Girder Highway Bridges," Center for Civil Engineering Earthquake Research, Department of Civil and Environmental Engineering, University of Nevada, Reno, Nevada, Report No. CCEER-08-03, September 2008.
- CCEER 08-04 Saiidi, M., Ghasemi, H. and Hook, J., "Long Term Bridge Performance Monitoring, Assessment & Management," Proceedings, FHWA/NSF Workshop on Future Directions," Center for Civil Engineering Earthquake Research, Department of Civil and Environmental Engineering, University of Nevada, Reno, Nevada, Report No. CCEER 08-04, September 2008.
- CCEER 09-01 Brown, A., and Saiidi, M., "Investigation of Near-Fault Ground Motion Effects on Substandard Bridge Columns and Bents," Center for Civil Engineering Earthquake Research, Department of Civil and Environmental Engineering, University of Nevada, Reno, Nevada, Report No. CCEER-09-01, July 2009.
- CCEER 09-02 Linke, C., Pekcan, G., and Itani, A., "Detailing of Seismically Resilient Special Truss Moment Frames," Center for Civil Engineering Earthquake Research, Department of Civil and Environmental Engineering, University of Nevada, Reno, Nevada, Report No. CCEER-09-02, August 2009.

- CCEER 09-03 Hillis, D., and Saiidi, M., "Design, Construction, and Nonlinear Dynamic Analysis of Three Bridge Bents Used in a Bridge System Test," Center for Civil Engineering Earthquake Research, Department of Civil and Environmental Engineering, University of Nevada, Reno, Nevada, Report No. CCEER-09-03, August 2009.
- CCEER 09-04 Bahrami, H., Itani, A., and Buckle, I., "Guidelines for the Seismic Design of Ductile End Cross Frames in Steel Girder Bridge Superstructures," Center for Civil Engineering Earthquake Research, Department of Civil and Environmental Engineering, University of Nevada, Reno, Nevada, Report No. CCEER-09-04, September 2009.
- CCEER 10-01 Zaghi, A. E., and Saiidi, M., "Seismic Design of Pipe-Pin Connections in Concrete Bridges," Center for Civil Engineering Earthquake Research, Department of Civil and Environmental Engineering, University of Nevada, Reno, Nevada, Report No. CCEER-10-01, January 2010.
- CCEER 10-02 Pooranampillai, S., Elfass, S., and Norris, G., "Laboratory Study to Assess Load Capacity Increase of Drilled Shafts through Post Grouting," Center for Civil Engineering Earthquake Research, Department of Civil and Environmental Engineering, University of Nevada, Reno, Nevada, Report No. CCEER-10-02, January 2010.
- CCEER 10-03 Itani, A., Grubb, M., and Monzon, E., "Proposed Seismic Provisions and Commentary for Steel Plate Girder Superstructures," Center for Civil Engineering Earthquake Research, Department of Civil and Environmental Engineering, University of Nevada, Reno, Nevada, Report No. CCEER-10-03, June 2010.
- CCEER 10-04 Cruz-Noguez, C., Saiidi, M., "Experimental and Analytical Seismic Studies of a Four-Span Bridge System with Innovative Materials," Center for Civil Engineering Earthquake Research, Department of Civil and Environmental Engineering, University of Nevada, Reno, Nevada, Report No. CCEER-10-04, September 2010.
- CCEER 10-05 Vosooghi, A., Saiidi, M., "Post-Earthquake Evaluation and Emergency Repair of Damaged RC Bridge Columns Using CFRP Materials," Center for Civil Engineering Earthquake Research, Department of Civil and Environmental Engineering, University of Nevada, Reno, Nevada, Report No. CCEER-10-05, September 2010.
- CCEER 10-06 Ayoub, M., Sanders, D., "Testing of Pile Extension Connections to Slab Bridges," Center for Civil Engineering Earthquake Research, Department of Civil and Environmental Engineering, University of Nevada, Reno, Nevada, Report No. CCEER-10-06, October 2010.
- CCEER 10-07 Builes-Mejia, J. C. and Itani, A., "Stability of Bridge Column Rebar Cages during Construction," Center for Civil Engineering Earthquake Research, Department of Civil and Environmental Engineering, University of Nevada, Reno, Nevada, Report No. CCEER-10-07, November 2010.
- CCEER 10-08 Monzon, E.V., "Seismic Performance of Steel Plate Girder Bridges with Integral Abutments," Center for Civil Engineering Earthquake Research, Department of Civil and Environmental Engineering, University of Nevada, Reno, Nevada, Report No. CCEER-10-08, November 2010.
- CCEER 11-01 Motaref, S., Saiidi, M., and Sanders, D., "Seismic Response of Precast Bridge Columns with Energy Dissipating Joints," Center for Civil Engineering Earthquake Research, Department of Civil and Environmental Engineering, University of Nevada, Reno, Nevada, Report No. CCEER-11-01, May 2011.

- CCEER 11-02 Harrison, N. and Sanders, D., "Preliminary Seismic Analysis and Design of Reinforced Concrete Bridge Columns for Curved Bridge Experiments," Center for Civil Engineering Earthquake Research, Department of Civil and Environmental Engineering, University of Nevada, Reno, Nevada, Report No. CCEER-11-02, May 2011.
- CCEER 11-03 Vallejera, J. and Sanders, D., "Instrumentation and Monitoring the Galena Creek Bridge," Center for Civil Engineering Earthquake Research, Department of Civil and Environmental Engineering, University of Nevada, Reno, Nevada, Report No. CCEER-11-03, September 2011.
- CCEER 11-04 Levi, M., Sanders, D., and Buckle, I., "Seismic Response of Columns in Horizontally Curved Bridges," Center for Civil Engineering Earthquake Research, Department of Civil and Environmental Engineering, University of Nevada, Reno, Nevada, Report No. CCEER-11-04, December 2011.
- CCEER 12-01 Saiidi, M., "NSF International Workshop on Bridges of the Future – Wide Spread Implementation of Innovation," Center for Civil Engineering Earthquake Research, Department of Civil and Environmental Engineering, University of Nevada, Reno, Nevada, Report No. CCEER-12-01, January 2012.
- CCEER 12-02 Larkin, A.S., Sanders, D., and Saiidi, M., "Unbonded Prestressed Columns for Earthquake Resistance," Center for Civil Engineering Earthquake Research, Department of Civil and Environmental Engineering, University of Nevada, Reno, Nevada, Report No. CCEER-12-02, January 2012.
- CCEER 12-03 Arias-Acosta, J. G., Sanders, D., "Seismic Performance of Circular and Interlocking Spirals RC Bridge Columns under Bidirectional Shake Table Loading Part 1," Center for Civil Engineering Earthquake Research, Department of Civil and Environmental Engineering, University of Nevada, Reno, Nevada, Report No. CCEER-12-03, September 2012.
- CCEER 12-04 Cukrov, M.E., Sanders, D., "Seismic Performance of Prestressed Pile-To-Bent Cap Connections," Center for Civil Engineering Earthquake Research, Department of Civil and Environmental Engineering, University of Nevada, Reno, Nevada, Report No. CCEER-12-04, September 2012.
- CCEER 13-01 Carr, T. and Sanders, D., "Instrumentation and Dynamic Characterization of the Galena Creek Bridge," Center for Civil Engineering Earthquake Research, Department of Civil and Environmental Engineering, University of Nevada, Reno, Nevada, Report No. CCEER-13-01, January 2013.
- CCEER 13-02 Vosooghi, A. and Buckle, I., "Evaluation of the Performance of a Conventional Four-Span Bridge During Shake Table Tests," Center for Civil Engineering Earthquake Research, Department of Civil and Environmental Engineering, University of Nevada, Reno, Nevada, Report No. CCEER-13-02, January 2013.
- CCEER 13-03 Amirihormozaki, E. and Pekcan, G., "Analytical Fragility Curves for Horizontally Curved Steel Girder Highway Bridges," Center for Civil Engineering Earthquake Research, Department of Civil and Environmental Engineering, University of Nevada, Reno, Nevada, Report No. CCEER-13-03, February 2013.
- CCEER 13-04 Almer, K. and Sanders, D., "Longitudinal Seismic Performance of Precast Bridge Girders Integrally Connected to a Cast-in-Place Bentcap," Center for Civil Engineering Earthquake Research, Department of Civil and Environmental Engineering, University of Nevada, Reno, Nevada, Report No. CCEER-13-04, April 2013.

- CCEER 13-05 Monzon, E.V., Itani, A.I., and Buckle, I.G., "Seismic Modeling and Analysis of Curved Steel Plate Girder Bridges," Center for Civil Engineering Earthquake Research, Department of Civil and Environmental Engineering, University of Nevada, Reno, Nevada, Report No. CCEER-13-05, April 2013.
- CCEER 13-06 Monzon, E.V., Buckle, I.G., and Itani, A.I., "Seismic Performance of Curved Steel Plate Girder Bridges with Seismic Isolation," Center for Civil Engineering Earthquake Research, Department of Civil and Environmental Engineering, University of Nevada, Reno, Nevada, Report No. CCEER-13-06, April 2013.
- CCEER 13-07 Monzon, E.V., Buckle, I.G., and Itani, A.I., "Seismic Response of Isolated Bridge Superstructure to Incoherent Ground Motions," Center for Civil Engineering Earthquake Research, Department of Civil and Environmental Engineering, University of Nevada, Reno, Nevada, Report No. CCEER-13-07, April 2013.
- CCEER 13-08 Haber, Z.B., Saiidi, M.S., and Sanders, D.H., "Precast Column-Footing Connections for Accelerated Bridge Construction in Seismic Zones," Center for Civil Engineering Earthquake Research, Department of Civil and Environmental Engineering, University of Nevada, Reno, Nevada, Report No. CCEER-13-08, April 2013.
- CCEER 13-09 Ryan, K.L., Coria, C.B., and Dao, N.D., "Large Scale Earthquake Simulation of a Hybrid Lead Rubber Isolation System Designed under Nuclear Seismicity Considerations," Center for Civil Engineering Earthquake Research, Department of Civil and Environmental Engineering, University of Nevada, Reno, Nevada, Report No. CCEER-13-09, April 2013.
- CCEER 13-10 Wibowo, H., Sanford, D.M., Buckle, I.G., and Sanders, D.H., "The Effect of Live Load on the Seismic Response of Bridges," Center for Civil Engineering Earthquake Research, Department of Civil and Environmental Engineering, University of Nevada, Reno, Nevada, Report No. CCEER-13-10, May 2013.
- CCEER 13-11 Sanford, D.M., Wibowo, H., Buckle, I.G., and Sanders, D.H., "Preliminary Experimental Study on the Effect of Live Load on the Seismic Response of Highway Bridges," Center for Civil Engineering Earthquake Research, Department of Civil and Environmental Engineering, University of Nevada, Reno, Nevada, Report No. CCEER-13-11, May 2013.
- CCEER 13-12 Saad, A.S., Sanders, D.H., and Buckle, I.G., "Assessment of Foundation Rocking Behavior in Reducing the Seismic Demand on Horizontally Curved Bridges," Center for Civil Engineering Earthquake Research, Department of Civil and Environmental Engineering, University of Nevada, Reno, Nevada, Report No. CCEER-13-12, June 2013.
- CCEER 13-13 Ardakani, S.M.S. and Saiidi, M.S., "Design of Reinforced Concrete Bridge Columns for Near-Fault Earthquakes," Center for Civil Engineering Earthquake Research, Department of Civil and Environmental Engineering, University of Nevada, Reno, Nevada, Report No. CCEER-13-13, July 2013.
- CCEER 13-14 Wei, C. and Buckle, I., "Seismic Analysis and Response of Highway Bridges with Hybrid Isolation," Center for Civil Engineering Earthquake Research, Department of Civil and Environmental Engineering, University of Nevada, Reno, Nevada, Report No. CCEER-13-14, August 2013.

- CCEER 13-15 Wibowo, H., Buckle, I.G., and Sanders, D.H., "Experimental and Analytical Investigations on the Effects of Live Load on the Seismic Performance of a Highway Bridge," Center for Civil Engineering Earthquake Research, Department of Civil and Environmental Engineering, University of Nevada, Reno, Nevada, Report No. CCEER-13-15, August 2013.
- CCEER 13-16 Itani, A.M., Monzon, E.V., Grubb, M., and Amirhormozaki, E. "Seismic Design and Nonlinear Evaluation of Steel I-Girder Bridges with Ductile End Cross-Frames," Center for Civil Engineering Earthquake Research, Department of Civil and Environmental Engineering, University of Nevada, Reno, Nevada, Report No. CCEER-13-16, September 2013.
- CCEER 13-17 Kavianipour, F. and Saiidi, M.S., "Experimental and Analytical Seismic Studies of a Four-span Bridge System with Composite Piers," Center for Civil Engineering Earthquake Research, Department of Civil and Environmental Engineering, University of Nevada, Reno, Nevada, Report No. CCEER-13-17, September 2013.
- CCEER 13-18 Mohebbi, A., Ryan, K., and Sanders, D., "Seismic Response of a Highway Bridge with Structural Fuses for Seismic Protection of Piers," Center for Civil Engineering Earthquake Research, Department of Civil and Environmental Engineering, University of Nevada, Reno, Nevada, Report No. CCEER-13-18, December 2013.
- CCEER 13-19 Guzman Pujols, Jean C., Ryan, K.L., "Development of Generalized Fragility Functions for Seismic Induced Content Disruption," Center for Civil Engineering Earthquake Research, Department of Civil and Environmental Engineering, University of Nevada, Reno, Nevada, Report No. CCEER-13-19, December 2013.
- CCEER 14-01 Salem, M. M. A., Pekcan, G., and Itani, A., "Seismic Response Control Of Structures Using Semi-Active and Passive Variable Stiffness Devices," Center for Civil Engineering Earthquake Research, Department of Civil and Environmental Engineering, University of Nevada, Reno, Nevada, Report No. CCEER-14-01, May 2014.
- CCEER 14-02 Saini, A. and Saiidi, M., "Performance-Based Probabilistic Damage Control Approach for Seismic Design of Bridge Columns," Center For Civil Engineering Earthquake Research, Department Of Civil and Environmental Engineering, University of Nevada, Reno, Nevada, Report No. CCEER-14-02, May 2014.
- CCEER 14-03 Saini, A. and Saiidi, M., "Post Earthquake Damage Repair of Various Reinforced Concrete Bridge Components," Center For Civil Engineering Earthquake Research, Department Of Civil and Environmental Engineering, University of Nevada, Reno, Nevada, Report No. CCEER-14-03, May 2014.
- CCEER 14-04 Monzon, E.V., Itani, A.M., and Grubb, M.A., "Nonlinear Evaluation of the Proposed Seismic Design Procedure for Steel Bridges with Ductile End Cross Frames," Center For Civil Engineering Earthquake Research, Department Of Civil and Environmental Engineering, University of Nevada, Reno, Nevada, Report No. CCEER-14-04, July 2014.
- CCEER 14-05 Nakashoji, B. and Saiidi, M.S., "Seismic Performance of Square Nickel-Titanium Reinforced ECC Columns with Headed Couplers," Center For Civil Engineering Earthquake Research, Department Of Civil and Environmental Engineering, University of Nevada, Reno, Nevada, Report No. CCEER-14-05, July 2014.
- CCEER 14-06 Tazarv, M. and Saiidi, M.S., "Next Generation of Bridge Columns for Accelerated Bridge Construction in High Seismic Zones," Center For Civil Engineering Earthquake Research, Department Of Civil and Environmental Engineering, University of Nevada, Reno, Nevada, Report No. CCEER-14-06, August 2014.

- CCEER 14-07 Mehrsoroush, A. and Saiidi, M.S., “Experimental and Analytical Seismic Studies of Bridge Piers with Innovative Pipe Pin Column-Footing Connections and Precast Cap Beams,” Center For Civil Engineering Earthquake Research, Department Of Civil and Environmental Engineering, University of Nevada, Reno, Nevada, Report No. CCEER-14-07, December 2014.
- CCEER 15-01 Dao, N.D. and Ryan, K.L., “Seismic Response of a Full-scale 5-story Steel Frame Building Isolated by Triple Pendulum Bearings under 3D Excitations,” Center For Civil Engineering Earthquake Research, Department Of Civil and Environmental Engineering, University of Nevada, Reno, Nevada, Report No. CCEER-15-01, January 2015.
- CCEER 15-02 Allen, B.M. and Sanders, D.H., “Post-Tensioning Duct Air Pressure Testing Effects on Web Cracking,” Center For Civil Engineering Earthquake Research, Department Of Civil and Environmental Engineering, University of Nevada, Reno, Nevada, Report No. CCEER-15-02, January 2015.
- CCEER 15-03 Akl, A. and Saiidi, M.S., “Time-Dependent Deflection of In-Span Hinges in Prestressed Concrete Box Girder Bridges,” Center For Civil Engineering Earthquake Research, Department Of Civil and Environmental Engineering, University of Nevada, Reno, Nevada, Report No. CCEER-15-03, May 2015.
- CCEER 15-04 Zargar Shotorbani, H. and Ryan, K., “Analytical and Experimental Study of Gap Damper System to Limit Seismic Isolator Displacements in Extreme Earthquakes,” Center For Civil Engineering Earthquake Research, Department Of Civil and Environmental Engineering, University of Nevada, Reno, Nevada, Report No. CCEER-15-04, June 2015.
- CCEER 15-05 Wieser, J., Maragakis, E.M., and Buckle, I., “Experimental and Analytical Investigation of Seismic Bridge-Abutment Interaction in a Curved Highway Bridge,” Center For Civil Engineering Earthquake Research, Department Of Civil and Environmental Engineering, University of Nevada, Reno, Nevada, Report No. CCEER-15-05, July 2015.
- CCEER 15-06 Tazarv, M. and Saiidi, M.S., “Design and Construction of Precast Bent Caps with Pocket Connections for High Seismic Regions,” Center For Civil Engineering Earthquake Research, Department Of Civil and Environmental Engineering, University of Nevada, Reno, Nevada, Report No. CCEER-15-06, August 2015.
- CCEER 15-07 Tazarv, M. and Saiidi, M.S., “Design and Construction of Bridge Columns Incorporating Mechanical Bar Splices in Plastic Hinge Zones,” Center For Civil Engineering Earthquake Research, Department Of Civil and Environmental Engineering, University of Nevada, Reno, Nevada, Report No. CCEER-15-07, August 2015.
- CCEER 15-08 Sarraf Shirazi, R., Pekcan, G., and Itani, A.M., “Seismic Response and Analytical Fragility Functions for Curved Concrete Box-Girder Bridges,” Center For Civil Engineering Earthquake Research, Department Of Civil and Environmental Engineering, University of Nevada, Reno, Nevada, Report No. CCEER-15-08, December 2015.
- CCEER 15-09 Coria, C.B., Ryan, K.L., and Dao, N.D., “Response of Lead Rubber Bearings in a Hybrid Isolation System During a Large Scale Shaking Experiment of an Isolated Building,” Center For Civil Engineering Earthquake Research, Department Of Civil and Environmental Engineering, University of Nevada, Reno, Nevada, Report No. CCEER-15-09, December 2015.

- CCEER 16-01 Mehraein, M and Saiidi, M.S., “Seismic Performance of Bridge Column-Pile-Shaft Pin Connections for Application in Accelerated Bridge Construction,” Center For Civil Engineering Earthquake Research, Department Of Civil and Environmental Engineering, University of Nevada, Reno, Nevada, Report No. CCEER-16-01, May 2016.
- CCEER 16-02 Varela Fontecha, S. and Saiidi, M.S., “Resilient Earthquake-Resistant Bridges Designed For Disassembly,” Center For Civil Engineering Earthquake Research, Department Of Civil and Environmental Engineering, University of Nevada, Reno, Nevada, Report No. CCEER-16-02, May 2016.
- CCEER 16-03 Mantawy, I. M, and Sanders, D. H., “Assessment of an Earthquake Resilient Bridge with Pretensioned, Rocking Columns,” Center For Civil Engineering Earthquake Research, Department Of Civil and Environmental Engineering, University of Nevada, Reno, Nevada, Report No. CCEER-16-03, May 2016.
- CCEER 16-04 Mohammed, M, Biasi, G., and Sanders, D., “Post-earthquake Assessment of Nevada Bridges using ShakeMap/ShakeCast,” Center For Civil Engineering Earthquake Research, Department Of Civil and Environmental Engineering, University of Nevada, Reno, Nevada, Report No. CCEER-16-04, May 2016.
- CCEER 16-05 Jones, J, Ryan, K., and Saiidi, M, “Toward Successful Implementation of Prefabricated Deck Panels to Accelerate the Bridge Construction Process,” Center For Civil Engineering Earthquake Research, Department Of Civil and Environmental Engineering, University of Nevada, Reno, Nevada, Report No. CCEER-16-05, August 2016.



Nevada Department of Transportation  
Rudy Malfabon, P.E. Director  
Ken Chambers, Research Division Chief  
(775) 888-7220  
kchambers@dot.nv.gov  
1263 South Stewart Street  
Carson City, Nevada 89712